UNIVERSITY OF BIRMINGHAM

Characterisation of platelet receptor CLEC-2 in thrombosis and inflammation

By Joshua Henry Bourne

Submitted to the University of Birmingham for the degree of
DOCTOR OF PHILOSOPHY

Institute of Cardiovascular Science
College of Medical and Dental Science
University of Birmingham
October 2021

Abstract

Platelets have an established role in thrombosis and haemostasis. C-type lectin-like receptor 2 (CLEC-2) is highly expressed on platelets and a subpopulation of myeloid cells, and is critical in lymphatic development. Using a recently developed mouse model for platelet-specific deletion of platelet-CLEC-2, CLEC1b$^{fl/fl}$GPIb-Cre, we show that CLEC-2 contributes to thrombus stability in mice. However, CLEC-2 inhibition in human blood using monoclonal antibody, AYP1, or recombinant CLEC-2 did not translate these observations to human. This presents CLEC-2 as a promising therapeutic target in thromboinflammatory or inflammatory disease, without detriment to thrombosis and haemostasis. We show that hemin, the oxidised form of haem released post-haemolysis, is a novel CLEC-2 ligand which can activate and aggregate platelets through its hemITAM domain. Interestingly, anti-malarial drug hydroxychloroquine is able to inhibit hemin-induced mouse and human platelet activation, but not ROS generation. In a mouse model of thrombosis, the ferric chloride injury of the carotid artery, we demonstrate that hydroxychloroquine treatment presents small, non-occlusive thrombi, compared to saline-treated controls. This may present hemin-CLEC-2 as a promising therapeutic target in thromboinflammatory disease. Beyond thrombosis, platelets contribute to the development, progression and resolution of the inflammatory response. CLEC-2 is protective during mouse models of sepsis, and other inflammatory diseases. Here we show that CLEC-2 reduces tissue inflammation by regulating inflammatory macrophage activation and trafficking from inflamed tissue during murine peritonitis through its ligand, podoplanin. Treatment using recombinant CLEC-2-Fc induces the rapid emigration of peritoneal inflammatory macrophages to mesenteric lymph nodes, thus reducing the accumulation of inflammatory macrophages in the inflamed peritoneum. Macrophage efflux to draining lymph nodes induces T cell priming. In conclusion, we show that CLEC-2 reduces the inflammatory phenotype of macrophages and their accumulation, leading to diminished tissue inflammation. Both the thromboinflammatory and immunomodulatory functions of CLEC-2 present strategies to reduce tissue inflammation and inflammatory thrombi, and could be therapeutically exploited to limit disease progression.

Publications arising from this thesis

BOURNE, J. H., COLICCHIA, M., DI, Y., MARTIN, E., SLATER, A., ROUMENINA, L. T., DIMITROV, J. D., WATSON, S. P. & RAYES, J. 2020. Heme induces human and mouse platelet activation through C-type-lectin-like receptor-2. *Haematologica*.

BOURNE, J. H., BERISTAIN-COVARRUBIAS, N., ZUIDSCHERWOUDE, M., CAMPOS, J., DI, Y., GARLICK, E., COLICCHIA, M., TERRY, L. V., THOMAS, S. G., BRILL, A., BAYRY, J., WATSON, S. P. & RAYES, J. 2021. CLEC-2 Prevents Accumulation and Retention of Inflammatory Macrophages During Murine Peritonitis. *Front Immunol,* 12, 693974.

BOURNE, J. H., SMITH C.W., JOOSS N.J., DI Y., BROWN H.C., MONTAGUE S.J., THOMAS, M.R., POULTER, N.S., RAYES, J. and WATSON, S.P. 2021. Characterization of platelet-CLEC-2 in models of hemostasis and arterial thrombosis in mice and humans. (*Submitted*)

BOURNE, J. H., COLICCHIA, M., HOGG, R. and RAYES, J. Hydroxychloroquine limits hemin-driven thrombosis. (*In preparation*)

BOURNE, J. H. 2021. Angiogensis Protocols - Quantification of leukocyte-endothelial cell interaction during *in vitro* models of thrombosis at arterial and venous shear rates. *Springer Nature*. (*In print*)

KHAN, A. R., **BOURNE, J.H.**, COLICCHIA, M., NEWBY, M.L., ALLEN, JD., CRISPIN, M., YOUD, E., MURRAY, PG., TAYLOR, G., STAMATAKI, Z., RICHTER, AG., CUNNINGHAM, AF., PUGH, M., RAYES, J. 2021. Stimulation of vascular organoids with SARS-CoV-2 antigens increases endothelial permeability and regulates vasculopathy. *medRxiV*.

Reviews:

RAYES, J., **BOURNE, J. H.,** BRILL, A. & WATSON, S. P. 2020. The dual role of platelet-innate immune cell interactions in thrombo-inflammation. *Res Pract Thromb Haemost,* 4**,** 23-35.

D'ALESSANDRO, E., BECKER, C., BERGMEIER, W., BODE, C., **BOURNE, J.H**. et al., 2020. Thrombo-Inflammation in Cardiovascular Disease: An Expert Consensus Document from the Third Maastricht Consensus Conference on Thrombosis. *Thromb Haem.* 120(4): 538-64.

Acknowledgments

Firstly, thank you to Steve Watson, who gave me the amazing opportunity to work in the Birmingham platelet group, for his guidance, Wasps tickets and memorable long speeches. This extends to the staff at the BMSU for training and accommodation, Ying, Beata, Lourdes and Gayle, for always knowing every answer to every question and Deano, for his expertise in Birmingham City and microscopy.

Thanks especially go to all of the lab members in the platelet group, who have been particularly accommodating and forever entertaining. Special thanks go to Chris for his memorable good moods and charm, to Joossy for exposing me to her unmatched German wit, to Joana for reminding me that I'm not "Gen Z" and can't wear straight legged jeans, to Rachel for sitting next to the kettle, Martina for keeping me up to date with the latest Tinder scene, and Alex for being a persistent reminder that I'm not at rock bottom.

My friends outside the lab have provided welcome breaks from science, more often than not resulting in what is now a two-day hangover – thank you. Rob, I, Ab and Az have provided much-needed venting and eating environments which I'll forever be grateful for. My family, Mom, Dad, Els and Pebs have been wonderful, and your motivation throughout has made this possible. Thank you to Nan and Grandad for putting up with my unpredictable golf, and always saying the right things, when I need to hear it.

Thank you to Lol, who has been my everything. From 7am coffees in the med-school on a dreary Monday winter morning, to backpacking through Bali, your support and belief in me never waivers. Our future is so bright, and the work will pay off so soon.

And finally, Julie – my 'science Mom'. The time and effort you've given me is ineffable. I'll never forget the support you've given me.

Dedicated to Jeanette Caddick (1946-2015)
Who always knew ‘her boy’ would be a doctor.
Forever grateful for your belief.

“Now this is a story all about how
My life got flip turned upside down…”

The Fresh Prince of Bel-Air

Table of contents

List of Figures

CHAPTER 1

CHAPTER 2

CHAPTER 3

CHAPTER 4

CHAPTER 5

LIST OF TABLES

CHAPTER 1

CHAPTER 2

Abbreviations

ACD	-	Acid citrate-dextrose
ADAM	-	A disintegrin and metalloproteinase
ADP	-	Adenosine 5'-diphosphate
ARDS	-	Acute respiratory distress syndrome
ATP	-	Adenosine 5'-triphosphate
a.u.	-	Arbitrary units
AUC	-	Area under the curve
BMDMs	-	Bone marrow-derived macrophages
BSA	-	Bovine serum albumin
BTK	-	Bruton tyrosine kinase
Ca^{2+}	-	Calcium
cAMP	-	Cyclic adenosine monophosphate
CARS	-	Compensatory anti-inflammatory response syndrome
CEACAM	-	Carcinoembryonic antigen-related cell adhesion molecule
cGMP	-	Cyclic guanosine monophosphate
CLEC-2	-	C-type lectin-like receptor 2
COX	-	Cyclooxygenase
CSF1R	-	Colony-stimulating factor 1 receptor
DAG	-	1, 2-diacylglycerol
DAMPs	-	Damage-associated molecular patterns
DCS	-	Dense canalicular system
DC-SIGN	-	Dendritic cell-specific intracellular adhesion molecule 3-grabbing nonintegrin

DIC	-	Disseminated intravascular coagulation
diSPIM	-	Dual-view inverted selective plane illumination microscopy
DMEM	-	Dulbecco's Modified Eagle Medium
DNA	-	Deoxyribonucleic acid
DVT	-	Deep vein thrombosis
EAE	-	Experimental autoimmune encephalomyelitis
ECGM	-	Endothelial Cell Growth Media
EDTA	-	Ethylenediaminetetraacetic acid
Egr-2	-	Early Growth Response Gene-2
ELISA	-	Enzyme-linked immunosorbent assay
ERM	-	Ezrin, radixin and moesin proteins
FBS	-	Foetal bovine serum
GFP	-	Green fluorescent protein
GM-CSF	-	Granulocyte-macrophage colony stimulating factor
GP	-	Glycoprotein
GPCR	-	G-protein coupled receptor
GPO	-	Glycine-proline-hydroxyproline
G-protein	-	Guanine nucleotide-binding proteins
GPVI	-	Glycoprotein VI
HCQ	-	Hydroxychloroquine
hFc-CLEC-2	-	Recombinant human CLEC-2-Fc
HIV	-	Human immunodeficiency virus
HO-1	-	Haem-oxygenase 1
HUS	-	Haemolytic uremic syndrome
HUVECs	-	Human umbilical vein endothelial cells

ICAM	-	Intercellular adhesion molecule 1
ICF	-	Immunocytofluorescent
IFNγ	-	Interferon gamma
IgG	-	Immunoglobulin G
IHF	-	immunohistofluorescent
IL	-	Interleukin
IP3	-	Inositol 1, 4, 5-triphosphate
ITIM	-	Immunoreceptor tyrosine- based inhibitory motif
ITAM	-	Immunoreceptor tyrosine-based activation motif
IVC	-	Inferior vena cava
JAK-STAT	-	Janus kinase-signal transducer and activator of transcription
LDL	-	Low density lipoprotein
LECs	-	Lymphatic endothelial cells
LFA-1	-	Lymphocyte function-associated antigen-1
LPM	-	Large peritoneal macrophages
LPS	-	Lipopolysaccharide
MAC-1	-	Macrophage antigen-1
MAPK	-	Mitogen-activated protein kinase
M-CSF	-	Macrophage colony stimulating factor
MLN	-	Mesenteric lymph node
MMP	-	Metalloproteinase
NETs	-	Neutrophil extracellular traps
NO	-	Nitric oxide
NOS	-	Nitric oxide synthase
OCS	-	Open canalicular system

OCT	-	Optical cutting temperature
OxLDL	-	Oxidised low-density lipoproteins
PAMPs	-	Pathogen-associated molecular patterns
PAR	-	Protease activating receptor
PBS	-	Phosphate buffered saline
PBS-T	-	Phosphate buffered saline with 0.1 % Tween 20
PDGF	-	Platelet-derived growth factor
PECAM-1	-	Platelet endothelial cell adhesion molecule-1
PF4	-	Platelet factor 4
PGI_2	-	Prostacyclin
PI3K	-	Phosphoinositide 3-kinase
PIP3	-	Phosphatidylinositol-3, 4, 5-trisphosphate
PKA	-	Protein kinase A
PKG	-	Protein kinase G
PLAG	-	Platelet aggregation-stimulating
PLC	-	Phospholipase C
PLF	-	Peritoneal lavage fluid
PPAR	-	Peroxisome proliferator-activated receptors
PPP	-	Platelet poor plasma
PRP	-	Platelet rich plasma
PS	-	Phosphatidylserine
PTK	-	Protein tyrosine kinase
qPCR	-	Quantitative polymerase chain reaction
rCLEC-2-Fc	-	Recombinant mouse CLEC-2-Fc
RNA	-	Ribonucleic acid

ROS	-	Reactive oxygen species
rpm	-	Rotations per minute
RPMI	-	Roswell Park Memorial Institute Medium
RT	-	Room temperature
SARS	-	Severe acute respiratory syndrome
SFK	-	Src family kinase
SH	-	Src homology 2 domain-containing protein-tyrosine phosphatase-1
SIM	-	Structured illumination microscopy
SIRS	-	Systemic inflammatory response syndrome
SLe^x	-	Sialyl Lewis X
SPM	-	Small peritoneal macrophages
TBS	-	Tris buffered saline
TBS-T	-	Tris buffered saline with 0.1 % Tween 20
TGF-β	-	Transforming growth factor-β
TLR4	-	Toll-like receptor 4
TLT-1	-	Triggering receptor expressed on myeloid cells-like transcript 1
TNF-α	-	Tumour necrosis factor-α
TxA_2	-	Thromboxane A_2
VCAM	-	Vascular cell adhesion molecule
VEGF	-	Vascular endothelial growth factor
vWF	-	von Willebrand Factor
WB	-	Western blotting
WT	-	Wild type

Chapter 1

General Introduction

1.1 An overview on classical platelet functions

Platelets are small, anuclear cell fragments important in health, but are also contributors to pathophysiology. Demonstrated to have several roles post-injury or infection, platelets are best described to regulate the maintenance of circulating blood volume through the generation of a vascular plug at the site of injury. Upon vascular injury or rupture, exposure of the sub- or activated-endothelium initiates platelet activation, which leads to conformational changes in their shape, the translocation of activation markers from intracellular stores to the platelet surface, and subsequent increased interaction with other circulating platelets, leukocytes, endothelial cells and clotting factors, together contributing to clot formation. Whilst platelets are important for maintenance of haemostasis, they have also been observed to drive unwanted complications in disease, in particular inflammatory and thrombotic diseases. More recently, platelets were shown to be involved in development and cancer progression, with different platelet receptors involved at different stages and different organs. The regulation of platelet-cell interaction, their ability to form a vascular plug, alongside various other bodily functions create interesting and effective translational therapeutic targets to treat thrombosis, thromboinflammation, and/or inflammatory-related diseases.

1.2 Platelet physiology

1.2.1 Platelet structure and anatomy

First described in 1882 by Giulo Bizzozero, platelets were microscopically observed in both circulating blood and in blood harvested from living mammals (Ribatti and Crivellato, 2007). Mature human platelets are typically 2-3 microns in size, and have a somewhat unique cellular assembly. To support the plasma membrane, platelets utilise an actin cytoskeleton with a microtubule system which upkeeps conformational changes during platelet activation and spreading (Bearer et al., 2002, Poulter et al., 2015). The proportion of polymerised actin within the cell fragment is fundamental to the organisation of filaments, and hence platelet shape (Bearer et al., 2002).

Whilst the cell fragments are anuclear, platelets have unique mitochondria which are few, but highly active, with a high adenosine 5'-triphosphate (ATP) turnover (Zharikov and Shiva, 2013). Aside from the classical 'powerhouse' of the cell function, platelet mitochondria have been shown to be vital in dictating intracellular signalling via reactive oxygen species (ROS) generation, and cytochrome c production to dictate platelet activation and apoptosis, respectively (Hamanaka and Chandel, 2010, Nunnari and Suomalainen, 2012). In the absence of a nucleus, platelets are incapable of upregulating protein expression transcriptionally post-phosphorylation of intracellular signalling components, subsequently unable to undergo *de novo* protein synthesis. Instead, platelets store biologically active molecules which are critical in the classical, and non-classical functions in

intracellular granules (Flaumenhaft, 2003). Of the three major granules, the most prominent is the alpha granule, which contains P-selectin, GPIIb/IIIa, fibrinogen and von Willebrand Factor (vWF) which are released upon platelet activation; alpha granules also contain inflammatory cytokines and chemokines (Harrison and Cramer, 1993). The second major granule are the dense granules, which also secrete proteins during activation, such as serotonin, adenosine 5'-diphosphate (ADP) and ATP. Platelets also contain lysosomes, which store glycohydrolases, but are less prevalent. Both granules and lysosomes are vital in thrombi formation and growth, alongside the recruitment of leukocytes in thrombosis and inflammation (Heijnen and van der Sluijs, 2015), and reside in the central cytoplasm – coined 'hyalomere'.

For dynamic transport and access to the intracellular components of the platelet hyalomere, two canalicular systems are utilised; (i) an open (OCS) and (ii) dense canalicular system (DCS) (Bearer et al., 2002). The DCS is responsible for calcium (Ca^{2+}) sequestration, alongside the synthesis of various unsaturated fatty acids and subsequent lipid mediators. That being said, it has been shown that the majority of granular release is through the OCS, leading to protein release through pores into the extracellular space (Allen et al., 1979, Stenberg et al., 1984). The phospholipid bilayer accommodates the expression of constituently expressed proteins, which can be used to trigger platelet activation, alongside those released from degranulation.

1.2.2 Platelet production

Platelets are derived from their progenitor in the haematopoietic lineage, the megakaryocyte. Megakaryocytes are responsible for almost all organelles and proteins comprised within the mature platelet, both constituently expressed and those released through degranulation; other proteins such as fibrinogen are uptaken from blood plasma. In early development, prior to sufficient marrow cavity infrastructure, megakaryopoiesis occurs in the liver and yolk sac (Bluteau et al., 2013). Post-development, megakaryocytes reside predominantly in the bone marrow, but are also found in the lung, and rarely in peripheral blood (Ogawa, 1993, Lefrançais et al., 2017). Murine megakaryocytes are also found in the spleen, albeit this is not translated to humans (Schmitt et al., 2001). Alongside other circulating blood cells, megakaryocytes are derived from a haematopoietic stem cell, and subsequent common myeloid progenitor **(Figure 1.1)**. The progenitor can differentiate into burst- or colony-forming, immature megakaryocytes, albeit both lineages ultimately differentiate to mature megakaryocytes (Briddell et al., 1989). In distinct response to thrombopoietin, a growth-development cytokine, megakaryocytes enlarge to 100-500 μm to facilitate platelet production (Long et al., 1982, Kaushansky, 2005, Kaushansky and Drachman, 2002). It is estimated that thousands of proplatelets develop along the branches formed from the megakaryocyte pseudopods (Patel et al., 2005), although this is not replicated over the 14-day *ex vivo* bone marrow differentiation process (Thon and Italiano, 2010, Sim et al., 2016).

In health, around two thirds of platelets are in constant circulation, with the remaining stored in the spleen. Normal platelet counts in humans are 150-400x10^6/ml. During illness or blood-loss, platelet count is replenished through increased megakaryocyte differentiation from the bone marrow (Patel et al., 2005, Ghoshal and Bhattacharyya, 2014). Humans can produce up to 10^{11} platelets/day, with a lifespan of 8-10 days (Fritz et al., 1986, Lebois and Josefsson, 2016); old platelets are phagocytosed in the liver and spleen.

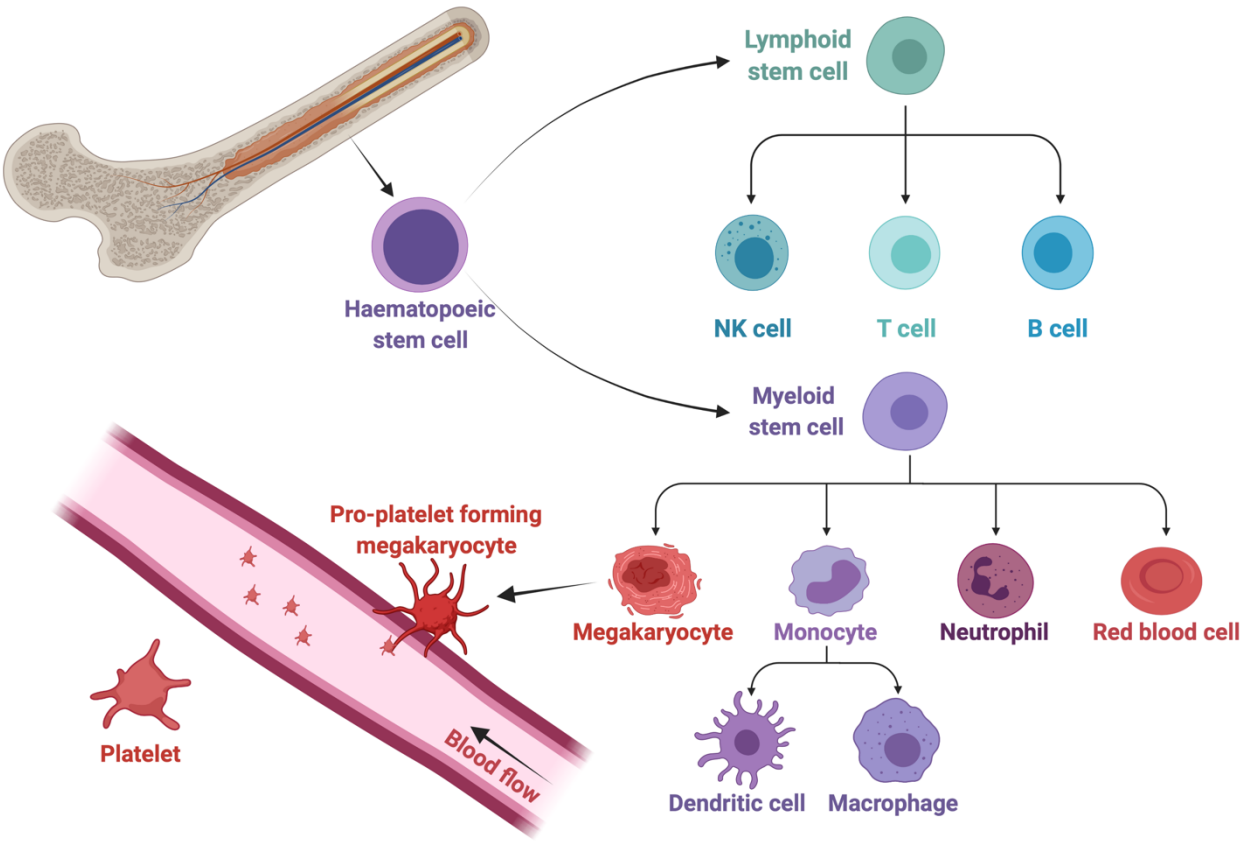

Figure 1.1 - Differentiation of specialised cells from haematopoietic stem cells

Haematopoietic stem cells, found in bone marrow, differentiate to common progenitors in response to specific stimuli. Progenitors can further differentiate to specialised cells under particular conditions, in this case – platelets from megakaryocytes. *Figure made using BioRender.*

1.2.3 The dynamic role of platelets

Platelets circulate the body in vasculature to maintain and preserve vascular integrity in the absence of injury and inflammation (Gupta et al., 2020). However, platelets play critical roles post-trauma or infection. Upon injury, activated platelets reduce blood loss (haemostasis) through the formation of a haemostatic plug in the cardiovascular system. Pathogenic-driven clot formation can also occur (thrombosis). Thrombosis and haemostasis were long believed to be the sole function of the platelet (Ghoshal and Bhattacharyya, 2014, Tomaiuolo et al., 2017), albeit more recently, classical and non-classical functions beyond primary thrombosis have been discovered. Alongside significant roles in inflammation driven thrombosis (thromboinflammation) (Nieswandt et al., 2011, Jackson et al., 2019), platelets have been demonstrated to interact with inflammatory cells to not only drive thrombosis, but also to have immunomodulatory functions in dictating the inflammatory response to pathogen- and sterile-driven inflammation (Rayes et al., 2020). Platelet-cell interactions have been established to drive thrombosis, thromboinflammation and inflammation, through crosstalk with the endothelium, erythrocytes, neutrophils, monocytes and macrophages. The pro-thrombotic and immunomodulatory functions of platelets are promising therapeutic targets to treat vascular diseases such as atherosclerotic plaque, peripheral artery disease or ischaemic stroke, inflammatory diseases such as inflammatory bowel disease, arthritis or sepsis, and even cancer.

1.3 Thrombus formation

Thrombus formation involves multiple cell types, proteins and signalling events which culminates to a vascular plug which ultimately promotes haemostasis. In response to a platelet stimulus, most commonly the exposure of collagen from the subendothelium, a sequence of events is initiated. (i) platelets adhere to exposed collagen fibres, (ii) are stabilised for firm adherence, (iii) then spread and recruit further platelets by protein secretions, and (iv) thrombus growth **(Figure 1.2)**.

i. Collagen exposure and initial platelet adherence

In health, platelets are marginalised by red blood cells to force a mild interaction with the non-activated, intact endothelium. Forming as much as 40% of total protein in the blood vessel walls, collagen is critical in both the tissue integrity of the endothelium, but also in driving thrombosis (Farndale et al., 2004). Located immediately below endothelium in the underlying matrix, collagen is both an efficient and convenient tool utilised to restrict haemostasis. Upon vascular injury, vascular integrity is disrupted, forcing blood – and hence platelets – to flow over collagen-containing connective tissue. Collagen types I, II, III and IV, the most common in vasculature, can support platelet adhesion up to a high shear rate in microcirculation of $2000s^{-1}$ (Sixma et al., 1997, Sixma et al., 1995). Platelet receptor glycoprotein (GP)-Ib-V-IX indirectly binds collagen through vWF to initiate initial platelet adhesion (Verkleij et al., 1998). Vascular injury exposes both vWF and collagen in the subendothelium, although inflammation-driven thrombosis induces the release of vWF on the endothelial surface to promote platelet adhesion. The passive binding to vWF is

insufficient to drive stable adhesion, and causes platelet rolling along the endothelium.

ii. Stabilised adhesion and activation

Initial platelet binding to collagen and vWF through glycoproteins allows for increased platelet receptor-ligand interaction, and formation of firm adhesion with collagen fibres. Platelet receptor glycoprotein (GP)VI is critical for platelet interaction with collagen, and when within close vicinity, initiates platelet activation and subsequent stable adhesion (Nieswandt et al., 2001a). GPVI is essential at all shear rates, unlike integrin $\alpha 2\beta 1$ (Savage et al., 1998). GPVI crosslinking initiates a strong 'inside-out' signalling to activate integrins $\alpha 2\beta 1$ and $\alpha IIb\beta 3$, inducing a switch in conformational shape and their binding affinity to collagen (Nieswandt et al., 2001a, Watson et al., 2005). Activation of integrins $\alpha 2\beta 1$ and $\alpha IIb\beta 3$ allows for greater interaction with collagen and vWF, respectively, to further promote further stable platelet adhesion (Verkleij et al., 1998).

iii. Platelet spreading and recruitment

Despite classically having a discoid shape when non-activated in circulation, platelets have a highly irregular shape upon activation. Through an extension of pseudopodia, and subsequent lamellipodia, platelets flatten to have an increased surface area at the site of injury (Lee et al., 2012, Durrant et al., 2017). Activated platelets secrete thromboxane A_2 (TxA_2) and ADP from granules, which drive the recruitment of further platelets independent of collagen (Wu et al., 1996), and also promotes further platelet spreading. Procoagulant enzyme complexes are formed on platelet surfaces through phosphatidylserine (PS) exposure through platelet-

membrane inversion upon activation. In turn, thrombin is generated from prothrombin – a major platelet activator through protease activated receptor (PAR)-1 and PAR-4 (PAR-3 and PAR-4 in mice which are PAR-1-deficient) (Arachiche et al., 2013).

iv. Thrombus growth

Thrombin released from recruitment, and collagen-adhered platelets not only acts as a strong platelet agonist, but also converts fibrinogen, produced in the liver and found in blood plasma, to fibrin. Fibrin acts as a web to not only recruit and activate more platelets but also hold the thrombi together, to successfully inhibit blood loss at the site of vascular disruption. Initially thought to be a GPVI-dependant mechanism (Alshehri et al., 2015a), GPIIb/IIIa has been shown as the major fibrin receptor (Moroi et al., 2021). Moroi et al. demonstrated that only dimeric, and not monomeric, GPVI binds fibrin in clots, although at low levels compared to GPIIb/IIIa. Clots are then able to strengthen the plug formed through contraction generated by non-muscle myosin II to generate retraction of the actin cytoskeleton to pull platelets together. Clot retraction leads to restoration of homeostasis (Farndale et al., 2004).

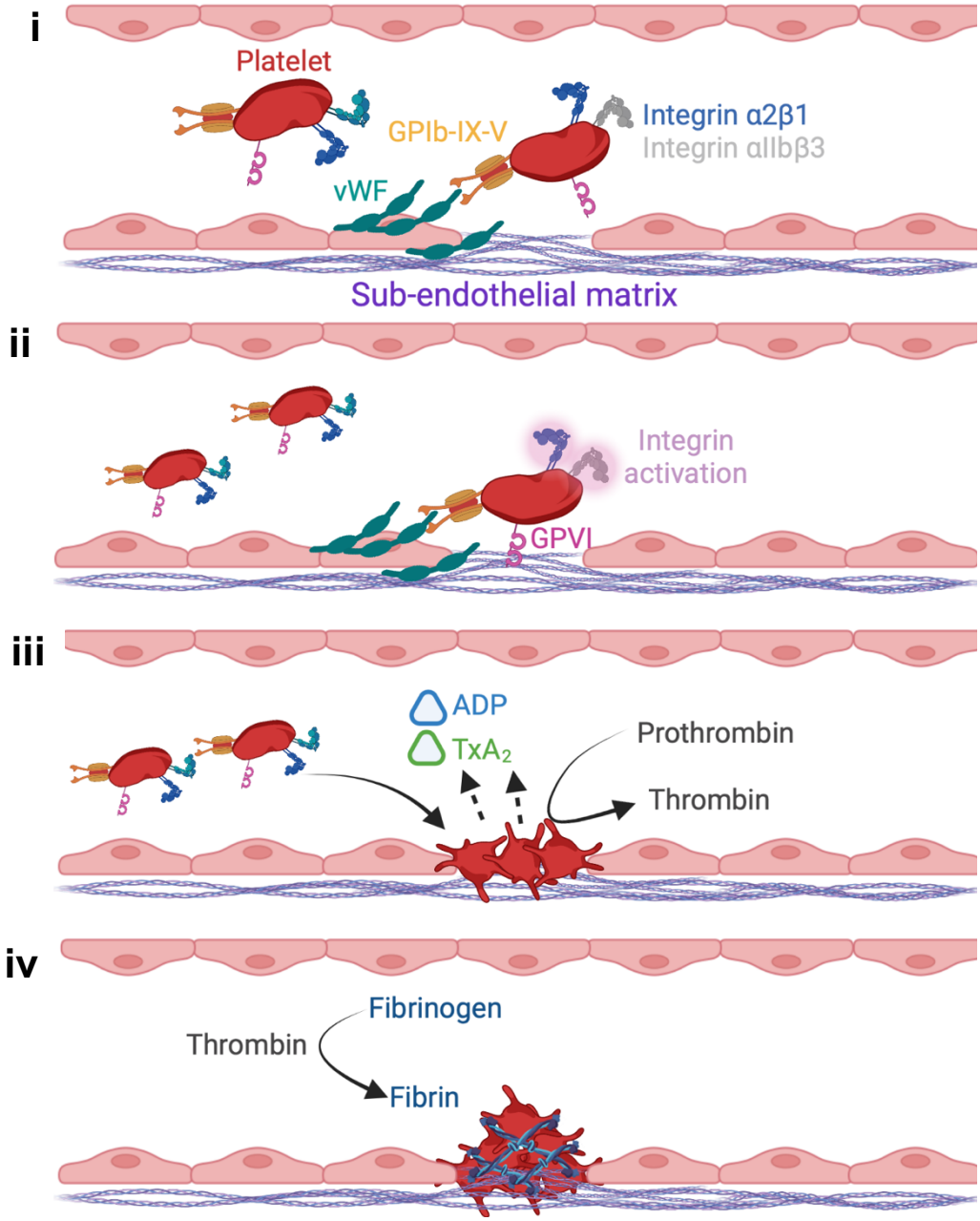

Figure 1.2 – Stages of thrombus formation. The major stages of thrombus formation post-vascular integrity disruption: (i) collagen exposure and initial platelet adherence through GPIb-IX-V binding to vWF and collagen, (ii) stabilised platelet adhesion through GPVI and subsequent integrin activation to promote further firm adhesion, (iii) platelet spreading and their further recruitment through the secretion of ADP and TxA_2 and (iv) thrombus growth and stabilisation by the formation of a fibrin web which retracts to form a haemostatic plug. *Figure made using BioRender.*

1.3.1 Platelet activation signalling

Platelet activation through receptor crosslinking and Ca^{2+} mobilisation from granule release is mediated by external agonists or adhesion proteins; platelets are otherwise biologically active, but non-activated in physiology. Receptors regulating platelet activation which are important in thrombosis and haemostasis can be categorised into two major domains – G protein-coupled receptors (GPCRs) and protein tyrosine kinase (PTK)-linked receptors **(Figure 1.3)** (Offermanns, 2006, Furman et al., 1994).

GPCRs make up the largest family of proteins in the human genome sequence (Pierce et al., 2002, Fredriksson et al., 2003). They are impressively diverse and can be activated by a range of ligands with a variety of chemical properties, subsequently inducing a range of intracellular signalling pathways through the guanine nucleotide-binding proteins (G proteins) (Offermanns, 2006). The tertiary phase **(Figure 1.2)** in thrombus formation utilises the assorted application of GPCRs to accommodate TxA_2- and ADP-regulated platelet activation and recruitment through a positive feedback loop (Wu et al., 1996); platelet activation by the ligands further drive their secretion.

TxA_2 is derived from arachidonic acid, stored as phospholipids in the platelet membrane, through oxygenation by cyclooxygenase and TxA_2 synthase (Paul et al., 1999). Whilst a positive feedback loop is well understood in context of GPCR-TxA_2 crosslinking, it is not known if TxA_2 is a strong agonist for platelet activation, or a mediator for activation of other ligands. TxA_2 binds to and activates the platelet-

receptor, thromboxane receptor, a Gq-coupled receptor which leads to phospholipase C (PLC) phosphorylation, and subsequent induction of intracellular Ca^{2+} release (Hechler and Gachet, 2011); Ca^{2+} is an essential second messenger for platelet activation (Varga-Szabo et al., 2009).

ADP is released from dense granules (Heijnen and van der Sluijs, 2015), but can also be secreted by activated or disrupted endothelial cells through its metabolism by ectonucleoside triphosphate diphosphohydolase1 (Yau et al., 2015). It activates platelets through GPCR receptors, P2Y1 and P2Y12 (Offermanns, 2006, Hechler and Gachet, 2011). The P2Y1 receptor, similar to the thromboxane receptor, is Gq-coupled and also signals through PLC. Interestingly, P2Y12 signals through a different pathway, as they are Gi-coupled. Downstream of receptor P2Y12 activation, cyclic adenosine monophosphate (cAMP) formation by adenyl cyclase is inhibited, subsequently reducing the activity of protein kinase A (PKA), and phosphorylation of protein kinase B (PKB) downstream of phosphoinositide 3-kinase (PI3K) (Cattaneo, 2015).

Aside from TxA_2 and ADP, thrombin is also a GPCR agonist, binding to platelets through PAR-1 and -4 (Adam et al., 2003). Distinct from other GPCRs, PARs are not simply activated through direct ligand binding, but through cleavage of their N-terminus to expose a ‘tethered ligand’. The tethered ligand remains bound, and signals through Gq- and G_{13}-coupled receptors (Offermanns, 2006, Hechler and Gachet, 2011, Cattaneo, 2015). Mice are deficient in PAR-1, but instead function through PAR-3 and PAR-4; different PARs have varying affinity to ligands, and have

varying activating capabilities. Thrombin acts to cleave fibrin from fibrinogen, and stabilise thrombus formation (as mentioned in 1.3).

PTK-linked receptors are essential for the first stages of platelet activation, and are important in the initial binding of platelets to exposed collagen, post vascular disruption. The role of platelet integrins is well established in the field, which signal through PTKs. Integrins are heterodimeric glycoproteins, which are integral in the platelet membrane to facilitate platelet-ligand or platelet-cell interaction (Furman et al., 1994).

Integrins $\alpha 2\beta 1$ and $\alpha IIb\beta 3$ (GPIIb/IIIa) are important in firm adhesion of platelets to collagen-containing sub-endothelial tissue. The heterodimer integrin $\alpha IIb\beta 3$ is the most abundance integrin with up to 80,000 copies, and is distinct to platelets (Bennett, 2005, Bennett, 2015). The receptor can bind to soluble fibrinogen, fibronectin and vWF (Furman et al., 1994, Nieswandt et al., 2001a). Upon activation, inside-out signalling drives a conformational change in receptor shape to increase the affinity to ligands. Unlike integrin $\alpha IIb\beta 3$, $\alpha 2\beta 1$ has a more relevant function in initial platelet adhesion, and can only process weak activation signals. Platelet activation through these integrins initiates platelet cytoskeleton rearrangement to stimulate platelet spreading (Poulter et al., 2015).

Before firm platelet adhesion can be initiated, platelet arrest from circulation is stimulated through the GPIb-IX-V complex. This consists of a GPIbα, GPIbβ, GPIX and GPV subunits (Andrews et al., 2003, Ravanat et al., 2010), which together form a vWF receptor complex. GPIbα is the largest of the aforementioned, and is integral

in binding to vWF, factor XII and thrombin to initiate a coagulation sequence (Madabhushi et al., 2014). The GPIbα tail, along with support by GPIbβ, is bound to a dimeric actin crosslinking scaffold protein, Filamin A.

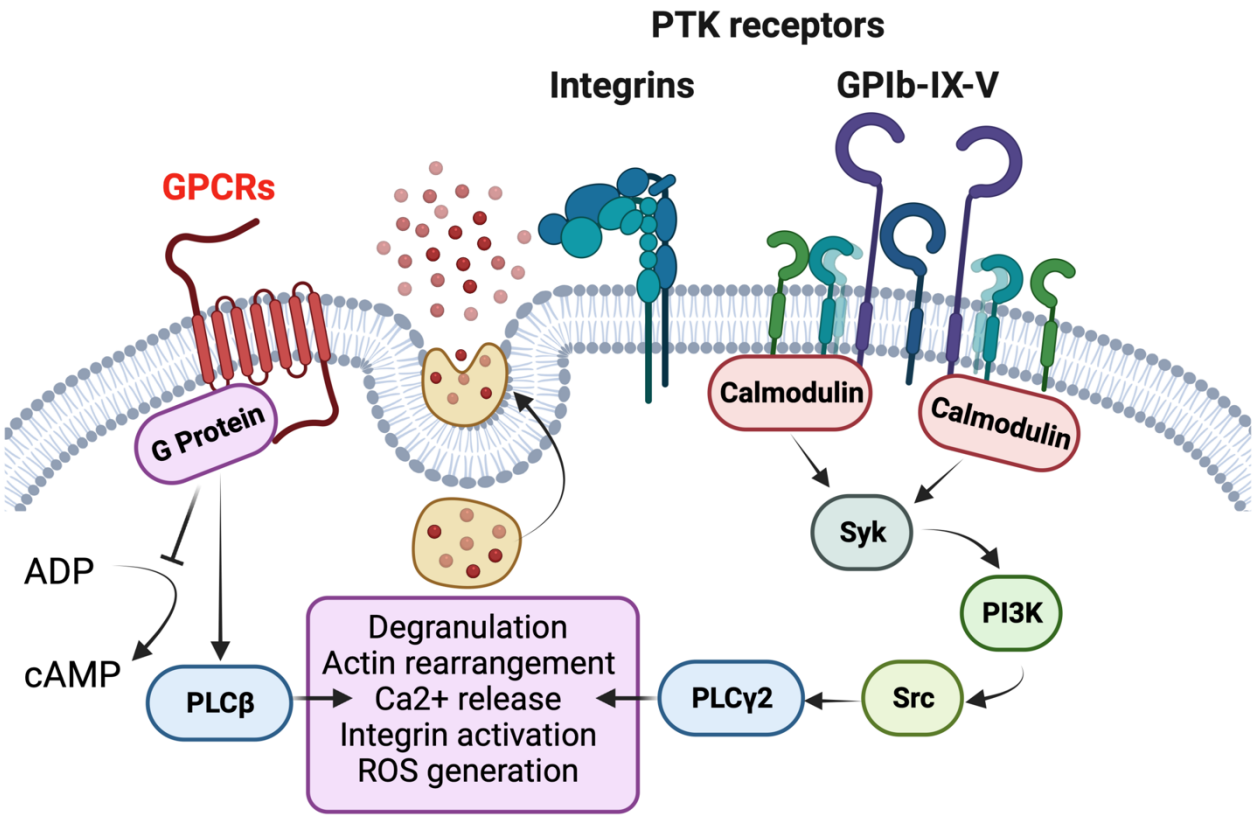

Figure 1.3 - Classical GPCR and PTK-linked receptor signalling. The GPCR and PTK-linked receptors induce signalling pathways integral to platelet activation and subsequent thrombus formation. Receptor-ligand binding initiates a phosphotyrosine signalling cascade, leading to αIIbβ3 activation and degranulation, leading to a positive feedback loop to drive further activation and platelet recruitment. *Figure made using BioRender.*

immunoreceptor tyrosine-based activation motif (**ITAM**) receptors, upon crosslinking by the relevant ligands, distinctly activate platelets through an intracellular signalling pathway independent of GPCRs, and unlike PTK-linked receptors, have either an ITAM of hemITAM domain. These domains facilitate Src family kinase (SFK) phosphorylation, leading to PLCγ2 activation (Rayes et al., 2018), and have been shown to regulate canonical and non-canonical functions of platelets. The structure and function of ITAM receptors will be discussed later in this thesis.

1.3.2 Preventing platelet activation in physiology

Platelets have little function in physiology, and whilst thrombosis and haemostasis are essential mechanisms in homeostasis, spontaneous platelet activation would be detrimental. With this in mind, mechanisms to prevent platelet activation are necessary to allow passive interaction with the non-activated, intact endothelium as a result of margination by erythrocytes. Endothelial cells have an arsenal of platelet-inhibiting mechanisms.

Nitric Oxide (NO) is synthesised by NO synthase (NOS), an enzyme with three isoforms; NOS-III is most commonly found in the endothelium, unlike NOS-I- and NOS-II which is mainly found in inflammatory cells and the nervous system (Ghosh and Salerno, 2003). Upon Ca^{2+}-dependant NO release from the endothelium, the soluble gas diffuses to the luminal portion of the vessel to interact with platelets. NO is sensed by guanylyl cyclase in the platelet cytoplasm, which subsequently drives intracellular cyclic guanosine monophosphate (cGMP) to activate protein kinase G

(PKG). PKG activation forces a reduction in intracellular, bioavailable Ca^{2+}, and hence eliminates cell activation (Mitchell et al., 2008). The short half-life of NO allows for a rapid turnover of the soluble gas, alongside constitutive expression and release from the endothelium, leading to a careful balance to remove spontaneous platelet activation, simultaneously allowing platelet activation in response to a strong agonist.

In many ways, **prostacyclin** (PGI_2) is thought to be the opposite to TxA_2 in platelet functionality (Offermanns, 2006, Mitchell et al., 2008). Platelets express PGI_2 receptors on their surface, which are classical GPCRs, but also intracellular peroxisome proliferator-activated receptors (PPARs), specifically PPARβ/∂ and PPARγ, which are ligand-activated transcription factors of the nuclear hormone family (Pierce et al., 2002, Offermanns, 2006, Stitham et al., 2007). Interestingly, PPARγ has been shown to negatively regulate GPIIb/IIIa outside-in signalling through protein kinase A (Unsworth et al., 2017). PGI_2 receptor activation initiates GPCR-dependant adenylate cyclase production of cAMP; TxA_2 signalling inhibits cAMP production. Resultant PKA phosphorylation decreases intracellular bioavailability of Ca^{2+}, and hence reduces cellular activity.

Alongside endothelial secretions to limit platelet activation, endothelial cells express an integral membrane enzyme, **CD39**, which is key in the hydrolysis of ADP and/or ATP (Antonioli et al., 2013). An accumulation of ATP has been shown to exacerbate thrombin-induced vascular permeability, through a loss of endothelial barrier function, to promote thrombus growth (Gündüz et al., 2003). Reduction in adenosine residue generation has been shown to be essential in silencing endothelial

activation, and subsequent thrombus generation (Koszalka et al., 2004, Zernecke et al., 2006).

Aside from anti-platelet mechanisms developed by the endothelium, platelets also express anti-activating qualities through the immunoreceptor tyrosine- based inhibitory motif (ITIM). Platelet endothelial cell adhesion molecule-1 (PECAM-1), G6b-B, triggering receptor expressed on myeloid cells-like transcript 1 (TLT-1), and carcinoembryonic antigen-related cell adhesion molecule (CEACAM) each have been demonstrated to contain ITIMs (O'Brien et al., 2004, Mazharian et al., 2012, Geer et al., 2018, Smith et al., 2018, Ye et al., 2020). They are linked to Src homology 2 domain-containing protein-tyrosine phosphatase-1 (SH1) and -2 (SH2), which regulate the dephosphorylation of integral intracellular signalling components (Mazharian et al., 2013, Geer et al., 2018). As a result of dephosphorylation, free intracellular Ca^{2+} is decreased, and hence so is cell activity.

1.4 Platelets beyond haemostasis

As eluded to thus far, platelets have significant functions during pathophysiological conditions beyond conventional hemostasis. The past 20 years have enlightened platelets as contributors to vascular integrity and permeability, infection- and sterile-driven inflammation and tissue repair. Platelets alone are somewhat innocent bystanders in these processes, however through their interaction with the endothelium or myeloid cells, they can drive these processes to restore homeostasis. Interestingly, alongside storing mediators of a platelet-activating positive-feedback loop, platelet granules simultaneously store pro- and anti-

inflammatory mediators, including tumour necrosis factor-α (TNF-α) and transforming growth factor-β (TGF-β), chemokines such as RANTES and platelet factor 4 (PF4), endothelial cell regulators such as sphingosine-1-phosphate and serotonin, and also growth factors such as platelet-derived growth factor (PDGF) and vascular endothelial growth factor (VEGF) (Golebiewska and Poole, 2015, Rayes et al., 2020). Secretion of these factors can all be released instantly post-platelet activation by an agonist. The dynamic capabilities of platelets make them fascinating therapeutic targets to modulate various platelet functions beyond haemostasis.

Platelets have a dynamic, and heavily dependable role during local inflammatory conditions through maintenance of **vascular integrity and permeability** (Ho-Tin-Noé et al., 2018). Classically, collagen exposure post-trauma leads to platelet recruitment and haemostasis. That being said, inflammatory bleeding outlines a mechanism distinct from typical thrombosis and haemostasis. Inflammatory hemostasis is primarily GPIIb/IIIa-independent, although it can also be GPIIb/IIIa-dependent during cortical inflammation-induced ischemia-reperfusion injury (Kingma et al., 2000). Neutrophil extravasation-induced vascular permeability is recovered through platelet recruitment during inflammation (Hillgruber et al., 2015), through binding to endothelial tight junctions and 'conducting' neutrophils through their transmigration process. This emphasises the importance of platelets during inflammation through limitation of inflammatory bleeding. Simultaneously, platelet recruitment during inflammation can increase vascular permeability, leukocyte recruitment, and oedema through the release of chemokines and permeability factors, such as PF4, RANTES and VEGF (Golebiewska and Poole, 2015, Rayes et al., 2020). The dynamic and significant role of platelets is carefully regulated

throughout the inflammatory process dependant on the vascular bed, inflammatory stimuli and local tissue microenvironment (Boulaftali et al., 2014, Gros et al., 2015). It is not known if the vascular bed, or the inflammatory stimuli regulates differential platelet receptor contribution to inflammatory haemostasis, although it has been shown that GPIbα is critical in inflamed alveolar vascular integrity, but not in the inflamed skin vascular integrity, which has been shown to be GPIbα-independent (Boulaftali et al., 2014, Rayes et al., 2018).

Post inflammation-driven vascular injury, **wound healing** is integral to efficient restoration of tissue to restrict inflammation-induced organ dysfunction. Interestingly, platelet-rich plasma (PRP) has been revealed to be a safe, non-invasive and beneficial therapeutic to treat inflammatory-induced wound healing (Chicharro-Alcántara et al., 2018), outlining the importance of platelets and its secretions in this process. Platelets promote the release of cytokine, chemokine, and growth factors, support fibrin generation and regulate immune cell recruitment and subsequent activation (Eisinger et al., 2018, Rayes et al., 2020). Metalloproteinase (MMP) release from platelets, and platelet-induced MMP release from leukocytes and endothelial cells promote leukocyte recruitment and migration to the injury site, allowing sufficient wound repair (Seizer and May, 2013). Activated platelets have been shown to upregulate the secretion of endothelial cell-MMP-1, -2 and -9, and isolated monocyte-MMP-9 to retain leukocytes at the site of injury (May et al., 2002, Galt et al., 2001). Additionally, Wichaiyo et al. (2019) demonstrated key roles for ITAM receptors GPVI and C-type lectin-like receptor (CLEC-2) in wound healing, through a loss of platelet-regulated vascular integrity. Deletion of either the ITAM, or hemITAM receptor results in a mild bleeding phenotype during post wound-injury,

alongside a loss of blood/lymphatic separation upon CLEC-2 deletion (Haining et al., 2020); double-deletion during wound healing has complete loss of vessel integrity, and leads to inflammatory bleeding (Bender et al., 2013). Blood loss to tissue from vasculature drives fibrin formation from fibrinogen through thrombin generation, consequently inhibiting leukocyte recruitment. This utilises platelets as a promising target for wound healing, however receptor-targeting is highly dependent on the inflammatory-stimuli and -location.

1.5 ITAM Receptors

Despite initiating platelet adhesion and activation, signals accompanying the vWF-GPIb-IX-V or integrin complexes promote complete platelet activation. ITAM receptors are distinct, as such characterised in their two tyrosine residues in sequence in the cytoplasmic tail; a conserved YxxI/$Lx_{(6\text{-}12)}$YxxI/L motif (Underhill and Goodridge, 2007). Uniquely, ITAM receptors have an ability to cluster, which increases the local concentrations of signalling molecules, and hence induces a strong platelet activation. These receptors were first found in a population of B and T cells (Reth, 1989, Underhill and Goodridge, 2007), but have now been described across all haematopoietic lineages. In human platelets, ITAM receptors GPVI, FcγRIIA and hemITAM receptor CLEC-2 are expressed, and signal through Syk family kinases and Syk (Hughes et al., 2010b). Mice are deficient in the genetic equivalent of human FcγRIIa (McKenzie et al., 1999).

1.5.1 GPVI

GPVI is a type 1 transmembrane protein exclusively expressed within the platelet/megakaryocyte lineage. In humans, there are 3000-4000 copies of GPVI on a platelet (Nieswandt and Watson, 2003, Best et al., 2003). It is a member within the superfamily of immunoglobulin receptors, and contains 2 immunoglobulin domains, alongside a mucin-like stalk region – a site with a high affinity for glycosylation, and a short cytoplasmic tail. It is associated with an FcR gamma-chain, and distinctly signals through this linked domain (Berlanga et al., 2002). Interestingly, GPVI was first discovered to be relevant to platelets through identification of patients with autoimmune thrombocytopaenia, lacking responsiveness to collagen-induced platelet activation (Sugiyama et al., 1987); other platelet-agonists induced normal activation and aggregation. Genetic deletion of platelet receptors in mice have been critical in establishing the contribution of platelet receptors to thrombus formation. The specificity of GPVI-expression to platelet/megakaryocyte lineage allows for a simple, global GPVI knockout to be generated (Lockyer et al., 2006). Mice lacking GPVI are born in mendelian ratio, and are indistinguishable to their littermate control; the mice present small, non-occlusive thrombi with mild bleeding phenotypes (Nieswandt et al., 2000, Nieswandt et al., 2001a, Kato et al., 2003a). Interestingly, a family in Chile has been discovered to be GPVI-deficient, and present a mild bleeding phenotype similar to the -deficient mice (Nagy et al., 2020). It is now accepted that GPVI is critical in thrombus formation at mid- and high-shear conditions.

GPVI activation by its ligands begins a cascade of events by an initial Src family kinase-mediated phosphorylation of the two tyrosine kinases observed in the cytoplasmic tail through a relevant FcRγ ITAM. Subsequently, the SH2 of Syk is recruited, whereby it partakes in a chain of auto- and trans-phosphorylation through SFK, causing the rapid phosphorylation of LAT, an adapter protein, which culminates various effector proteins such as phosphatidylinositol-3, 4, 5-trisphosphate (PIP3) (Rayes et al., 2019). This rapid and strong sequence of events climaxes in the phosphorylation of Phospholipase (PL)Cγ2, which can bind to the already phosphorylated LAT and PIP3 to instigate a positive feedback loop to further increase platelet activation. This is extended via second messenger enrolment of inositol 1, 4, 5-triphosphate (IP3) and 1, 2-diacylglycerol (DAG), causing intracellular release of Ca^{2+} from the platelet dense granules and protein kinase activation (Nieswandt and Watson, 2003, Watson et al., 2005, Rayes et al., 2019). This cascade of events induces the previously described dense and alpha granule release from intracellular stores, to activate platelet integrins α2β1 and αIIbβ3. Subsequent classical platelet remodelling occurs through actin reorganisation leading to platelet spreading, and hence platelet activation and aggregation.

A critical feature of GPVI is not only its strong activation of platelets, but also its ability to remain 'non-activated'. GPVI has been closely studied as a receptor which is able to limit its shedding to restrict GPVI-mediated platelet activation. Proteolytic cleavage of the GPVI ectodomain has demonstrated induction of GPVI signalling (Gardiner et al., 2004); shedding is induced by ligand binding. Interestingly, activation of ITAM receptors CLEC-2 and FcγRIIA also induces GPVI shedding. The strength, affinity and molarity of the ligand can regulate the rate of GPVI shedding,

which can be over minutes or even hours (Gardiner et al., 2007, Andrews et al., 2007). Overall, the ability of GPVI to signal is regulated through metalloproteinases of the disintegrin and metalloproteinase (ADAM) family, specifically ADAM10 and ADAM17 (Bender et al., 2010). ADAM17 contributes predominantly to GPIb and also to GPVI shedding; GPVI cleavage is more dominantly induced by ADAM10. Interestingly, soluble GPVI is found in the blood plasma of patients with thrombotic events, including ischaemic stroke, but also inflammatory events such as sepsis (Montague et al., 2018). G6b-B is a platelet protein which acts on GPVI to prevent its shedding through tyrosine phosphatases SHP1 and SHP2 in circulating platelets; prevention of GPVI shedding inhibits GPVI-induced platelet activation (Rayes et al., 2019). Shedding has also been shown to be induced through high shear stress, similar to GPIbα (Chen et al., 2015).

GPVI has previously been thought to be strongly activated through collagen, and binding to laminins, albeit much weaker than collagen. More recently, Fibrin has also been demonstrated to bind monomeric GPVI (Alshehri et al., 2015a, Poulter et al., 2017, Pallini et al., 2021). Collagen binds to dimeric, but not monomeric, GPVI through the D1 domain of the receptor's short chain, through a glycine-proline-hydroxyproline (GPO) sequence at micromolar affinity (Miura et al., 2002). Furthermore, fibrin and fibrinogen acts to promote thrombus growth and stabilisation through binding the GPVI D-region. However, fibrin activation of GPVI in physiological levels has recently been questioned, as inhibition of GPVI and GPVI-signalling did not alter platelet coverage of plasma- or blood-fibrin (Zhang et al., 2020). immobilised fibrinogen activates human, but not mouse platelets (Mangin et al., 2018).

Research suggests that GPVI promotes classical platelet functions, but also has roles in arthritis, macrophage activation and sepsis. Intriguingly, GPVI dysfunctionality has been described to be acquired in patients post-sepsis, whereby their washed platelets had no/reduced response to collagen *ex vivo* (Weiss et al., 2021).

1.5.2 FcγRIIA

FcγRIIA is another ITAM receptor, which consists of 2 extracellular IgG sites, alongside a transmembrane domain, and an ITAM-bound intracellular tail. Similar to GPVI, its crosslinking and activation and downstream phosphorylation of SFKs results in platelet activation. The ITAM receptor is a platelet activator, and has been shown to be crosslinked by a wide range of bacteria (Arman et al., 2014); low affinity binding of immunoglobulin G (IgG) induce receptor clustering and integrin engagement (Brandt et al., 1995, Reilly et al., 2001). FcγRIIA has also been demonstrated to co-stimulate platelets through its interaction with the GPIbα-IX-V complex-vWF interaction. Interestingly, unlike monomeric IgG, IgG-expressing immune complexes bind FcγRIIA with high affinity, and leads to systemic shock through serotonin (Cloutier et al., 2018). FcγRIIA has important roles beyond classical haemostasis and thrombosis, in immunomodulatory functions of platelet biology post-infection or trauma. Cloutier et al. demonstrated that post-immune complex-driven shock, ‘empty’ platelets (platelets lacking granules) were allowed to re-enter circulation so as not to initiate a secondary systemic shock in a FcγRIIA-dependent manner. The role of FcγRIIA has been well described to be critical in

leukocyte immunoregulation through binding and internalisation of IgG-expressing cells (Worth et al., 2006). The 5000 copies of human platelet-FcγRIIA is not translated to mice, hence a transgenic, humanised mouse is required to research the contribution of FcγRIIA to immunoregulation; the receptor has been demonstrated to bind and internalise IgG-expressing complexes, similar to leukocytes (Capel et al., 1994, Worth et al., 2006). Albeit deficient in mice, FcγRIIA is believed to be important in the inflammatory response through clearance of immune cell debris.

The third platelet-ITAM receptor, CLEC-2, differs in its activation and functions through a hemITAM domain **(Figure 1.4)**. CLEC-2 has major functions in both classical and non-classical platelet functions.

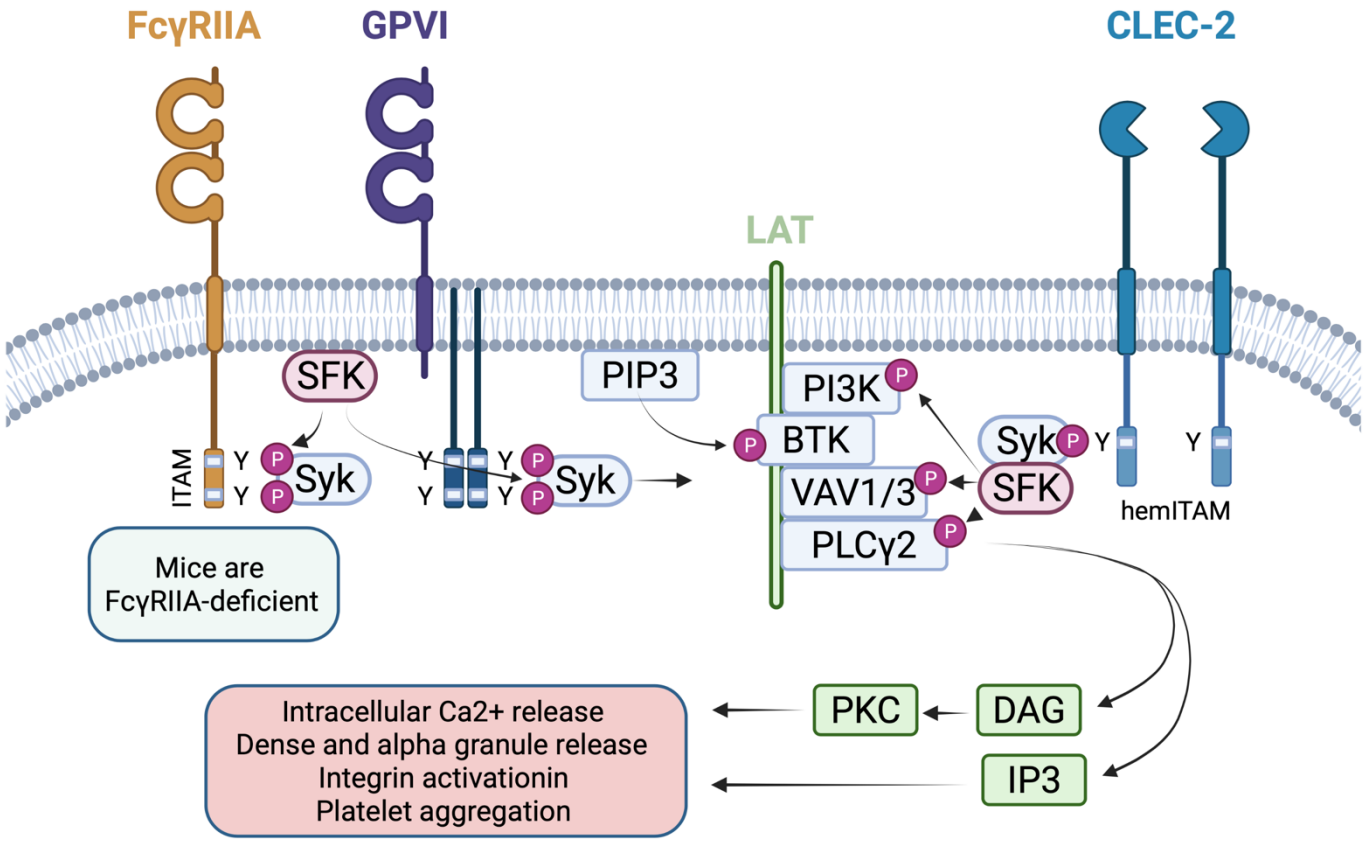

Figure 1.4 – ITAM and hemITAM platelet signalling pathways. Platelets receptors GPVI and FcγRIIA (ITAM), alongside CLEC-2 (hemITAM) signalling through a well conserved SFK-mediated Syk phosphorylation to initiate PLCγ2 phosphorylation, and subsequent platelet activation. ITAM receptors have both classical and non-classical platelet functions. Adapted from Rayes et al. (2019). *Figure made using BioRender.*

1.6 C-type Lectin-like receptor 2

1.6.1 CLEC-2 Structure

CLEC-2 is a type II transmembrane receptor with roles in thrombosis and haemostasis, but also highly critical roles in immunomodulation. The receptor contains 229 amino acids, and is primarily composed of an extracellular ligand-binding C-type lectin-like domain, a transmembrane helix and stalk region, and a short cytoplasmic tail. Classified by solving the crystal structure of the extracellular domain, CLEC-2 is a member of subgroup V of the C-type lectin superfamily (Watson et al., 2007); categorisation is dependent on the extracellular domain fold. The fold is reliant on the trio of disulphide bridges amid residues, presenting a glycosylation site. The stalk region has another glycosylation site, and may contain an additional disulphide bond, although this is under speculation (Watson et al., 2007, Martin et al., 2021). The CLEC-2-cytoplasmic tail of human CLEC-2 has a 33 amino acid sequence, and unlike GPVI and FcγRIIA, contains a single conserved YxxL motif – this is defined as a hemITAM. Upstream of the hemITAM contains amino acids required for CLEC-2 receptor activation upon ligand-activation (Hughes et al., 2013). Unfortunately, the structure of CLEC-2 in mice is yet to be published, but is predicted to be similar to human CLEC-2 due to positional conservation of the N-linked glycosylation sites and disulphide bonds with c-type lectin-like domain to an 84% similarity of sequence homology and residues between species (Martin et al., 2021).

1.6.2 CLEC-2 signalling and clustering

There is no evidence of the C-type lectin-like domain self-dimerising (Watson et al., 2009), however in the presence of the stalk region of CLEC-2, the receptor is presented as a dimer. Whilst CLEC-2 is distinct from GPVI and FcγRIIA in its single, hemITAM domain-bound cytoplasmic tail, they signal in a similar way utilising the Syk-SH2 domains to bind the duo of activated, phosphorylated receptors (Rayes et al., 2019). CLEC-2 activation by its ligands begins a cascade of events through SFK and SH2 of Syk is recruited, causing the rapid phosphorylation of LAT through auto- and trans-phosphorylation by SFK, and subsequently, PIP3 recruitment (Rayes et al., 2019). As with the other ITAM receptors, PLCγ2 is phosphorylated to instigate a positive feedback loop to further increase platelet activation and Ca^{2+} release in an IP3- and DAG-mediated fashion. This cascade induces dense and alpha granule release from intracellular stores, to activate platelet integrins α2β1 and αIIbβ3, to instigate classical platelet activation (**Figure 1.4**).

Interestingly, platelet aggregation through CLEC-2 has a characteristic 'lag' phase, which is proposed to be a result of necessary receptor clustering to induce aggregation (Pollitt et al., 2010). In fact, crosslinking CLEC-2 with its ligand, podoplanin, induces rapid clustering to the centre of the platelet, within 10nm of each other, to form a single unit (Pollitt et al., 2014). This mechanism occurs in a Syk/Src-dependant manner, but is also dependant on translocation of receptor-agonist complexes to the signalling region in the membrane (Martyanov et al., 2020).

1.6.3 CLEC-2 expression

CLEC-2, encoded by the C-type lectin domain family 1-member B (*Clec1b*), was first discovered in a C-type lectin genetic screen (Colonna et al., 2000), and subsequently found to be expressed on human and mouse platelets and megakaryocytes in the years later (Suzuki-Inoue et al., 2006, Suzuki-Inoue et al., 2007). More recently, the receptor has also been demonstrated to be active on a small sub-population of myeloid cells at low levels (Lowe et al., 2015). Interestingly, research prior to Lowe et al. suggested an assortment of CLEC-2 expression across haematopoietic lineages (Tang et al., 2010). An altered clone (17D9) of a CLEC-2 antibody demonstrated constitutive CLEC-2 expression in $CD11b^{hi}Gr\text{-}1^{hi}$ cells, splenic-B lymphocytes, -natural killer cells and -dendrites, bone marrow derived- and peripheral-dendrites (Kerrigan et al., 2009, Mourão-Sá et al., 2011). This particular clone also presented an upregulation of CLEC-2 in $F4/80^{+}$ macrophages post-thioglycolate-induced peritonitis, but not $CD11b^{hii}Gr\text{-}1^{hi}$ cells. It was concluded, using the **INU1** antibody clone, that CLEC-2 is expressed constitutively and exclusively on the **megakaryocyte lineage** and **$CD11b^{hi}Gr\text{-}1^{hi}$** cells myeloid cells. Remarkably, CLEC-2 is shown to be acquired, but not produced, on peripheral B lymphocytes from an unknown source (Lowe et al., 2015). This acquired CLEC-2 appears to be lost upon entrance to secondary lymphoid organ, which is intriguing, as it is well accepted that, unlike GPVI, CLEC-2 is not shed (Gitz et al., 2014). Lowe et al also confirmed that a unique domain of mesenteric lymph node (MLN)-activated dendritic cells can acquire CLEC-2.

1.7 CLEC-2 ligands

CLEC-2 is a powerful platelet-activating receptor, signalling in a Syk/Src-dependant manner through its hemITAM domain. Although CLEC-2-agonist binding induces platelet activation, the receptor has been demonstrated to have important roles in immunomodulation and inflammation driven thrombosis.

1.7.1 Rhodocytin

The first ligand to both mouse and human platelet-CLEC-2 to be discovered was a toxin from the venom of the Malayan pit viper (*Calloselasma rhodostoma*), rhodocytin. The non-glycosylated toxin is a powerful platelet activator, producing a so-called 'all or nothing' response, before inducing a classical lag phase and subsequent platelet aggregation. Interestingly, it was first thought that rhodocytin bound to platelet-activating receptors integrin $\alpha 2\beta 1$ and/or GPIb-IX-V (Huang et al., 1995), however rhodocytin-induced aggregation still occurred in response to deficiency in either receptor (Bergmeier et al., 2001, Suzuki-Inoue et al., 2001). Incidentally, CLEC-2 was discovered as the sole receptor to rhodocytin, which activated platelets in a Syk/Src-dependant manner (Suzuki-Inoue et al., 2006). Furthermore, deletion of PLCγ2 or LAT reduced rhodocytin-induced platelet aggregation, leading to identification of CLEC-2 as the first C-type lectin to signal in this way on platelets. The snake venom was shown to bind through its C and N termini to the 'non-canonical' binding face of CLEC-2 (Nagae et al., 2014). Whilst this binding site may appear unique, it is interestingly simultaneously utilised by the endogenous CLEC-2-ligand, podoplanin.

1.7.2 Podoplanin

Podoplanin is a type I, mucin-type transmembrane glycoprotein, which is relatively well conserved in a trans-cellular and -species fashion, with homologues in humans, mice and more. The protein's structure is yet to be solved, and sequential analysis does not reside similarities with known structures to date (Martin et al., 2021). It is made up of a heavily glycosylated extracellular region, a single transmembrane domain, and an extremely short, 9 amino acid long intracellular tail (Martín-Villar et al., 2005). In fact, despite the size of the tail, it is essential to the integrity of podoplanin expression in the cell membrane post-development, and inhibits its shedding (Haining et al., 2020). In spite of a lack of complete conservation of podoplanin, several residues have been identified to regulate its functionality. For example, motifs in the podoplanin intracellular are able to bind to ezrin and moesin of the ezrin, radixin, moesin (ERM) protein family – integral in actin cytoskeletal remodelling (Martín-Villar et al., 2006). The stalk is heavily glycosylated with up to 24 sites in human podoplanin (Christou et al., 2008), which accommodate its interaction with transmembrane ligands such as CD44 and CD9 **(Figure 1.5)**. The extracellular region is constructed of specific repeats of platelet aggregation-stimulating (PLAG) domains; PLAGs are short sequences of amino acids. To date, 4 PLAG domains critical in podoplanin-induced platelet activation have been identified, conserved within mammals, but with varying contribution to platelet activation – PLAG1 (29-EDDTETTG-36), PLAG2 (38-EGGVAMPG-45), PLAG3 (47-EDDVVTPG-54) and PLAG4 (81-EDLPT-85). Podoplain-CLEC-2 crosslinking has important implications in thromboinflammation and modulating the inflammatory response.

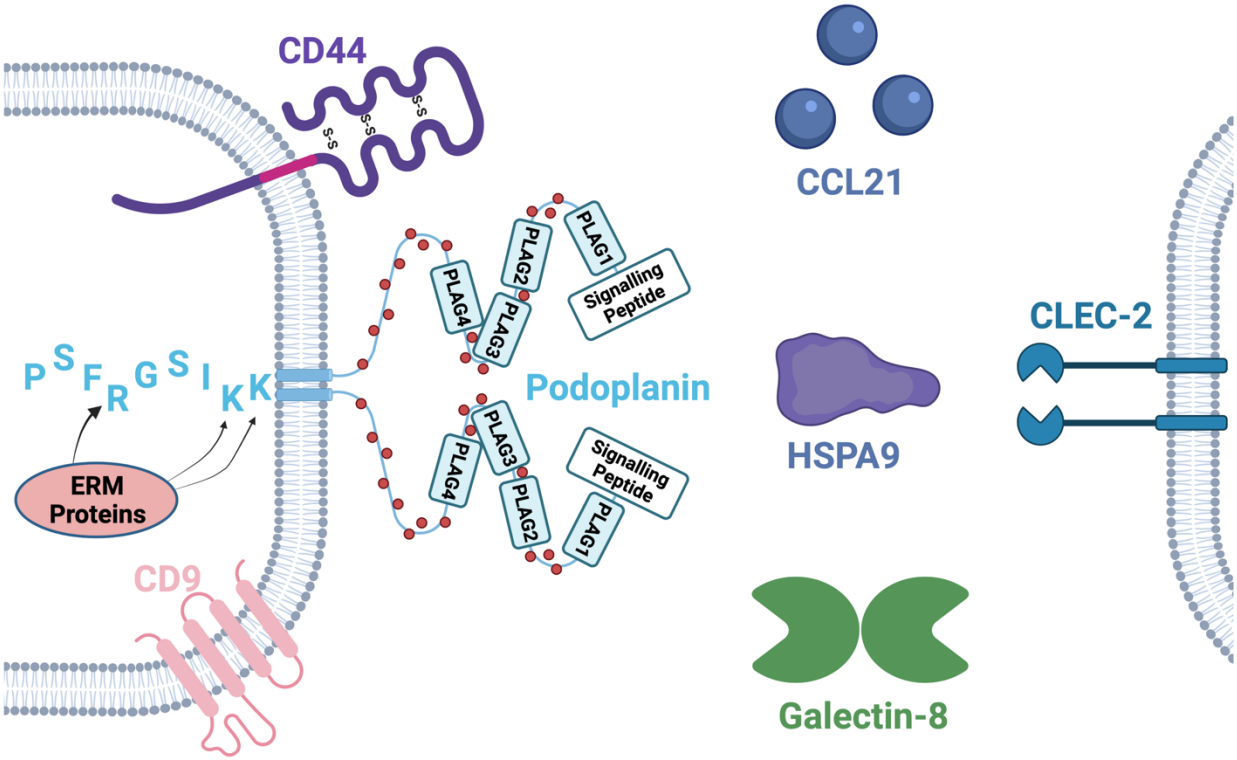

Figure 1.5 – The structure of podoplanin and its binding partners. Podoplanin contains a heavily glycosylated extracellular region with PLAG domains, a single transmembrane domain, and an extremely short, 9 amino acid long intracellular tail. Its structure accommodates binding to intracellular ligand (ERM proteins), transmembrane ligands (CD9 and CD44) and extracellular ligands (HSPA9, CCL21, Galectin-8 and CLEC-2). *Figure made using BioRender.*

The expression of podoplanin in physiology resides outside of vasculature. Due to the vast nature and multi-functionality of podoplanin, it had multiple names throughout its discovery in early literature. The protein has been described as antigen **E11** in lymphatic endothelial cells (LECs) (Wetterwald et al., 1996), **gp38** in fibroblast reticular cells and specialised epithelial cells (Farr et al., 1992), **T1a/rTI$_{40}$** in alveolar type I epithelial cells (Rishi et al., 1995), **PA2.26** unregulated on keratinocytes (Scholl et al., 1999), **OTS-8** upregulated on osteoblasts (Nose et al., 1990) and **aggrus**, a platelet-activating protein (Kato et al., 2003b). The name podoplanin was finally coined amongst its homologues for its expression on kidney podocytes, and its function of flattening (or 'planing') podocyte foot processes (Matsui et al., 1999). Podoplanin has also been shown to be upregulated on stromal and myeloid cells, monocytes and macrophages, alongside upregulation during cancer (Bourne et al., 2021).

Beyond binding to ERM proteins, the small podoplanin intracellular tail has further functions through signalling with its transmembrane co-ligands. **CD44** is a protein demonstrated to be critical in migration and adhesion in multiple cells types in humans and mice (Martín-Villar et al., 2010). Co-localisation and simultaneous upregulation of CD44 and podoplanin during cancer instigated discovery that these proteins bind in a glycosylation dependant-manner. Furthermore, a tumour suppressor, tetraspanin **CD9**, has been shown to mediate podoplanin-regulated cell migration; CD9 restricts podoplanin-induced migration (Nakazawa et al., 2008). Recently, podoplanin-induced fibroblast spreading and contractility has been shown to be CD44- and CD9-dependant (de Winde et al., 2021). These signalling pathways, although not entirely understood, have characterised podoplanin as a cell

migratory protein, presenting this phenotype in cancer, wound healing and leukocyte trafficking. Aside from CLEC-2, podoplanin has extracellular ligands Galectin-8, Heat shock protein (HSP)A-9 and CCL21. There are very few studies on the function of podoplanin expression on LECs, however podoplanin-**Galectin-8** interaction is believed to promote LEC adhesion (Cueni and Detmar, 2009). **HSPA-9** has been shown to be secreted by podoplanin-expressing oral squamous cell carcinomas, to crosslink cell surface-podoplanin and increase cell growth and invasiveness (Tsuneki et al., 2013). The function of podoplanin-CCL21 will be further discussed in Chapter 5.

Podoplanin was first discovered to bind to platelet-CLEC-2 due to the increasing description of platelet-contribution to cancer progression. In turn, there were further reports of tumour cell-induced platelet aggregation – specifically through aggrus (now podoplanin)-CLEC-2 interaction (Suzuki-Inoue et al., 2006). Similar to rhodocytin, podoplanin utilises the non-canonical binding face of CLEC-2 to crosslink the platelet-activating receptor. Crystallisation studies have revealed an interaction between a well conserved region of PLAG2 and 3 on podoplanin (EDXXXT/S) and four arginine regions of CLEC-2 (Nagae et al., 2014). The absence of podoplanin in healthy murine and human vasculature eludes a redundant or negligible role for the CLEC-2-podoplanin axis in classical haemostasis, however podoplanin upregulation during pathophysiological conditions, and platelet extravasation during inflammation to podoplanin-expressing tissue leads to inflammation driven thrombosis (thromboinflammation).

1.7.3 Hemin

Haem is an Fe^{3+} ion-containing protoporphyrin IX with an associated chloride ligand, which is rapidly converted to hemin immediately upon oxidisation. Hemin is integral to oxygen transfer in circulation by erythrocytes, making up a significant aspect of the 2 α- and β-subunits of haemoglobin (Hargrove et al., 1997). Despite its residency in the vasculature, hemin can be released post-trauma and is understood to be a strong platelet agonist, although the mechanism is not well understood. High dose hemin induces programmed platelet cell death induced by iron, coined ferroptosis. This is morphologically and biochemically dissimilar to classical apoptosis and necrosis. Ferroptosis occurs through the release of iron and free radicals mediated by haem-oxygenase-1 to induce hemin-facilitated lipid peroxidation and ROS generation (NaveenKumar et al., 2018, NaveenKumar et al., 2019). During pathophysiological conditions where haem is released from erythrocytes, hemin concentrations can range from 2 to 50 μM (Gouveia et al., 2017). Interestingly, thrombi are found at a range of severities of haemolytic disease, suggesting a mechanism distinct from ferroptosis regulating platelet activation at low-dose hemin. However, prior to this thesis, the mechanism through which hemin activates platelet at a low dose was yet to be discovered. This will be investigated in Chapter 4, whereby we demonstrate that hemin is a novel endogenous ligand to CLEC-2.

1.7.4 Other endogenous and exogenous ligands

Platelet-CLEC-2 has further ligands beyond CLEC-2 which are independent of classical ITAM signalling, and in fact do not utilise canonical platelet functions.

Human immunodeficiency virus **(HIV)-1** was previously associated with platelet interaction in infected platelets, however HIV-driven thrombosis has not been described. Interestingly, Chaipan et al. (2006) reported that alongside fellow lectin, dendritic cell-specific intracellular adhesion molecule 3-grabbing nonintegrin (DC-SIGN), platelet-CLEC-2 is able to bind and internalise HIV-1, without HIV-CLEC-2 induced platelet activation; kinases downstream of the hemITAM domain are unchanged.

There are further exogenous ligands beyond rhodocytin, such as diesel exhaust particles, the large polysaccharide, dextran sulfate and the complex polysaccharide, fucoidan (*murine exclusive*) (Alshehri et al., 2015b, Kardeby et al., 2019), but the functional relevance of these interactions is not known. CLEC-2-synthetic exogenous ligand binding is predominantly electrostatic; they have the ability to not only crosslink CLEC-2, but also to induce CLEC-2 receptor clustering on an individual platelet, as well as form a bridge between CLEC-2 and other membrane receptors (Rayes et al., 2019). These ligands also bind to GPVI, and facilitate formation of a CLEC-2-GPVI complex to induce platelet activation.

1.8 The innate immune system

Haematopoietic-derived innate immune cells are differentiated from a common myeloid progenitor cell **(Figure 1.1)**. Upon recognition of a pathogen, neutrophils, representing approximately 70% of peripheral blood leukocytes, are generally the first responders during infection and are recruited to the localised site. Following microbial challenge, a specialised subset of tissue-resident macrophages, such as

(but not limited to) perivascular macrophages which line blood vessels, are rapid responders. They are able to alert circulating neutrophils through the release of chemokines such as CXCL1, CXCL2, CCL2, CCL3 and CCL4, which are strong neutrophil chemoattractants to promote their extravasation (Kim and Luster, 2015). These strong, pro-inflammatory neutrophils are believed to have short life-span to avoid excessive inflammation (Prame Kumar et al., 2018).

Endothelial cells, which line and provide structure to vessels, upregulate the expression of 2 carbohydrate-binding c-type lectins upon inflammatory stimuli: P-selectin and E-selectin. Selectins recognise a host of glycan epitopes on a lactosamine backbone, specifically the selectin-binding terminal tetrasaccharide, sialyl Lewis X (sLe^x) (Munro et al., 1992). Human circulating leukocytes express sLe^x within protein scaffolds including PSGL-1, CD43 and CD44 (Woodman et al., 1998, Huo and Xia, 2009, McDonald and Kubes, 2015). sLe^x-expressing leukocytes form weak, transient bonds with the endothelium through selectins, as they are pushed along the vessel through a force generated by the flow of erythrocytes; as old bonds break, new ones are formed. Upon activation as a result of infection-, lesion- or sterile-induced inflammation, constitutively expressed neutrophil integrins, Mac-1 (CD11b/CD18) and lymphocyte function-associated antigen-1 (LFA-1; CD11a/CD18), undergo a conformational change to form strong bonds with selectins expressed on the endothelium to promote their firm adhesions and extravasation (Shamri et al., 2005, Hyun et al., 2019). Despite having the shortest half-life of the leukocytes (6 to 10 hours), they are equipped with potent anti-microbial activity and can quickly release NETs to ‘trap’ bacteria (McCracken and Allen, 2014).

Monocytes are derived from a common haematopoietic stem cell to neutrophils, and are generated and stored at low levels in bone marrow in response to growth-stimulating cytokines IL-3, macrophage-colony stimulating factor (M-CSF) and granular (G)M-CSF, and during inflammation, factor increasing monocytopoeisis; stores are also kept in the spleen (Wolf et al., 2019). Mice deficient in circulating neutrophils show a large reduction in migrating inflammatory monocytes at the site of infection (Soehnlein et al., 2008). Monocyte recruitment is delayed compared to neutrophils, but they persist for longer and can infiltrate tissues through their extravasation from vasculature, whereby they can differentiate into macrophages or dendritic cells. The ingestion of apoptotic neutrophils by inflammatory macrophages induces macrophage re-polarisation, which switches their phenotype from pro-inflammatory, to one with anti-inflammatory and repair properties (Poon et al., 2014), and resolving the inflammatory response.

1.8.1 Monocyte-derived macrophages

Monocytes released into circulation with a half-life of less than 24 hours (McCracken and Allen, 2014). Alongside their presence in circulation, they can also be released form storage in the subcapsular red pulp in the spleen under pathological conditions, such as ischemic myocardial infarction, which promotes wound repair (Italiani and Boraschi, 2014). In the absence of inflammation, monocytes are cleared by stromal macrophages in the bone marrow, spleen, or liver. Following inflammation or infection, monocytes are recruited to the inflammatory site by chemoattractants (such as CCL2), adhere to the activated endothelium and migrate into tissue where they differentiate into macrophages or dendritic cells *in situ*. During inflammation,

infiltrating monocytes replenish the existing pool of tissue-resident macrophages. The maintenance of the balance between monocytes and macrophages in tissue is predominantly preserved through stromal-derived M-CSF (Italiani and Boraschi, 2014).

1.8.2 Macrophage activation and polarisation

Macrophages have two classical sub-categories based on their inflammatory phenotype which each play specific roles in the immune response and its regulation. Activated M1 macrophages have pro-inflammatory properties, and alternatively M2 macrophages have anti-inflammatory, pro-resolution and repair properties (Italiani and Boraschi, 2014). M1 and M2 macrophages can differentiate from circulating monocytes which have migrated to tissue in response to infection. However, more recently, these categories have become accepted in the community to be a spectrum from pro- to anti-inflammatory phenotypes (Chávez-Galán et al., 2015). Macrophage differentiation from monocytes requires M-CSF binding to its receptor, colony-stimulating factor 1 receptor (CSF1R), a homodimeric type III receptor tyrosine kinase constituently expressed on monocytes and hematopoietic stem cells (Hamilton, 2008). Although the exact mechanisms have not been fully understood, the M-CSF-CSF1R axis is thought to initiate a downstream phosphorylation cascade, leading to monocyte cytoskeletal remodelling. Pyk2, a non-receptor tyrosine kinase, has been shown to phosphorylate focal adhesion proteins expressed on macrophages, and may be downstream of CSF1R (Pixley and Stanley, 2004, Pixley, 2012).

Tissue resident macrophages such liver Kupffer cells, peritoneal and alveolar macrophages, sufficiently reside and maintain a homeostatic balance in their respective tissue (the liver, peritoneum and lungs, respectively) at a steady state via self-proliferation (Hashimoto et al., 2013). Tissue macrophages have an inherent anti-inflammatory phenotype, due to enrichment in interleukin (IL)-10, but undergo an immediate morphological change upon infection. Alongside vascular permeability at the site of infection, various cytokines (Inflammatory – TNF-α, IL-6; immunoregulatory – IL-12, IFN-γ) and chemokines (Neutrophil recruitment – CXCL1, CXCL2, IL-1α) are produced to initiate a strong pro-inflammatory response (Dempsey et al., 2003). M2 macrophages have an anti-inflammatory phenotype, and express anti-inflammatory cytokines, chemokine and low quantities of organ damaging ROS and NO, unlike M1 macrophages (**Table 1)**.

Infiltrating M1 macrophages are produced in response to infection or inflammation. GM-CSF is a chemokine which is involved in the differentiation of pro-inflammatory macrophages. Unlike M-CSF, GM-CSF is differentially expressed in response to stimulation (such as infection), produced by many activated cell types including T-cells and the activated endothelium (Fleetwood et al., 2005). GM-CSF binds to the heterodimeric CSF2R receptor on monocytes (Hamilton, 2008). Activation of the GM-CSF receptor has been shown to initiate several pathways: the Janus kinase-signal transducer and activator of transcription (JAK-STAT) pathway, the mitogen-activated protein kinase (MAPK) pathway and the PI3K pathway leading to the upregulation of proinflammatory genes (Fleetwood et al., 2005). M1 macrophages have a pro-inflammatory phenotype and express CD80 and CD86, produce pro-inflammatory cytokines, chemokines and high quantities of ROS and NO (**Table 1)**.

Table 1 – M1 vs M2 macrophages

Macrophage	M1	M2
Activation	Classical	Alternative
Stimuli	IFNγ, LPS, GM-CSF	IL-10, IL-4, M-CSF, Immune Complexes
Inflammatory-cytokines	High levels	Low levels
Antigen presentation	Yes	No
ROS generation	High	Low
NO generation	Yes	No
Function	Pathogen clearing	Resolution and repair

ROS – reactive oxygen species. NO – Nitric oxide.

1.9 CLEC-2 beyond thrombosis and haemostasis

1.9.1 CLEC-2 functionality during development

CLEC-2 is understood to have only a minor or negligible role in haemostasis (Rayes et al., 2019, Rayes et al., 2020). That being said unlike GPVI-deficient patients identified in Chile, CLEC-2-deficient patients are yet to be described. It has been speculated that this may be because of the critical function CLEC-2 has in **lymphatic development** (Haining et al., 2020). The lymphatic vascular systems act in tandem to the blood vascular systems, which drain tissue interstitial fluid and supplies oxygen and nutrients to tissue, respectively. Removal of proteins, cells and

fluids accommodates their relocation back to circulation, which necessitates a distinct separation between the two vascular systems. Lymphatic development begins early in murine embryos (day 10), whereby the circulatory system is already functioning (Uhrin et al., 2010). LECs lining the vasculature are distinct from blood vasculature endothelial cells, through the expression of markers Lyve-1 and podoplanin (Alitalo and Carmeliet, 2002). That being said, deletion of Lyve-1 does not alter lymphatic development (Gale et al., 2007), but disruption of Syk resulted in a striking 'leaky' phenotype with non-distinct blood-lymphatic separation (Abtahian et al., 2003). Furthermore, the deletion of podoplanin or its receptor, CLEC-2, resulted in neonatal murine death (Uhrin et al., 2010, Suzuki-Inoue et al., 2010), associated with unsystematic, blood-filled lymphatics and severe oedema. Further studies have identified that deletion of signalling proteins downstream of CLEC-2, such as Syk, SLP-76 and PLCγ2 mimics the effect of CLEC-2-deletion (Bertozzi et al., 2010, Finney et al., 2012). Observations through numerous methods of CLEC-2 or podoplanin depletion throughout various phases of murine development have demonstrated that CLEC-2-function is critical to lymphatic structure throughout life. However, Haining et al. (2020) concluded podoplanin signalling was not essential post-development. This suggests that the CLEC-2-podoplanin axis could safely be targeted in other functions of CLEC-2 in pathophysiology.

Whilst CLEC-2 is not understood to have important roles in haemostasis, alongside lymphatic development, CLEC-2 has been demonstrated to have important thrombo-inflammatory and immunomodulatory functions. ITAM receptors GPVI and FcγRIIA have not been described to have significant functions pre-development.

1.9.2 CLEC-2 functionality post-development

1.9.2.1 Sterile inflammation

Deep vein thrombosis (DVT) is a thrombo-inflammatory disease which can lead to vascular occlusion and cardiovascular dysfunction. Commonly developed in muscle fascia of peripheral limbs, DVT has also been observed in the major central arteries. Interestingly, the location, but not size, of the thrombus formed dictates clinical prognosis. It is thought this regulates the severity of the resulting pulmonary embolism, which is a common cause of DVT-induced mortality (Stone et al., 2017). Furthermore, thrombi from DVT scars the endothelium, which in turn, promotes the possibility of recurrent DVT; 5 % of patients have a second episode within 1 year, and up to 10 % within 2 years (Farzamnia et al., 2011). DVT models are well, and easily reproduced in mice through ligation (stasis or stenosis) of the inferior vena cava. Platelets initially bind to the endothelium as singlets or minor aggregates in a GPIbα-dependant fashion (Li et al., 2020a) and neutrophils promote DVT through neutrophil extracellular trap release and inflammasomes assembly (Campos et al., 2021). Unlike wild type controls, P-selectin-deficient mice do not form neutrophil extracellular traps (NETs), and hence have reduced DVT-driven thrombus growth (Etulain et al., 2015, Stark et al., 2016). Interestingly, podoplanin (albeit from an unknown source) is observed to be upregulated immediately below the endothelium of the vena cava post-stenosis, and its abundance correlated with the severity of DVT in mice. Mice deficient in CLEC-2 were protected from thrombus formation, suggesting podoplanin-CLEC-2-dependant platelet activation in this model (Payne et al., 2017). Mechanical thrombectomy is most effective in immediate limitation of

DVT-induced organ damage, however treatment is commonly reliant on anti-coagulants such as warfarin, and anti-platelet drugs for effective long-term treatment to limit secondary incidents.

During experimental autoimmune encephalomyelitis (EAE), a murine model for brain inflammation disease such as **multiple sclerosis**, the podoplanin-CLEC-2 axis has been shown to be neuroprotective. EAE is induced through sensitisation to myelin antigens to induce an autoimmune response, and hence echoing the human inflammatory demyelinating disease (Constantinescu et al., 2011). Podoplanin has been shown to negatively regulate $CD4^+$ T cell and Th17 cell inflammatory response to post-EAE, whereby deletion of podoplanin or CLEC-2 increased EAE-induced inflammatory responses (Peters et al., 2015, Nylander et al., 2017).

Intriguingly, podoplanin overexpression on Th17 cells during **rheumatoid arthritis** further promoted, and not limited, the inflammatory response through the secretion of pro-inflammatory cytokine, IL-17 (Noack et al., 2016). Furthermore, CLEC-2 is reported to limit **liver recovery** post-toxic injury, through inhibiting neutrophil recruitment and subsequent TNF-α production necessary (Chauhan et al., 2020). This elucidates the diversity and complexity of the CLEC-2-podoplanin axis across disease types, and how it could be exploited therapeutically.

1.9.2.2 Infection-driven inflammation

As well as critical roles in inflammation-driven thrombosis, and regulating leukocyte function, platelets can interact with bacterial-, fungal- or viral-pathogens directly. As

earlier described, HIV can bind and be internalised by hemITAM receptor, CLEC-2 (also through DC-SIGN) (Chaipan et al., 2006). Also, previously mentioned ITAM receptor FcγRIIa has the ability to activate platelet through binding and internalisation of IgG-expressing cells, especially gram-negative and -positive bacteria (Watson et al., 2016). Interestingly, the platelet/megakaryocyte lineage express receptors for early immuno-recognition of pathogens, toll-like receptors (TLRs). TLR 1-6 and 9 have been described to regulate platelet function and activity in response to infection, through a 'sensory' mechanism, but not classical activation (Semple and Freedman, 2010).

Typhoid is a systemic, potentially fatal, infection induced by *Salmonella Typhimurium*. Whilst the systemic inflammatory response can lead to organ dysfunction, thrombosis is also observed in the spleen, liver and kidneys. Interestingly, the specialised liver macrophage Kupffer cell (alongside other macrophage sub-populations) is shown to upregulate podoplanin upon inflammatory stimuli – in this case *Salmonella* (Hitchcock et al., 2015). Deletion of haematopoietic-lineage podoplanin or platelet-CLEC-2 presented decrease in liver thrombi, without altering homeostasis (Hitchcock et al., 2015).

Sepsis is a complicated, dynamic disease which has a systemic inflammatory response syndrome (SIRS) and a compensatory anti-inflammatory response syndrome (CARS) phase. A blurred shift between these two indistinct stages leads to an exaggerated and sustained inflammatory response to stimuli, furthered through a cytokine storm and eventual sepsis-induced organ dysfunction. Platelet depletion has been shown to be detrimental during sepsis in mice (Rayes et al., 2017),

outlining not only the direct anti-microbial function of platelets, but also their immunomodulatory function during disease. Platelet reperfusions have been shown to limit pro-inflammatory cytokine concentration (such as TNF-α) in blood plasma to promote survival (Xiang et al., 2013). Platelet-CLEC-2, but not GPVI, has been demonstrated to be protective during murine sepsis models, through limiting the resultant cytokine storm. Furthermore, Platelet-CLEC-2 bound to podoplanin-expressing monocytes have been demonstrated to limit inflammation through complement inhibition, whereby CLEC-2 deletion in mice exacerbated liver dysfunction post-sepsis (Xie et al., 2020).

Acute respiratory distress syndrome (**ARDS**), the build-up of fluid in the alveolar space post-infection, currently has no therapeutic intervention. More recently, severe acute respiratory syndrome (SARS), and SARS-CoV-2 have been demonstrated to induce sever inflammatory responses, resulting in alveolar dysfunction and endothelial permeability (Khan, 2021). Podoplanin- or CLEC-2-deficienncy in haematopoietic cells and platelets, respectively, exacerbated lung function post intratracheal lipopolysaccharide instillations (Lax et al., 2017). As with sepsis and *Salmonella* infection, the CLEC-2-podoplanin axis has a protective immunomodulatory function in the lung through platelet-macrophage interaction.

There are distinct ITAM mechanisms mediating platelet-leukocyte interaction which can be exploited to limit thrombo-inflammatory and inflammatory disease. It is clear that different platelet-leukocyte interactions contribute with differential efficacy dependant on disease, location, and inflammatory microenvironment. Furthermore,

mechanisms mediating the cellular response upon podoplanin-CLEC-2 crosslinking is yet to be elucidated, and will be further explored in chapter 5.

1.10 Aims of the thesis

Antiplatelet therapy is an aged and overused strategy to limit thrombosis and thromboinflammation. Severe off-target effects with excess bleeding, and inflammatory-driven bleeding outline a clear desire for more specific targeting. HemITAM receptor, CLEC-2, has been well reported to play a minor role in hemostasis, and has simultaneously been shown to modulate various platelet thromboinflammatory and immunomodulatory functions. To date, investigation into platelet-CLEC-2 in the context of arterial thrombosis has been limited to antibody inhibition of the receptor, or its genetic depletion using a PF4-Cre recombinase mouse; once believed to be specific to the megakaryocyte lineage, has now been reported to expressed in various haematopoietic cells. Furthermore, the podoplanin-CLEC-2 axis is well reported to drive platelet activation and inflammation-driven thrombosis, albeit implications of CLEC-2-podplanin crosslinking on leukocyte function is yet to be elucidated. These queries will be addressed through:

1. Characterisation of a novel, megakaryocyte lineage-specific CLEC-2-deficient mouse using a GPIb-Cre recombinase model in arterial thrombosis by intravital microscopy and *ex vivo* flow adhesion models.

2. Investigation into the mechanism through which platelet-agonist, hemin, is able to bind and activate platelets in a mechanism distinct from ferroptosis.

This will be furthered using hemin-binding compound, hydroxychloroquine as a drug to limit thrombus growth post-ferric chloride induces thrombosis and visualised by intravital microscopy.

3. Studying the implications of CLEC-2 on leukocyte trafficking, specifically investigating podoplanin-expressing inflammatory macrophage migration and their fate in the resolution of inflammation.

Platelet receptor CLEC-2 have been demonstrated to have classical functions in platelet activation and aggregation through its known ligands, podoplanin and rhodocytin. Due to the absence of a known ligand in human vasculature during physiology, we hypothesise that platelet-CLEC-2 will not contribute to arterial thrombosis. We also hypothesise that there is a mechanism beyond ferroptosis through which hemin aggregates platelets. CLEC-2 has also been shown to have non-classical, immunomodulatory functions during inflammation. We hypothesise that crosslinking podoplanin-expressing inflammatory macrophages with CLEC-2 increase macrophage migratory activity.

Chapter 2

Methods and materials

2.1 Materials

All antibodies, secondary antibodies, agonists, inhibitors, and cytokines (including ELISAs) are outlined in **Table 2.1, 2.2, 2.3, 2.4 and 2.5**, respectively. Gifted reagents are outlined, and we thank Dr Farndale (university of Cambridge) and Dr Eble (University of Münster) for these.

Table 2.1 – Primary antibodies

Primary antibody (Clone number)	Host or conjugated fluorophore	Use: working concentration	Source
AnnexinV	APC	Whole Blood:1/100 ICF: 1/100	BD Pharmingen
CCL21 (polyclonal)	Biotinylated	IHF: 1/200	R&D
CD11b (m1/70)	Biotin	ICF: 1/100	eBioScience
CD11c (N418)	FITC	ICF: 1/100	eBioScience
CD16/32 (93)	Rat	ICF: 1/200	eBioScience
CD19 (eBio1D3)	APC-Cy7	ICF: 1/100	eBioScience
CD3 (145-2C11)	PE-Cy7	ICF: 1/100	eBioScience
CD4 (RM4-5)	PE-Cy5.5	ICF: 1/100	eBioScience
	PE	ICF: 1/100	invitrogen
	BV421	ICF: 1/100	BioLegend
CD41 (MWReg30)	FITC	ICF: 1/100	BioLegend
	Rat	ICF: 1/200 IHF:1/100	BD Bioscience
	DyLight488	*in vivo*: 01µg/kg	Emfret
CD44 (IM7)	AF647	ICF: 1/100	BioLegend

	Rat	ICF: 1/200	Tonbo Bioscience
CD45 (30-F11)	APC	ICF: 1/100	Tonbo Bioscience
	APC-Cy7	ICF: 1/100	Invitrogen
CD80 (16-10A1)	FITC	ICF: 1/100	Tonbo Bioscience
CD8a (53-6.7)	PE	ICF: 1/100	eBioScience
CLEC-2 (17D9)	FITC	ICF: 1/100	Internally sourced
Egr-2 (erongr2)	PE	ICF: 1/100	Invitrogen
ERM (Polyclonal)	Rabbit	ICF:1/50	Cell Signalling
	eFluor450	ICF: 1/100	eBioScience
F4/80 (BM8)	Rabbit	ICF: 1/200 IHF:1/100	abcam
	APC	ICF: 1/100	eBioScience
Fibrinogen (Polyclonal)	FITC	Whole Blood: 1/100	Dako
GPIb (Polyclonal) depleting antibody	Rat	*in vivo*: 0.1mg/kg	Emfret
iNOS (CXNFT)	AF488	ICF: 1/100	eBioScience
	Rat	ICF: 1/200	BioLegend
Ly6C (HK1.4)	PERCP-Cy5.5	ICF: 1/100	eBioScience
Ly6G (1A8)	V450	ICF: 1/100	BD Horizon
P-Selectin (RMP-1)	PE	Whole Blood: 1/100	BioLegend
PAC-1 (MA5-28564)	FITC	ICF: 1/100	Invitrogen
Pan Syk (4D10)	Mouse	WB: 1/200	Santa Cruz
Phospho-PLCγ2 (Y1217)	Rabbit	WB: 1/50	Cell Signalling
Phospho-Syk (pY525/6)	Rabbit	WB: 1/100	Cell Signalling
Phospho-PKA (RRXS*/T*)	Rabbit	WB: 1/100	Cell Signalling

PLC2γ2 (B-10)	Mouse	WB: 1/200	Santa Cruz
Podoplanin (8.1.1)	PE	ICF: 1/100	BioLegend
	Syrian Hamster	ICF: 1/200 IHF:1/100 WB:1/100 IP:1/100	eBioScience
SytoxRed	TxRed	ICF: 1/800	ThermoFisher
Ter119 (TER119)	Rat	ICF: 1/200	BioLegend
β-Actin (polyclonal)	Rabbit	WB: 1/500	abcam

Primary antibodies used for experiments involving whole blood, in vivo studies, immunocytofluorescent (ICF) imaging and analysis, immunohistofluorescent (IHF) imaging and western blotting (WB). Company-recommended immunoglobulin isotype controls for each antibody were used for flow cytometry analysis and immunofluorescent imaging as required.

Table 2.5 – Secondary antibodies and stains

Secondary antibody (Clone number)	Host or conjugated fluorophore	Use: working concentration	Source
Anti-biotin AF568	Streptavidin	ICF: 1/1000 IHF:1/200	BioLegend
Anti-biotin AF647	Streptavidin	ICF: 1/1000 IHF:1/200	BioLegend
Anti-hamster AF488	Goat	ICF: 1/1000 IHF:1/200	Invitrogen
Anti-hamster AF568	Goat	ICF: 1/1000 IHF:1/200	Invitrogen
Anti-hamster AF647	Goat	ICF: 1/1000 IHF:1/200	Invitrogen
Anti-hamster HRP	Goat	WB: 1/10000	Jackson Immuno Research
Anti-rabbit AF405	Goat	ICF: 1/1000 IHF:1/200	Invitrogen
Anti-rabbit AF488	Goat	ICF: 1/1000 IHF:1/200	Invitrogen

Anti-rabbit AF568	Goat	ICF: 1/1000 IHF:1/200	Invitrogen
Anti-rabbit AF647	Goat	ICF: 1/1000 IHF:1/200	Invitrogen
Anti-rabbit HRP	Donkey	WB: 1/10000	ThermoFisher
Anti-rat AF405	Goat	ICF: 1/1000 IHF:1/200	Invitrogen
Anti-rat AF488	Goat	ICF: 1/1000 IHF:1/200	Life Technology
DiOC6		Whole Blood: (2μM)	Sigma

Secondary antibodies used in experiments with immunocytofluorescent (ICF) imaging and analysis, immunohistofluorescent (IHF) imaging and western blotting (WB).

Table 2.6 - Agonists

Agonist	Target	Source
Collagen III	GPVI Integrins	Sigma
CRP	GPVI Integrins	Dr Farndale (University of Cambridge)
E Coli Bioparticles	Phagocytes	Incucyte
Hemin	TLR-4 CLEC-2	Frontier Scientific
Horm Collagen	GPVI Integrins	Takeda
Lipopolysaccharide O55:B5	TLR-4	Sigma
PAM3CSK4	TLR-1/2	InvivoGen
PGN-SA	TLR-2	InvivoGen
Rhodocytin	CLEC-2	Dr Eble (University of Münster)
Thrombin	PAR-1 (human) PAR-3 (mouse) PAR-4 (both)	Sigma
Zymosan	TLR-2/Dectin-1	InvivoGen

Table 2.7 - Inhibitors

Inhibitor	Target	Source
AEBSF	Serine Proteases	Calbiochem
Aprotinin	Serine Proteases	Sigma
AYP-1	CLEC-2	Internally generated
Cangrelor	P2Y12	The Medicines Company
Citrate	Calcium chelation	BD
EDTA	Calcium chelation	Acros Organics
Eptifibatide (Integrilin)	GPIIb/IIIa	GSK
Heparin	Thrombin Factor Xa	BD
Hydroxychloroquine	Heme	Sigma
Ibrutinib	BTK	Stratech Scientific
Leupeptin	Cysteine- serine-threonine-proteases	Enzo Life Science
NAC	Oxidants	Sigma
Pepstatin	Aspartyl Proteases	Sigma
PP2	Src Kinase	Tocris
PPACK	Thrombin	Cambridge Biosciences
Prostacyclin	PKA	Cayman Chemicals
PRT-060318	Syk Kinase	Portola Pharmaceuticals Inc.
Sodium Orthovanadate	Tyrosine phosphatases	Sigma
TAK-242	TLR-4	EMD Millipore Corp.

Table 2.8 – Cytokines, chemokines and ELISAs

Cytokines, chemokines and ELISAs	Source
Angiopoetin-2	R&D
C5a	PeproTech
CCL2	PeproTech
CCL21	PeproTech
CCL4	PeproTech
CCL5	PeproTech
CXCL1	PeproTech
CXCL2	PeproTech
GM-CSF	PeproTech
IL-10	PeproTech
IL-2	PeproTech
IL-6	PeproTech
Lactate dehydrogenase	abcam
M-CSF	PeproTech
MMP-9	R&D
TNF-α	PeproTech

2.1.1 Recombinant protein generation

Recombinant (murine and human) CLEC-2-Fc (rCLEC-2-Fc) was designed by cloning the extracellular domain region of CLEC-2 into mammalian expression vector pFuse-rIgG-Fc (InvivoGen), an Fc-fusion protein expression plasmid (rabbit). The construct was used to stable transfect HEK-293T cells by polyethylenimine (PEI) MAX 4K (PolySciences). The stable line was established by antibiotic, Zeocin (ThermoFisher), selection and functional screening. rCLEC2-Fc was then purified from the cell culture supernatant by protein-A affinity beads using chromatography, followed by validation utilising sodium dodecyl sulphate-polyacrylamide gel electrophoresis (SDS-PAGE) and western blotting to confirm expected molecular weights. Protein production, isolation and validation was performed in house and carried out my Mrs Ying Di (University of Birmingham).

2.1.2 Mice and genetic alterations

All murine *in vivo* experiments were performed in accordance with UK law (Animal Scientific Procedures Act 1986) with approval of the local ethics committee and UK Home Office approval under PPL P2E63AE7B, PP9677279 and P0E98D513 granted to the Birmingham Platelet Group (University of Birmingham). Wild type (WT) C57BL/6 mice (8-14 weeks; males and females) were purchased from Harlan Laboratories (Oxford, UK). Platelet-specific CLEC-2-deficient mice were generated using a lox-Cre recombination, by crossing mice on a C57BL/6 background with *CLEC1b* flox sites, with a mouse containing a novel, platelet-specific GPIbCre site (**CLEC1b$^{fl/fl}$GPIbCre**) (Nagy et al., 2019, Haining et al., 2020). Cre-negative, CLEC-2-floxed mice were used in Chapter 3 as littermate controls. GPVI-deficient mice

used in Chapter 3 had a global GPVI knockout (Lockyer et al., 2006), which were crossed with CLEC1b$^{fl/fl}$GPIbCre mice; Cre-negative mice had normal CLEC-2 expression, but deficient in GPVI (**GPVI-/- CLEC1b$^{fl/fl}$GPIbCre**). Throughout Chapter 5, haematopoietic-specific podoplanin-deficient mice were used, using lox-Cre recombination through Vav-iCre (**PDPN$^{fl/fl}$Vav-iCre**) (Siegemund et al., 2015). Cre-recombinase was confirmed by polymerase chain reaction and SDS-PAGE; genotyping performed by Dr Beata Grygielska. LifeAct-GFP mice were also used for fluorescent microscopy of F-Actin, tagged with green fluorescent protein (GFP) in Chapter 5 (Riedl et al., 2010).

2.1.3 Human Tissue and plaque processing

Pooled plaque homogenate material used in Chapter 3 was obtained through Dr Mark Thomas (UHB and SWBH NHS trust) from patients with atherosclerotic disease, and its use was approved by the North-West Haydock Research Ethics Committee (ref: 20/NW/0001). Homogenate was embedded in optical cutting temperature (OCT) gel, snap frozen in liquid nitrogen, and stored at -80 ^{o}C. 10 atherosclerotic plaque samples were collected from patients with coronary artery diseases who underwent surgery for high-grade carotid artery stenosis and stored at -80 °C after sampling. Cryo-sections were taken from each atherosclerotic plaque specimen for histological analysis purposes. Specimens were placed in a single 500 ml borosilicate glass laboratory reagent bottle immersed in liquid nitrogen (-160 °C) and crushed with glass mortar to a fine powder. 20 ml of PBS was then added to the glass containing atherosclerotic plaque homogenate, thawed at 37 °C for 3 min, transferred into 50 ml Falcon tube. Atherosclerotic plaque homogenate was sonicated (10 times, 5 s at 12 % amplitude) on ice for tissue dispersal, followed by centrifugation (500 *xg*, 1 min). The supernatant was retrieved, and protein

concentration measured with a standard bicinchoninic acid protein assay. Plaque material was then spotted onto a Maastricht flow chamber.

2.2 Human and murine blood

2.2.1 Human blood

Venous blood was drawn from healthy, consenting, drug-free volunteers using a 25-guage butterfly needle into 3.2 % trisodium citrate BD Vacutainers (Becton Dickinson, Oxford, UK). Ethical approval for use of human blood was granted by the University of Birmingham Research Ethics Committee to the Birmingham Platelet Group (ref: UHSP/22/BTVR/07).

2.2.2 Human washed platelet isolation

10 % acid citrate-dextrose (ACD) (Sigma) was added to the 9 ml blood-filled vacutainer within 1 h of drawing, before centrifugation at 200 *xg* for 20 min at room temperature (RT) with reduced brake deceleration (7/10) and a swinging bucket. The top section of plasma (PRP) was taken, avoiding erythrocytes and the buffy coat (leukocyte) layer. Potent platelet activation inhibitor, PGI_2, was added to the PRP at 1 µg/ml, prior to inversion and centrifugation at 1000 *xg* for 10 min at RT. The platelet pellet was then isolated by removal of the platelet-poor plasma (PPP), before pellet resuspension in 25 ml Modified Tyrode's buffer (1 mg/ml glucose anhydrous, pH 7.3) with 10 % ACD; supernatant was disposed of as biological waste. PGI_2 was again added (1 µg/ml) to the platelet mixture, before centrifugation at 1000 *xg* for 10

min at RT. Supernatant was discarded, and the pellet was resuspended to $2x10^8$ platelets per ml, counted using a Coulter Z2 Particle Count and Size Analyser (Beckman Coulter Ltd.). Platelets were rested for at least 30 min before use, to allow for PGI_2 degradation, as described (Suzuki-Inoue et al., 2006).

2.2.3 Murine blood

2.2.3.1 Blood collection for washed platelet preparation

Prior to blood collection, mice were anaesthetised using isofluorane in a scavenging chamber. Mice were then terminally narcosed using a nasal CO_2 mask, and the inferior vena cava (IVC) was isolated through the peritoneum. Blood was slowly drawn using a 25-gauge needle and 1 ml syringe, containing 10 % ACD. Once drawn, blood was added to a 1.5 ml Eppendorf containing 200 µl Modified Tyrode's buffer. Mice were terminally bled and confirmed by cervical dislocation.

2.2.3.2 Whole blood collection for flow adhesion

Blood was drawn as described in 2.2.3.1, however heparin (20 U/ml) was used as the anti-coagulant in the 1 ml syringe. 800 µl of heparinised blood was added to 400 µl Modified Tyrode's buffer with 2 mM calcium. Mice were terminally bled and confirmed by cervical dislocation.

2.2.3.3 Whole blood collection for daily platelet quantification

Mice were restrained using a restraint tube, minimising stress on the animal. The hind left or right leg (alternated daily) was extended and immobilised by pinching the thigh immediately above the knee. Hair around the area was clipped and skin was cleaned, before piercing the lateral saphenous vein using a 26-gauge needle. 50 µl blood was collected using a heparinised glass capillary tube into 5 µl ethylenediaminetetraacetic acid (EDTA; 0.5 M). Bleeding was ceased by gentle pressure.

2.2.3.4 Blood collection for inflammation assays

Prior to blood collection, mice were anaesthetised using isofluorane in a scavenging chamber. The mouse was held by the scruff, adding pressure to bulge the eye, inserting a heparinised capillary tube laterally. 200 µl blood was collected into 5 µl EDTA (0.5 M) in a 1.5 ml Eppendorf. Mice were terminally bled and confirmed by cervical dislocation. Cells in whole blood were quantified using an ABX Pentra 80 automated haematology analyser (HORIBA).

2.2.4 Murine washed platelet isolation

Blood collected in 2.2.3.1 was centrifuged using a Microcentaur (Sanyo) at 2,000 rotations per minute (rpm), for 5 min at RT. The PRP and upper third of erythrocytes was collected, and transferred to a new Eppendorf. PRP was further isolated from erythrocytes by centrifugation at 200 *xg* for 6 min at RT with reduced brake (7/10) in

a swinging bucket. PRP was collected, avoiding the erythrocytes, and added to a new Eppendorf. To increase yield, the remaining erythrocytes and small amount of PRP were washed with a further 200 µl Modified Tyrode's buffer, and centrifuged at 200 *xg* for 6 min at RT with reduced brake (7/10) in a swinging bucket. The PRP was again collected, alongside the platelet ring immediately above the erythrocytes, which was pooled with the first collected PRP; remaining cells were discarded. PRP was made up to 1 ml using Modified Tyrode's buffer, and treated with PGI_2 (1 µg/ml), before inversion and centrifugation at 1000 *xg* for 6 min at RT. Supernatant was discarded, and the platelet pellet was resuspended in 400 µl Modified Tyrode's buffer. Cells were normalised to $2x10^8$ platelets/ml, after quantification using a Coulter Z2 Particle Count and Size Analyser. Platelets were rested for at least 30 min before use, as described (Suzuki-Inoue et al., 2006).

2.3 Cell culture

2.3.1 General technique

Cell lines were cultured in a humidified incubator at 5 % CO2 and 37 ^oC. RAW264.7 cells and bone marrow-derived macrophages (BMDMs) were cultured in Dulbecco's Modified Eagle Medium (DMEM) (ThermoFisher), and L929 cells were cultured in Roswell Park Memorial Institute Medium (RPMI)-1640 (ThermoFisher); both (complete) mediums contained 10 % heat-inactivated foetal bovine serum (FBS), 1 % penicillin-streptococcus (Sigma) and 2.5 mM L-Glutamine (Sigma). Human umbilical vein endothelial cells (HUVECs; Promocell) were cultured using Endothelial Cell Growth Media (ECGM; Promocell) with 1 % penicillin-streptococcus. HUVECs

were cultured up to passage 6. All cells were passaged (1:4) using Trypsin-EDTA solution at 80 % confluency, and media was changed every 2-3 days.

2.3.2 Bone marrow isolation from mice

Wild type mice were culled by cervical dislocation, and the hind legs were excised above the pelvic-hip joint. The tibia was isolated from the femur by bending around the knee, dislocating and cutting through the joint. Skin was peeled from the muscle, and muscle was cleaned from the bones using scissors and sterile paper towels. Bones were sterilised using sterile 70 % ethanol solution, and were cut on one end of the femur and tibia under a laminar flow hood. Both bones were added to a 0.6 ml Eppendorf tube, which has been punctured at its bottom using a 21-guage needle. The bone-containing 0.6 ml Eppendorf tube was inserted to a 1.5 ml Eppendorf containing 100 µl DMEM. Eppendorfs were centrifugated at 1000 *xg* for 10 s (RT) to flush bone marrow from the femur and tibia. Supernatant was removed, and cells were used for experimentation.

2.3.3 Macrophage media preparation from fibroblasts

Murine fibroblast cell line, L929, were cultured in an T175 cm^2 cell culture flask until complete confluence was achieved. Upon confluence, cells were cultured in 50 ml of complete DMEM for 7 days, which was then removed and centrifugated at 500 xg for 5 min (RT) and filtered through a 0.22 µm sterile filter, before storage in 10 ml aliquots at -20 ^oC. This technique generates a rich solution containing M-CSF and IL-3, promoting macrophage differentiation (Weischenfeldt and Porse, 2008).

2.3.4 BMDM generation

Complete macrophage media was created using complete DMEM, supplemented with 20 % L929 supernatant. The bone marrow pellet (described in 2.3.2) was resuspended in 20 ml complete macrophage media, and cells were seeded in a 15 cm petri dish for 7 days to generate BMDMs. On day 5, cells were supplemented with 5 ml of complete macrophage media. On day 7, cell media was removed and cells were treated with 10 ml ice-cold phosphate buffered saline (PBS)-ethylenediaminetetraacetic acid (EDTA; 1 mM), before gentle agitation using a cell scraper.

2.4 Molecular biology – qPCR

Cells were incubated in 1 ml TRIzol (TRI-reagent, Invitrogen) in 6-well plates, before 200 µl chloroform was added, collected in a 1.5 ml Eppendorf, shaken, and incubated at RT for 10 min before centrifugation (12000 *xg* for 15 min at 4 ^{o}C). The upper, cleared fraction was taken and mixed with 500µl of isopropanol. This was shaken for 15 s and incubated at RT for 10 min before centrifugation (12000 *xg* for 10 min at 4 ^{o}C). The supernatant was drained, and the resultant pellet was washed in 75 % ethanol, before brief vortex and centrifugation (7500 *xg* for 5 min at 4 ^{o}C). The supernatant was removed, and the pellet was air-dried before being suspended in 20 µl nuclease-free water. Ribonucleic acid (RNA) was quantified using Nanodrop 2000 (ThermoFisher) and complementary DNA was transcribed from messenger RNA using PrimeScript (Clontech, Takara. 3 µl cDNA was added to 5 µl PCR-grade

water, 10 µl Lightcycler 480 SYBR Green 1 mastermix (Roche) and 2 µl murine podoplanin primers (Sino Biological). GAPDH (Origene) was used as a housekeeping control for $\Delta\Delta$CT calculations, which has been shown to be consistently expressed across multiple conditions in RAW264.7 cells (Bao et al., 2019). Using a PCR thermocycler, the following program was performed: pre-incubation (5 min, 95 ^{o}C), amplification (10 s, 95 ^{o}C; 10 s, 60 ^{o}C; 10 s, 72 ^{o}C), melting curve (5 s, 95 ^{o}C; 1 min, 65 ^{o}C) and cooling (30 s, 40 ^{o}C). PCRs were performed in triplicate, and a $\Delta\Delta$CT value was calculated and normalised to unstimulated control (Livak and Schmittgen, 2001).

2.5 Cell biology

2.5.1 Western blotting

Cells in 6-well plates were washed in PBS, before incubation in 100 µl ice-cold NP-40 cell lysis buffer (300 mM NaCl, 20 mM Tris, 2 mM EGTA, 2 mM EDTA, 2 % NP-40), supplemented with protease inhibitors 2.5 mM Na_3VO_4, 100 µg/ml AEBSF, 5 µg/ml leupeptin, 5 µg/ml aprotinin and 0.5 µg/ml pepstatin (pH 7.4). Protein concentration was estimated by Bradford reagent (Biorad) using bovine serum albumin (BSA) at known concentrations (1.5-0.03 mg/ml) as a standard curve, and absorbance was calculated in duplicate (750 nm). Protein electrophoresis of 20 µg protein was performed in Tris-Glycine SDS running buffer (Biorad) alongside a molecular weight ladder (ThermoFisher). Protein was transferred to a PVDF membrane by electroblotting, before blocking with 5 % BSA-Tris-buffered saline with 0.1 % Tween 20 (TBS-T) for 1 h at RT, and incubating in primary antibody (Table

1.1) overnight at 4 °C. The membrane was thrice washed, before incubation in secondary antibody (Table 2.2) 1 h at RT, before thrice washing and revealing by ECL Western Blotting Substrate (ThermoFisher) and imaging by an Odyssey Imaging System (LI-COR Biosciences).

2.5.2 Immunoprecipitation

Immunoprecipitation was performed in whole cell lysate using anti-podoplanin antibody (clone 8.1.1) bound to protein A-sepharose beads, as described by Krishnan et al. (2013). 400 µg protein (extracted and quantified as in 2.5.1), was precleared with 30 µl beads in 1 ml NP-40 lysis buffer for 1 h at 4 °C in rotation. Supernatant was taken post-centrifugation for 15 min at 1000 *xg* at 4 °C, and added to 30 µl beads containing 2 µg anti-podoplanin antibody. Mixture was incubated overnight at 4 °C, before centrifugation for 15 min at 1000 *xg* at 4 °C. Supernatant was discarded and beads were thrice washed in ice-cold NP-40 lysis buffer. Immunoprecipitated protein was quantified by western blot (2.5.1).

2.5.3 Flow cytometry

Cells were scraped in ice-cold 1ml PBS-EDTA (1mM), and pelleted by centrifugation (500 *xg*, 5 min at RT) in polystyrene test tubes. Major macrophage Fc-receptors were blocked (anti-CD16/CD32, 1:100) in 100µl 10 % mouse serum-PBS for 1 h at 4 °C, before washing in 1 ml PBS and centrifugation (500 *xg*, 5 min at RT) and resuspension in 100 µl primary antibody mix (Table 2.1) for 30 min at 4 °C. Cells were washed in 1 ml PBS and centrifugated (500 *xg*, 5 min at RT), before

resuspension in 200 µl PBS. Receptor surface expression was assessed by an Accuri C6 Plus flow cytometry (BD Bioscience, Oxford, UK), a CyAn ADP Analyzer (Beckman) or a CytoFLEX Flow Cytometer (Beckman). Median fluorescence intensity (MFI) or percentage of positive expression compared to isotype control was quantified using FlowJo v8. Fluorescence compensation was calculated using either fluorescence beads, or cells with a known positive protein marker for each colour.

2.5.4 Cytokine and chemokine quantification

Cytokines and chemokines were taken from cell media supernatant, or peritoneal lavage, and quantified by sandwich-enzyme-linked immunosorbent assay (ELISA; Peprotech). Supernatant/peritoneal lavage fluid (PLF) was aliquoted to avoid repetitive freeze-thawing. 96-well, half area microplates were coated with capture antibodies (1 µg/ml) in 50 µl PBS overnight (RT). Plates were thrice washed in TBS-T, and supernatant/PLF was added to the plate, alongside a standard curve (2000 – 31.25 pg/ml) – all in duplicate for 1 h at 37 ^{o}C. The plate was thrice washed in TBS-T, and incubated with an avidin-bound detection antibody (1 µg/ml) for 1 h 37 ^{o}C. The plate was again thrice washed in TBS-T, and incubated with HRP-conjugated streptavidin at 1:4000 (ThermoFisher) for 30 min at RT. Cells were thrice washed with TBS-T, before treatment with 100 µl ABTS (PeproTech), and absorbance quantification after 15 min incubation at 405 nm by a Microplate Reader (ThermoFisher).

2.5.5 Surface plasma resonance and absorbance spectroscopy

Real-time interaction profiles were obtained after injection of increasing concentrations of hemin (19.5–625 nM) over recombinant CLEC-2-Fc immobilized on a CM5 sensor chip (Cytiva) to calculate **plasma surface resonance**. The association and dissociation phases were followed for 5 min, each. Data was quantified using a Langmuir global analyses model. **UV-vis absorbance spectroscopy** was performed using differential spectra generated of CLEC-2-Fc (2 μM) with increasing concentrations of hemin (0.5–16 μM). The differential spectra were obtained after subtraction of the spectra of hemin at a given concentration from the spectra of the same concentration of hemin in the presence of the protein. The measurements were done at 25 °C in optical cell with 10 mm light path. Experimentation and quantification of surface plasma resonance and absorbance spectroscopy was performed by Dr Jordan Dimitrov (University of Paris).

2.6 Immunostaining

2.6.1 Immunohistochemistry

Paraffin embedding and sectioning was performed on murine lungs, livers and kidneys post-endotoxemia. Organs were washed in ice-cold PBS, before being fixed overnight in 4 % paraformaldehyde (PFA) overnight. Organs were dehydrated using increasing concentrations of ethanol for 30 min each (70 %, 80 %, 90 % and 100 %) followed by 2 h Histoclear (National Diagnostics). Organs were paraffin embedded,

and oriented and mounted onto blocks. Tissues were sectioned at 6 microns and collected onto polylysine adhesion slides (ThermoFisher).

For antibody staining, sections were de-waxed and rehydrated in xylene (twice for 2 min) and then ethanol (100 %, 90 %, 75 %, 50 %, 30 %; 30 s each) before water (5 min). Antigens were retrieved in citrate buffer for 15 min in the microwave, cooled and washed in PBS-T. Samples were blocked with 3 % endogenous peroxidase (Dako) for 10 min, before blocking in 3 % BSA-PBS-T for 1 h (RT). Primary antibody was incubated in block solution overnight at 4 ^{o}C, before thrice washing in PBS-T, and incubation with a biotinylated secondary antibody in block (30 min at RT). Sections were incubated with phosphatase-conjugated streptavidin for 30 min at RT, before thrice washing with PBS-T. IMPACT DAB substrate chromogen solution (VectorLab) was added, and observed by a brightfield microscope, and was rinsed with water once revealed. Slides were dehydrated 3 min each in ethanol (75 %, 90 %, 100 %), before xylene overnight. Slides were mounted using Hydromount (National Diagnostics) and imaged using an Axioscan 7 Slide Scanner Microscope (Zeiss).

2.6.2 Immunohistofluorescent staining

Murine lungs, livers and kidneys were snap frozen in OCT post-endotoxemia using liquid nitrogen. Lungs were not inflated, and the kidney capsule was removed. Organs were sectioned at 6 microns, and stored at -80 ^{o}C. Slides were allowed to dry for 30 min, circled using a hydrophobic pen and washed in PBS-T (5 min). Slides were incubated in ammonium chloride (20 mM) to quench auto-fluorescence for 15

min, RT. After a 5 min PBS-T wash, sections were 1 % BSA blocked with 5 % goat serum for 1 h at RT. Primary antibody (Table 2.1) was incubated overnight at 4 ^{o}C, before thrice washing in PBS-T and a 1 h incubation with a secondary antibody (Table 2.2). Slides were thrice washed before mounting using Hydromount and imaged using an Axioscan 7 Slide Scanner Microscope.

2.7 Microscopy

2.7.1 Confocal microscopy

Cells were cultured on sterilised, 13 mm round glass coverslips (ThermoFisher), and washed with PBS post-experimentation. Cells were fixed in 4 % PFA for 10 min, before blocking in 1 % BSA-PBS. Cells were incubated in primary antibody in block buffer overnight at 4 ^{o}C, before thrice washing with PBS-T, and incubating with secondary antibody for 1 h at RT. Coverslips were flat-mounted using Hydromount, and imaged using a Zeiss LSM780 confocal microscope (Zeiss). Images were acquired using an inverted confocal microscope (Zeiss LSM 780) using a 1.49 NA 64X oil- immersion objective. Argon-ion lasers 405 nm, 457-514 nm and 561 nm were used to excite fluorophores. Z-stack images were acquired, and were compressed upon analysis for maximum fluorescence intensity.

2.7.2 diSPIM microscopy

BMDMs derived from LifeAct-GFP mice were allowed to spread on collagen-coated #1.5H slides. Murine platelets were stained using CellMask Deep Red (Invitrogen).

Cells were imaged in phenol red free DMEM supplemented with 2 % FBS at 37 °C and 5 % CO_2. Fluorescence was acquired on a Marianas LightSheet (Intelligent Imaging Innovations, Denver, CO, USA), a dual inverted Selective Plane Illumination Microscope (diSPIM) fitted with two perpendicular 0.8 NA, 40x water immersion objectives and ORCA-Flash4.0 V3 sCMOS cameras (Hamamatsu), driven by SlideBook software (Intelligent Imaging Innovations). Volumes were captured every minute in slice scan mode, with a step size of 0.5 µm and 488 nm and 640 nm excitation wavelengths. Time lapse images of maximal intensity projections were visualised using Arivis. Images were acquired by Dr Malou Zuidscherwoude (University of Birmingham).

2.7.3 SIM microscopy

BMDMs were allowed to spread on collagen-coated #1.5H glass coverslips for 2 h. Cells were then fixed in prewarmed 4 % PFA in PEM buffer (0.8M PIPES, 4 mM EGTA, 1 mM $MgSO_4$) for 15 min, before autofluorescence quenching by ammonium chloride (50 mM), and permeabilisation by 0.1 % Triton X-100 (10 min, RT). Cells were blocked in 1 % BSA, 2 % goat serum in PBS for 1h (RT), before incubating with primary antibody overnight (Table 2.1) at 4 ^{o}C. Cells were thrice washed, and incubated with secondary antibodies (Table 2.2) for 1 h at RT. Coverslips were flat-mounted with VECTASHIELD antifade mounting medium (Vector Labs). SIM imaging was performed on a Nikon N-SIM-S system with Nikon Perfect Focus in 3-D SIM mode, using a Nikon 1.49x Na oil Objective, Chroma ET525/50m and ET595/50m excitation filters, and an ORCA Flash4.0 sCMOS camera (Hamamatsu). Illumination was with 488 nm and 561 nm lasers. Capture and subsequent

reconstruction was performed in Nikon NIS Elements 5 – stack and a maximum score of less than 8 were discarded. Composite Images were visualised and adjusted for figures using ImageJ. Images were acquired by Miss Evelyn Garlick (University of Birmingham).

2.7.4 Electron microscopy

BMDMs were allowed to spread on collagen-coated #1.5H glass coverslips for 1 h in the presence or absence of platelets. Cells were PBS washed, before fixation in 2.5 % glutaraldehyde. Cells were treated with osmium tetroxide, and imaged using a Philips XL30 FEG ESEM in high vacuum mode at 20 kV and 2500 x magnification.

2.7.5 Microscopy analysis

Images acquired were obtained and exported using Zeiss Zen Black microscope software and analysed using Image J software. Macros were constructed using ImageJ to quantify cell size and circularity.

2.8 Functional biology

2.8.1 Platelet lumi-aggregometry

Washed platelets (2.2.2 and 2.2.3.1) normalised at $2x10^8$ /ml were incubated at 37 ^oC for 2 min, before recalcification with $CaCl_2$ (2 nM), inhibitor treatment (1:100) and incubating for 1 min during stirring conditions at 1200 rpm using a Chrono-Log Lumi-

aggregometer (Havertown). Platelets were then stimulated with an agonist (1:100) and measurement began. Percentage of aggregation was quantified by measurement of final aggregation after 6 min (unless otherwise stated) compared to starting point, relative to the baseline. In some cases, inhibitor treatment was for longer time periods which are outlined in relevant legends.

2.8.2 Flow adhesion assays

µ-slide VI 0.1 and 0.4 (Ibidi) – Whole blood was flown over Horm collagen (surfaces coated with 100 µg/ml) or HUVECs through a µ-slide VI 0.1 or 0.4, respectively. For HUVEC seeding, flow chambers were coated with 0.5 % pre-warmed gelatin for 1 h, before washing with sterile PBS. HUVECs were cultured to complete confluence in a T75 cell culture flask, pelleted and resuspended in 200 µl ECGM. 30 µl of cell suspension was added to each of the channels in the chamber, and allowed to adhere for 1 h. Cells were washed and allowed to culture overnight, before 1 % BSA-PBS blocking. Blood was perfused at arterial flow rate (1000 s^{-1}) and shear stress (10 dyn.s/cm^2) unless specified. Blood was treated with 2 µM DioC6 (ThermoFisher, USA) and 40 µM PPACK. **Maastricht flow chamber** – Whole blood was flown over Horm collagen (surfaces coated with 100 µg/ml; Nycomed Pharma GmbH), Human collagen III (Sigma Aldrich), or pooled plaque homogenate (500 µg/ml) through a Maastricht parallel flow chamber at arterial shear rate (1000 /s). Blood was treated with 40 µM PPACK and recalcified. P-Selectin (anti-CD62P, BioLegend), active αIIbβ3 (anti-Fibrinogen, Dako), phosphatidylinositol (PS)-exposure (Annexin V, ThermoFisher) and brightfield images were taken post-flow. Images were acquired

using an EVOS M5000 Imaging system by fluorescence and transmitted light imaging (20X lens). Images were analyzed using ImageJ (van Geffen et al., 2019).

2.8.3 Macrophage chemotaxis migration

Lipopolysaccharide (LPS; O55:B5)-treated (1 µg/ml, 24 h) BMDM were incubated for 1 h with rCLEC-2-Fc (10 µg/ml) or IgG isotype (10 µg/ml). Cells were scraped and seeded onto the upper layer of an 8µm pore polycarbonate inserts transwell (Corning) (Boyden, 1962). Migration of BMDM towards CCL21 (30 ng/ml) was assessed after 4 h at 37 ^{o}C. The top layer of the insert was scraped, and cells on the lower side were fixed with 4 % PFA for 10 min. Cells were immunostained with Hoechst 33342 (1:10000) for 10 min, before mounting with Hydromount, and migrated cell nuclei counted by using an EVOS M5000 Imaging system.

2.8.4 Macrophage wound healing

Confluent, LPS-treated BMDM (1 µg/ml, 24 h were washed and scratched using a 96-pin 800 µm-wide mechanical WoundMaker. Cells were thrice washed (until no cells were visible in the wound) and were then co-cultured in the absence or presence of platelets or recombinant murine CLEC-2-Fc for 96 h at 37 ^{o}C. Cells were imaged every 2 h using an Incucyte SX-5 Live-Cell microscope (Satorius). Wound closure was quantified using ImageJ, and calculated as percentage of closure at each timepoint by:

$$100 - \left(\frac{wound\ size}{wound\ size\ t = 0} \right)$$

2.8.5 Phagocytosis assay

LPS-treated BMDM were incubated in the absence or presence of platelets for 1 h. pH sensitive, AlexaFluor488-conjugated, *Escherichia Coli* covered (K-12 strain) BioParticles ($3x10^6$ beads/condition) were added for an additional 4 h at 37 ^oC. Total green fluorescence was quantified by a mask generated by Incucyte Systems on images taken using an Incucyte SX-5 Live-Cell microscope (Satorius).

2.9 *In vivo* murine assays

2.9.1 Lipopolysaccharide-induced peritonitis

Male and female mice (20-25 g) were challenged with LPS (O55:B5) at 10 mg/kg in 200 µl sterile saline solution for 22 h (Frimodt-Møller, 1993). After 18 h, mice were treated with 100 µg recombinant murine CLEC-2-Fc or IgG isotype control for 4 h (**Figure 2**). Mice were monitored for clinical severity throughout. After 22 h, mice were anaesthetised by isofluorane, and bled retro-orbitally (2.2.3.4). A peritoneal lavage was then performed by infecting 2 ml of ice-cold PBS-EDTA (1 mM) into the peritoneum, and retrieving 1 ml after 1 min. Organs were then taken, and prepared for either immunostaining (2.6) or for flow cytometry (2.5.3) after homogenisation using a 25-guage needle, and filtration using a 22-micron filter. Mesenteric lymph nodes were taken and prepared for either flow cytometry, immunostaining, or culture *ex vivo* after homogenisation, and subsequent stimulation with low-dose LPS (10 ng/ml).

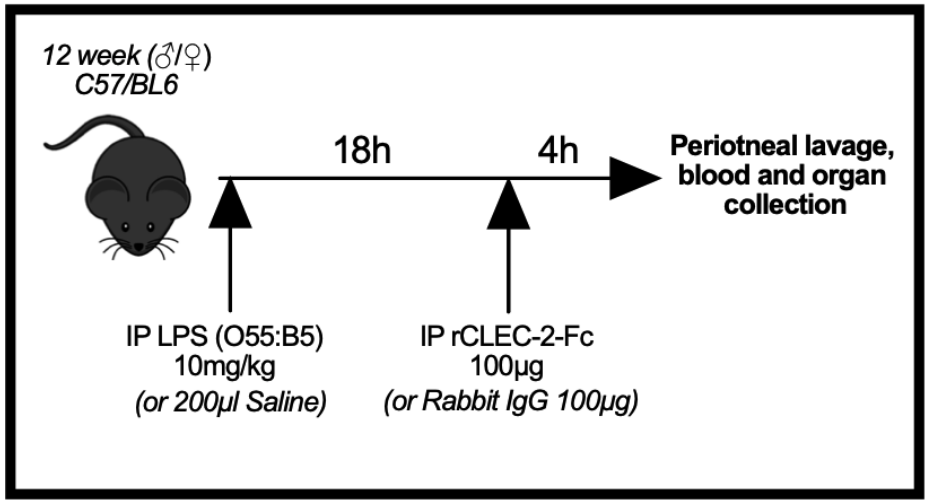

Figure 2 – Methodology to induce peritonitis by LPS. Mice were challenged with LPS (10 mg/kg) for 18 h before treatment with rCLEC-2-Fc or IgG Isotype control (100 µg) for 4 h. Mice were culled 22h post-challenge and tissue was processed.

2.9.2 in vivo thrombosis models

2.9.2.1 Preparation for surgery

Mice (20-25 g) were anaesthetised intraperitoneally by avertin (*2,2,2-Tribromoethanol*; Sigma), before securing to a heated pad and performing a tracheostomy using trachea tubing secured by suture. An anti-GP1bβ X488 at 0.1 µg/kg (Emfret, Germany) was administered for platelet detection by cannulation of the jugular vein. Further anaesthetic was maintained via the cannula throughout surgery.

2.9.2.2 Ferric chloride-induced thrombosis

The carotid artery was exposed by blunt dissection using sterile black plastic, and thrombi was generated by administration of 10 % $FeCl_3$-soaked filter paper (1 mm x 2 mm) for 3 min. The injury site was imaged for 25 min by time-lapse microscopy (Li et al., 2016).

2.9.2.3 Laser-induced thrombosis

The cremaster muscle was isolated in male mice by cutting the scrotum, and dissecting the muscle using a thermocautery over a glass coverslip. Thrombi was generated by laser injuries of the arterioles during constant perfusion of warmed 0.9 % saline buffer. Thrombus was observed for 3 min by time-lapse microscopy of simultaneous fluorescence and bright field images (Stalker, 2020).

2.9.2.4 Platelet-depletion

Mice were challenged with an anti-GPIbα, platelet depleting antibody at 0.1 mg/kg by intraperitoneal injection (Rayes et al., 2017); platelet count was analysed by saphenous bleed (2.2.3.3) daily and quantified by an ABX Pentra 80 automated haematology analyser.

2.9.2.5 Analysis

Images were acquired using an Olympus, upright spinning disk confocal microscope and 4X Nikon air lens or 40X Nikon water-immersed lens for $FeCl_3$ and laser injuries, respectively). Images were analysed using Slidebook6 software (Intelligent Imaging Innovations),

2.10 Statistical analysis

All data is presented as mean±SD, unless otherwise stated. The statistical significance between 2 groups was analyzed using an unpaired t-test and the statistical difference between multiple groups *in* vitro using one-way ANOVA with Tukey's multiple comparisons test. The statistical significance for *in vivo* experiments were determined by a Kruskal-Wallis test, unless otherwise stated, using Prism 8 (GraphPad Software Inc, USA). Statistical significance was represented by stars: *$p < 0.05$ **$p < 0.01$ ***$p < 0.001$ ****<0.0001

Chapter 3

Platelet-CLEC-2 in models of arterial thrombosis in humans and mice

3.1 Aim

The aim of this chapter was to investigate the role of platelet-ITAM receptor, CLEC-2, in arterial thrombosis in humans and mice. This was investigated *in vivo* using a recently generated, megakaryocyte lineage-specific GPIb recombinase mouse (Nagy et al., 2019) for specific deletion of platelet-CLEC-2. Furthermore, human CLEC-2-blocking antibody, AYP1, which blocks CLEC-2-podoplanin interaction, was used to investigate the role of human platelet-CLEC-2 in *ex vivo* functional assays.

3.2 Introduction

Platelets critically limit blood loss post-injury. Conversely, undesired vascular occlusion resulting from common cardiovascular disorders such as atherosclerotic plaque rupture can be fatal. Whilst current anti-platelet therapeutics are effective in unwanted vascular occlusion, they are commonly coined ‘blood thinners’, elucidating unwanted and often detrimental bleeding characteristics in patients upon trauma.

3.2.1 Modern anti-coagulant drugs

Current anti-thrombosis therapeutics can be categorised into anti-coagulant, and anti-platelet targeting. **Anti-coagulants** commonly used in patients at high risk of deep vein thrombosis, or a prior history of blood clotting, include warfarin and heparin. First described in 1918 extracted from dried powdered liver with ether, heparin is the most commonly prescribed anti-coagulant globally (Hemker, 2016). Modern unfractionated heparin is derived from porcine intestinal- or bovine lung-

mucosal tissue, and works through binding, and subsequently activating plasma resident glycoprotein, antithrombin III (Nutescu et al., 2016). Through antithrombin III-heparin complexes, Factors IXa-XIIa are inhibited, therefore preventing the generation of GPCR agonist, thrombin, from prothrombin (described in 1.3.1). Furthermore, fibrin generation from fibrinogen is also inhibited, therefore removing two pro-coagulant stimuli from circulation. Warfarin is a vitamin K antagonist, and through interference with enzyme vitamin K reductase, reduces the activity of γ-glutamyl carboxylase to inhibit the activation of Factors VII, IX and X, alongside thrombin generation (Ageno et al., 2012). **Anti-platelet** drugs are prescribed to patients with arterial diseases, post-coronary surgery, or that are currently having a heart attack. Amazingly described in 1500 BC Egyptian medical records, acetylsalicylic acid (aspirin) is derived from the willow tree. Mechanistically, the anti-platelet drug is a non-selective cyclooxygenase (COX) inhibitor, and pharmaceutically inhibits COX-1 and -2 activity. COX-1 is essential for TxA_2 biosynthesis (Patrignani et al., 1999); TxA_2 induced platelet activation is described in 1.3.1. Another target for patients with thrombosis is fibrinolysis. **Anti-fibrinolytic** drugs prevent fibrin breakup to promote clot stability (Hoylaerts et al., 1981), however this strategy merely limits symptoms, without treating the cause.

Whilst anti-coagulant, anti-platelet and anti-fibrinolytic therapeutics are effective, they have 6-8 days of activity, and induce severe haemostatic defects. Furthermore, patients can become refractory, or in severe haemolytic disease, platelet activation cannot be blocked by classical drugs. There is a clear demand for anti-thrombotic therapeutics without detriment to platelet-regulated homeostasis.

3.2.2 CLEC-2 in arterial thrombosis

Platelets express ITAM receptors, which are critical in classical and non-classical platelet functions (Rayes et al., 2019). GPVI-deficient mice present small, non-occlusive thrombi with mild bleeding phenotypes (Nieswandt et al., 2000, Nieswandt et al., 2001b). Furthermore, CLEC-2 has been demonstrated to contribute to thrombus stability during *in vivo* $FeCl_3$-induced thrombosis models in mice (May et al., 2009, Suzuki-Inoue, 2011, Bender et al., 2013). Interestingly, discrepancy in the field has led to ambiguity to the contribution of platelet CLEC-2 to thrombus formation, as it was shown that CLEC-2 was not required at arterial shear flow rates ($1700s^{-1}$) (Hughes et al., 2010a). Furthermore, an endogenous, vascular-resident ligand to CLEC-2 was not described, hence imploring further mystery to how CLEC-2 supports thrombus growth and vascular occlusion.

Endogenous CLEC-2-ligand, podoplanin, is constitutively expressed on alveolar epithelial cells, fibroblasts, lymphatic endothelial cells and podocytes in physiology (Quintanilla et al., 2019). However, the glycoprotein is also upregulated during inflammation on macrophages, TH17 cells and fibroblasts, and is also expressed on cancer cells; podoplanin is absent in healthy vasculature (Quintanilla et al., 2019). Podoplanin could potentially activate platelets following lesion of advanced atherosclerotic plaque (Hatakeyama et al., 2012). **Atherosclerosis** is a thrombo-inflammatory disease which results from a culmination of inflammatory response to oxidised lipids and endothelial dysfunction, which leads to a plaque formation. Platelet-leukocyte interaction has been demonstrated to be critical in disease progression, as depletion of platelets, neutrophils or monocytes drastically reduces

plaque size post-rupture (Ylitalo et al., 1994, Massberg et al., 2002, Drechsler et al., 2010). GPVI-laminin interaction promotes atherosclerotic progression, through platelet activation and spreading, which builds on an intact plaque (Inoue et al., 2006). The role of GPVI is switched upon the separation of plaque material to be collagen-driven, as a result of endothelial breach and sub-endothelial exposure. Interestingly, platelet-driven atheroprogression also occurs independently of classical platelet-activating receptors (Rayes et al., 2020). Platelets encourage monocyte and/or macrophage uptake of oxidised low-density lipoproteins (OxLDLs), and their recruitment to the inflamed endothelium (Badrnya et al., 2014) directly through PSGL-1, CD40L and through secretion of RANTES and PF4. Murine models targeting these axes demonstrated promising targets to treat atherosclerosis, albeit translation to humans have been disappointing (Rainger et al., 2015). Interestingly, podoplanin was co-localised to smooth muscle cells and macrophages, with increased expression within advanced lesions (Hatakeyama et al., 2012). This could provide justification for CLEC-2 as a therapeutic target for patients with, or at high risk of atherosclerotic plaque.

In the absence of a vascular-resident ligand, Haining et al. (2017) generated a novel mouse with normal CLEC-2 expression, but with a Y7A knock-in at the first exon of *clec1b*, to inhibit CLEC-2 signalling through its hemITAM domain. Interestingly, thrombus size in these mice were non-occlusive and smaller versus wild type controls, suggesting that CLEC-2 contributes to thrombus formation independently of its signalling domain. Furthermore, bleeding defects were not observed in the Y7A mice, providing further justification to progress CLEC-2 as a therapeutic target in thrombosis and haemostasis.

3.2.3 The 'leaky' PF4-Cre recombinase mouse

Research on murine platelet-CLEC-2 in thrombosis and haemostasis models has previously relied on antibody inhibition-induced downregulation by INU1, or genetic deletion by platelet factor PF4-Cre recombinase in mice (Tiedt et al., 2007). The PF4-Cre was the gold-standard in platelet specificity, with >99.9 % genetic deletion, due to the early presentation of PF4 in development. More recently, PF4 has been shown to be expressed in mast cells, microglia, monocytes and T cells (Calaminus et al., 2012, Abram et al., 2014, Pertuy et al., 2015), and not specifically to the megakaryocyte lineage. The 'leaky' PF-4-Cre, alongside potential antibody inhibition of CLEC-2 on other cell types, may have contributed to a phenotype nonspecific to platelet-CLEC-2 in thrombus formation in mice. It is evident that a mouse with a higher specificity to platelet-receptor deletion is required to characterise CLEC-2 in thrombosis and haemostasis.

In this chapter, we investigate the role of CLEC-2 during murine *in vivo* and *in vitro* models of thrombosis and haemostasis using megakaryocyte lineage-specific GPIb-Cre mice for genetic deletion of CLEC-2 (Nagy et al., 2019). The CLEC1b$^{fl/fl}$GPIb-Cre^{+} mouse exhibits a 98.7 % deletion of platelet-specific CLEC-2, without deletion in myeloid cells (Nagy et al., 2019, Haining et al., 2020). We have also investigated the role of CLEC-2 in human blood using Fab and F(ab)$_2$ fragments of CLEC-2-blocking antibody, AYP1, which blocks CLEC-2-podoplanin interaction, and through the use of human dimeric recombinant CLEC-2 (hFc-CLEC-2) during an *ex vivo* model of thrombosis by whole blood flow adhesion on immobilised matrix or inflammatory endothelial cells at various shear rates.

3.3 Results

3.3.1 Platelet-CLEC-2-deficient mice have reduced platelet and erythrocyte counts but a normal leukocyte count

Previous studies investigating the role of CLEC-2 on platelets in arterial thrombosis in mice have used a CLEC1b$^{fl/f}$PF4-Cre model to selectively delete the hemITAM receptor on platelets. However, several groups have shown that the PF4-Cre transgene also deletes CLEC-2 on a sub-population of myeloid cells (Pertuy et al., 2015, Calaminus et al., 2012, Abram et al., 2014), thereby making it unclear if the phenotype is due solely to deletion on platelets. In view of this, we have extended this work to CLEC1b$^{fl/fl}$GPIb-Cre mice, as expression of GPIb-Cre transgene is restricted to the megakaryocyte/platelet lineage (Fujita et al., 1998, Nagy et al., 2019), and compared the result to both wild type mice and to GPVI-deficient mice. We have previously reported that CLEC1b$^{fl/fl}$GPIb-Cre are born at a Mendelian ratio with a mild reduction in platelet count, possibly as a result of a defect in blood-lymphatic separation (Haining et al., 2020). Here, we report a 20.7±4.6 % reduction in circulating platelet count **(Figure 3.1A),** but unchanged mean platelet volume and erythrocyte and white blood cell (monocyte, neutrophil and lymphocyte) counts **(Figure 3.1B-G)** in CLEC-2$^{fl/fl}$GPIbCre^{+} mice, compared to the Cre^{-} littermates.

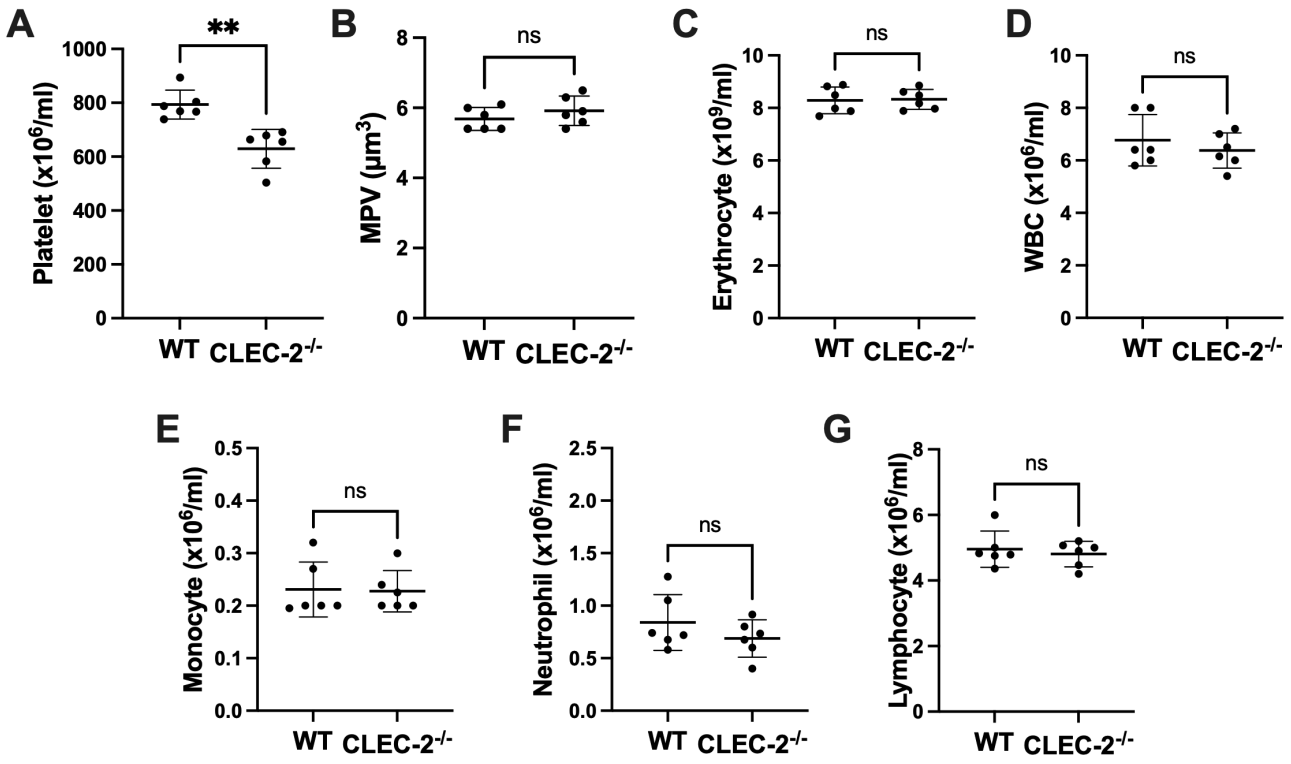

Figure 3.1 - Platelet-CLEC-2-deficiency leads to a reduction in platelet count.

Whole blood from wild type (WT; CLEC1b$^{fl/fl}$GPIb-Cre^{-}) or platelet-CLEC-2-deficient (CLEC-2$^{-/-}$; CLEC1b$^{fl/fl}$GPIb-Cre^{+}) mice was analysed for **(A)** Platelet count, **(B)** mean platelet volume (MPV), **(C)** erythrocyte count, **(D)** white blood cell (WBC) count, **(E)** monocyte count, **(F)** neutrophil count and **(G)** lymphocyte count (n=6). The statistical significance between 2 groups was analysed using an unpaired t-test. *$p < 0.05$ **p<0.01

3.3.2 Platelet-CLEC-2 contributes to thrombus formation in $FeCl_3$ and laser injury models in the arterial circulation

Using the $FeCl_3$-induced thrombosis model of the carotid artery (Li et al., 2016, Haining et al., 2017, Smith et al., 2018), we show that thrombus growth post-injury is mildly impaired in the absence of platelet-CLEC-2, and more substantially in the absence of GPVI. The CLEC1b$^{fl/fl}$GPIb-Cre mouse did not present carotid artery occlusion 25 min post-injury **(Figure 3.2A)**, and presented a 47.3±19 % decrease in thrombus size, versus littermate controls **(Figure 3.2B, C)**. GPVI-deficient mice also had non-occlusive thrombi post-injury, but presented a more substantial 76.0±23 % decrease in thrombus size over 25 min **(Figure 3.2A-C)**. Interestingly, the initiation of thrombus formation was not dependant on either CLEC-2, nor GPVI (**Figure 3.2D)**, which has been previously reported (May et al., 2009). Together, these data are in line with reports using the PF4-Cre mouse, and those utilising CLEC-2-blocking mouse antibody INU1, reporting that CLEC-2 is important for vascular occlusion and thrombus growth. However, previous investigation into CLEC-2 has been somewhat limited to the carotid artery, a microenvironment with low shear flow rates compared to microcirculation throughout the peripheral circulatory system.

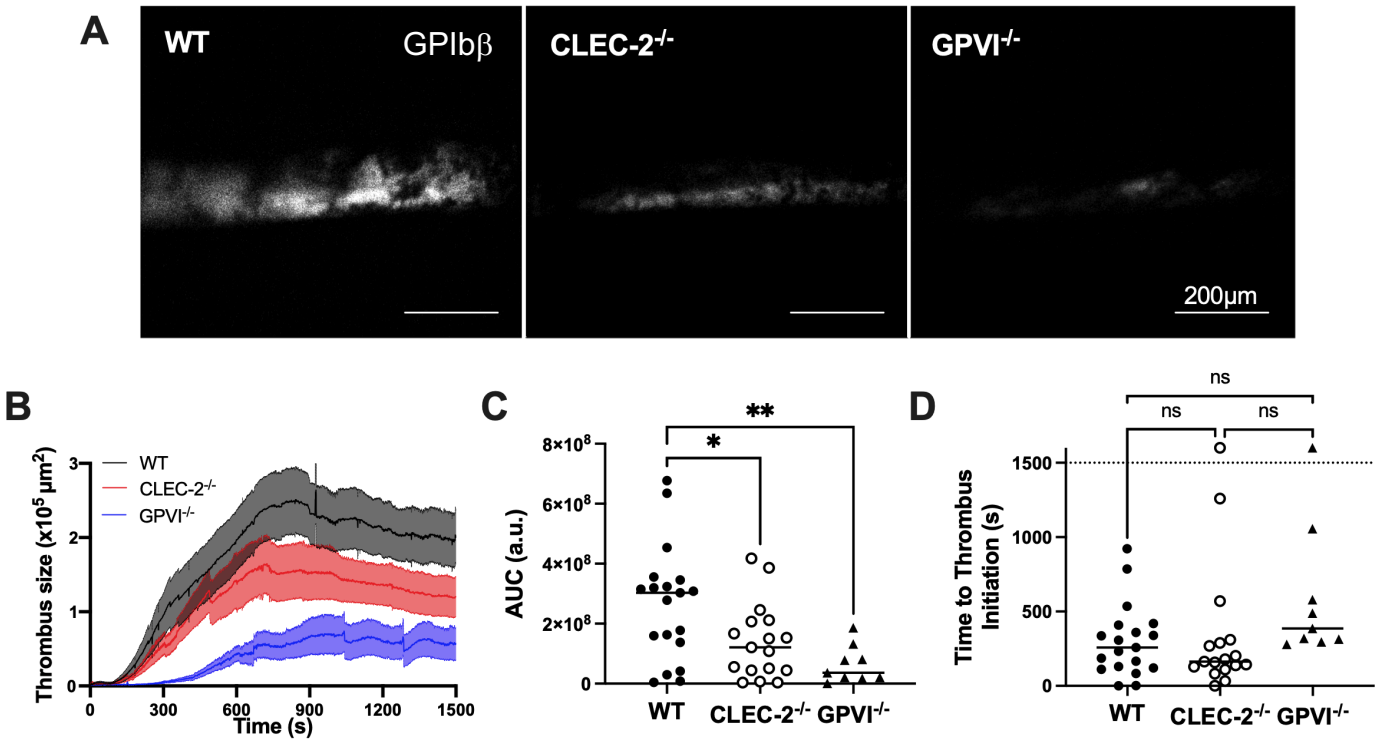

Figure 3.2 - Platelet CLEC-2-deficiency results in non-occlusive thrombus formation post-$FeCl_3$ injury in arterial thrombosis in mice. (A-D) Wild type (WT; CLEC1b$^{fl/fl}$GPIb-Cre^{-}), Platelet-CLEC-2-deficient (CLEC-2$^{-/-}$; CLEC1b$^{fl/fl}$GPIb-Cre^{+}) or GPVI-deficient (GPVI$^{-/-}$CLEC1b$^{fl/fl}$GPIb-Cre^{-}) mice were challenged with $FeCl_3$-soaked filter paper (10%, 3 min) on the carotid artery. **(A)** Representative images are shown at 25 min post-injury, and **(B)** thrombus size was quantified over 25 min by GPIbβ-antibody fluorescence using confocal microscopy; **(C)** the area under the curve (AUC) was calculated (a.u.=arbitrary units). **(D)** The time taken for a thrombus to reach 1x10^5 µm^2 was calculated (n=19 WT; n=17 CLEC-2$^{-/-}$; n=9 GPVI$^{-/-}$). The statistical difference between multiple groups using one-way ANOVA with Tukey's multiple comparisons test. *$p < 0.05$ **$p < 0.01$

3.3.3 Platelet-CLEC-2 contributes to thrombus stability in the arterial microcirculation post-laser injury of the cremaster

In order to assess whether the role of CLEC-2 is maintained across locations at high shear flow rates, as well as previously reported larger arteries, with medium shear flow rates, we used a laser-injury model of arterioles in the cremaster muscle. The thrombus size over 3 min was notably smaller in injuries in the absence of platelet-CLEC-2 **(Figure 3.3A, B)**. Although the initiation and the time to peak thrombus formation was not dependant on platelet-CLEC-2 compared to littermate controls **(Figure 3,3C)**, the peak thrombus size was significantly reduced **(Figure 3.3D)**. These results show a defect in arterial thrombus formation in mice deficient in platelet-CLEC-2, in line with previous results in a PF4-Cre mouse model (Bender et al., 2013, Haining et al., 2017). This demonstrates a contribution for CLEC-2 in arterial thrombosis in mice in two models at medium and high shear flow.

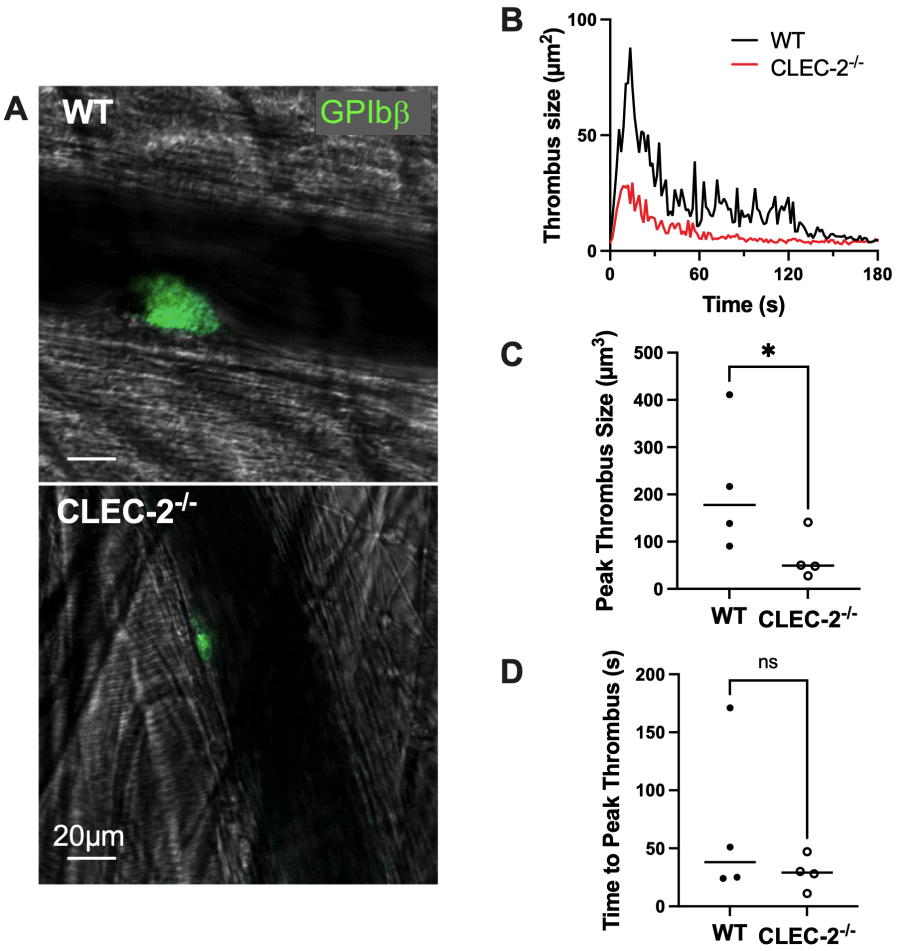

Figure 3.3 - Platelet CLEC-2-deficiency results in unstable thrombus formation in cremaster arterioles in mice. (A-D) WT or Platelet-CLEC-2$^{-/-}$ mice were challenged by a laser injury in arterioles of the cremaster muscle. **(A)** Representative images are shown at 30 s post-injury (median peak time with images shown of the median injury). **(B)** Thrombus size was observed over 3 min by GPIbβ-antibody fluorescence using confocal microscopy; **(C)** the peak thrombus size and **(D)** time to reach peak thrombus size was calculated. (n=4; median of 8-10 injuries/mouse are presented). The statistical significance between 2 groups was analysed using an unpaired t-test. *$p < 0.05$

3.3.4 Platelet-CLEC-2 regulation of thrombus stability is not dependant on a lower platelet count in GPIb-Cre^{+} mice

The decrease in thrombus formation could be due to the loss of CLEC-2 and/or the decrease in platelet count. To address this, C57BL/6 mice were treated with an intraperitoneal injection with a GPIbα platelet-depleting antibody, and the recovery in platelet count monitored. The $FeCl_3$-injury model was then performed in mice in which the platelet count had been lowered by >95 % and ~50 % at 24 and 72 h, respectively **(Figure 3.4A)**. A 50 % reduction in platelet count was used to mirror the reduced platelet count observed in CLEC1b$^{fl/fl}$GPIb-Cre mice. Thrombus formation was abolished in mice with a >95 % reduction in platelet count but unaltered in mice with a ~50 %, relative to saline-treated mice **(Figure 3.3A-C)**. This shows that the 36 % reduction in platelet count in CLEC1b$^{fl/fl}$GPIb-Cre mice, compared to littermate controls, is not the cause of the reduction in thrombus formation.

Together, data from Figures 3.2-3.4 confirm earlier reports that platelet-CLEC-2 plays an important role in the formation of thrombi in the arterial circulation, and that this is independent of the reduction in platelet count.

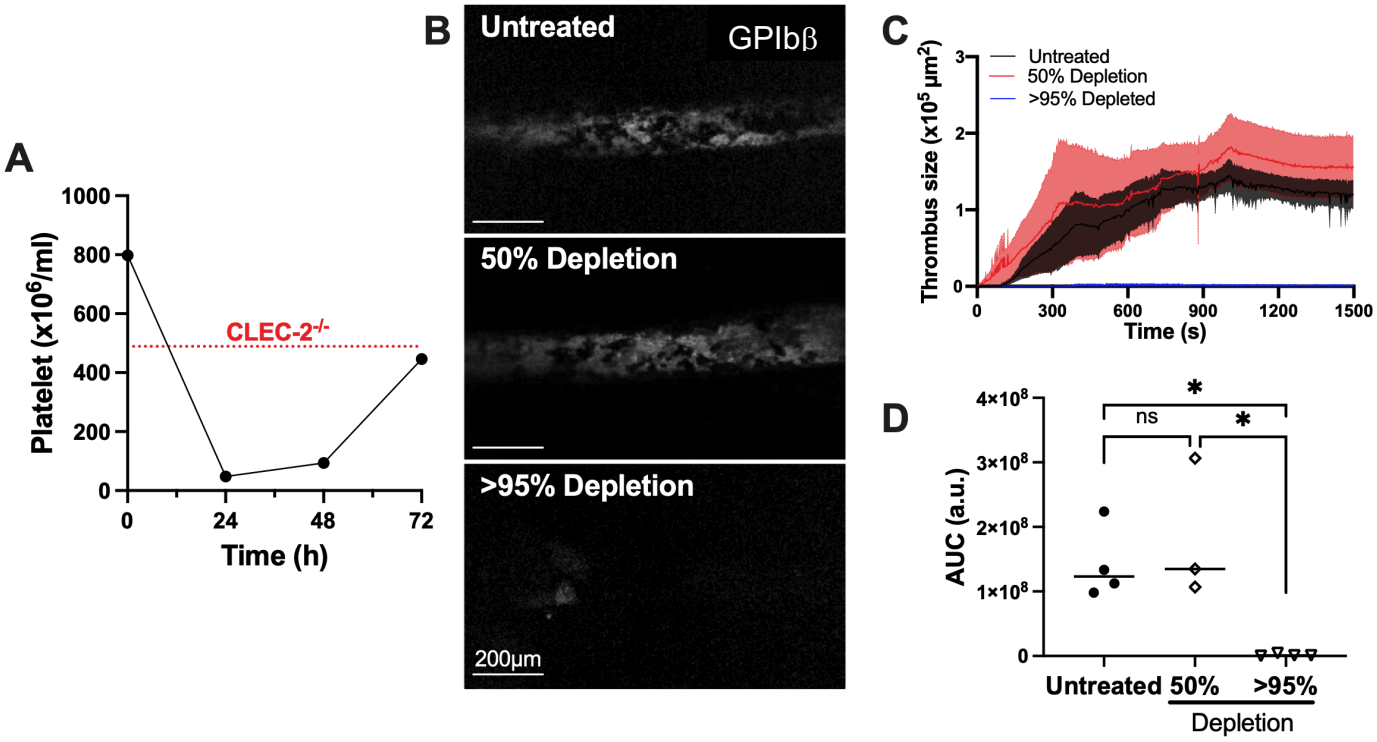

Figure 3.4 - Platelet CLEC-2-deficiency reducing thrombus size is independent of platelet count. (A-D) C57BL/6 mice were treated intraperitoneally with 200 µl saline, or a platelet-depletion antibody (0.1 mg/kg), and challenged 24 h, or 72 h post-treatment (>95 % and 50 % depletion, respectively) with $FeCl_3$-soaked filter paper (10 %, 3 min) on the carotid artery. **(A)** Platelet count was monitored over 72 h by saphenous bleed. **(B)** Representative images are shown at 25 min post-injury, **(C)** thrombus size was observed over 25 min by GPIbβ-antibody fluorescence using confocal microscopy and **(D)** the area under the curve (AUC) was calculated (a.u.=arbitrary units). The statistical difference between multiple groups was analysed using a one-way ANOVA with Tukey's multiple comparisons test. *$p < 0.05$

3.3.5 CLEC-2 contributes to thrombus formation over collagen *ex vivo* in mice

The contribution of CLEC-2 to thrombus formation was further investigation *ex vivo*, using an Ibidi µ-Slide VI 0.1 flow chamber coated with Horm collagen (100 µg/ml). The platelet count of platelet-CLEC-2-deficient mice was normalised to the WT littermate control using washed CLEC-2-deficient platelets in whole blood **(Figure 3.5A)**. Blood perfused at 1000 s^{-1} presented a decrease in thrombus surface coverage by 38±11 % after 4 min in platelet-CLEC-$2^{-/-}$ mice compared to WT controls **(Figure 3.5B-E)**. There was no change in surface coverage between the genotypes until 2 min into perfusion, suggesting a distinct role for CLEC-2 in thrombi growth, but not in thrombus initiation **(Figure 3.5B-D)**.

These data show that CLEC-2 contributes to the growth and/or stability of thrombi at arterial rates of shear in mice.

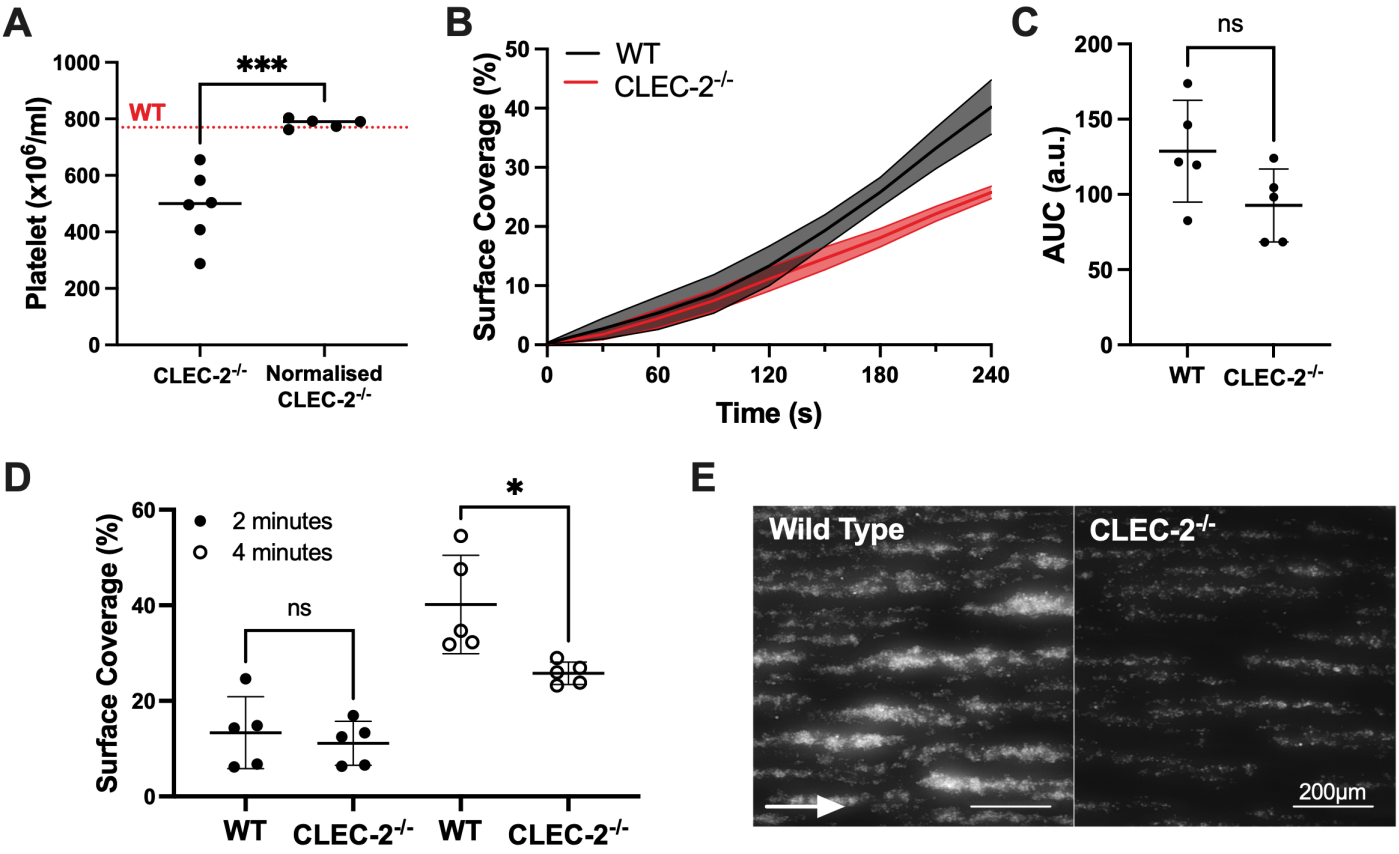

Figure 3.5 - Platelet-CLEC-2 promotes thrombus stability at arterial shear in mice *ex vivo*. (A) Washed platelets from a CLEC1b$^{fl/fl}$GPIb-Cre mouse was donated to CLEC1b$^{fl/fl}$GPIb-Cre whole blood *ex vivo* to match WT platelet counts. **(B)** Thrombus surface coverage over 4 min, measured using DioC6 fluorescence (2 µM) **(C)** subsequent area under the curve (AUC) was calculated (a.u.=arbitrary units) and thrombus formation after **(D)** 2 and 4 min. **(E)** Representative images shown after 4 min (n=5); arrow indicates direction of flow. The statistical significance between 2 groups was analysed using an unpaired t-test and the statistical difference between multiple groups was analysed using a one-way ANOVA with Tukey's multiple comparisons test. *$p < 0.05$, **p<0.01, ***$p < 0.001$

3.3.6 CLEC-2 inhibition by AYP1-F(ab) does not reduce thrombus generation on collagen and plaque at arterial shear in human blood *in vitro*

Studies were designed to investigate the contribution of CLEC-2 to thrombus formation using F(ab) fragments of the human CLEC-2-blocking antibody, AYP1. The mAb AYP1 F(ab) (10 µg/ml) blocked and markedly reduced rhodocytin- **(Figure 3.6A, B)** and podoplanin-expressing HEK-293T cell-induced **(Figure 3.6C, D)** platelet aggregation.

We used an Ibidi µ-slide 0.1 and Maastricht flow chamber models to study the effect of AYP1 F(ab) on thrombus formation. F(ab) (10 µg/ml) did not alter thrombus generation (surface area and thrombus height) **(Figure 3.7A-C)**, nor platelet activation (phosphatidylserine (PS) expression, P-selectin (CD62P) presentation and αIIbβ3 activation) **(Figure 3.7D-F),** when perfused over Horm collagen at arterial shear rate (1000 s^{-1}) in the Maastricht flow chamber. Similarly, neither F(ab), nor $F(ab)_2$ fragments of AYP1 (10 µg/ml) significantly altered thrombus generation over Horm collagen in the Ibidi µ-Slide VI 0.1flow chamber at 1000 s^{-1} **(Figure 3.8A-D).**

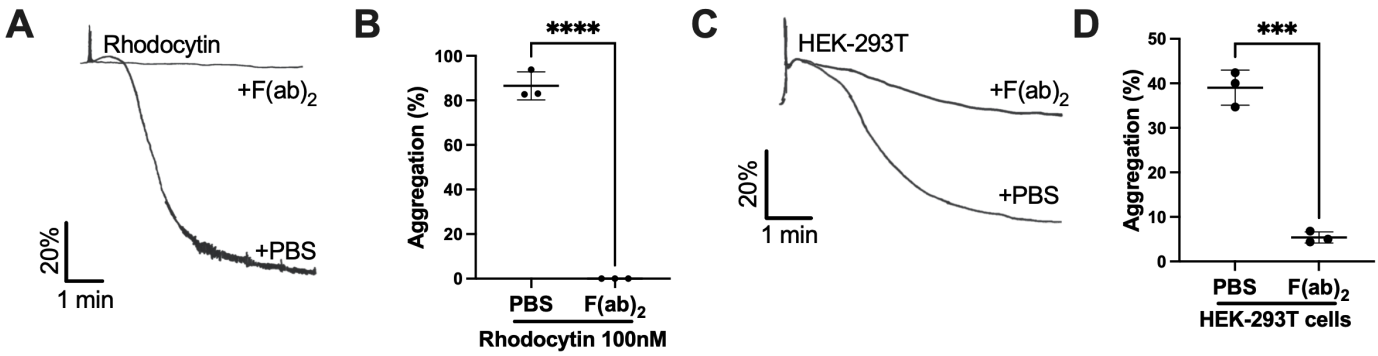

Figure 3.6 - Fragments of CLEC-2-blocking antibody AYP1 inhibit rhodocytin and podoplanin-induced platelet aggregation. (A-D) Washed platelet aggregation was assessed by light transmission aggregometry, in the presence or absence of AYP1 fragment, $F(ab)_2$ (10 µg/ml). **(A)** Representative platelet aggregation trace induced by rhodocytin (100 nM) and **(B)** final aggregation (n=3). **(C)** Representative platelet aggregation trace induced by HEK-293T cells and **(D)** final aggregation (n=3). The statistical significance between 2 groups was analysed using an unpaired t-test with Mann Whitney correction. ***$p < 0.001$, ****$p<0.0001$.

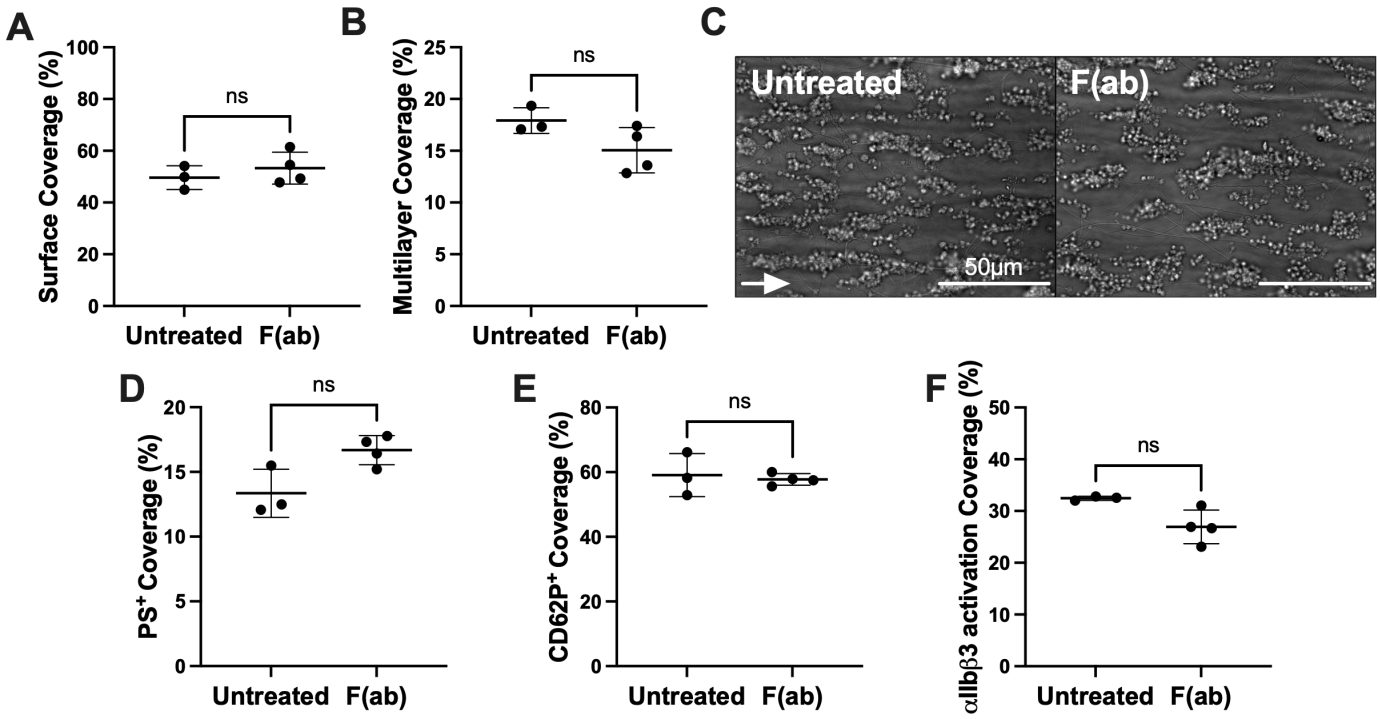

Figure 3.7 - CLEC-2 inhibition by AYP1 fragments does not alter thrombus formation, nor platelet activation in human blood perfused Horm collagen.

(A-F) Whole blood from healthy volunteer donors was perfused through a Maastricht flow chamber at 1000 s^{-1}, in the presence or absence of F(ab) (10 µg/ml) 10 min prior to perfusion. The flow chamber was coated with Horm collagen (100 µg/ml). **(A)** Thrombus surface coverage and **(B)** and multi-layered thrombi after 4 min. **(C)** Representative images shown after 4 min (n=3; arrow indicates direction of flow). **(D)** Phosphatidylserine (PS) exposure, **(D)** P-selectin expression (CD62P) and **(D)** Integrin αIIbβ3 activation was calculated from fluorescent images as shown. The statistical significance between 2 groups was analysed using an unpaired t-test with Mann Whitney correction.

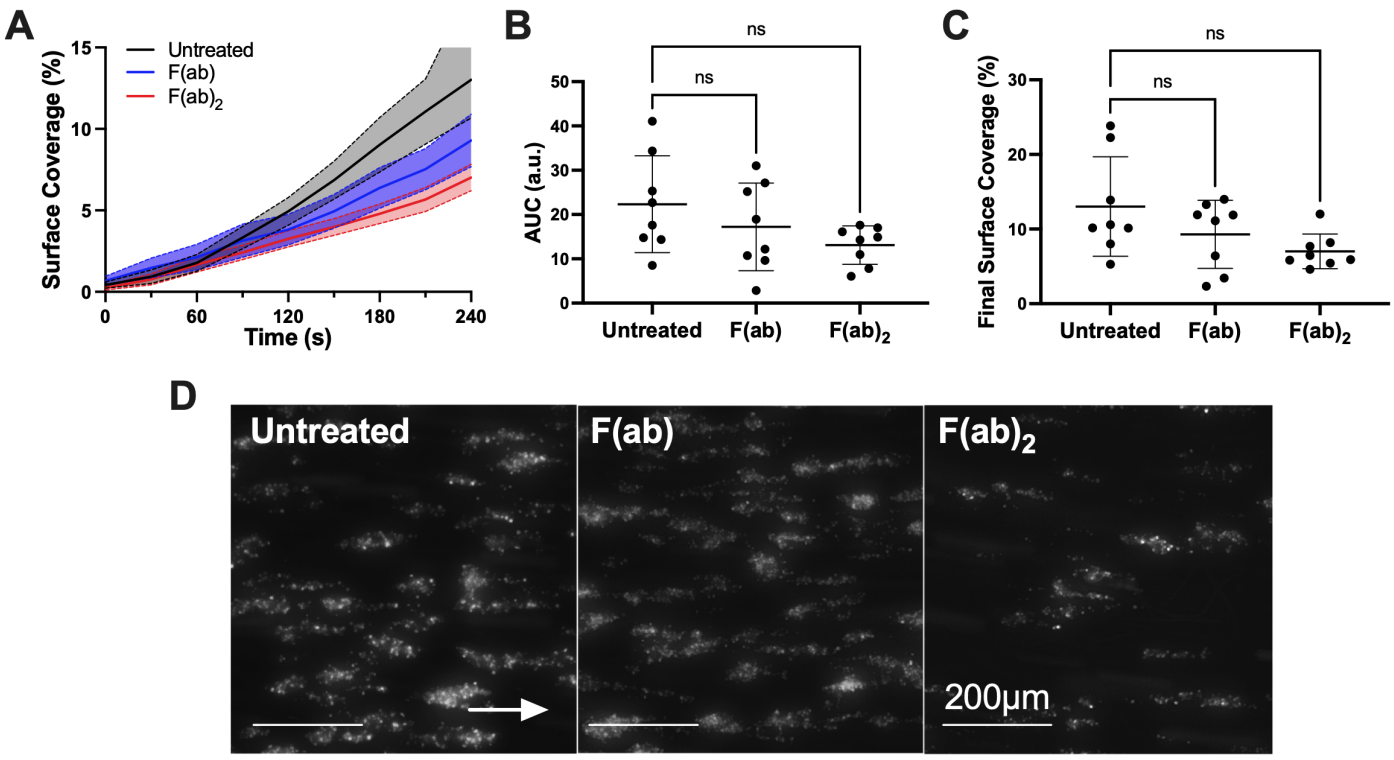

Figure 3.8 CLEC-2 inhibition by AYP1 fragments does not alter thrombus formation in human blood perfused over Horm collagen. Whole blood from healthy volunteer donors was perfused over Horm collagen-coated (100 µg/ml) in an Ibidi µ-Slide VI 0.1 flow chamber at 1000 s^{-1}, in the presence or absence of F(ab) (10 µg/ml), $F(ab)_2$ (10 µg/ml) for 10 min prior to perfusion. **(A)** Thrombus surface coverage over 4 min, measured using DioC6 fluorescence (2 µM), **(B)** subsequent area under the curve (AUC) was calculated (a.u.=arbitrary units) and **(C)** thrombus formation after 4 min. **(D)** Representative images shown after 4 min (n=5; arrow indicates direction of flow). The statistical significance between multiple groups was analysed using one-way ANOVA with Tukey's multiple comparisons test.

The subendothelium is composed of collagens type I and type III; horm collagen is predominantly equine type I collagen. For this reason, we extended the studies in the Maastricht flow model to collagen type III. AYP1 F(ab) (10 µg/ml) did not alter thrombus surface coverage, height, or activation **(Figure 3.9A-F)**. Atherosclerotic plaque contains a variety of extracellular matrix proteins and debris of various cells including podoplanin-positive macrophages (Hatakeyama et al., 2012), which may be critical in driving atherosclerosis-induced arterial disease. To replicate plaque-driven thrombosis in a large-artery intima, plaque homogenate was pooled and sectioned to allow blood perfusion over the material in a Maastricht flow chamber at arterial sheer rate (1000 s^{-1}). Platelets adhered to the plaque homogenate after 4 min, and platelet coverage, thrombus height, nor platelet activation was altered in the presence of AYP1 F(ab) (10 µg/ml), compared to the untreated control **(Figure 3.10A-F).**

These results demonstrate that blockade by AYP1 has no effect on thrombus formation when human blood is perfused over collagen types I and III, and atherosclerotic plaque at arterial shear in two widely used flow models.

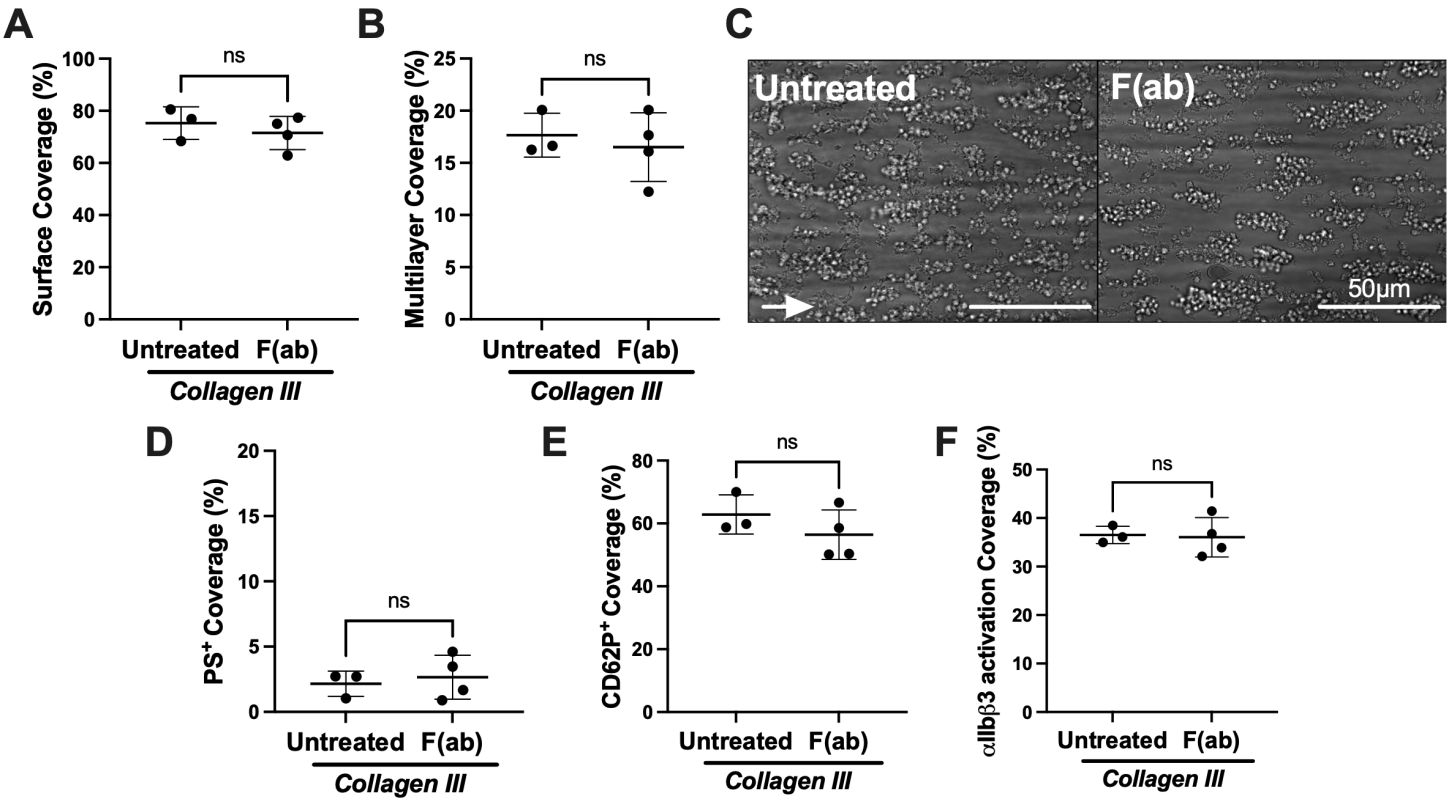

Figure 3.9 - CLEC-2 inhibition by AYP1 fragments does not alter thrombus formation, nor platelet activation in human blood perfused over collagen III.

(A-F) Whole blood from healthy volunteer donors was perfused through a Maastricht flow chamber at 1000 s^{-1}, in the presence or absence of F(ab) (10 µg/ml) 10 min prior to perfusion. The flow chamber was coated with collagen III (100 µg/ml). **(A)** Thrombus surface coverage and **(B)** and multi-layered thrombi after 4 min. **(C)** Representative images shown after 4 min (n=3; arrow indicates direction of flow). **(D)** Phosphatidylserine (PS) exposure, **(E)** P-selectin expression (CD62P) and **(F)** Integrin αIIbβ3 activation was calculated from fluorescent images. The statistical significance between 2 groups was analysed using an unpaired t-test with Mann Whitney correction.

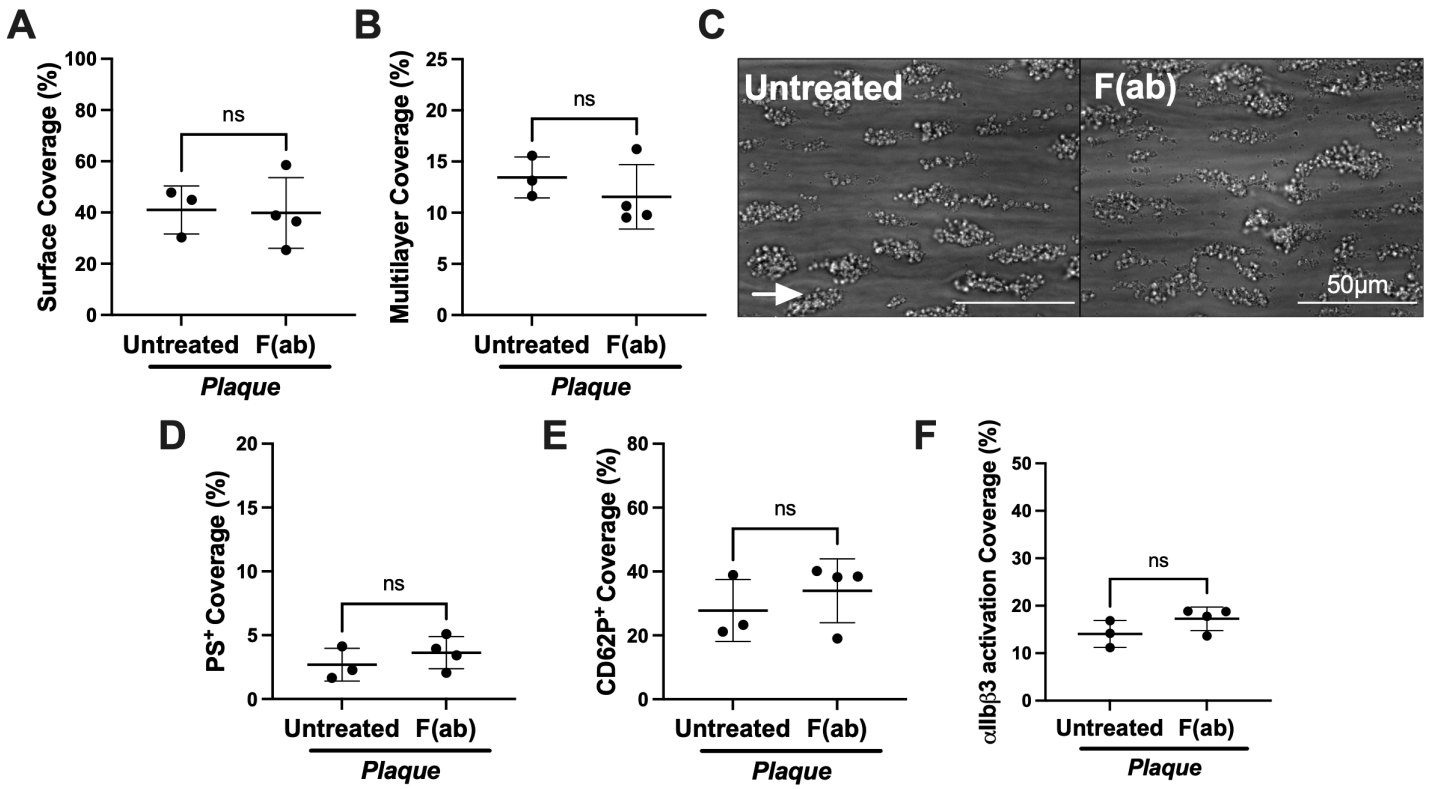

Figure 3.10 - CLEC-2 inhibition by AYP1 fragments does not alter thrombus formation, nor platelet activation in human blood perfused over plaque material. (A-F) Whole blood from healthy volunteer donors was perfused through a Maastricht flow chamber at 1000 s^{-1}, in the presence or absence of F(ab) (10 µg/ml) 10 min prior to perfusion. The flow chamber was coated with collagen III (100 µg/ml). **(A)** Thrombus surface coverage and **(B)** and multi-layered thrombi after 4 min. **(C)** Representative images shown after 4 min (n=3; arrow indicates direction of flow). **(D)** Phosphatidylserine (PS) exposure, **(E)** P-selectin expression (CD62P) and **(F)** Integrin αIIbβ3 activation was calculated from fluorescent images. The statistical significance between 2 groups was analysed using an unpaired t-test with Mann Whitney correction.

3.3.7 CLEC-2-ligand inhibition by recombinant human CLEC-2-Fc does not alter thrombus surface coverage

The ligand for CLEC-2 that supports thrombus formation in mice, and potentially in human, is not known; the only candidate is hemin, which is formed from lysed red blood cells. Interestingly, AYP1 does not block hemin-induced aggregation (Data shown in Figure 4.3) (Bourne et al., 2020). Therefore, we utilised recombinant human dimeric CLEC-2 (hFc-CLEC-2) to block a potential role of hemin, or an unknown CLEC-2-ligand that binds to a distant binding site to AYP1. hFc-CLEC-2 (10 µg/ml) blocked rhodocytin- **(Figure 3.11A, B)** and podoplanin-expressing HEK-293T cell-induced **(Figure 3.11C, D)** platelet aggregation.

We have demonstrated that hFc-CLEC-2 inhibits hemin-induced platelet aggregation (Data shown in Figure 4.3) (Bourne et al., 2020). Interestingly, blood treatment with hFc-CLEC-2 did not alter thrombus formation when perfused over Horm collagen in an Ibidi µ-slide VI 0.1 flow chamber, or the Maastricht flow chamber **(3.12A-D).**

These results provide further evidence against a role for CLEC-2 in thrombus formation on collagen at arterial shear in humans.

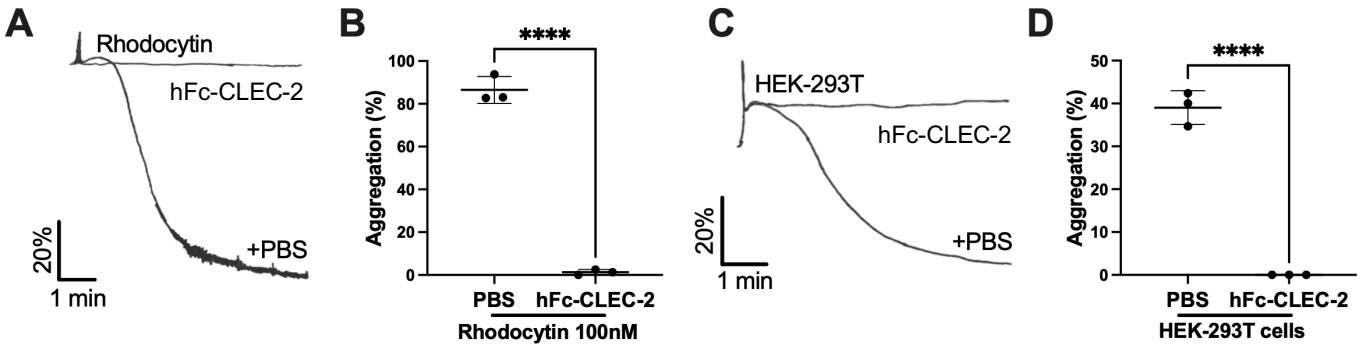

Figure 3.11 – Recombinant CLEC-2-Fc inhibits rhodocytin and podoplanin-induced platelet aggregation. (A-D) Washed platelet aggregation was assessed by light transmission aggregometry, in the presence or absence of recombinant human CLEC-2-Fc (hFc-CLEC-2) (10 µg/ml). **(A)** Representative platelet aggregation trace induced by rhodocytin (100 nM) and **(B)** final aggregation (n=3). **(**C**)** Representative platelet aggregation trace induced by HEK-293T cells and **(D)** final aggregation (n=3). The statistical significance between 2 groups was analysed using an unpaired t-test with Mann Whitney correction. ****p<0.0001.

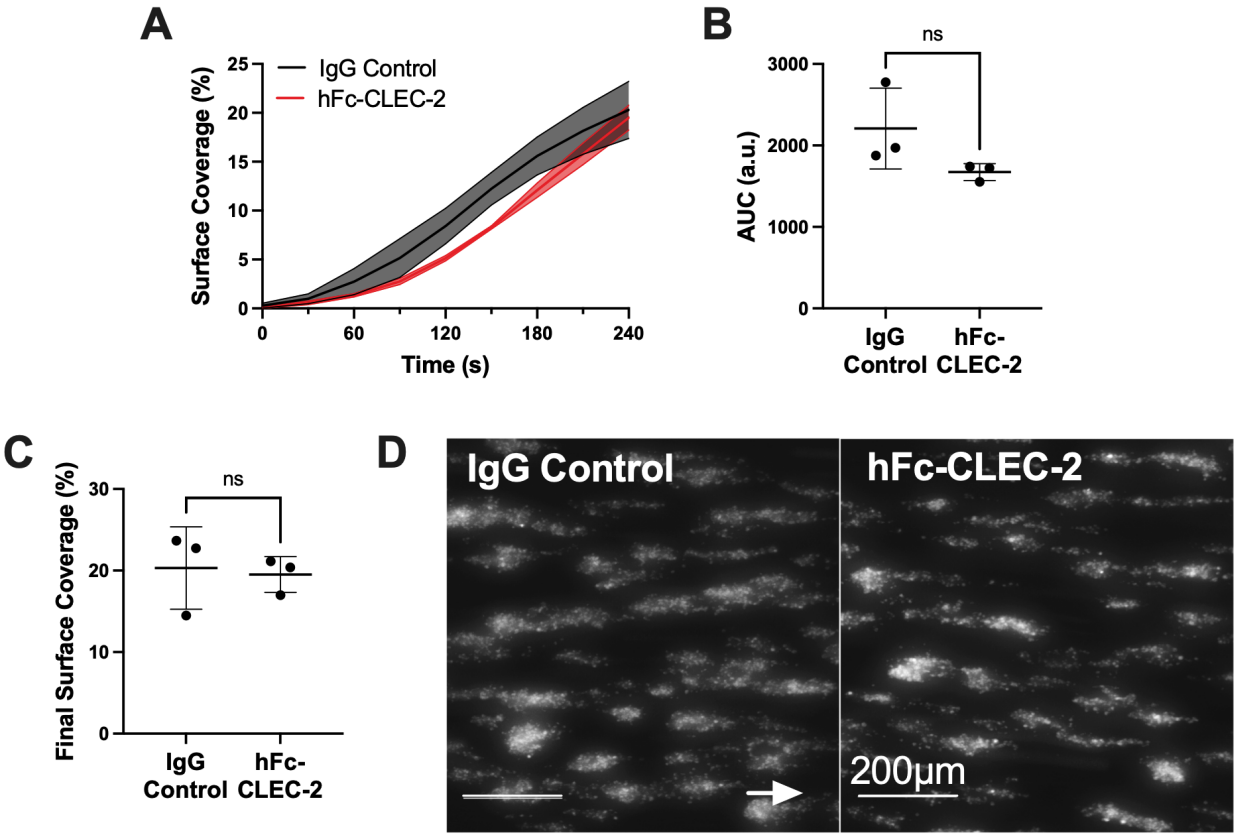

Figure 3.12 - Recombinant human CLEC-2-Fc does not alter thrombus formation in human blood perfused over Horm collagen. (A-D) Whole blood from healthy volunteer donors was perfused over Horm collagen-coated (100 µg/ml) in a µ-Slide VI 0.1 flow chamber at 1000 s^{-1}, in the presence or absence of hFc-CLEC-2 for 10 min prior to perfusion. **(A)** Thrombus surface coverage over 4 min, measured using DioC6 fluorescence (2 µM), **(B)** subsequent area under the curve (AUC) was calculated (a.u.=arbitrary units) and **(C)** thrombus formation after 4 min. **(D)** Representative images shown after 4 min (n=3; arrow indicates direction of flow). The statistical significance between 2 groups was analysed using an unpaired t-test with Mann Whitney correction.

3.3.8 AYP1-F(ab)$_2$ inhibition of CLEC-2 does not alter platelet adherence or leukocyte recruitment in blood perfused over endothelial cells

The endothelium is essential in thrombus formation during inflammatory events; adhesion receptors drive leukocyte recruitment, and vWF-GPIb interaction at high shear drives platelet recruitment to potentiate their aggregation (Kroll et al., 1991). We investigated if CLEC-2 plays a role in either leukocyte recruitment through platelet-leukocyte interaction, or in platelet adhesion to the endothelium through vWF. To model human vasculature, a monolayer of HUVECs were cultured in an Ibidi µ-slide VI 0.4 and TNF-α activated to promote the expression of intercellular adhesion molecule 1 (ICAM1) and vascular cell adhesion molecule (VCAM-1) (Zhou et al., 2007). The Maastricht flow chamber was not used in this assay due to limitations in live cell imaging. Surface coverage after 3 min of blood perfusion was significantly increased over TNF-α-activated EC versus the unstimulated control **(Figure 3.13A, B).** CLEC-2-inhibition at venous shear stress by F(ab)$_2$ did not alter leukocyte recruitment **(Figure 3.12C, D)**, nor surface coverage over activated EC **(Figure 3.13E-G)**. Surface coverage was also unchanged in the presence of F(ab)$_2$ at arterial shear **(Figure 3.13H-J)**.

As a whole, our data suggests that CLEC-2 does not contribute to leukocyte recruitment, nor platelet adhesion at arterial or venous shear rates over TNF-α-activated EC. Importantly, these EC are human umbilical vein EC, therefore the contribution of CLEC-2 to thrombus formation on other vascular beds requires further elucidation.

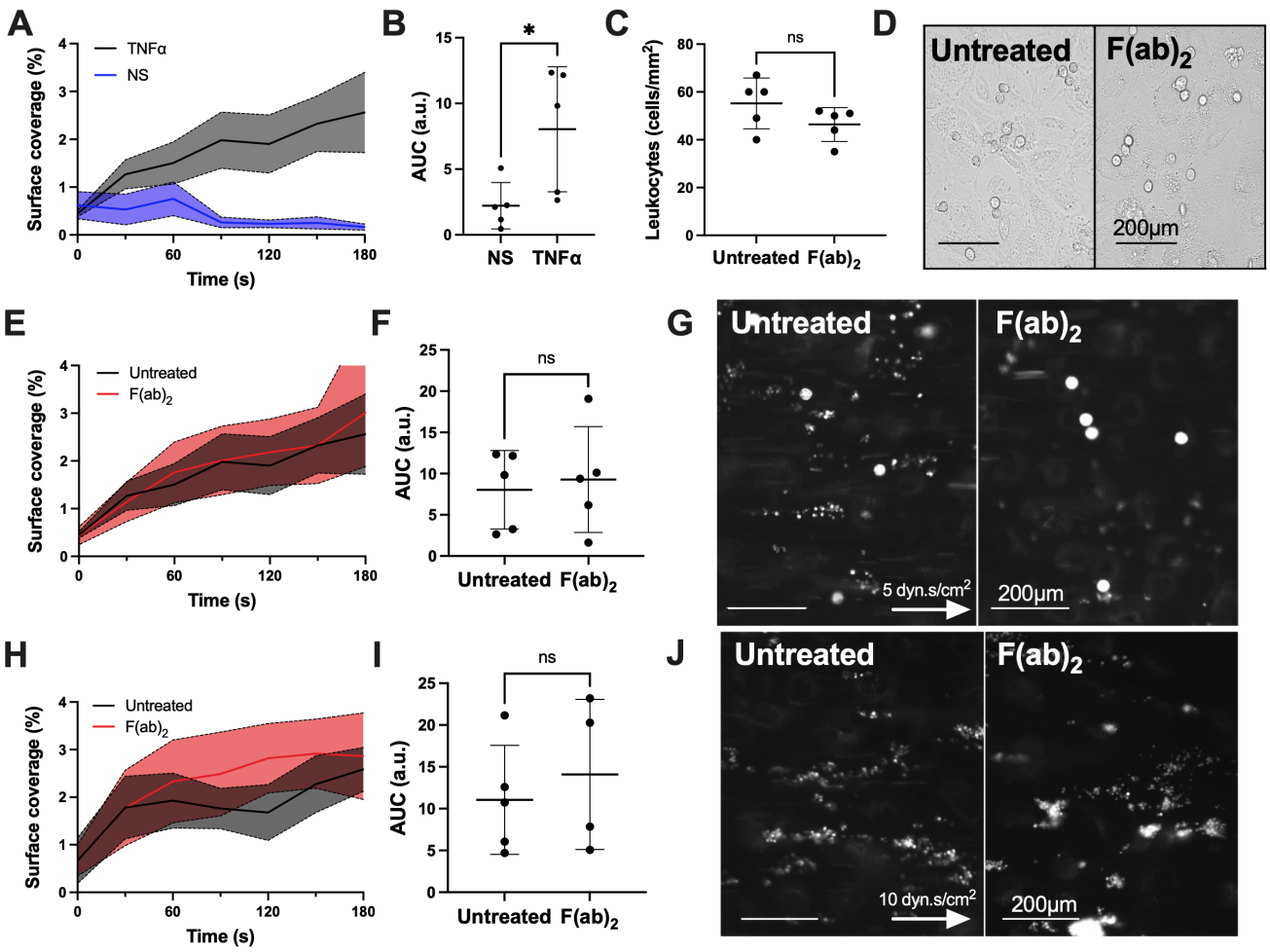

Figure 3.13 - CLEC-2 inhibition by F(ab)$_2$ does not alter thrombus formation or leukocyte recruitment over activated endothelial cells. (A-B) Whole blood from healthy volunteer donors was perfused in a μ-Slide VI 0.4 flow chamber over 24 h-TNF-α activated (10 ng/ml), or unstimulated, human umbilical vein endothelial cells (HUVEC) for 3 min. **(A)** Thrombus surface coverage over 3 min, measured using DioC6 fluorescence (2μM), **(B)** subsequent area under the curve (AUC) was calculated (a.u.=arbitrary units). **(C-G)** Whole blood from healthy volunteer donors was perfused at venous shear stress (5 dyn.s/cm^2) over 24 h-TNF-α activated (10 ng/ml) HUVEC for 3 min in the presence or absence of F(ab)$_2$ (10 μg/ml) for 10 min prior to perfusion. **(C)** Leukocyte recruitment and **(D)** representative images were taken post-perfusion. **(E)** Thrombus surface coverage over 3 min, measured using

DioC6 fluorescence (2 μM), **(F)** subsequent area under the curve (AUC) was calculated (a.u.=arbitrary units). **(G)** Representative images shown after 4 min (n=3; arrow indicates direction of flow). **(H-J)** Whole blood from healthy volunteer donors was perfused at arterial shear stress (10 dyn.s/cm^2) over 24 h-TNF-α activated (10 ng/ml) HUVECs for 3 min in the presence or absence of F(ab)$_2$ (10 μg/ml) for 10 min prior to perfusion. **(H)** Thrombus surface coverage over 3 min, measured using DioC6 fluorescence (2 μM), **(I)** subsequent AUC was calculated. **(J)** Representative images shown after 4 min (n=3; arrow indicates direction of flow). The statistical significance between 2 groups was analysed using an unpaired t-test with Mann Whitney correction. *$p < 0.05$

3.4 Discussion

In this chapter, we have used a novel CLEC1b$^{fl/fl}$GPIb-Cre mouse to confirm previous reports that CLEC-2 contributes to thrombus stability following a $FeCl_3$ injury of the carotid artery. This confirms and extends previous observations with the CLEC1b$^{fl/fl}$PF4-Cre mouse which deletes CLEC-2 on platelets and on a limited number of myeloid cells, and therefore strengthens the argument that the defect in thrombus formation is due to deletion of CLEC-2 on platelets. In addition, we provide evidence against a role for CLEC-2 in thrombus formation of human platelets on collagen under arterial rates of flow. Through the use of F(ab) and $F(ab)_2$ fragments of the CLEC-2 blocking antibody AYP1. This conclusion extends to multiple surfaces, namely Horm collagen, human collagen III, atherosclerotic plaque and activated (inflammatory) HUVECs. This suggests that CLEC-2 may not contribute to arterial thrombosis in humans consistent with the absence of an identified ligand for CLEC-2 in human blood.

Endogenous CLEC-2 ligand, podoplanin, has not been shown to exist in human vasculature during physiology, but is critical during inflammatory driven thrombosis (Payne et al., 2017, Hitchcock et al., 2015). Absent in tissue-resident, anti-inflammatory M2 macrophages, podoplanin is transcriptionally upregulated on pro-inflammatory, monocyte-derived M1 macrophages during inflammatory conditions (Bourne et al., 2021). Atherosclerosis is a leading cause of morbidity globally, whereby critical vasculature is occluded by plaque material; M1 and M2 macrophages are reported to contribute to progressing and regressing atherosclerotic plaques, respectively (Bobryshev et al., 2016). Initiated by low

density, lipoprotein (LDL)-cholesterol trapping through endocytosis of the endothelium and subsequent endothelial cell activation, activated mononuclear leukocytes enter the endothelium. Upon migration into the sub-endothelial space (intima), monocytes differentiate to phagocytic macrophages, which uptake OxLDLs and form foam cells – a tissue-specialised macrophage. OxLDLs have been demonstrated to upregulate adhesion markers on the endothelial, leukocytes and smooth muscle tissue (Guyton et al., 1990). Interestingly, podoplanin presentation in advanced atherosclerotic plaque lesions has been correlated with disease severity in human aortas – expression was localised to macrophages and smooth muscle cells (Hatakeyama et al., 2012). Despite thought that the podoplanin-CLEC-2 axis may prove a promising anti-thrombotic target, it has been shown that platelet-adhesion to recombinant podoplanin only occurs through CLEC-2 at venous shear rates to stabilise platelet adhesion in a src/syk-dependant manner (Navarro-Núñez et al., 2015). There was no role for podoplanin at arterial shear, perhaps due to the low CLEC-2-podoplanin affinity in humans (4 μM) compared to mice (15 nM) (Watson et al., 2007, Christou et al., 2008, Lombard et al., 2018). This echoes our observation of a limited role for CLEC-2 when healthy human blood was perfused over pooled plaque homogenate.

Unlike ITAM receptors GPVI and FcγRIIa, CLEC-2 expression is maintained upon activation and is not shed (Gitz et al., 2014). Interestingly, initial research into the role of CLEC-2 in arterial thrombosis utilised murine CLEC-2 irreversibly-binding antibody, INU1, or CLEC-2-/- chimeras (May et al., 2009, Suzuki-Inoue, 2011). Both groups reported a reduction in arterial thrombus formation, however antibody inhibition of CLEC-2 increased tail bleeding time. This was furthered by the

introduction of the PF4-cre mouse, then thought to induce platelet-specific deletion of CLEC-2. Similar to previous investigations, a reduction in thrombus size, without arterial occlusion is described in these mice (Bender et al., 2013). This concurs with phenotypes we observe in this study using the novel GPIb-Cre mice to generate platelet-specific, CLEC-2-deficient mice. That being said, any contribution of CLEC-2 to arterial thrombosis has been accepted to be independent of classical ITAM signalling, confirmed through the generation of CLEC-2-presenting, ITAM-defective Y7A mice (Haining et al., 2017, Hughes et al., 2010a). This suggests that in mice, CLEC-2 acts as an adhesion receptor, and not a platelet-activating receptor; albeit the CLEC-2-binding 'anchor' remains under speculation. It has been suggested that CLEC-2 may bind to itself in both humans and mice with an affinity of 278 nM and 499 nM, respectively (Suzuki-Inoue, 2011), however this requires further investigation.

The crystal structure of murine CLEC-2 is unsolved, but is predicted to be similar to human CLEC-2 due to positional conservation of the N-linked glycosylation sites and disulphide bonds within the c-type lectin-like domain (Martin et al., 2021). In this study, we observe a key role for CLEC-2 in thrombus stability, regulating vascular occlusion in mice, but not humans. Irrespective of structure similarities, phenotypic disparities may be a result in the vast difference of receptor expression levels between the species. Human platelets have been described to have 2000-3700 copies of CLEC-2 receptor expression on the cell surface (Gitz et al., 2014), whereas murine platelets express around 40,000 copes (Dunster et al., 2020, Zeiler et al., 2014). Concurrently, there are large variations in ligand binding affinities trans-species; podoplanin binds a 100-fold higher affinity in mice (Lombard et al., 2018),

whereas hemin binds at an indifferent molarity (**data shown in chapter 4.6**) (Bourne et al., 2020). Copy number and/or ligand-binding affinity may explain the large difference observed in the significant way CLEC-2 contributes the thrombus growth in mice, but not humans.

Whilst we observe a limited role for CLEC-2 in human arterial thrombosis, this may provide exciting prospects for targeting fellow ITAM receptor GPVI as an anti-thrombotic target. GPVI is platelet specific, and using mice with a global GPVI-knockout (alongside CLEC-2$^{-/-}$GPIb-Cre^{-}) in this study significantly delayed the initiation and growth of thrombi post-ferric chloride injury. It is likely that any delayed thrombus formation observed in this mouse is thrombin-dependant. Alongside no haemostatic defects (Bender et al., 2011, Bender et al., 2013), GPVI inhibition is platelet specific and could prove to be the future in artery anti-thrombotic therapy.

In this study, whilst *in vivo* studies were blinded throughout procedures, presentation of blood-filled lymph nodes was evident in platelet-CLEC-2-deficient mice (Haining et al., 2017); to combat bias, analysis was blinded. A drawback of our studies in humans in the simplicity of the flow adhesion models – flowing over collagen does not accurately represent vasculature as the *in vivo* models do. In an attempt to battle simplicity, we perfused blood over TNF-α-activated HUVECs (Tull et al., 2006, Kuckleburg et al., 2011). However, vascular beds other than that performed in our study, such as pulmonary or hepatic sinusoidal endothelial cells, may induce discrepancy in CLEC-2 contributions to thrombosis (Jambusaria et al., 2020); this requires further elucidation. In the future, it may also be interesting to perform *in vivo*

thrombosis models in mice with humanised CLEC-2 and GPVI to observe if the copy number of CLEC-2 dictated the receptor's contribution to thrombus stability.

To conclude, we observe a clear role for CLEC-2 during murine thrombosis in major arteries and arterioles, as well as in *ex vivo* flow adhesion models. Inhibition of CLEC-2 by CLEC-2-blocking F(ab) fragments of AYP1, nor ligand inhibition by hFc-CLEC-2 modified thrombus surface coverage at arterial shear flow rates. Altogether, data shows that CLEC-2 does not contribute to arterial thrombosis in humans.

Chapter 4

Hemin induces platelet aggregation through CLEC-2 and is blocked by hydroxychloroquine

Data from this chapter has been published:

BOURNE, J. H., COLICCHIA, M., DI, Y., MARTIN, E., SLATER, A., ROUMENINA, L. T., DIMITROV, J. D., WATSON, S. P. & RAYES, J. 2020. Heme induces human and mouse platelet activation through C-type-lectin-like receptor-2. *Haematologica*.

Publication available in **Appendix 1**

4.1 Aims

The aim of this chapter was to explore the mechanism through which human and mouse platelets are activated by hemin, the oxidised form of haem. Using $FeCl_3$-induced arterial thrombosis, a model known to release free haem following injury. We aimed to pharmaceutically target arterial thrombus generation *in vivo* in a ferric chloride-induced model of arterial thrombosis using anti-malarial drug, hydroxychloroquine (HCQ).

4.2 Introduction

4.2.1 Intravascular haemolysis

Haemolysis involves the lysis of red blood cells, which releases their content into the neighbouring liquid or tissue, and can be categorised as intravascular or extravascular haemolysis. This process can be constructive, as it promotes the removal of damaged or senescent (biologically inactive) erythrocytes from circulation, hence allowing fresh cells to enter circulation in their 120-day cycle (Dhaliwal et al., 2004). Removal of erythrocyte debris largely occurs in the liver, through monocyte and macrophage (specifically Kupffer cell)-dependant phagocytosis, but can also occur in the spleen (Theurl et al., 2016). Conversely, erythrocyte lysis can also be detrimental in exacerbating the inflammatory response to infection or trauma and promoting thrombo-inflammation, subsequently leading to organ dysfunction in disease. Proteins which are classically critical during physiology, such as haemoglobin, suddenly become highly toxic to the circulatory

microenvironment upon release into circulation. The presence of intracellular erythrocyte proteins in blood plasma is associated with nitric oxide and ROS imbalance, haem-induced activation of neutrophils and monocytes, alongside platelet activation. Furthermore, haem and haemoglobin can be found to be extravasated to tissue post-haemolysis, which further drives organ damage. Unlike intravascular haemolysis, intracellular erythrocyte content is not found in plasma post-extravascular haemolysis, as protein is contained by phagocytosing, tissue-resident macrophages, and stored as ferritin deposits (Rapido et al., 2017). During physiology, defence mechanisms are in place to accommodate the inevitable presence haemoglobin and haem in blood plasma, and to limit their toxicity; notably haptoglobin and haemopexin.

4.2.2 Scavenging system

Alongside pro-thrombotic mediators such as ADP and arginase, haem and haemoglobin are drivers in haemolysis-dependant thrombus generation. Erythrocyte destruction is somewhat inevitable, as a results of high shear flow rates in the microcirculation (Sohrabi and Liu, 2017). Furthermore, haemolysis can occur during pathogen-driven infection, or as a result of trauma, such as crush syndrome (Orf and Cunnington, 2015, Okubo et al., 2018). Haem is detected following rhabdomyolysis, which is the destruction of muscles whereby haem is released from myoglobin. With this in mind, means are required to remove toxic intracellular components released as a result of haemolysis. There are both extracellular and intracellular mechanisms in plasma to limit haemolysis-induced injury. Extracellular plasma glycoprotein, **haptoglobin**, is produced in the liver which functions to limit kidney injury through

irreversibly binding to free haemoglobin. The highly stable haptoglobin-haemoglobin binding has a high affinity, and the physiological concentration of haptoglobin (38-208 mg/dL) is sufficient to clear 3 g of haemoglobin (Sadrzadeh and Bozorgmehr, 2004). Upon binding, the haptoglobin-haemoglobin complex is cleared by Kupffer cells in the liver, $CD164^{+}$ macrophages or hepatocytes (Schaer et al., 2006, Kristiansen et al., 2001). The complex clearance removes the prospect for the iron contained within haemoglobin to be oxidised. Upon internalisation from the phagocytosing cells, hemin is released from haemoglobin post-degradation to be further processed by secondary clearance proteins haem-oxygenase 1 (HO-1) and haemopexin.

Second extracellular plasma protein, **haemopexin,** is also upregulated during inflammatory conditions. Interestingly, the glycoprotein produced in the liver has the highest, and irreversible binding affinity for free haem (<1 pM) (Lin et al., 2015). The haemopexin-haem complex is recognised by hepatocytes and macrophages in the liver through the low-density lipoprotein receptor-related protein-1 and are subsequently phagocytosed (Immenschuh et al., 2017). Upon cellular internalisation, hemin is released into the cell cytoplasm, whereby it can either by catabolised by HO-1, or can be recycled and repurposed into haem-based proteins such as haemoglobin. Haemopexin is immunoprotective during multiple inflammatory diseases (Hahl et al., 2013, Poillerat et al., 2020), and has been shown to limit the sepsis-induced cytokine storm during sepsis through inhibiting complement activation (Immenschuh et al., 2017, Poillerat et al., 2020). Furthermore, mice deficient in haemopexin have severe acute kidney post-haemolytic stress, which was blocked with haemopexin treatment in these mice (Ofori-Acquah et al., 2020).

HO-1 is an intracellular enzyme which is able to catabolise free hemin into free iron, alongside by-products biliverdin and carbon monoxide (Chung et al., 2008). Subsequent to binding to free haem in plasma, HO-1 accelerates its oxidative degradation through cleaving haem at the α-methene carbon bridge (Tenhunen et al., 1969). Its expression is relatively low during physiology (with the exception of the spleen), unlike its constituently expressed isoform HO-2, but is upregulated during pathophysiological conditions (Maines et al., 1986). HO-1 is immunosuppressive and immunoprotective during haemolytic diseases, such as sepsis, whereby the enzyme is rapidly upregulated (Immenschuh et al., 2017). Mice deficient in HO-1 accelerates $FeCl_3$- and hemin-induced vascular occlusion *in vivo* and clot size *ex vivo* in perfusion models (Peng et al., 2004). Not only is HO-1 protective through removing free, pro-inflammatory haem, but bilirubin, a product of metabolised biliverdin released from haem catalysis, has been shown to act as an antioxidant *in vitro*, protecting endothelial cells from oxidation-driven inflammation (Ziberna et al., 2016). Secondary biproduct, carbon monoxide, also has vasodilatory and anti-inflammatory properties.

In physiology extracellular mechanisms are sufficient to limit free haem. Failing that, intracellular HO-1 acts as a backup to reduce free haem. Together, they inhibit haem-induced inflammation.

4.2.3 Haemolysis in congenital and infectious disease

Haemolytic disorders arise upon chronic and sustained lysis of red blood cells, premature to their 120-day life expectancy. Genetic predisposition can lead to diseases, such as sickle cell disease and haemolytic uremic syndrome (HUS), or otherwise diseases are acquired, such as sepsis-induced autoimmune haemolytic anaemia (Chaplin and Zarkowsky, 1981). Patients can display early signs of haemolytic disease through anaemia, as a result of erythrocyte lysis at a higher rate than their production. However more generally, patients present later with acute renal injury, and eventual organ dysfunction, which can lead to haemolytic-induced mortality (Qian et al., 2010).

Sickle cell disease is an inherited single point mutation, which leads to morphological modifications in red blood cell structure and reduces oxygen affinity. Sickle erythrocytes have an altered membrane rigidity, as a result of modifications in their lipid bilayer, alongside subsequent cellular dehydration (Allan and Raval, 1983, Kuypers, 2014). These alterations in morphology leads to a high probability of haemolysis premature to their expected life span, which is reduced by >75 %, compared to healthy erythrocytes (Quinn et al., 2016). Furthermore, 2, 3-diphosphoglycerate is upregulated in sickle erythrocytes, which interacts with the β-globin subunit to reduce oxygen-binding affinity for haemoglobin (Rogers et al., 2013). As in physiology, erythrocyte lysis leads to the release of intracellular proteins such as haem and haemoglobin. However, the overwhelming and sustained rate of haemolysis in patients with sickle cell disease completely exhausts the scavenging mechanisms of HO-1, haemopexin and haptoglobin, and hence they are no longer

sufficient to metabolise these proteins. This results in large quantities of free haem, 2 to 50 μM, in blood plasma (Gouveia et al., 2017), inducing a crisis in patients. Together, these characteristics induce varying severity of unpredictable symptoms of pain and widespread organ damage. The complexities and multidimension of sickle cell disease makes treatment of acute and chronic symptoms challenging, whereby life expectancy in patients in reduced by 3 decades (Kato et al., 2018). HCQ is used to induce foetal haemoglobin expression and reduce leukocyte count, hence increasing oxygen affinity and simultaneously reducing the inflammatory response (McGann and Ware, 2015). Other, more invasive treatments include haematopoietic stem cell transplantations and erythrocyte transfusions, to replenish circulating red blood cell count. However, these methods are somewhat futile, and further replenishment is necessary in succession of the 120-day life cycle of a red blood cell.

Sepsis and other systemic inflammatory events have demonstrated extraordinary levels of free haem, following haemolysis, relative to the severity of inflammation (Adamzik et al., 2012, Janz et al., 2013). The pathogenesis and leukocyte-driven inflammatory events of sepsis will be explored in Chapter 5, but ultimately sepsis-induced inflammation is exacerbated by resultant haemolysis and free haem and haemoglobin. The presence of free haem during sepsis has been shown to detriment clinical outcome (Larsen et al., 2010). LPS has been shown to bind to haemoglobin during inflammatory events, which induces morphological changes and subsequently generates “microbicidal free radicals” – a molecule with dual toxicity in circulation (Bahl et al., 2011). The mechanisms through which sepsis induces intravascular haemolysis is somewhat ambiguous, perhaps due to the complex and dynamic

nature of the pro- and anti-inflammatory events in septic patients. It has been speculated that lysis could be a result of disseminated intravascular coagulation (DIC) (Bahl et al., 2014), complement-induced immune haemolysis (Stowell et al., 2012), microvascular stasis (Koch et al., 2001) or LPS-induced manipulation of the erythrocyte membrane (Poschl et al., 2003, Nagel et al., 2015). Whilst the direct origin of haemolysis if unknown, it is likely to be a combination of the listed causes, adding to the complexities of the disorder and hence the difficultly to treat. There is currently minimal treatment for sepsis. More recently inhibition of the complement system during paroxysmal nocturnal haemoglobinuria has limited inflammation-driven haemolysis (Schubert and Roth, 2015), although this unfortunately was not translated to sepsis, due to the multifactorial nature of haemolysis in septic patients.

4.2.4 Haemolytic disease-induced hypoxia

Hypoxia (low tissue oxygen level) is induced by hypoxemia (low blood oxygen level), and is a common symptom of severe haemolytic disease. The cause of hypoxia in these patients is often multifactorial (Machogu and Machado, 2018), hence highly difficult to treat, but is generally a result of cardio-respiratory dysfunction and hypoventilation. Hypoxia is commonly associated with episodes of crisis and increased haemolysis. This could be explained through hypoxia-induced red blood cell membrane dysfunction by modulation of blood viscosity, and hypoxia-regulated erythrocyte-ATP release (Dietrich et al., 2000, Wang et al., 2005a, Huang et al., 2011). ATP induces the activation of endothelial cells through P2Y receptors, and NO production (Wang et al., 2005a). Furthermore, alongside promoting haemolysis,

hypoxia has been shown to downregulate HO proteins, hence inducing a positive feedback loop of increasing severity.

4.2.5 Haem and platelet ferroptosis

Haem is an Fe^{3+} ion-containing protoporphyrin IX with an associated chloride ligand, which is rapidly converted to hemin immediately upon oxidisation (Camejo et al., 1998). Haem is integral to multiple haemoproteins, most importantly haemoglobin, which is critical to oxygen storage and transfer in circulation by erythrocytes, and makes up a significant aspect of the 2 α- and β-subunits of haemoglobin, therefore is essential in all aerobic bodily functions. The iron-containing compound consists of a tetrapyrrole ring, and is used for the catalysis of oxidoreduction systemically (Roumenina et al., 2016) In physiology, haem exclusively resides in vasculature, and is beneficial when contained within erythrocytes. Its toxicity upon exhaustion of the haem and haemoglobin scavenging systems during haemolytic disease not only induces high levels of inflammation through oxidative stress and lipid peroxidation (Chiabrando et al., 2014), but also is understood to be a strong platelet agonist, although the mechanism is not well understood.

Classical cell death is categorised into apoptosis (programmed cell death) and necrosis (unplanned, externally-modulated cell death), however new mechanisms with distinct characteristics such as autophagy have been described (Glick et al., 2010). First described in 2012, a mechanism distinct from previously described death pathways was identified – ferroptosis (Dixon et al., 2012). This iron-dependant cell death was characterised by a build-up of ROS, and is both morphologically and

biologically dissimilar to previously described pathways. Specifically, cells do not swell as in necrosis, shrink as in apoptosis, nor have a canonical membrane bilayer as in autophagy (Li et al., 2020b). Interestingly, ferroptosis induces mitochondrial shrinkage through dissemination of the mitochondrial cristae, in turn inducing cell death (Yang and Stockwell, 2008, Dixon et al., 2012). The mechanism for this event is well understood, and includes classical death regulator, P53, but also GPX4, which mediates cellular lipid peroxidation. Iron-containing haem is an inducer of ferroptosis in cells (NaveenKumar et al., 2018).

Free haem in patients undergoing haemolytic crisis induces severe DIC. Platelet ferroptosis occurs through the release of iron and free radical ions post-haemolysis, normally mediated by HO-1, to induce hemin-facilitated lipid peroxidation and ROS generation (NaveenKumar et al., 2018, NaveenKumar et al., 2019). During haemolytic diseases such as sickle cell disease, platelets express high levels of activation markers, P-selectin and activated integrin αIIbβ3 (Zhang et al., 2016). Interestingly, thrombi are found at a range of severities of haemolytic disease, suggesting that the concentration of haem may dictate the number of aggregates found in patients. ADP was initially thought to be contributing to vaso-occlusive crisis during sickle cell disease, however the DOVE (Determining effects of platelet inhibition on vaso-occlusive events) study showed blocking P2Y12 did not improve outcome, suggesting another mechanism for platelet activation must exist (Hoppe et al., 2016). This may explain aggregation formation in patients with a lower concentration of free haem.

4.2.6 Haem-induced neutrophil and endothelial activation

Further to platelet activation, haem interacts with other cells in vasculature to promote additional inflammation and thrombus generation. Haem can directly activate endothelial cells through TLR4, and induce vascular occlusion during haemolytic disease through rapid upregulation of vWF and P-selectin on endothelial surfaces (Belcher et al., 2014). This rapid induction of endothelial activation promotes platelet adhesion to the endothelium, and hence indirectly promotes thrombus growth. Interestingly, sickle erythrocytes express an arsenal of unusually upregulated adhesion molecules, integrin $\alpha 4\beta 1$, platelet glycoprotein 4 and basal cell adhesion molecule to promote their adhesion to the endothelial wall (Wagner et al., 2004). This combination of haem-induced platelet adhesion and erythrocyte adhesion to the endothelium promote vaso-occlusion in haemolytic disease.

Neutrophils have specialised pattern recognition receptors to isolate and respond to lethal pathogens/compounds which are categorised to damage- (DAMPs) and pathogen-associated molecular patterns (PAMPs). Haem, recognised as a DAMP, is able to directly induce neutrophil infiltration and activation, characterised by increased ROS and pro-inflammatory cytokine, IL-8 (Graca-Souza et al., 2002). Interestingly, haem-induced neutrophil activation promotes the production of NETs (Kono et al., 2014, Chen et al., 2014). Whilst NETs are classically associated with pathogen capture to promote the resolution of inflammation, they are associated with vascular occlusion in haemolytic disease. Moreover, platelet-neutrophil aggregates are observed in patients with haemolytic disease, which further promotes neutrophil

activation through haem-activated, P-selectin expressing platelets (Polanowska-Grabowska et al., 2010).

4.2.7 Hydroxychloroquine

HCQ ($C_{18}H_{26}ClN_3$) is an alkylated 4-aminoquinoline and has precursors dating back to the 1600's by the Jesuits of Chile who discovered that the bark of the cinchona tree could cure malaria, coined 'quinine' in the 1900's (Fox, 1993). Wars and invasions led to extinction of the natural supply of the drug, hence the generation of synthetic alternatives with progressively decreasing side effects led to the development of HCQ. The drug is widely accepted, and a highly effective antimalarial; the mechanism through which the drug functions is not well understood. It has been speculated that the drug may function through modulating lysosomal activity, autophagy and/or inhibition of TLR-mediating signalling pathways (Schrezenmeier and Dorner, 2020). Interestingly, another mechanism has been described, speculating the antimalarial properties of HCQ through modulation of haem. Malaria is characterised by parasitic invasion of erythrocytes, whereby they digest the intracellular haemoglobin, which eventually leads to cerebral oxygen-deprivation (Fitch, 1998). Interestingly, parasites release intracellular haem post-haemoglobin digestion. To avoid the toxicity of free haem, parasites cleverly store haem in crystallised deposits, haemozoin. It has been shown that HCQ can bind to haem to form a complex which is free from haemozoin, and is hence toxic to parasites (Ginsburg and Geary, 1987, Martin et al., 2009, Combrinck et al., 2013). Although HCQ has been repurposed for use in patients with rheumatoid arthritis, the HCQ-haem complex has not been studied outside of malaria. We predict that the

drug may scavenge free haem in the context of haemolytic disease, and could be exploited therapeutically.

In this chapter, we investigate a novel mechanism of platelet activation through which haem can activate human and mouse platelets which can be exploited therapeutically. Furthermore, we utilise antimalarial HCQ in an attempt to limit free haem in circulation in an *in vivo* model of thrombosis by $FeCl_3$. Analysis extends to the aggregation and activation of human and mouse platelets by hemin in the presence of HCQ. Should this be effective, the drug could be applied to haemolytic disease to limit free haem, and hence reduce symptoms in patients.

4.3 Results

4.3.1 Hemin activates platelets in a dose-dependent manner

Haemolytic disease exhausts the scavenging system leading to free hemin in patients' blood plasma in concentrations ranging from 2 to 50 μM (Maeda et al., 2006, Gouveia et al., 2017) This is associated with haem-induced thrombosis, although the mechanism is not well understood. Here, we show that hemin induces swift platelet aggregation at a low concentration (3.12-12.5 μM) which is interestingly slow with reduced maximum aggregation at high dose (>25 μM), suggesting two distinct mechanisms **(Figure 4.1A, B)**. Hemin-induced aggregation in this fashion was associated with an increase in platelet activation, demonstrated by increased P-selectin upregulation and GPIIb/IIIa activation **(Figure 4.2A-D)**. Interestingly, annexin V was significantly upregulated upon activation by high dose hemin (>25μM), but not mid- or low-dose hemin **(Figure 4.2E)**, supporting a toxic effect of high doses on platelets. Hemin induced the phosphorylation of syk and PLCγ2 at all concentrations, without altering total protein expression of syk or PLCγ2, but to a lesser extent at 50μM **(Figure 4.2F)**. Syk phosphorylation suggests the inclusion of an ITAM receptors in hemin-mediated platelet activation, independent of ferroptosis.

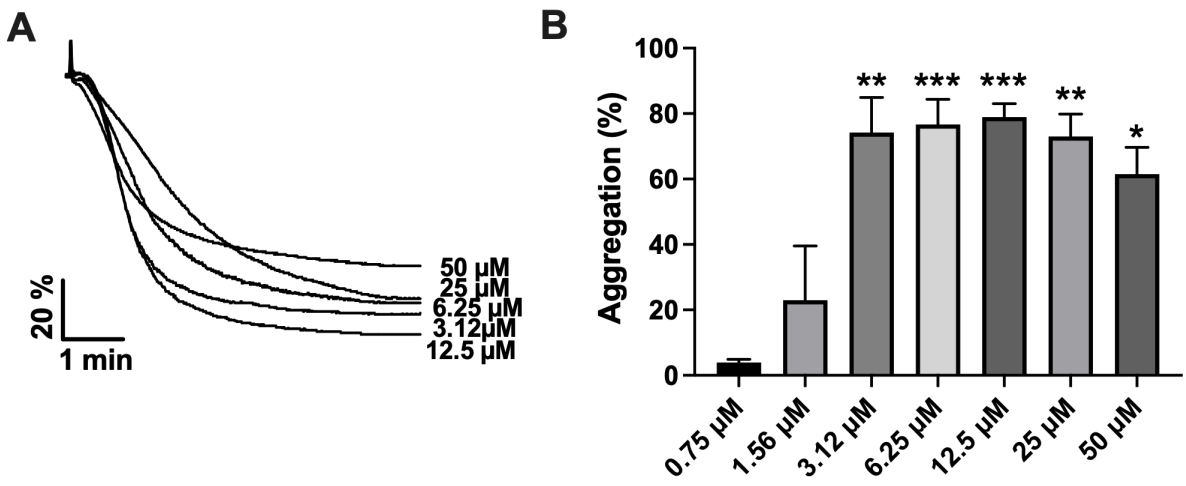

Figure 4.1 – Hemin-induced washed platelet aggregation. Washed platelet aggregation was assessed by light transmission aggregometry for 6 min under stirring conditions at 37 °C. **(A)** Representative platelet aggregation traces induced by hemin (2.12-50 µM) shown and **(B)** maximum aggregation was calculated (n=6). The statistical difference between multiple groups was analysed using a paired one-way ANOVA with Tukey's multiple comparisons test, *$p < 0.05$ **p < 0.01 ***p < 0.001.

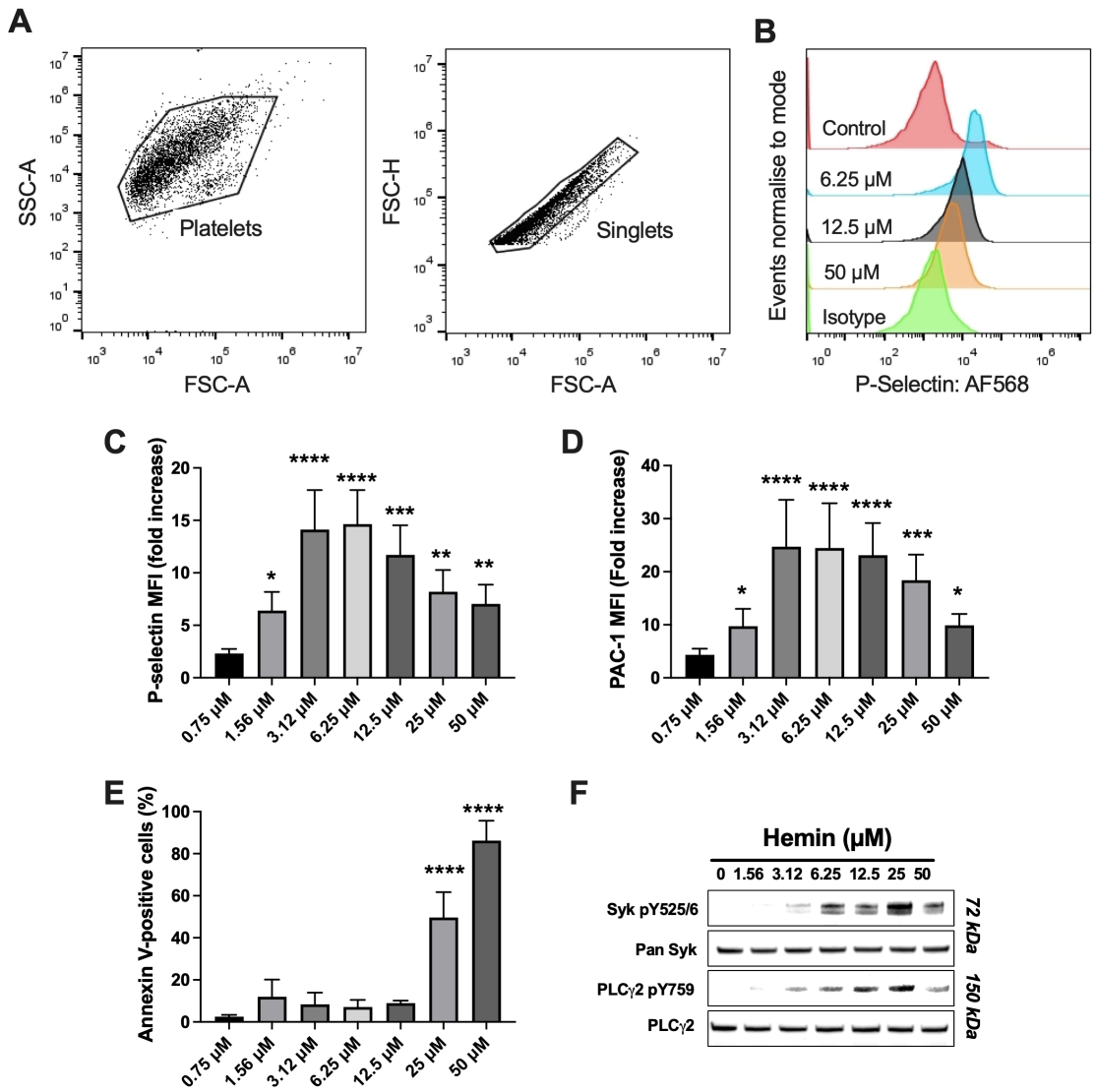

Figure 4.2 – Hemin-induced washed platelet activation and apoptosis. Washed platelets were incubated in the presence of hemin (0.75-50 µM) for 30 min. **(A-E)** Protein surface expression was quantified by flow cytometry, using a **(A)** gating strategy to identify live and single cells, for **(B, C)** P-selectin, **(D)** PAC-1 and **(E)** Annexin V versus an IgG isotype control (n=4). **(F)** Phosphorylated syk (pY525/6) and PLCγ2 (Y759) were assessed in whole platelet lysate post-hemin stimulation, alongside total syk and PLCγ2 controls. Western blot representative of 4 independent experiments. The statistical difference between multiple groups was analysed using a one-way ANOVA with Tukey's multiple comparisons test, *$p < 0.05$ **p < 0.01 ***p < 0.001 ****p < 0.0001.

4.3.2 Hemin activates human and mouse platelets through CLEC-2

To identify the receptor involved in hemin-mediated platelet activation, we screened extracellular and intracellular inhibitors for platelet receptors. Platelet activation by hemin (6.25 μM) was not altered by inhibition of the classical hemin receptor, TLR4, assessed using TAK-242, or by classical anti-platelet drugs targeting COX (indomethacin) or P2Y12 (Cangrelor). Platelet activation by hemin (6.25 μM) was inhibited by Src family kinase inhibitor PP2 (20 μM), syk inhibitor PRT-060318 (20 μM) or BTK inhibitor, Ibrutinib (500 nM) suggesting an implication of platelet-ITAM receptors. Addition of recombinant hFc-CLEC-2 (10 μg/ml), but not recombinant GPVI (hFc-GPVI; 10 μg/ml), inhibited platelet activation by hemin, identifying CLEC-2 as the receptor for hemin on platelets. CLEC-2 monoclonal antibody AYP1, which inhibits podoplanin-CLEC-2 interaction failed to inhibit platelet activation, suggesting that CLEC-2 does not share the same binding site with podoplanin (**Figure 4.3A, B)**. Interestingly mouse platelets were less sensitive to hemin, compared to human platelets. Hemin induced mouse platelet aggregation at concentrations higher than 12.5 μM **(Figure 4.4A, B)**. Mirroring humans, aggregation was induced to a lesser extent at 50 μM, compared to lower doses of hemin. As with human platelets, hemin-induced murine platelet activation was inhibited by PP2, PRT-060318, Ibrutinib and murine recombinant dimeric CLEC-2 (mFc-CLEC-2) and Integrilin **(Figure 4.4D)**. CLEC-2-blocking antibody, AYP1 failed to block hemin-induced aggregation. CLEC-2 specificity was further confirmed, as hemin does not aggregate CLEC-2-deficient murine platelets **(Figure 4.5A, B)**. This demonstrates that low- and mid-dose hemin activates platelets through CLEC-2.

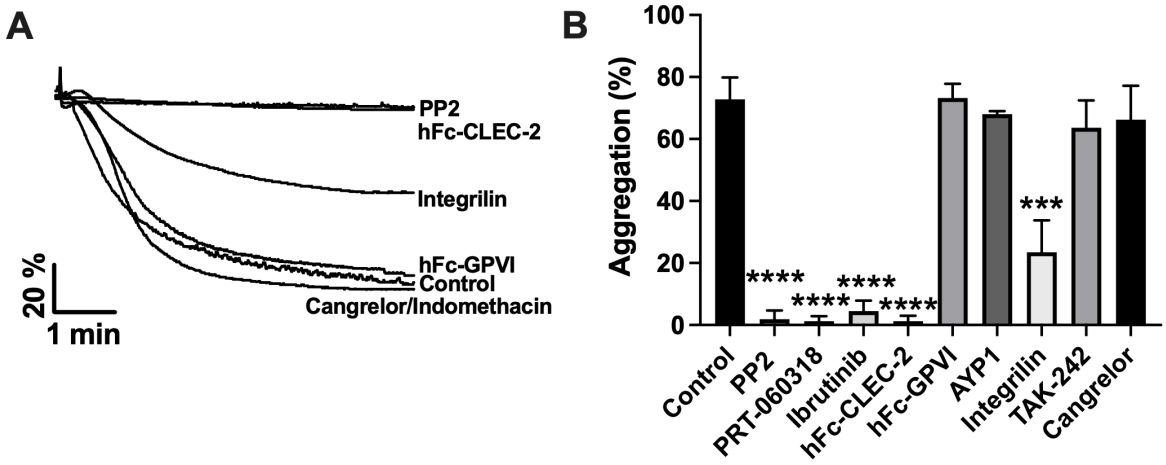

Figure 4.3 – Low-dose hemin activates human platelets in a syk-dependant manner. Washed platelet aggregation was assessed by light transmission aggregometry for 6 min under stirring conditions at 37 ^{o}C. **(A)** Representative aggregation traces of washed platelets activated by 6.25μM hemin and were pre-incubated with Ibrutinib (500 nM), PP2 (20 μM), PRT-060318 (20 μM), TAK-242 (10 μM), AYP1 (10 μg/ml), hFc-CLEC-2 (10 μg/ml), hFc-GPVI (10 μg/ml) or Cangrelor (10 μM) for 5 min at 37 ^{o}C shown. **(B)** Maximum aggregation was calculated (n=5). The statistical difference between multiple groups was analysed using a one-way ANOVA with Tukey's multiple comparisons test, ***$p < 0.001$ ****$p < 0.0001$.

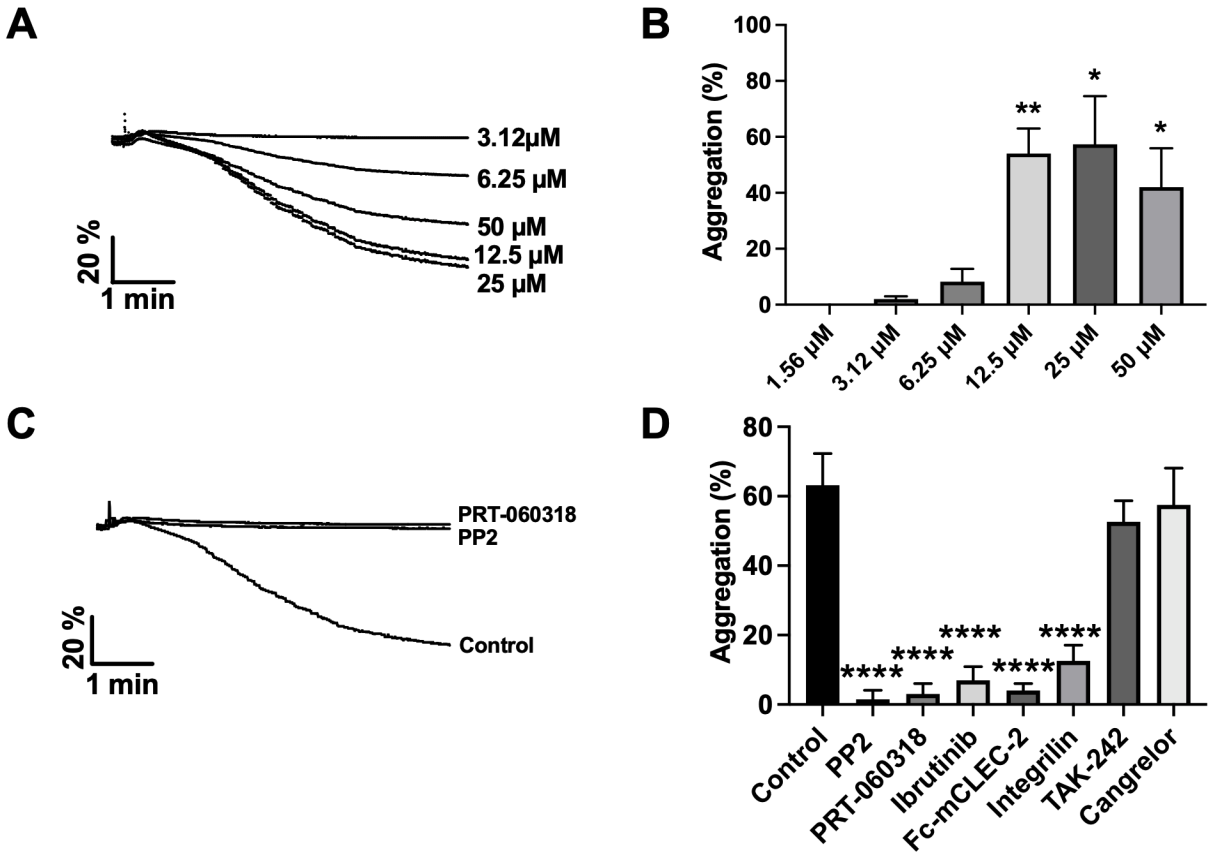

Figure 4.4 – Hemin activates and aggregates mouse platelets through CLEC-2. Washed platelet aggregation was assessed by light transmission aggregometry for 6 min under stirring conditions at 37 ^{o}C. **(A)** Representative platelet aggregation traces induced by hemin (1.56-50 µM) shown and **(B)** maximum aggregation was calculated (n=5). **(C)** Representative aggregation traces of washed platelets activated by 12.5µM hemin, with pre-incubated of Ibrutinib (500 nM), PP2 (20 µM), PRT-060318 (20 µM), TAK-242 (10 µM), or Cangrelor (10 µM) for 5 min at 37 ^{o}C shown and **(D)** maximum aggregation was calculated (n=6). The statistical difference between multiple groups was analysed using a one-way ANOVA with Tukey's multiple comparisons test, ***$p < 0.001$ ****$p < 0.0001$.

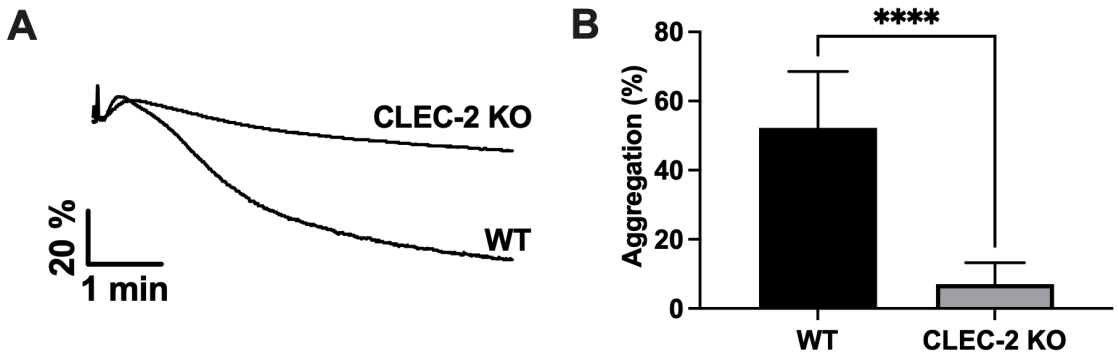

Figure 4.5 – CLEC-2-deficient platelets are not aggregated in response to hemin. Washed platelet aggregation from wild type (WT) or CLEC-2-deficient (CLEC-2 KO) mice was assessed by light transmission aggregometry for 6 min under stirring conditions at 37 ^{o}C. **(A)** Representative platelet aggregation traces induced by hemin (12.5 μM) are shown and **(B)** maximum aggregation was calculated (n=5). The statistical significance between 2 groups was analysed using an unpaired t-test, ****p<0.0001.

4.3.3 Hemin directly binds to human and mouse recombinant CLEC-2

The fact that recombinant CLEC-2 inhibits hemin mediated platelet aggregation suggests a direct interaction between hemin and CLEC-2. Using a surface plasmon resonance-based technique, we show hemin binding to both murine and human recombinant CLEC-2, both of which binding with a high affinity ~200nM **(Figure 6A, B).** Similar values of kinetic rate association and dissociation of hemin binding to mFc-CLEC-2 and hFc-CLEC-2. The interaction of hemin with human and mouse CLEC-2 was further confirmed by UV-vis absorbance spectroscopy **(Figure 6C, D)**. The differential absorbance spectra profiles presented spectra shifts of hemin by human and mouse CLEC-2, demonstrating direct binding.

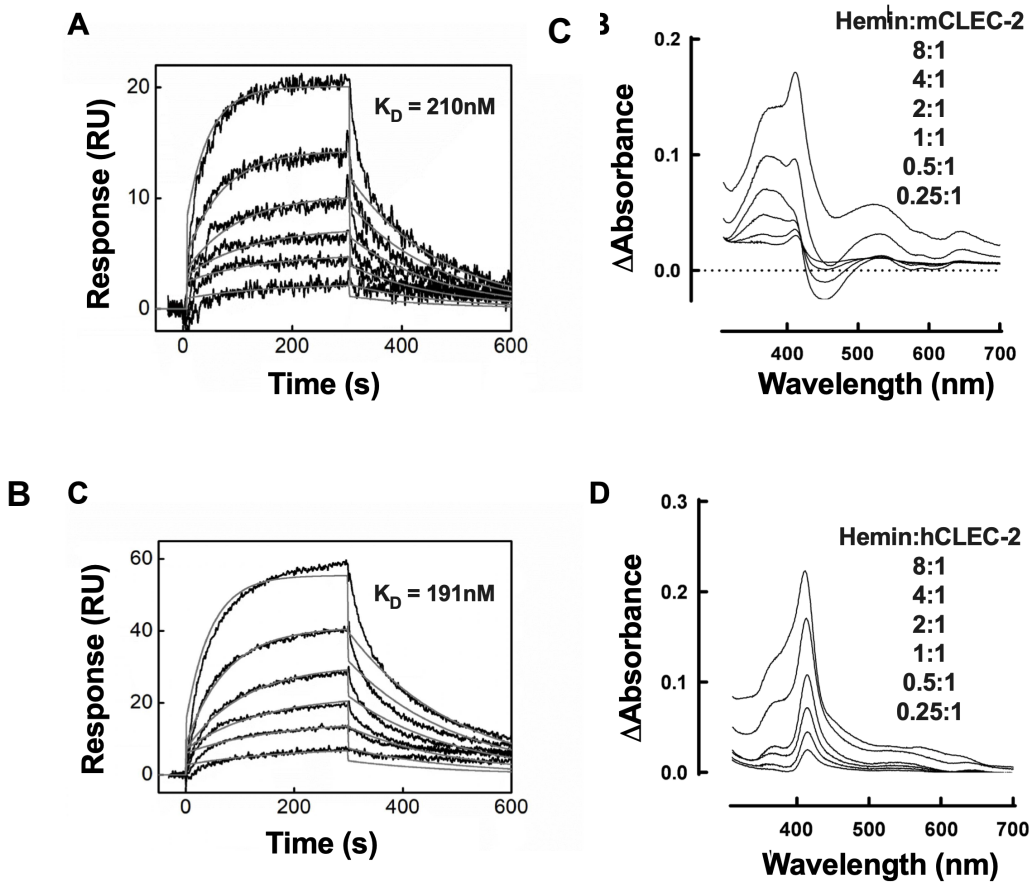

Figure 4.6 – Hemin binds to human and mouse hFc-CLEC-2. (A, B) Surface plasma resonance presented real-time interaction profiles obtained with increasing concentrations of hemin (5, 20, 50, 100, 250, 500nM) over **(A)** murine CLEC-2-Fc and **(B)** human hFc-CLEC-2 immobilised on a CM5 sensor chip. The association and dissociation phases were followed for 5 min. K_D was calculated using a Langmuir global analyses model. **(C, D)** UV-vis absorbance spectroscopy generated differential spectra post-titration of **(C)** mCLEC-2 or **(D)** hFc-CLEC-2 (2 μM) with increasing concentrations of hemin (0.5–16 μM). The differential spectra were obtained after subtraction of the spectra of hemin at a given concentration, from the spectra of the same concentration of hemin in the presence of the protein. The measurements were done at 25 °C in optical cell with 10 mm light path.

4.3.4 Hydroxychloroquine limits hemin-induced murine platelet activation through CLEC-2

HCQ is used in malaria to bind to haem, which increases its toxicity to parasite-containing erythrocytes. Its toxicity to platelets has not been reported, hence we wanted to investigate if the drug-hemin complex could be exploited therapeutically post-haemolysis. Interestingly, low- and mid-dose hemin-induced mouse platelet aggregation (10 and 25μM, respectively) was inhibited by pre-treatment with HCQ (50 μM) **(Figure 4.7A-D)**. This was translated to an *in vivo* model which has been shown to release haem, the $FeCl_3$-induced thrombosis model of the carotid artery. we show that thrombus growth and vascular occlusion post-injury is impaired with HCQ treatment (10 mg/kg), compared to saline-treated mice **(Figure 4.8A, B)**. Treatment presented a 69.5 % decrease in thrombus size, calculated by AUC and final thrombus size versus saline controls **(Figure 4.8C, D)**. To further understand how thrombus size was reduced, and if it was a result of hemin toxicity to platelets, we analysed platelet death and activation markers *ex vivo.* HCQ treatment of washed mouse platelets was associated with a significant decrease in P-selectin and annexin V presentation post low-, mid- and high-dose hemin (10, 25 and 50 μM, respectively) **(Figure 4.9A, B)**. It was also necessary to assess the specificity of HCQ inhibitory activity on hemin-induced platelet activation and aggregation. CRP-, thrombin-, nor rhodocytin-induced platelet aggregation was reduced when platelets were treated with HCQ **(Figure 4.10A-C)**. This demonstrates a specific role for the drug in inhibiting hemin-platelet-CLEC-2 binding to induce platelet activation, in mice.

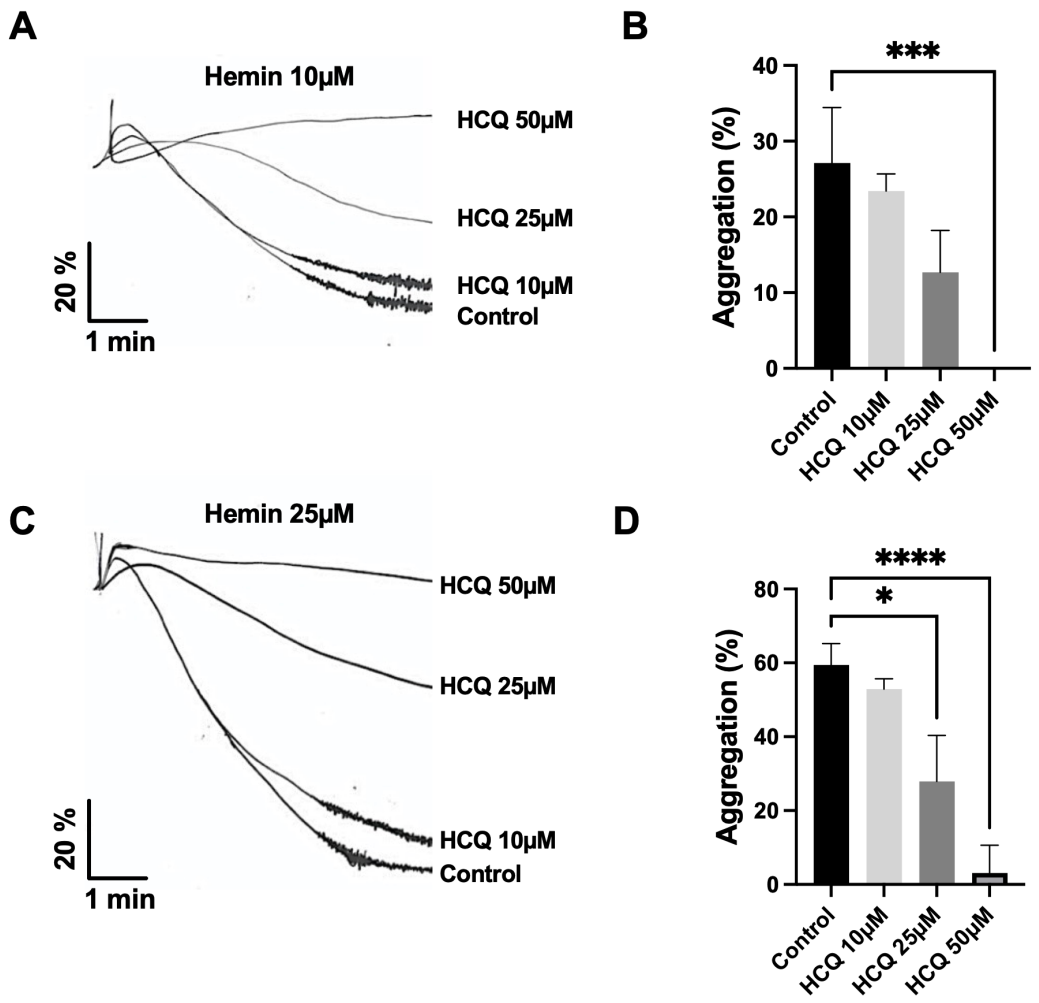

Figure 4.7 – Hydroxychloroquine inhibits hemin-induced mouse platelet aggregation. Washed mouse platelet aggregation was assessed by light transmission aggregometry for 6 min under stirring conditions at 37 ^{o}C. Platelets were pre-incubated with hydroxychloroquine (HCQ), or buffer for 5 min pre-aggregation at 37 ^{o}C. **(A)** Representative platelet aggregation traces induced by hemin (10 μM), in the absence or presence of HCQ (10-50 μM) are shown and **(B)** maximum aggregation was calculated (n=5). **(C)** Representative platelet aggregation traces induced by hemin (25 μM), in the absence or presence of HCQ (10-50 μM) are shown and **(D)** maximum aggregation was calculated (n=5). The statistical significance between 2 groups was analysed using a paired one-way ANOVA with Tukey's multiple comparison test, *p<0.05, ***p<0.001, p<0.0001.

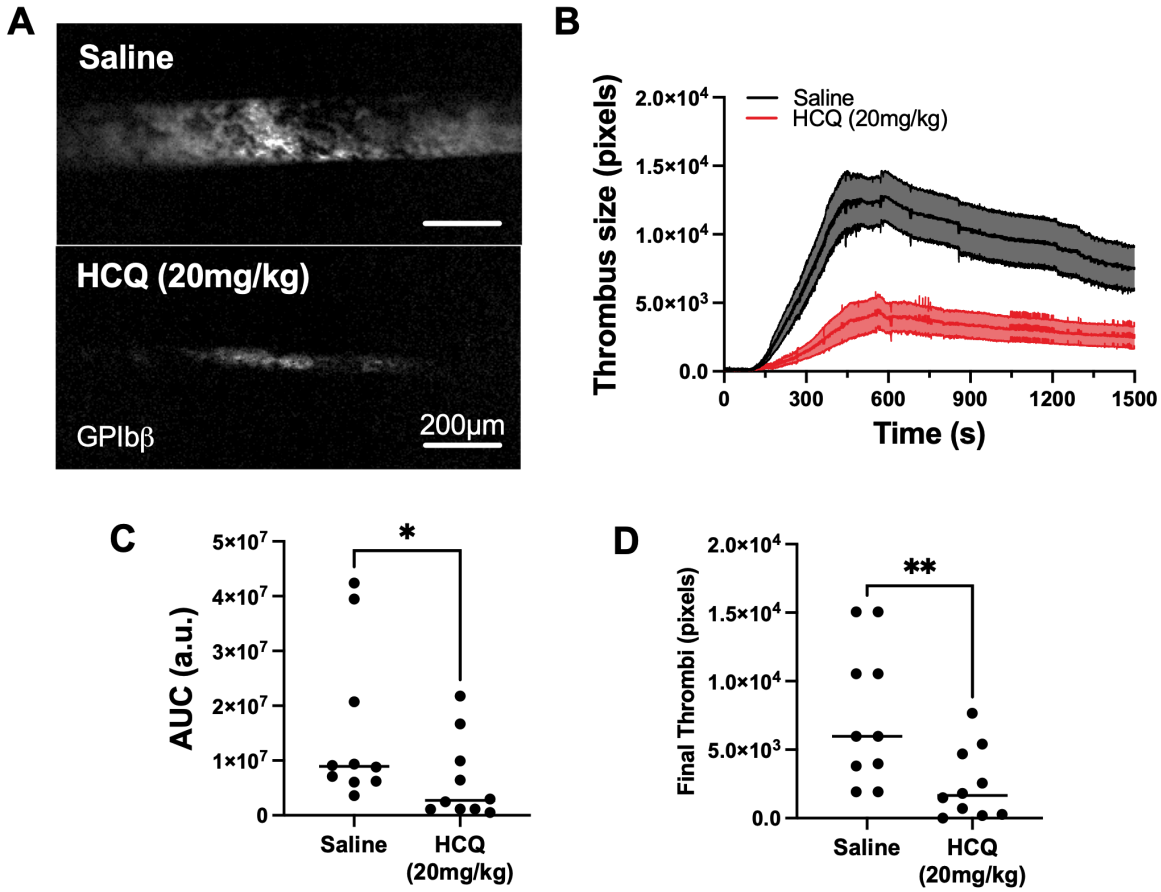

Figure 4.8 – Hydroxychloroquine reduces thrombus size post-$FeCl_3$ injury of the carotid artery in mice. Wild type mice were treated with hydroxychloroquine (HCQ; 10 mg/kg), or 200µl saline for 30 min prior to $FeCl_3$-soaked filter paper-challenge (10%, 3 min) on the carotid artery. **(A)** Representative images are shown at 25 min post-injury, and **(B)** thrombus size was quantified over 25 min by GPIbβ-antibody fluorescence using confocal microscopy. **(C)** The area under the curve (AUC; a.u.=arbitrary units) and **(D)** final thrombus size was calculated (n=10). The statistical difference between multiple groups using one-way ANOVA with Tukey's multiple comparisons test. *$p < 0.05$ **$p < 0.01$

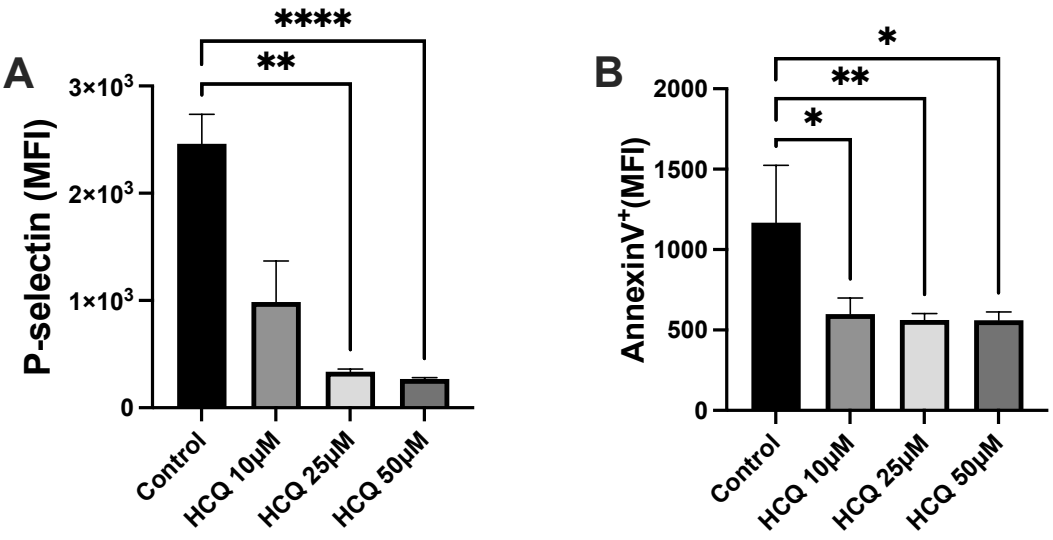

Figure 4.9 – Mouse platelet activation and apoptosis is inhibited by hydroxychloroquine. Washed platelets were incubated in the presence of hemin (10 μM), with or without hydroxychloroquine (HCQ) for 30 min. Protein surface expression was quantified by flow cytometry, for **(A)** P-selectin and **(B)** Annexin V (n=6). The statistical difference between multiple groups was analysed using a paired one-way ANOVA with Tukey's multiple comparisons test, *$p < 0.05$ **$p < 0.01$ ****$p < 0.0001$.

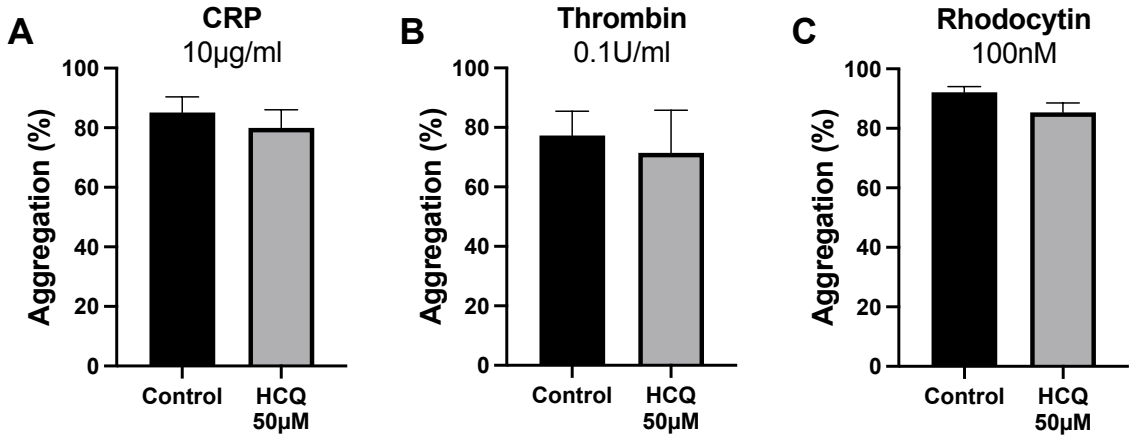

Figure 4.10 – CLEC-2, GPVI nor PAR-3/4 are inhibited by hydroxychloroquine in mice. Washed mouse platelet aggregation was assessed by light transmission aggregometry for 6 min under stirring conditions at 37 ^{o}C. Platelets were pre-incubated with hydroxychloroquine (HCQ), or buffer for 5 min pre-aggregation at 37 ^{o}C. Maximum aggregation was calculated induced by **(A)** CRP (10 µg/ml), **(B)** thrombin (0.1 U/ml) and **(C)** rhodocytin (100 nM), in the absence or presence of HCQ (50 µM) are shown (n=6). The statistical significance between 2 groups was analysed using a paired t-test.

4.3.5 Hydroxychloroquine inhibits hemin-induced platelet activation and aggregation by CLEC-2

If the specific inhibition of hemin-induced aggregation could be translated to human, it could provide a promising drug during haemolytic disease. Low- and mid-dose hemin-induced human platelet-aggregation (5 and 10 μM, respectively) was inhibited by 100 μM HCQ in a dose-dependent manner **(Figure 4.11A-D)**. This was associated with a decrease in P-Selectin and annexin V presentation in the presence of HCQ, post-hemin stimulation, compared to controls **(Figure 4.12A, B)**. Importantly, CLEC-2 and GPIb (CD42b) receptor levels were unchanged in the presence of HCQ, post-hemin stimulation **(Figure 4.12C, D)**.

It was necessary to assess the specificity of HCQ inhibitory activity on hemin-induced human platelet activation and aggregation. Aggregation induced by rhodocytin (100 nM) nor thrombin (0.1 U/ml) was altered by HCQ (100 μM) **(Figure 13A, B)**. Furthermore CRP-induced (3 and 10 μg/ml) human platelet aggregation was not altered, alongside no alterations in P-Selectin or annexin V presentation **(Figure 13C-E)**. This was echoed by unaltered TRAP-induced (100 μM) platelet aggregation and activation in the presence of HCQ post-hemin stimulation.

The clear specificity and translation quality of HCQ in limiting platelet aggregation and activation in response to hemin makes for an exciting drug and therapeutic target for patients with haemolytic disease.

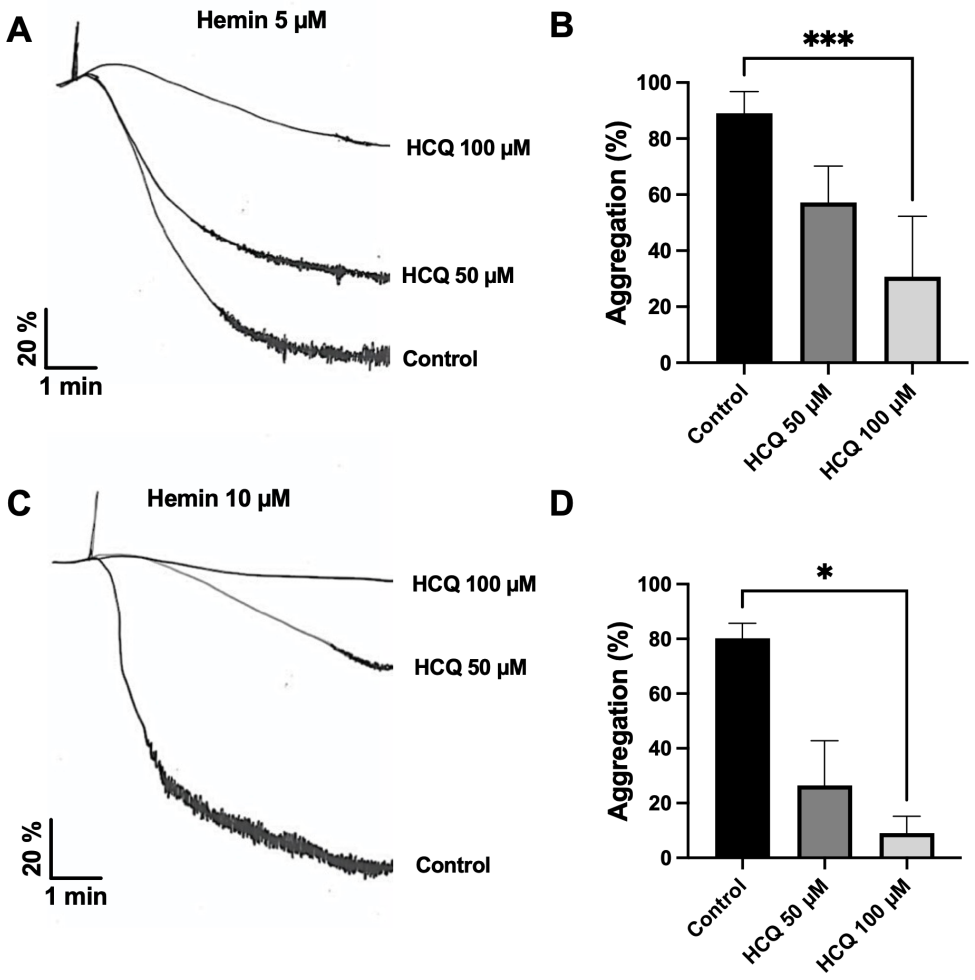

Figure 4.11 – Hydroxychloroquine inhibits hemin-induced human platelet aggregation. Washed platelet aggregation was assessed by light transmission aggregometry for 6 min under stirring conditions at 37 °C. Platelets were pre-incubated with hydroxychloroquine (HCQ), or buffer for 5 min pre-aggregation at 37 °C. **(A)** Representative platelet aggregation traces induced by hemin (5 µM), in the absence or presence of increasing concentrations of HCQ (50 and 100 µM) are shown and **(B)** maximum aggregation was calculated (n=6). **(C)** Representative platelet aggregation traces induced by hemin (10 µM), in the absence or presence of HCQ (50 and 100 µM) are shown and **(D)** maximum aggregation was calculated (n=6). The statistical difference between multiple groups was analysed using a paired one-way ANOVA with Tukey's multiple comparisons test, *$p < 0.05$ ***p<0.001.

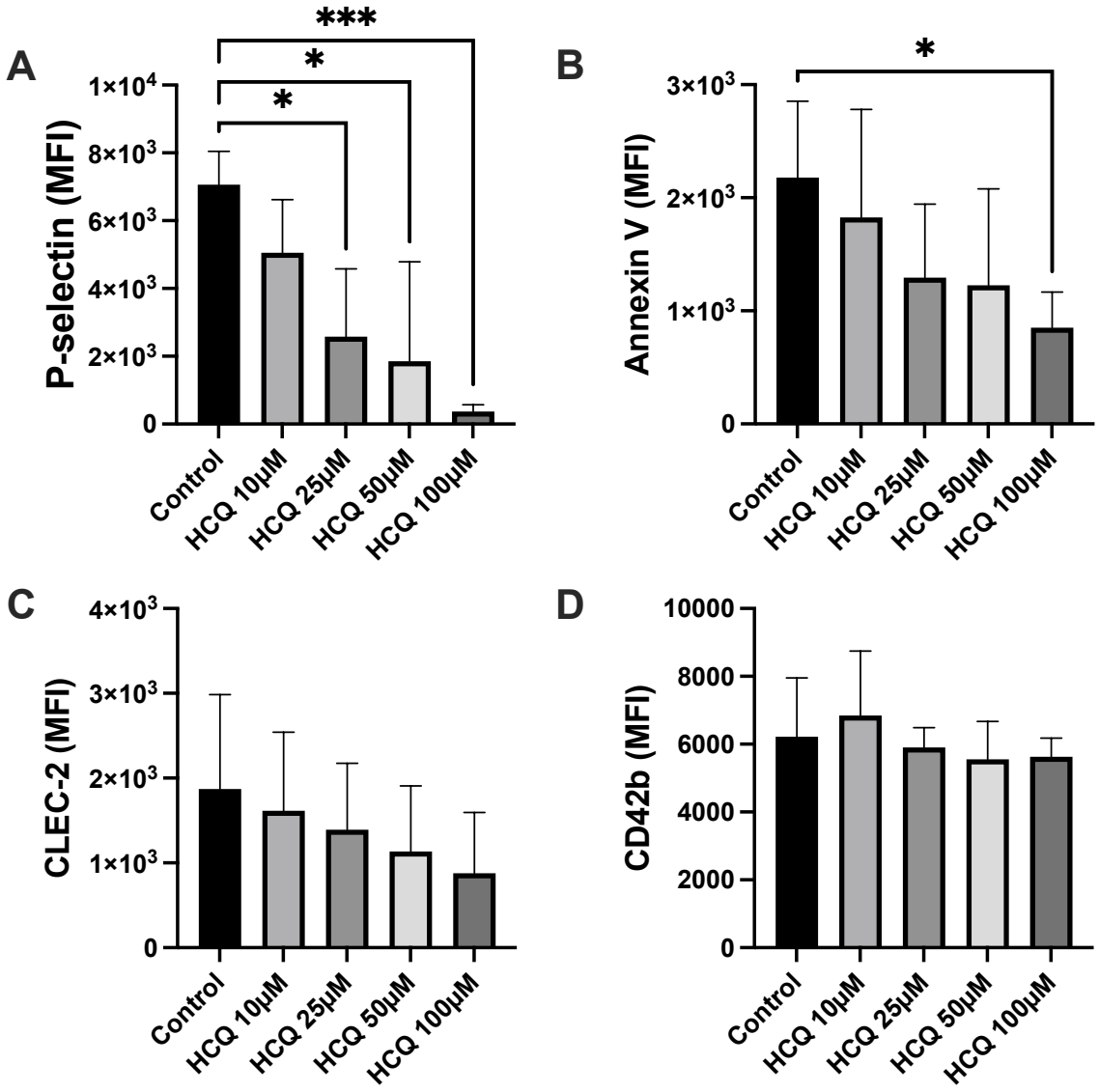

Figure 4.12 – Human platelet activation and apoptosis is inhibited by hydroxychloroquine. Washed platelets were incubated in the presence of hemin (10 μM), with or without hydroxychloroquine (HCQ) for 30 min. Protein surface expression was quantified by flow cytometry, for **(A)** P-selectin (n=6), **(B)** Annexin V (n=6), **(C)** CLEC-2 (n=4) and **(D)** CD42b (n=3). The statistical difference between multiple groups was analysed using a paired one-way ANOVA with Tukey's multiple comparisons test, *$p < 0.05$ ***$p < 0.001$.

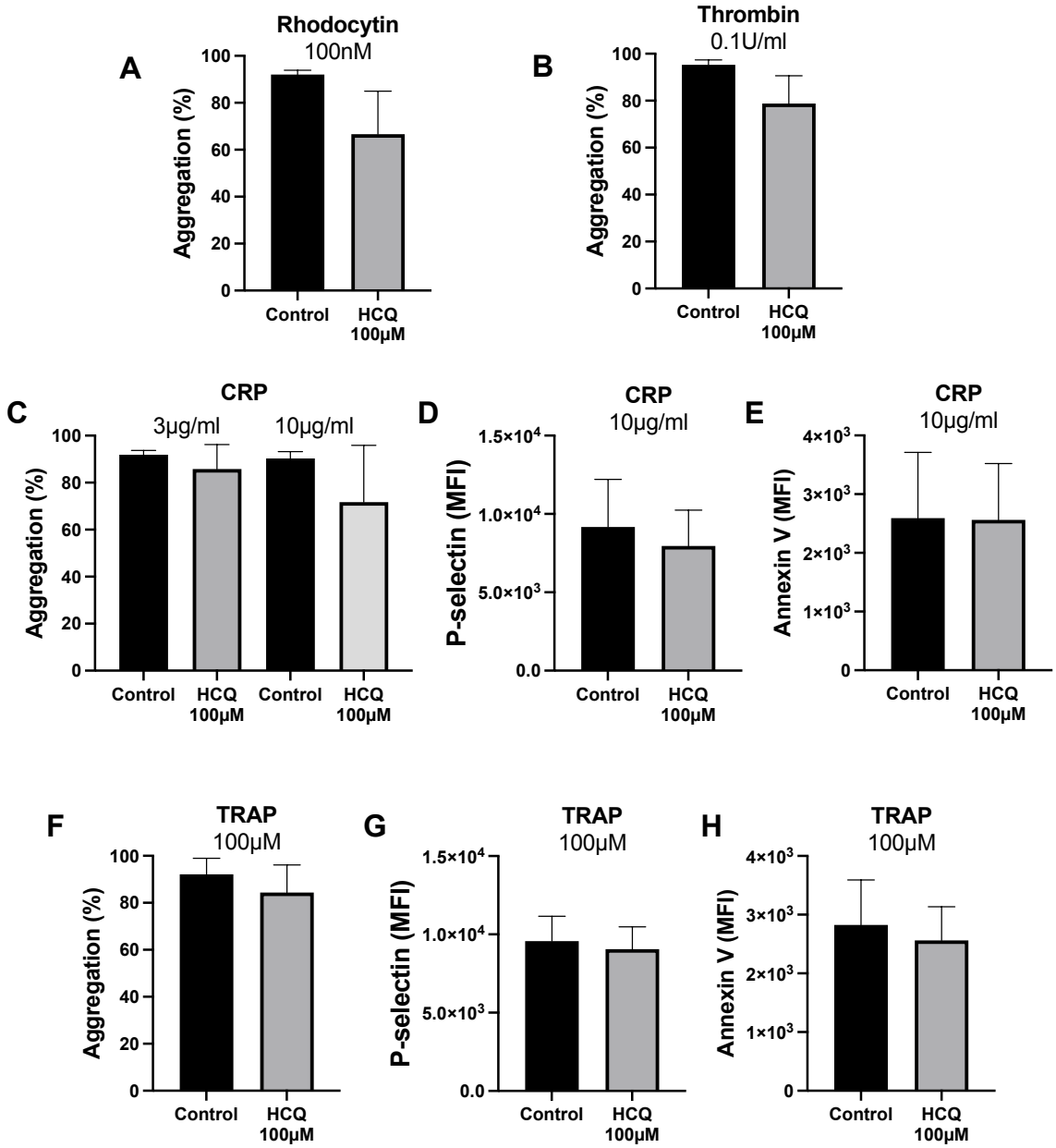

Figure 4.13 – CLEC-2, GPVI nor PAR-1/4 are inhibited by hydroxychloroquine in humans. (A-C, F) Washed mouse platelet aggregation was assessed by light transmission aggregometry for 6 min under stirring conditions at 37 ºC. Platelets were pre-incubated with hydroxychloroquine (HCQ), or buffer for 5 min pre-aggregation at 37 ºC. Maximum aggregation was calculated, induced by **(A)** rhodocytin (100 nM), **(B)** thrombin (0.1 U/ml), **(C)** CRP (3 μg/ml or 10 μg/ml) or TRAP (100 μM), in the absence or presence of HCQ (100 μM) are shown (n=3). **(D,**

E, G, H) Washed platelets were incubated in the presence of **(D, E)** CRP (10 µg/ml), or **(G, H)** TRAP (100µM) with or without hydroxychloroquine (HCQ) for 30 min. Protein surface expression was quantified by flow cytometry, for **(D, G)** P-selectin (n=6), **(E, H)** Annexin V (n=6). The statistical significance between 2 groups was analysed using an paired t-test.

4.3.6 Hydroxychloroquine does not inhibit hemin-induced ROS generation

Hemin can induce inflammation through not only platelet aggregation, but also through oxidation, specifically of lipoproteins (Camejo et al., 1998). Oxidation, in the context of platelets, can be assessed through ROS generation. As expected, low-dose hemin induces ROS generation, however this was not limited by HCQ **(Figure 4.14)**. Furthermore, ROS generation was not decreased by hFc-CLEC-2, PP2, Ibrutinib or PRT-060318, suggesting that hemin-mediated platelet activation in independent of ROS generation and is dependent on CLEC-2 activation.

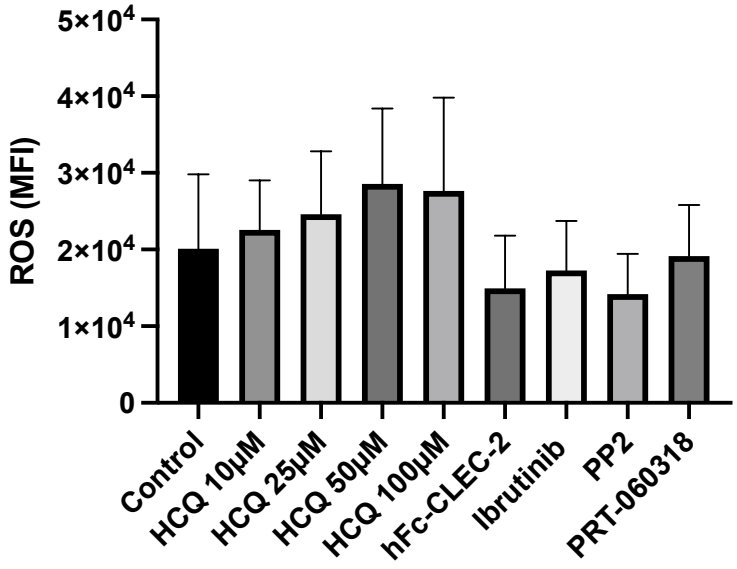

Figure 4.14 – Hydroxychloroquine treatment on hemin-induced ROS generation. Washed platelets were incubated in the presence of hemin (10 μM), with or without hydroxychloroquine (HCQ), hFc-CLEC-2 (10 μg/ml), Ibrutinib (500 nM), PP2 (20 μM) or PRT-060318 (20 μM) for 30 min. Using a FITC-conjugated DCFDA dye, reactive oxygen species (ROS) generation was detected by flow cytometry (n=3). The statistical difference between multiple groups was analysed using a one-way ANOVA with Tukey's multiple comparisons test.

4.4 Discussion

It is evident that the unpredictable nature of haemolytic disease makes therapeutic intervention challenging, therefore a specific mechanism for platelet activation is desired. In this chapter, we describe hemin as a novel ligand for platelet receptor, CLEC-2, inducing platelet activation and aggregation. During haemolytic events, the haem scavenging system becomes exhausted (Roumenina et al., 2016), leading to increased free haem in blood plasma (2-50 μM). We show that anti-malarial drug, HCQ, inhibits human and mouse platelet activation by hemin and limits thrombus formation in mice. The anti-malarial drug could be repurposed for use in haemolytic disease.

Platelet activation by hemin has previously been described through ferroptosis, but the receptors and mechanisms involved are not well known (NaveenKumar et al., 2018). In this study, we observe that platelets agglutinate at high dose hemin (50 μM), which is the extremity of haem detected during sickle cell crisis. Although, the dose of haem detected in patients cannot discriminate between free haem and haem bound with low affinity to plasma proteins like albumin. It is predicted that free hemin levels range between 2 and 8μM, which are relative to the low doses used in this study. We observed high levels of platelet death, and a mechanism with reduced PLCγ2-dependance, but allows platelet agglutination. Interestingly, a lower dose of hemin is here shown to be CLEC-2-dependant, which signals through its hemITAM domain in a syk-dependant manner to initiate PLCγ2 phosphorylation. Interestingly, platelet aggregation by hemin in the presence of CLEC-2-blocking antibody, AYP1 was not altered. Surface plasmon resonance demonstrates a very high affinity for

hFc-CLEC-2 and hemin (~200 nM) in human and mice. Furthermore, AYP1 blocks the interaction of CLEC-2 with its ligands podoplanin and rhodocytin, inhibiting platelet activation and aggregation (Gitz et al., 2014). Together, this suggests that hemin has a bind site on CLEC-2, distinct from its previously known ligands. Intriguingly, cobalt-hematoporphyrin, a compound which is structurally parallel to hemin aside from its cobalt core, has been shown block podoplanin and rhodocytin induced platelet aggregation (Tsukiji et al., 2018). It could be expected these compounds have similar binding sites, however cobalt-hematoporphyrin does not activate platelets, therefore suggesting distinct binding sites. It is important to note, that platelet aggregation is not completely abolished in CLEC-2-deficient platelets (7% aggregation). This suggests a second platelet receptor inducing a low level of aggregation in mice (or indeed a supportive role), which has been described as GPVI (Oishi et al., 2021). However, we observed this was not the case in humans, through using hFc-GPVI. Aggregation in human platelets is almost entirely abolished using hFc-CLEC-2, suggesting an almost exclusive mechanism for hemin-induced platelet activation.

Hemin has been demonstrated to induce lipid peroxidation, a process through which oxidants (including free radicals or ROS) attack lipids to induce inflammation (Ayala et al., 2014). The porphyrin ring of hemin is lipophilic (Kumar and Bandyopadhyay, 2005), which induces hemin binding to cellular lipids and subsequently inducing an impairment of the lipid bilayer. Although we demonstrate that HCQ limits platelets activation and aggregation *in vitro* and thrombus formation *in vivo,* the drug does not limit ROS generation post-stimulation with low-dose hemin. Iron-induced ROS is observed during multiple vascular diseases, including haemolytic anaemia,

atherosclerosis and vasculitis and reperfusion injury (Kumar and Bandyopadhyay, 2005). In these diseases, effective therapeutics are natural sources of antioxidants, such as vitamin E or resveratrol (Petrovic et al., 2020). Our data supports multiple mechanisms by which hemin alters platelet function, including CLEC-2-dependent platelet activation and aggregation and CLEC-2-independent oxidative stress and ROS generation. Therefore, dual therapies targeting CLEC-2 and oxidative stress might be required to limit thrombosis and inflammation in haemolytic diseases and reduce vascular occlusion

We demonstrate that HCQ limits thrombus growth post $FeCl_3$-injury.
Arterial topical application of $FeCl_3$ causes major oxidative stress through free-radical-dependant lipid peroxidation and endothelial damage. However, it has also been shown, through transmigration of the ferric ion through pores in the endothelium, that $FeCl_3$ can induce erythrocyte haemolysis directly (Tseng et al., 2006). This may hint that hemin released by haemolysed red blood cells can contribute to thrombus formation post-$FeCl_3$ injury. That being said, the concentration of free haem in this model is unknown; the haem scavenging system is not exhausted as it is in haemolytic disease presentation such as sickle cell crisis, and it is likely free haem is rapidly scavenged by hemopexin. *Ex vivo* investigation suggests that HCQ inhibits hemin-CLEC-2 platelet aggregation, and induces syk phosphorylation. However, the role of CLEC-2 during murine arterial thrombosis was shown to be independent of ITAM signalling (Haining et al., 2017). It is possible that not only does hemin induce platelet activation through CLEC-2, but also provides a basis for a role for CLEC-2 as an adhesion receptor, acting through hemin. This could be further investigated through the use of the laser-induced thrombosis model

in arterioles. In spite of early users of the laser injury-induced thrombosis model reporting erythrocyte lysis (Hovig et al., 1974), modern uses observe no red blood cell damage, and simply laser-activated endothelial-driven fibrin formation (Stalker, 2020). This could show a role for haemopexin, specific to thrombosis involving haemolysis. Furthermore, the specificity of HCQ to limit platelet activation by hemin needs to be confirmed, for example, hemin classically activates the endothelium through TLR4, which likely contributes to thrombus growth through an upregulation of vWF generation and release (Belcher et al., 2014). Research into HCQ treatment of endothelial cells challenged with hemin is ongoing.

In this study, we investigated the interaction specifically between hemin and platelets, inhibited by HCQ. However, hemin has been shown to activate and induce inflammation through neutrophils, monocytes and various vascular beds (Graca-Souza et al., 2002, Wagner et al., 2004). In order to fully understand the and replicate hemin activity, an *in vitro* model must be created, perhaps using flow adhesion chambers or through the use of organoids. This way haemolysis occurrence on varied vascular beds can be investigated. Furthermore, the implication of HCQ treatment on hemin-induced endothelial activation can be observed *in situ*.

In conclusion, we provide evidence that hemin is a novel ligand to platelet-activating receptor, CLEC-2. We speculate that CLEC-2 may be promoting thrombotic events during haemolytic disease, which could be limited by anti-malarial drug, HCQ. The dual nature of haem-induced lipid peroxidation suggests a role for an anti-oxidant,

alongside HCQ, in a dual therapy to limit haemolytic disease symptoms. This combination of treatment may be of benefit in patients with haemolytic disease.

Chapter 5

CLEC-2 prevents accumulation and retention of inflammatory macrophages during peritonitis

Data from this chapter has been published:

BOURNE, J. H., BERISTAIN-COVARRUBIAS, N., ZUIDSCHERWOUDE, M., CAMPOS, J., DI, Y., GARLICK, E., COLICCHIA, M., TERRY, L. V., THOMAS, S. G., BRILL, A., BAYRY, J., WATSON, S. P. & RAYES, J. 2021. CLEC-2 Prevents Accumulation and Retention of Inflammatory Macrophages During Murine Peritonitis. *Front Immunol,* 12**,** 693974.

Publication available in **Appendix 2**

5.1 Aims

Podoplanin-expressing macrophages have been demonstrated to activate, and aggregate platelets through ITAM receptor, CLEC-2. Furthermore, platelet-CLEC-2 has been shown to have important immunomodulatory functions during inflammation, however the mechanism is not well understood. In this chapter, we aim to establish how CLEC-2 regulates the inflammatory response during ongoing inflammation by interacting with podoplanin upregulated on inflammatory macrophages.

5.2 Introduction

During infection, the development of an adequate inflammatory response is critical to contain pathogen growth and spreading. Innate immune cells are recruited to the site of infection to clear pathogens through multiple mechanisms including the secretion of cytokines and anti-microbial molecules, phagocytosis and through release of extracellular traps (Campos et al., 2021). Following pathogen clearance, the resolution of the inflammation is critical to restore tissue homeostasis.

Alongside their role in thrombosis and haemostasis, platelets are emerging as vital regulators of the inflammatory response under sterile and infectious conditions (Morrell et al., 2014). The immunoregulatory functions of platelets, independent of thrombosis and haemostasis, are tightly regulated by the nature of the insult, the tissue and local microenvironment. Interestingly, distinct platelet receptors are engaged in different vascular beds and differentially regulate vascular integrity,

thrombosis and inflammation (Ho-Tin-Noé et al., 2018). Platelet-immune cell interactions play a pivotal role in balancing the immune response, however little is known on the functional relevance of these interaction during ongoing inflammation, and how it regulates the resolution of the inflammation. Therapeutic intervention of a sterile- or pathogen-induced inflammatory response through regulating platelet-leukocyte interaction by a specific axis could be a promising target for patients with chronic inflammatory disease, such as metabolic disorders, atherosclerosis or SARS-CoV-2.

5.2.1 Monocyte/macrophage migration and trafficking

During bacterial peritonitis, macrophage migration is critical for bacterial clearance. Macrophages are capable of migrating large distances and can move as fast as 10 μm/min in response to chemoattractants (Grabher et al., 2007). Dissimilar to fibroblasts, which utilise actin bundle anchorage points to migrate, macrophages form countless dot-like points of contacts to form temporary focal complexes and focal adhesions of varying phosphopaxillin contents (Grabher et al., 2007, Zaidel-Bar et al., 2007). Importantly, macrophages do not mature into large focal contacts with stress fibres attached, hence allowing them to manoeuvre through tissue. In addition to point and focal complexes, macrophages have podosomes which are short actin-rich adhesion molecules, accommodating migration (Wiesner et al., 2014). These qualities allow macrophages to respond to chemoattractants, not just within tissue, but allow tissue-resident macrophages to leave, and re-enter organs.

Resident macrophages are the initiators of the inflammatory response, and act as the 'patrollers' in tissue. Upon pathogen detection, they secrete neutrophil chemoattractants such as IL-1β, CXCL1, CXCL2 and CCL2 (Beck-Schimmer et al., 2005, Barry et al., 2013). Extravasation of neutrophils and monocytes by 2-D (through the endothelium) and then 3-D (through the endothelial matrix) migration in response to inflammation is critical to macrophage recruitment and retention (Cui et al., 2018). Macrophages have mechanisms to accommodate their migration through 2-D and 3-D structures: the amoeboid and mesenchymal systems. Amoeboid migration is an integrin-independent mechanism utilised by rapidly migrating leukocytes, such as dendritic cells and lymphocytes, which utilises 'flowing and squeezing' (Lämmermann et al., 2008). Interestingly, it has recently been shown that a moderate, but not high expression of integrins is required on M2 or tissue-resident macrophages to accommodate amoeboid migration (Cui et al., 2018). Mesenchymal migration is a much slower migratory mechanism generally utilised by M1 inflammatory macrophages, which is a classical adhesion-mediated process (Guiet et al., 2012, Čermák et al., 2018). Integrins are integral to macrophage mesenchymal migration, and of particular note is the family of β_2 subfamily: α_M and α_D are of particular note in macrophages (Cui et al., 2018). Interestingly Cui et al. (2018) demonstrated that integrin $\alpha_D\beta_2$ promotes inflammatory macrophage retention post-inflammation.

Leukocyte migration is dictated by a careful balance of chemotactic gradients through chemokine which are generated by specific tissues under inflammatory conditions. CCL2 is a strong chemoattractant for monocytes (also known as monocyte chemoattractant protein-1), and part of the C-C chemokine family. It is

secreted by a variety of cell types, such as endothelial, epithelial, smooth muscle cells and fibroblasts, either constituently, or upon oxidative stress or cytokine stimulation (Deshmane et al., 2009). Chemokines signal through GPCRs to induce strong intracellular kinase-mediate phosphorylation (Neel et al., 2005). The receptor for CCL2, CCR2, is expressed constituently on monocytes and macrophages. Interestingly, CCL2-CCR2 binding induces rapid CCR2 internalisation via arrestin in caveosomes (Garcia Lopez et al., 2009, Berchiche et al., 2011). From here, CCR2 can be either recycled or degraded in lysosomes. This careful balance of CCR2 expression regulates monocyte recruitment, and then retention during inflammation.

Upon neutrophil cell death during inflammation, macrophages (resident and monocyte-derived) engulf the apoptosed debris, coined ‘efferocytosis’ (Greenlee-Wacker, 2016). Neutrophil internalisation by macrophages induces the release of anti-inflammatory cytokines and chemokines, in turn repolarising the macrophage (Serhan and Savill, 2005). Furthermore, these macrophages are now able to repair or emigrate (Prame Kumar et al., 2018). The fate of these macrophages is unclear, as it has been shown both that they die locally or emigrate to draining lymph nodes (Bellingan et al., 1996, Cao et al., 2005, Gautier et al., 2013). However, it is clear that this mechanism is vital to the resolution of inflammation.

During inflammation, 3-D macrophage migration is dictated by chemokines, which differentially regulates the movement of M1 and M2 macrophages. There are 41 known chemokines which bind to 20 chemokine receptors on macrophages, 7 of which are specific to driving M1 macrophage migration through MEK1, ERK1/2 and PI3K cascades (Amin et al., 2003, Xuan et al., 2015). Differential effects of

chemokines on M1/M2 macrophage migration can be explained by increased expression of their ligand on the respective population, with the exception of CCR7. Interestingly CCR7 expression is conserved in M1 and M2 populations, but its ligand, CCL21 only induces M1 macrophage chemotaxis (Xuan et al., 2015). This suggests a mechanism involving CCL21, distinct from CCL21-CCR7 which is promoting inflammatory macrophage chemokine-induced migration.

5.2.2 Platelet-leukocyte interaction

Platelet-leukocyte interaction is a common occurrence during inflammation, due to upregulation and conformational changes of various inflammatory proteins on both platelets and myeloid cells. Platelet activation and subsequent recruitment to a site of inflammation-induced vascular permeability leads to extravasation of platelet-bound leukocytes, beyond the endothelium. Leukocyte recruitment is common in postcapillary venules, as a result of increased density of cell adhesion molecules and wall shear rate (Petri et al., 2008). Platelet-leukocyte aggregates are observed in the blood during sterile inflammation and following bacterial, viral and fungal infections (Assinger et al., 2019, Koupenova et al., 2019, Deppermann and Kubes, 2016, Speth et al., 2014). Activated platelets bind to neutrophils and monocytes, regulating both thrombosis and inflammation.

Platelets interact with neutrophils and monocytes in the blood through several mechanisms including:

Platelet-leukocyte

- P-selectin – PSGL-1
- CD40 Ligand (CD40L) – CD40
- GPIbα – Macrophage antigen-1 (MAC-1)
- GPIIb3a – MAC-1 (via fibrinogen or vWF)

The initial unstable interaction between P-selectin and PSGL-1 induces the subsequent activation and clustering of integrin $\alpha M\beta 2$ (MAC-1) on immune cells and firm adhesion through its interaction with GPIb-α and GPIIb/IIIa (Frenette et al., 2000, Wang et al., 2005b, Schwarz et al., 2002, Inwald et al., 2003). Whilst both MAC-1 and GPIbα are constituently expressed on their respective cell types, MAC-1 is believed to undergo a conformational modification to bind to GPIbα (Pluskota et al., 2008). Platelet-leukocyte interactions are further potentiated by CD40L interaction with CD40 on immune cells. Platelet binding to neutrophils initiates the release of various chemokines and cytokines, promotes ROS generation and the formation of NETs to promote pathogen clearance (Kim and Jenne, 2016).

Platelet secretion also plays a key role in promoting their interaction with monocytes and neutrophils. Platelets are an important source of chemokines in particular PF4 and RANTES (CCL5). Platelet activation leads to the deposition of these chemokines on the endothelium promoting neutrophil and monocyte recruitment to the endothelium (von Hundelshausen et al., 2005). PF4 is the most abundant protein

in α-granules, and is able to interact with neutrophils through LFA-1 to initiate neutrophil granular release. PF4 also interacts with monocytes, inhibiting their apoptosis and promotes their differentiation to macrophages (Scheuerer et al., 2000). Therefore, platelet interaction with leukocytes in the blood promotes the recruitment of both platelets and leukocytes at the site of inflammation and regulates inflammation and thrombosis.

Interestingly, although these receptor axes have been well researched, the contribution and significance of the platelet-leukocyte interaction through each receptor-ligand in varied inflammatory conditions, organs and/or vascular beds is not well elucidated.

5.2.3 Platelet-macrophage interaction

While most of the macrophages reside in tissues and are not in contact with the blood, the liver specialized macrophage Kupffer cells line the walls of the sinusoids and are constantly exposed to the blood flow. Under physiological conditions, platelets transiently interact with intravascular Kupffer cells via GPIbα-vWF and this interaction is stabilized during bacterial infection regulating endothelial permeability and host response against bacteria (Chimen et al., 2020). Platelets have been shown to protect against septic shock and decrease subsequent organ damage in LPS-challenged mice by regulating the inflammatory phenotype of macrophages (Xiang et al., 2013). It is currently not known how platelets enter the tissues during inflammation and infection and how this interaction occurs *in vivo*. *In vitro,* at low doses of LPS, platelets promote TNF-α secretion from bone-marrow derived

macrophages, whereas in the presence of high doses of LPS, platelets inhibit macrophage-dependent inflammation (Xiang et al., 2013). In human monocyte-derived macrophages, activated platelets promote LPS-mediated inflammatory cytokine release, which is largely dependent on platelet secretion (Scull et al., 2010).

Under inflammatory conditions, CLEC-2 was shown to interact with podoplanin upregulated on inflammatory macrophages (Kerrigan et al., 2012). The interaction of CLEC-2 with podoplanin induces platelet activation in a Src/Syk/PLCγ2-dependent manner. The structure, expression and function of podoplanin in Chapter 1.7.2. Of particular note, podoplanin binds to the ERM proteins through its intracellular tail (Krishnan et al., 2013, Krishnan et al., 2015). The ERM proteins are well understood to guide cellular migration through reorganisation of the actin cytoskeleton (Arpin et al., 2011).

5.2.4 Podoplanin function in myeloid cells

Podoplanin expression has been described in multiple myeloid cells, including murine macrophage cell line RAW264.7 cells, murine primary BMDMs, peritoneal macrophages (post-peritonitis), tumour-associated macrophages, and monocyte-derived macrophages in the inflamed lung, liver and skin (Kerrigan et al., 2012, Rayes et al., 2017, Lax et al., 2017, Hitchcock et al., 2015, Wichaiyo et al., 2019, Bieniasz-Krzywiec et al., 2019, Xie et al., 2020, Eisemann et al., 2019). However, little is known on the function of podoplanin in myeloid cells. Podoplanin is well reported to promote epithelial cell migration and subsequent metastasis during cancer (Quintanilla et al., 2019), but recent reports have identified a role for myeloid-

podoplanin during mouse models of breast cancer and gliomas (Eisemann et al., 2019, Bieniasz-Krzywiec et al., 2019). Podoplanin-expressing tumour-associated macrophages were shown to promote lymphangiogenesis through binding to LECs, specifically through LEC-derived galectin 8, in turn promoting cancer progression. Furthermore, podoplanin-expressing myeloid cells were identified to mediate glioma-induced immunosuppression (Eisemann et al., 2019). Alas, whilst it was suggested that podoplanin-expressing myeloid cell targeting could present a novel anti-cancer therapy, it could prove counterintuitive due to the high inflammation throughout cancer. During Sepsis, podoplanin-expressing macrophages and monocytes are anti-inflammatory, with the latter protecting liver function through complement inhibition (Rayes et al., 2017, Xie et al., 2020).

5.2.5 The CLEC-2-podoplanin axis during inflammation

A key role for the CLEC-2-podoplanin axis was shown to drive thromboinflammation in murine models of DVT and *Salmonella* infection-mediated thrombosis in the liver (Payne et al., 2017, Hitchcock et al., 2015). In the model of DVT, podoplanin was upregulated in the subendothelium triggering thrombosis at the site of vascular breaches in a CLEC-2-dependent manner. Following *salmonella* infection, an upregulation of podoplanin on macrophages in the liver is observed, forming inflammatory foci. At the site of endothelial damage, podoplanin induces thrombosis in the liver with limited capacity in containing bacteria.

Beside the role of CLEC-2-podoplanin in thromboinflammation, the CLEC-2-podoplanin axis has been shown to regulate the inflammatory response in multiple

models of inflammation. Interestingly, the axis has been shown to be both beneficial and detrimental. CLEC-2 is protective post-lung injury through podoplanin-expressing alveolar macrophages (Lax et al., 2017) and during murine models of multiple sclerosis (Nylander et al., 2017). However, CLEC-2 is detrimental and promotes inflammation in rheumatoid arthritis, as well as limiting liver regeneration (Takakubo et al., 2017, Chauhan et al., 2020).

Using a mouse model of sepsis induced by caecal ligation and puncture, CLEC-2 was shown be immunoprotective (Rayes et al., 2017). Deletion of CLEC-2 using a PF4-Cre mouse (CLEC1b$^{fl/fl}$PF4-Cre) or deletion of podoplanin from haematopoietic cells (PDPN$^{fl/fl}$VAVi-Cre), increased sepsis severity and exacerbated the cytokine storm in mice. The deleterious effect was associated with impaired macrophage recruitment to the infected peritoneum, increased bacterial load and dissemination and multiple organ damage. The mechanism by which platelet CLEC-2 regulates macrophage activation and migration is not known. Moreover, it was recently shown that PF4-Cre-generated KO mice have additional inflammatory and immunological anomalies as a result of nonspecific deletion in other hematopoietic lineages. Whether crosslinking podoplanin can regulate macrophage phenotype, fate or resultant tissue inflammation is not known. This is highly relevant in diseases describing platelet-bound podoplanin-positive macrophages such as atherosclerosis, rheumatoid arthritis and breast cancer (Inoue et al., 2015, Takakubo et al., 2017, Hatzioannou et al., 2016).

In this chapter, we investigate the mechanisms by which CLEC-2 regulates macrophage activation, accumulation and fate during ongoing inflammation. Our

study shows a key role for CLEC-2 in macrophage trafficking from inflamed tissues. This provides a rational to use recombinant CLEC-2-Fc as a therapeutic protein to limit macrophage accumulation in inflamed tissues and progression to chronic inflammation.

5.3 Results

5.3.1 LPS induces the expression of podoplanin on macrophages through TLR-4

Podoplanin expression was previously shown to be upregulated on LPS-treated RAW264.7 (RAW) cells, as well as on peritoneal macrophages during polymicrobial sepsis and skin macrophages during immune complex-mediated inflammation (Kerrigan et al., 2012). We first screened stimuli which significantly upregulates podoplanin on macrophages, using murine leukaemia-derived cell line, RAW264.7 macrophages. We investigated the effect of different TLR agonists from bacterial and fungal wall proteins on the expression of podoplanin. LPS (TLR-4 agonist from gram-negative bacteria), PGN-SA (TLR-2 agonist from gram-positive bacteria), PAM3CSK4 (TLR-1 and -2 agonist found in gram-negative and -positive bacteria) and Zymosan (TLR-2 agonist from fungus) upregulate podoplanin expression on the surface of RAW264.7 cells in a dose-dependent manner **(Figure 5.1A-D)**, and total podoplanin protein in the cell **(Figure 5.1E)**. Cells stimulated with other pro-inflammatory stimuli, such as hypoxia, pro-inflammatory cytokines (TNF-α) or staurosporine (an inducer of apoptosis) did not induce podoplanin expression (data not shown). Podoplanin is not expressed on naïve macrophages, and is transcriptionally upregulated post-LPS stimulation **(Figure 5.1F).** These podoplanin-expressing macrophages express classical inflammatory M1 macrophage markers CD80 and CD86 **(Figure 5.1G, H)** (Italiani and Boraschi, 2014)**.** Podoplanin upregulation by LPS occurs in a TLR-4 dependant manner, observed by treating RAW264.7 cells with TLR-4 small molecule inhibitor, TAK-242, which do not express

podoplanin post-LPS-stimulation **(Figure 5.1I, J)**. Our results suggest that during infection, TLR-4 activation by LPS, and to a lesser extent other TLRs, upregulate podoplanin expression on macrophages. Going forward, LPS is used to induce podoplanin expression on inflammatory macrophages, due to the large and consistent upregulation.

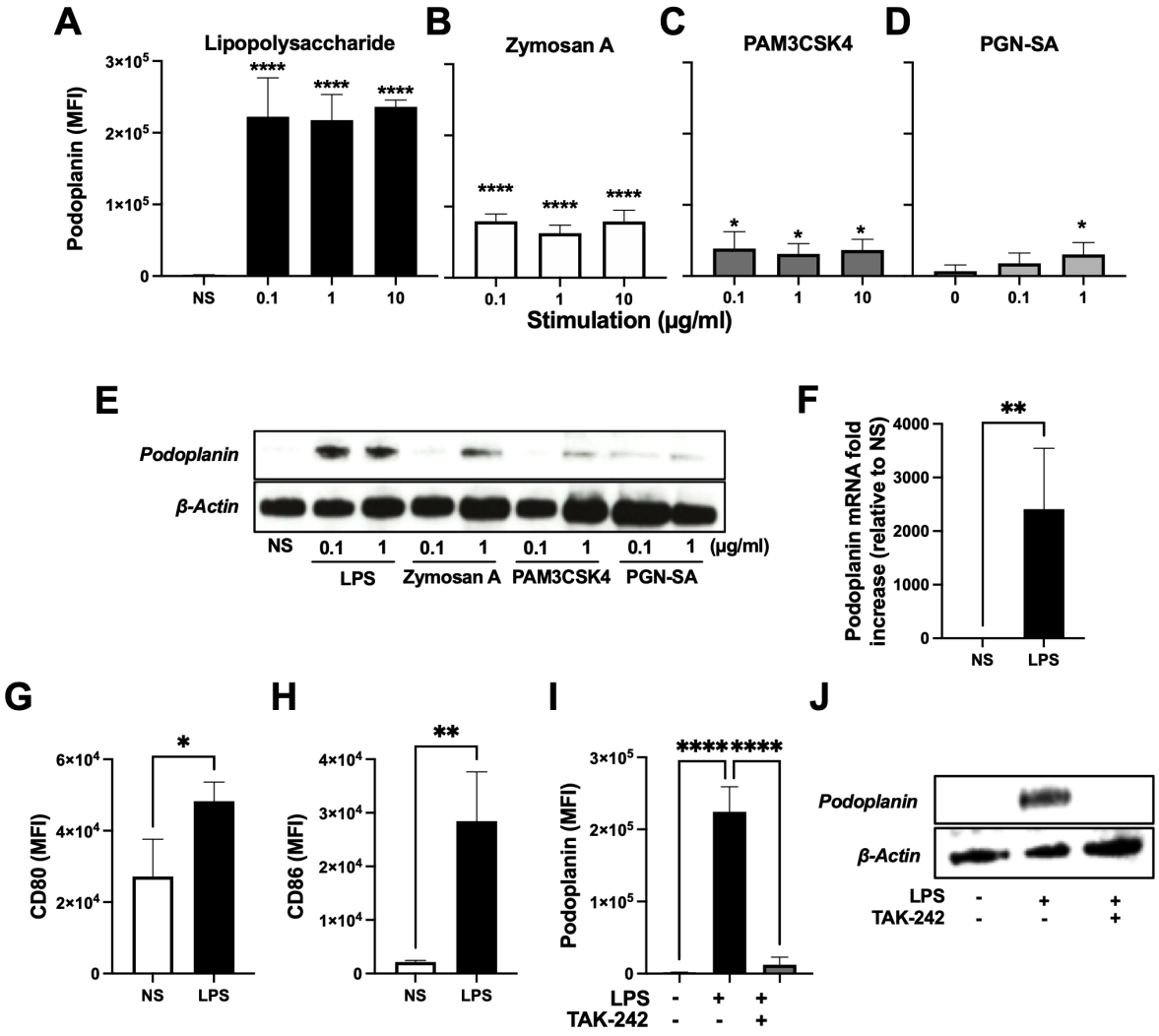

Figure 5.1 - LPS upregulates podoplanin on RAW264.7 cells through TLR-4.

RAW264.7 cells were incubated with increasing concentrations of **(A)** LPS, **(B)** Zymosan A, **(C)** PAM3CSK4 or **(D)** PGN-SA for 24 h. **(A-D)** Surface podoplanin expression assessed by flow cytometry and compared to non-stimulated cells (NS; n=3). **(E)** Total podoplanin levels were assessed in RAW264.7 lysates by western blot (image representative of 3 independent experiments). **(F)** Podoplanin transcription from isolated mRNA relative to NS control was quantified by qPCR (n=4). **(G, H)** RAW264.7 cells were stimulated with LPS (1 µg/ml) for 24 h. Macrophage maturation markers **(G)**

CD80 and **(H)** CD86 were quantified by flow cytometry (n=3). **(I, J)** RAW264.7 cells were treated with TAK-242 (1 μM), before stimulation with LPS (1 μg/ml) for 24 h. Podoplanin expression was quantified by **(I)** flow cytometry (n=3) and **(J)** western blot (image representative of 3 independent experiments). The statistical significance between 2 groups was analysed using a paired t-test and the statistical difference between multiple groups was tested using a one-way ANOVA with Tukey's multiple comparisons test, *$p < 0.05$ **$p < 0.01$ ****$p < 0.0001$.

5.3.2 Platelet-CLEC-2 upregulates podoplanin on podoplanin-expressing inflammatory macrophages and promotes spreading

Podoplanin-expressing inflammatory macrophages have been demonstrated to induce platelet aggregation in a CLEC-2-specific manner (Kerrigan et al., 2012). Whilst CLEC-2-podoplanin crosslinking is known to activate and aggregate platelets, the implications of the axis on macrophages is not known. Resting, washed platelets incubated with naïve RAW264.7 cells did not induce podoplanin expression. However, incubation of podoplanin-expressing RAW264.7 cells with platelets for 1h increased podoplanin expression two-fold **(Figure 5.2A)**. Incubation of CLEC-2-deficent platelets did not alter podoplanin expression, compared to control, without loss of platelet-binding **(Figure 5.2B, C)**. Interestingly, WT, nor CLEC-2-deficient platelets increased podoplanin expression in whole cell lysate **(Figure 5.2D)**. The rapid upregulation of podoplanin surface expression in the presence of platelets, alongside the absence of upregulation in lysate suggests a distinct role for CLEC-2 in releasing podoplanin from intracellular stores in macrophages.

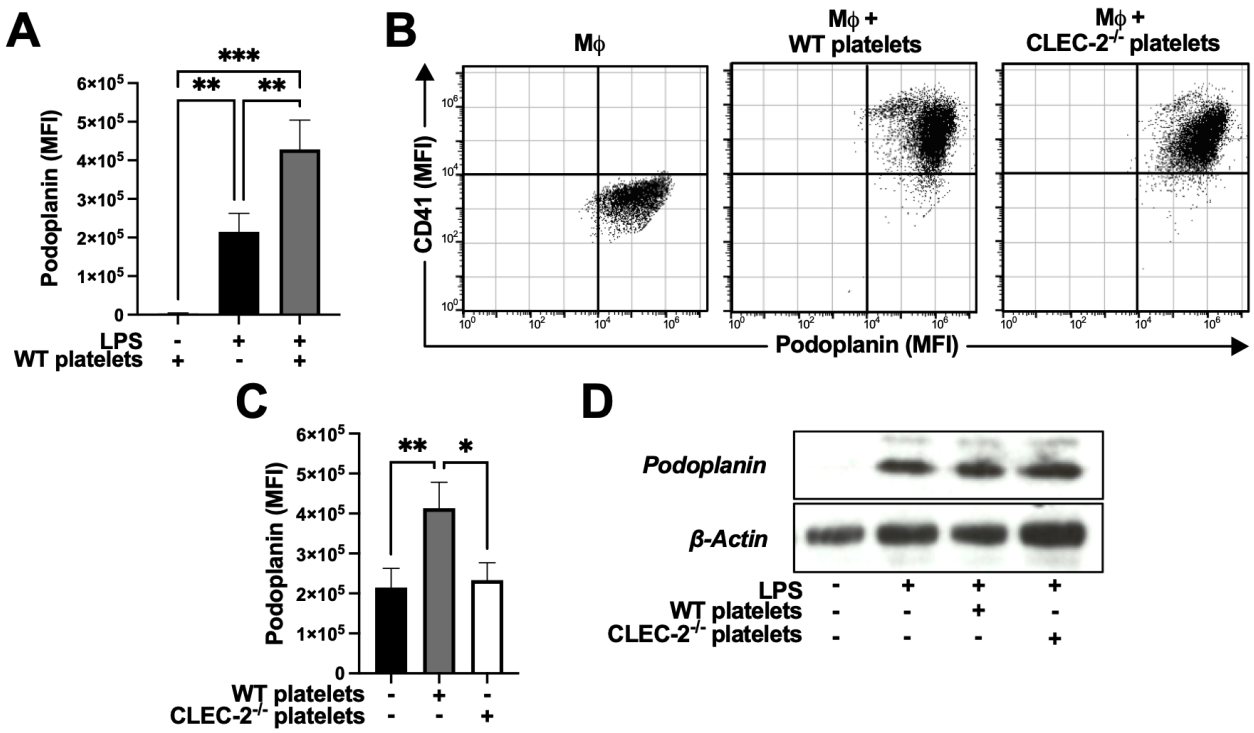

Figure 5.2 – Platelet CLEC-2 induces an upregulation of podoplanin surface expression on RAW264.7 cells. (A-D) RAW264.7 cells were challenged with LPS (1 µg/ml) for 24 h, before washing, and then incubated in the presence or absence of wild type (WT) or CLEC-2-deficient (CLEC-2$^{-/-}$) platelets (100 platelets:1 RAW264.7 cell) for 1 h. **(A)** Podoplanin surface expression was detected by flow cytometry (n=3). **(B)** Gating strategy for CD41 (platelet)-positive RAW264.7 cells. **(C)** Podoplanin surface expression was detected by flow cytometry (n=3). **(D)** Podoplanin expression was detected in RAW264.7 cell lysate by western blot (image representative of 3 independent experiments). The statistical significance between 2 groups was analysed using a paired t-test and the statistical difference between multiple groups was tested using a one-way ANOVA with Tukey's multiple comparisons test, *$p < 0.05$ **$p < 0.01$ ***$p < 0.001$.

To assess the distribution of podoplanin on macrophages post-LPS stimulation and upon incubation with platelets, RAW264.7 cells were imaged using immunofluorescence. LPS-stimulated macrophages appear to have intracellular stores of podoplanin in the cytoplasm, perhaps in lysosomes or endosomes. In fact, podoplanin was localized on the pseudopods of RAW264.7 cells in the presence of WT, but not CLEC-2-deficient platelets **(Figure 5.3A)**. This was associated with increased cell spreading, measured by cell size and loss of circularity **(Figure 5.3B, C).** The podoplanin intracellular tail contains 2 serines, 167 and 171, that are constitutively phosphorylated and are critical for the association with the ERM proteins and cell migration (Krishnan et al., 2013, Krishnan et al., 2015). Immunoprecipitation of podoplanin post-LPS-stimulation demonstrated a reduction in the presence of podoplanin phospho-serine residues in the presence of WT but not $CLEC2^{-/-}$ platelets, which has been shown to promote podoplanin association with the ERM proteins **(Figure 5.3D).**

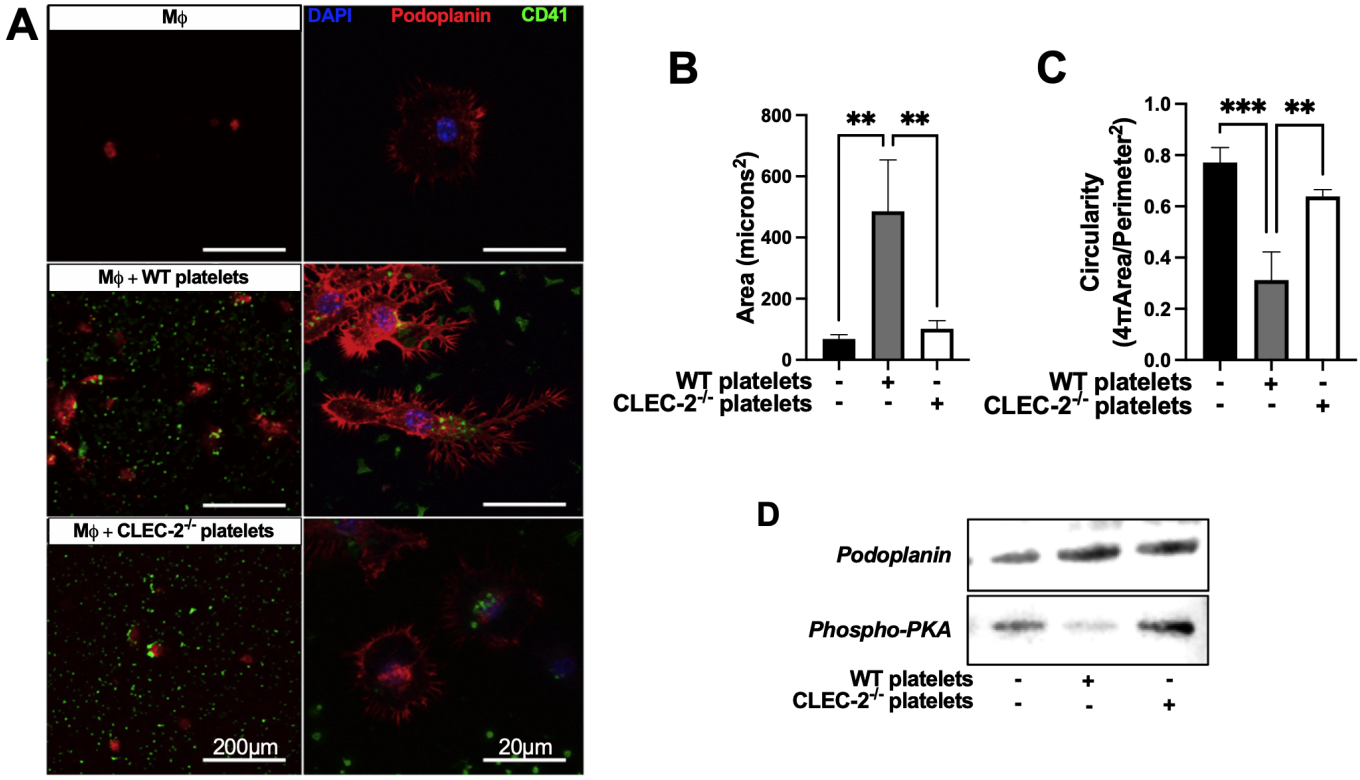

Figure 5.3 – Platelet-CLEC-2 increases macrophage spreading through podoplanin. (**A-C)** RAW264.7 cells were cultured and allowed to spread on glass coverslips in the presence of LPS (1 μg/ml) for 24 h (Mϕ). Cells were washed and cultured in the presence or absence of wild type (WT) or CLEC-2-deficient platelets (100:1) for 1 h, before fixation and staining for platelets (CD41, green), DAPI (blue) and podoplanin (red). **(A)** Fluorescence was detected by confocal microscopy, and images were quantified for **(B)** size and **(C)** circularity using scripts on ImageJ (n=3). **(D)** Podoplanin from 24 h LPS-stimulated (1 μg/ml) RAW264.7 cells were immunoprecipitated with anti-podoplanin antibody (8.1.1), and immunostained with anti-phospho-PKA substrate antibody (representative western blot of 3 independent experiments). The statistical difference between multiple groups was analysed using a one-way ANOVA with Tukey's multiple comparisons test, *$p < 0.05$ **$p < 0.01$ ***$p < 0.001$.

In order to more closely replicate the signalling events, functionality and platelet-macrophage interaction observed during inflammation *in vivo*, we utilised BMDMs Furthermore, we investigate the interaction of podoplanin with its intracellular ligand, CD44, which has been shown to regulate podoplanin-induced migration in squamous stratified epithelia (Martín-Villar et al., 2010). Similar to the cell line, RAW264.7, addition of WT, but not CLEC-2-deficient platelets for 1 h to LPS-stimulated BMDMs potentiates podoplanin and, also CD44 expression, as assessed by flow cytometry **(Figure 5.4A-C).** The distribution of podoplanin and CD44 was also altered by CLEC-2, associated with increased BMDM spreading, measured by increased cell area and loss of circularity **(Figure 5.4D-F).** Platelet-mediated cell spreading and cell spreading and pseudopods formation was confirmed using scanning electron microscopy **(Figure 5.4G).**

In order to confirm the role of platelets on actin remodelling, we observed LifeAct-GFP-derived inflammatory BMDMs spreading in the presence of platelets using diSPIM LightSheet microscopy for 1 h. As expected, inflammatory macrophages are sessile, and addition of WT platelets to LPS-activated BMDMs increased pseudopod formation, actin remodelling and mobility, compared to control **(Video 1 and 2)**. In contrast, actin remodelling, spreading and pseudopod formation decreased after the phagocytosis of platelets, showing distinct mechanism of cell-cell interaction and platelet phagocytosis on actin remodelling.

These results show that platelet CLEC-2 binding to podoplanin on inflammatory BMDM, or RAW264.7 cells, increases the expression and distribution of podoplanin and its transmembrane ligand CD44, to promote actin remodelling and cell mobility.

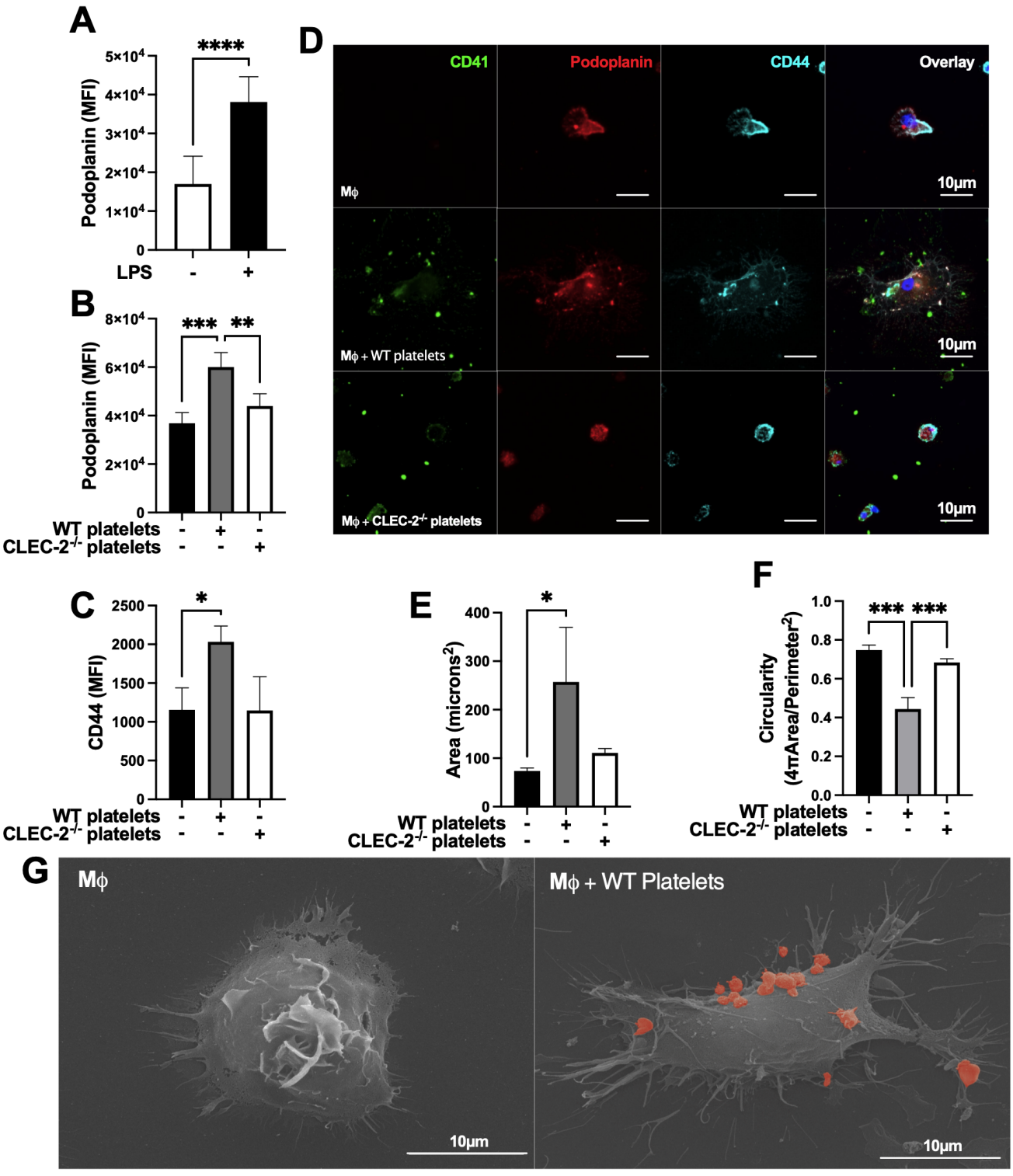

Figure 5.4 – Platelet-CLEC-2 upregulates podoplanin and CD44 expression on LPS-stimulated BMDMs. (A) BMDMs were incubated in the presence or absence of LPS (1 μg/ml) for 24 h. **(B, C)** LPS-stimulated BMDMs were co-cultured in the absence or presence of WT or CLEC-2-deficient platelets (100:1). **(A-C)** Median of

fluorescence intensity (MFI) of podoplanin (n=4) and CD44 (n=3) was detected by flow cytometry. **(D)** 24 h LPS-stimulated (1 μg/ml) BMDMs (Mϕ) were cultured on glass, and WT or CLEC-2-deficient platelets were added for 1 h. Platelets (CD41, green), podoplanin (red) and CD44 (cyan) were detected using confocal microscopy. Images are representative of 4 independent experiments. **(E)** Cell area and **(F)** circularity were analysed using ImageJ. **(G)** Mϕ were cultured on glass in the presence or absence of WT platelets (red) for 1 h, before fixing and imaging by electron microscopy. The statistical significance between 2 groups was analysed using an unpaired t-test and the statistical difference between multiple groups was analysed using a one-way ANOVA with Tukey's multiple comparisons test, *$p < 0.05$ **$p < 0.01$ ***$p < 0.001$ ****$p<0.0001$.

5.3.3 Platelet-CLEC-2 reduces the pro-inflammatory phenotype of the M1 BMDM and promotes wound closure

In numerous cell types and tissue environments, podoplanin regulates cell migration, however the CLEC-2-podoplanin axis is little explored. Furthermore, how and the extent which CLEC-2 dictates macrophage inflammatory function is unknown. Here, we show that addition of WT, but not CLEC-2-deficient platelets, to LPS-challenged BMDMs delayed the uptake of pH-sensitive fluorescent *E. Coli*-bound bioparticles compared to control, as assessed by Incucyte systems for live-cell microscopy **(Figure 5.5A, B)**. However, the final uptake of the beads was not affected **(Figure 5.5C)**. Crosslinking podoplanin by CLEC-2 expressed on WT platelets significantly reduced pro-inflammatory cytokine, TNF-α, secretion from BMDMs, whereas the levels of TNF-α were not altered by the addition of CLEC2-deficient platelets, compared to control **(Figure 5.5D).** No significant change in anti-inflammatory cytokine, IL-10, was observed following platelet addition **(Figure 5.5E)**. In a wound scratch assay, addition of WT platelets to a scratched monolayer of inflammatory BMDMs accelerated wound closure by two-fold (36±7.4 % wound closure for control versus 86±12.6 % closure in the presence of WT platelets) **(Figure 5.5F-H)**. Wound closure was also partially accelerated in the presence of $CLEC2^{-/-}$ platelets, although the maximal coverage did not exceed 66±18.2 %.

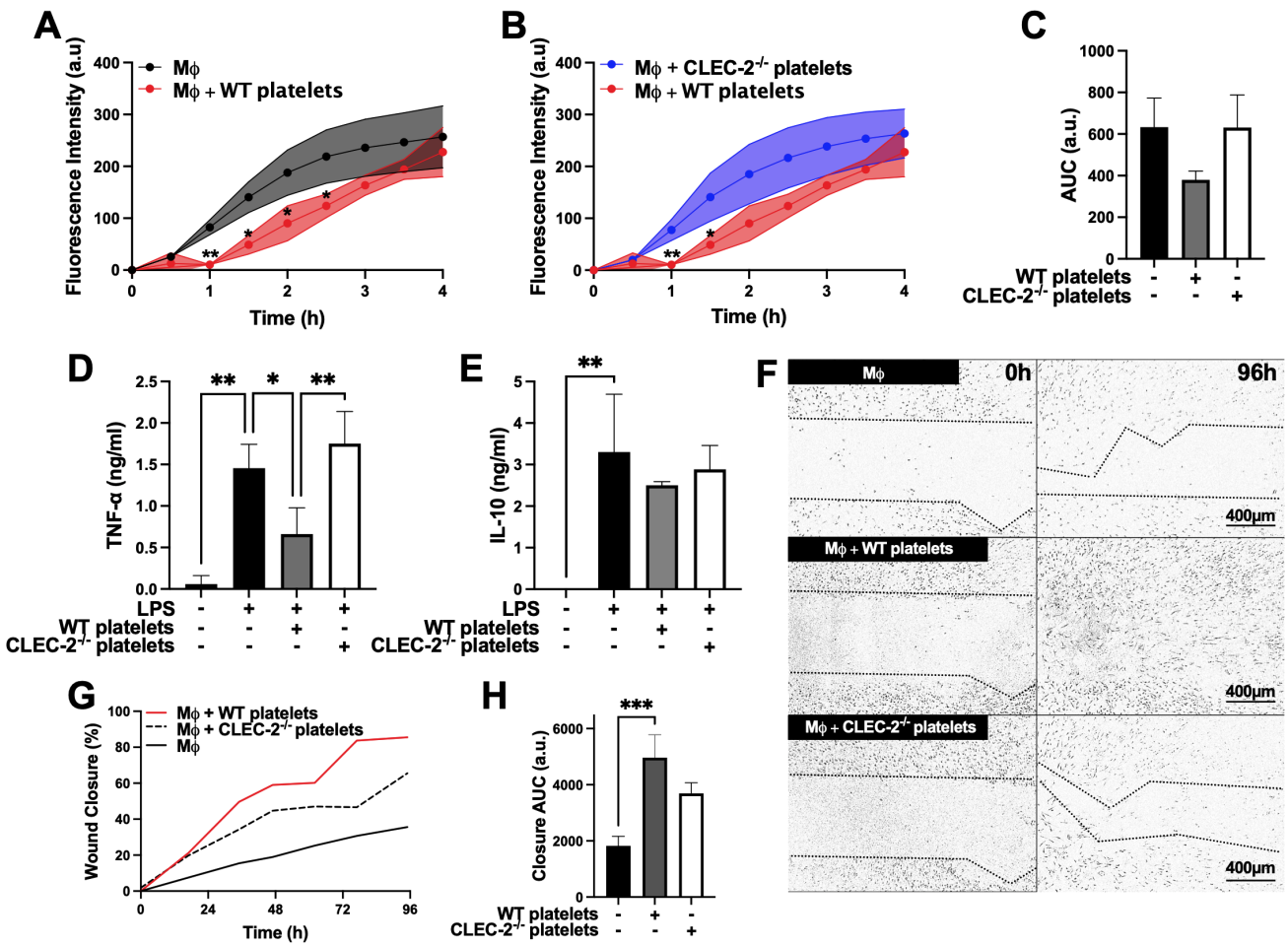

Figure 5.5 - Platelet CLEC-2 delays inflammatory BMDM phagocytic capacity and reduces TNF-α secretion. (A-C) pH sensitive Alexa Fluor-488 conjugated *Escherichia Coli* bioparticles (3x10^6 beads/condition) were added to LPS-treated BMDMs in the absence or presence of **(A)** WT platelets or **(B)** CLEC-2-deficient platelets (100:1) for 4 h. **(A, B)** Phagocytosis was visualised and quantified by time lapse-imaging using an Incucyte Live-cell analysis system. **(C)** Phagocytosis profiles were quantified at 4 h by detecting fluorescence /mm^3 using area under the curve (AUC; a.u. = arbitrary units; n=3). **(D)** TNF-α and **(E)** IL-10 secretion from LPS-treated BMDMs (24 h at 1 μg/ml) in the presence or absence of WT or CLEC-2-deficient platelets was quantified in the supernatant by ELISA (n=4). **(F-H)** Scratch wound migration of LPS-treated BMDMs (Mϕ) was monitored every 2 h for 96 h

using an Incucyte ZOOM system. Following wound scratch, **(F)** WT or CLEC-2-deficient platelets (100:1) were added to Mϕ. **(G)** Wound closure was quantified as percentage of closure using ImageJ. **(H)** Total wound closure was quantified by AUC at 96 h (n=3). The statistical significance between 2 groups was analysed using a paired t-test and the statistical difference between multiple groups was tested using a one-way ANOVA with Tukey's multiple comparisons test, *p < 0.05 **p < 0.01 ***p < 0.001.

To further assess the CLEC-2-podoplanin axis, we utilised macrophages derived from the bone marrow of mice with a haematopoietic-specific deletion of podoplanin. In the presence of LPS, these macrophages expressed significantly less podoplanin than WT controls, although were not completely podoplanin-deficient **(Figure 5.6)**. Interestingly, podoplanin deficiency from BMDMs did not affect their phagocytic activity **(Figure 5.7A, B)** suggesting a distinct role for podoplanin-crosslinking by CLEC-2. Podoplanin deficiency did not significantly alter wound closure, compared to WT BMDM **(Figure 5.7C-E)**, nor did the addition of WT or CLEC-$2^{-/-}$ platelets **(Figure 5.7C, F, G)**, showing a clear role for podoplanin in macrophage migration.

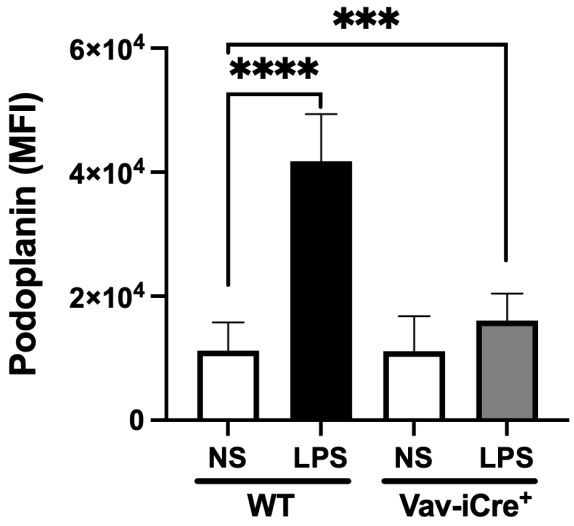

Figure 5.6 – Podoplanin expressed on BMDMs from PDPN$^{fl/fl}$Vavi-Cre^{+} mice. Wild type (WT) or podoplanin-deficient (Vav-iCre^{+}) BMDMs were cultured in the presence, or absence of LPS (1 µg/ml) for 24h. Podoplanin expression was assessed by flow cytometry. The statistical difference between multiple groups was analysed using a one-way ANOVA with Tukey's multiple comparisons test, *$p < 0.05$ **$p < 0.01$ ***$p < 0.001$.

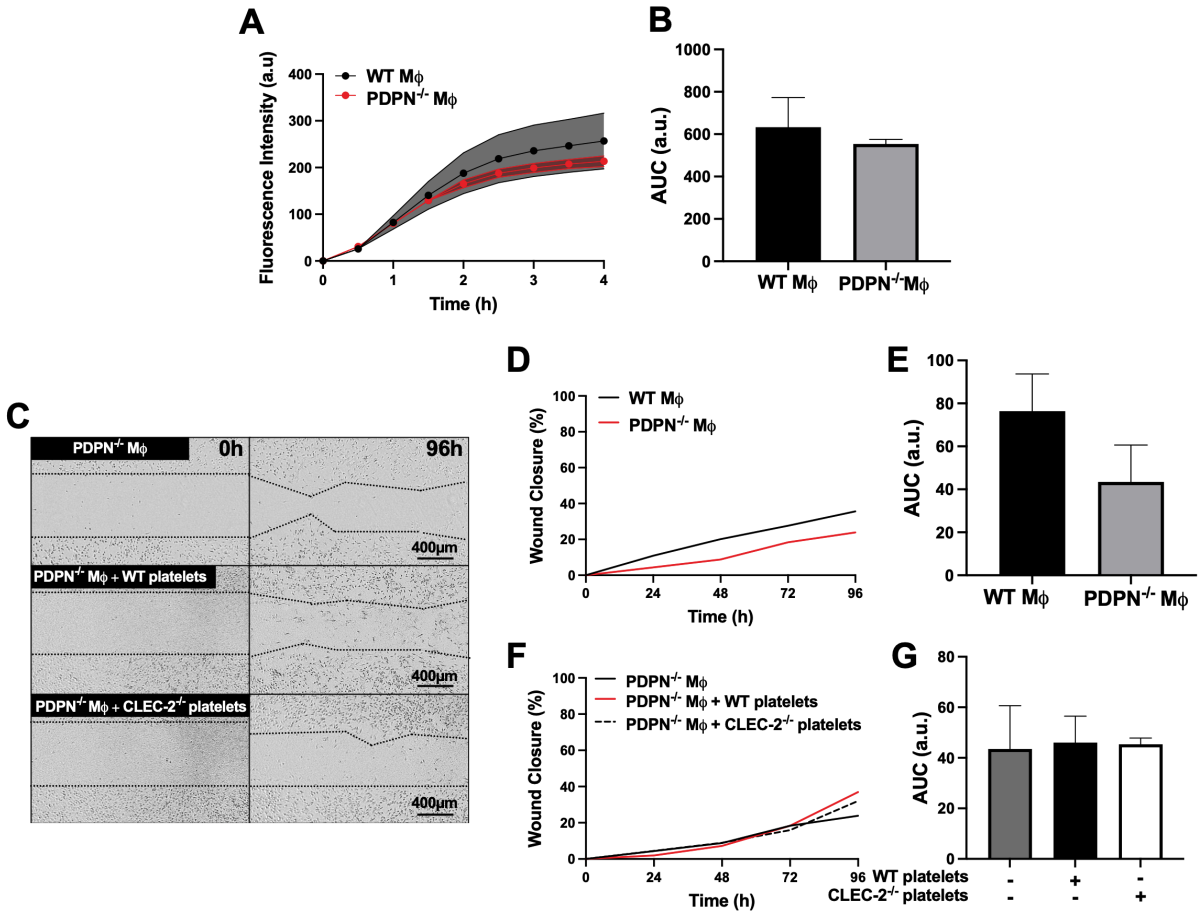

Figure 5.7 - Podoplanin deficiency does not reduce BMDM phagocytic capacity but inhibits platelet-induced wound closure. (A-G) Wild type (WT) or podoplanin-deficient BMDMs were LPS-stimulated (1 μg/ml) for 24 h (Mϕ). **(A, B)** Phagocytosis of pH sensitive Alexa Fluor-488 conjugated *Escherichia Coli* bioparticles ($3x10^6$ beads/condition) by WT or podoplanin-deficient ($PDPN^{-/-}$) Mϕ was visualized for 4 h and analysed using Incucyte SX-5 Live-Cell microscopy. (n=4). **(C-G)** Scratch wound migration of $PDPN^{-/-}$ Mϕ was monitored every 2 h for 96 h using an Incucyte ZOOM system. Following wound scratch, **(C)** WT or CLEC-2-deficient platelets (100:1) were added to Mϕ. **(D, F)** Wound closure was quantified as percentage of closure using ImageJ. **(E, G)** Total wound closure was quantified by area under the curve (AUC; a.u. = arbitrary units) at 96 h (n=3). The statistical significance between 2 groups was

analysed using an unpaired t-test and the statistical difference between multiple groups was tested using a one-way ANOVA with Tukey's multiple comparisons test.

5.3.4 The immunomodulatory function of CLEC-2 on macrophages is independent of platelet activation and secretion

Platelet activation has been shown to drive leukocyte recruitment and migration during inflammatory conditions, majorly through PF4 and RANTES secretion. In order to assess whether the immunomodulatory function of CLEC-2 was a result of platelet biology, or if it was a result of specific CLEC-2-podoplanin crosslinking, we used recombinant dimeric CLEC-2 (rCLEC-2-Fc) and IgG isotype controls. Addition of rCLEC-2-Fc to LPS-stimulated RAW264.7 cells or LPS-treated BMDM for 1 h increased podoplanin expression similar to WT platelets **(Figure 5.8A-B)**. Crosslinking podoplanin with rCLEC-2-Fc decreased TNF-α secretion **(Figure 5.8C)**.

Similar to WT platelets, rCLEC-2-Fc induced LPS-stimulated BMDM elongation along collagen fibres, compared isotype IgG control **(Figure 5.8D)** and accelerated wound closure **(Figure 5.8E-G)**, confirming the role of podoplanin crosslinking on macrophage migration. Podoplanin has been shown to bind to ERM proteins to regulate cell migration (Martín-Villar et al., 2006). We therefore investigated the interaction and distribution of the ERM proteins and podoplanin in inflammatory macrophages using 3D-SIM microscopy. Surprisingly, podoplanin did not colocalize with the ERM proteins in LPS-treated BMDM. However, addition of rCLEC-2-Fc increased the

association of ERM proteins with podoplanin **(Figure 5.8H)**, with an enrichment on the filopodia and migrating edges of the cell.

As expected, the addition of rCLEC-2-Fc to podoplanin-deficient BMDM did not induce wound closure **(Figure 5.9A-C)**, further confirming a distinct role for the CLEC-2-podoplanin axis. In line with this, rCLEC-2-Fc reduced the levels of iNOS, a marker of M1 inflammatory macrophages, without altering Early Growth Response Gene-2 (Egr-2), a marker of M2 anti-inflammatory macrophages **(Figure 5.10A, B)**. Furthermore, the expression of co-stimulatory receptor, CD80, was not modified in the presence of rCLEC-2-Fc **(Figure 5.10C)**. This suggests a distinct mechanism for the CLEC-2-podoplanin axis to decrease the BMDM inflammatory phenotype without altering its re-polarization.

Altogether, our results show that crosslinking podoplanin by CLEC-2, rather than platelet activation and secretion, is responsible for the immunomodulatory effect of CLEC-2 regulating macrophage inflammatory phenotype and their migration.

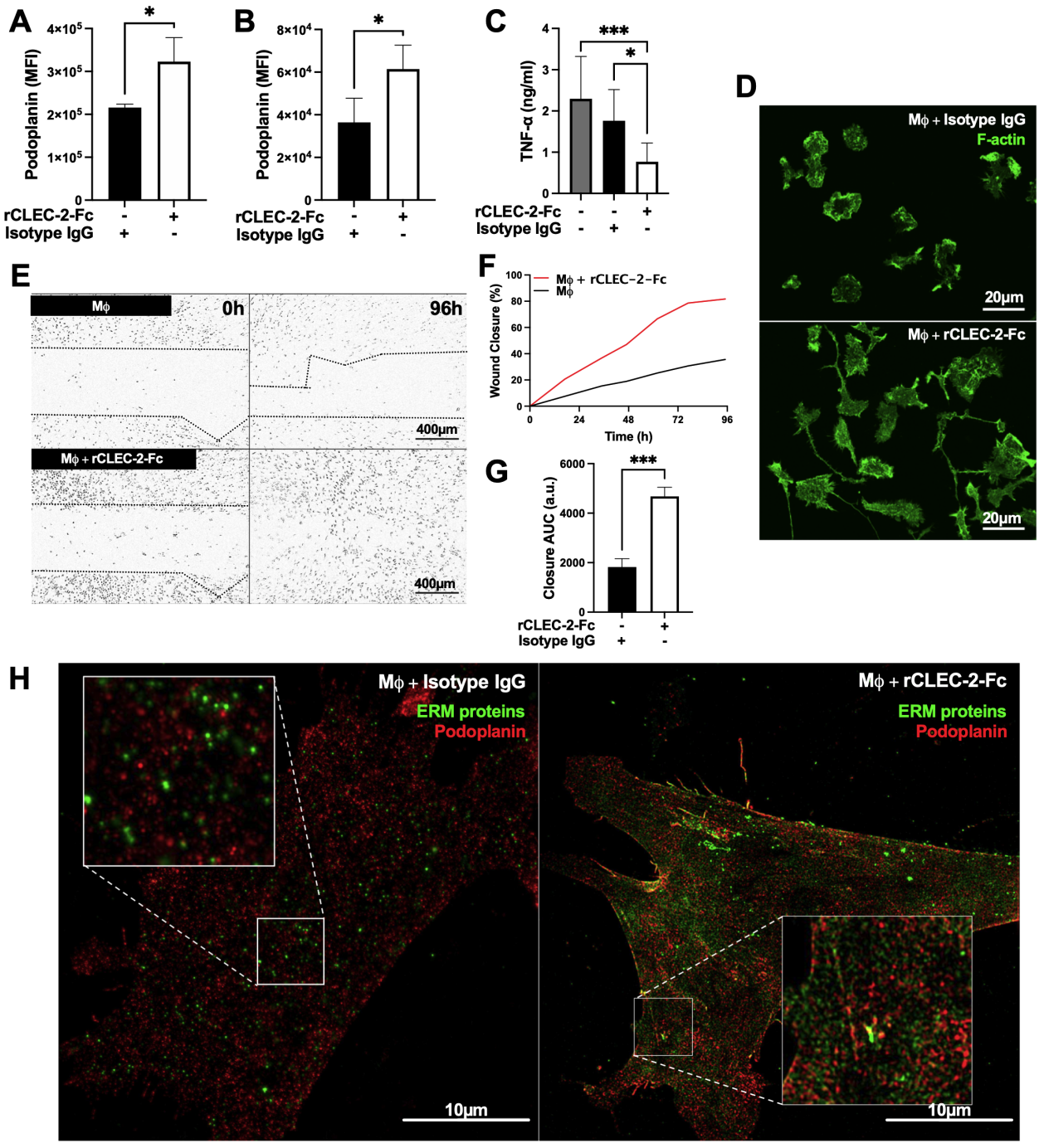

Figure 5.8 - Figure 3: rCLEC-2-Fc upregulates podoplanin expression, and promotes macrophage spreading and migration *in vitro*. **(A, B)** Surface podoplanin expression was detected by flow cytometry. 24 h LPS-stimulated (1 μg/ml) **(A)** RAW264.7 cells (n=3) or **(B)** BMDMs (Mϕ; n=4), were washed and incubated with recombinant CLEC-2-Fc (rCLEC-2-Fc; 10 μg/ml) or IgG isotype

control (10 μg/ml) for 1h. **(C)** Mϕ were washed, and cultured with rCLEC-2-Fc (10 μg/ml) or IgG isotype control (10 μg/ml) for 2 h before TNF-α secretion was quantified in the media supernatant by ELISA (n=4). **(D)** LifeAct-GFP-derived Mϕ were spread on collagen in the presence of rCLEC-2-Fc or IgG isotype control (10 μg/ml) for 2 h and measured with immunofluorescence by confocal microscopy. **(E-G).** Scratch wound migration of Mϕ in a monolayer was monitored every 2h for a total of 96h using an Incucyte ZOOM system. Following wound scratch, **(E)** rCLEC-2-Fc (10 μg/ml) was added to Mϕ. **(F)** Wound closure was quantified as percentage of closure compared to initial scratch size using ImageJ. **(G)** Total wound closure was quantified using area under the curve (AUC) at 96 h (a.u.= arbitrary units; n=3). **(H)** Mϕ were cultured on collagen in the presence of rCLEC-2-Fc or IgG isotype control (10 μg/ml) for 2 h. Podoplanin (red) and ERM protein (green) localisation was visualised using immunofluorescence by 3D-structured illumination microscopy (3D-SIM). The statistical significance between 2 groups was analysed using a paired t-test and the statistical difference between multiple groups was tested using a one-way ANOVA with Tukey's multiple comparisons test, $*p < 0.05$ $***p < 0.001$.

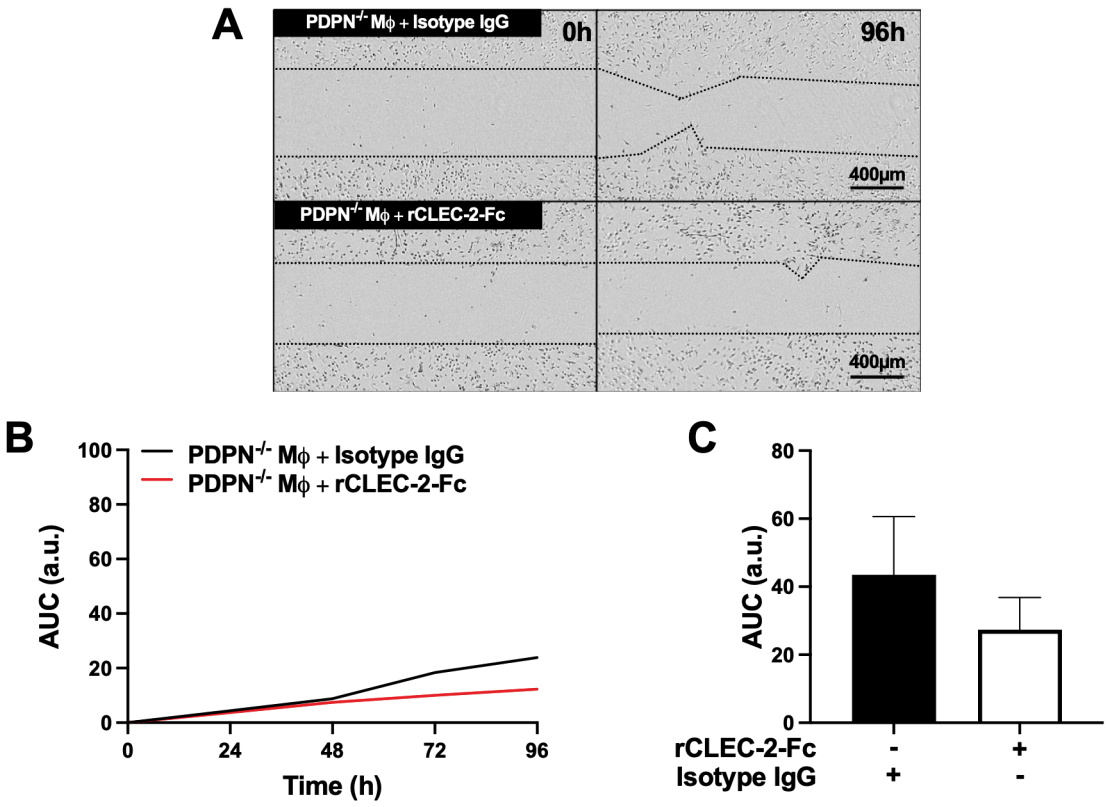

Figure 5.9 - BMDM podoplanin deficiency inhibits rCLEC-2-FC-induced wound closure. (A-C) Podoplanin-deficient BMDMs were LPS-stimulated (1 μg/ml) for 24 h (Mϕ). Scratch wound migration of podoplanin-deficient Mϕ was monitored every 2 h for 96 h using an Incucyte ZOOM system. Following wound scratch, **(A)** Isotype IgG (10 μg/ml), or rCLEC-2-Fc (10 μg/ml) was added to Mϕ. **(B)** Wound closure was quantified as percentage of closure using ImageJ. **(C)** Total wound closure was quantified by area under the curve (AUC) at 96 h (n=3). The statistical significance between 2 groups was analysed using a paired t-test.

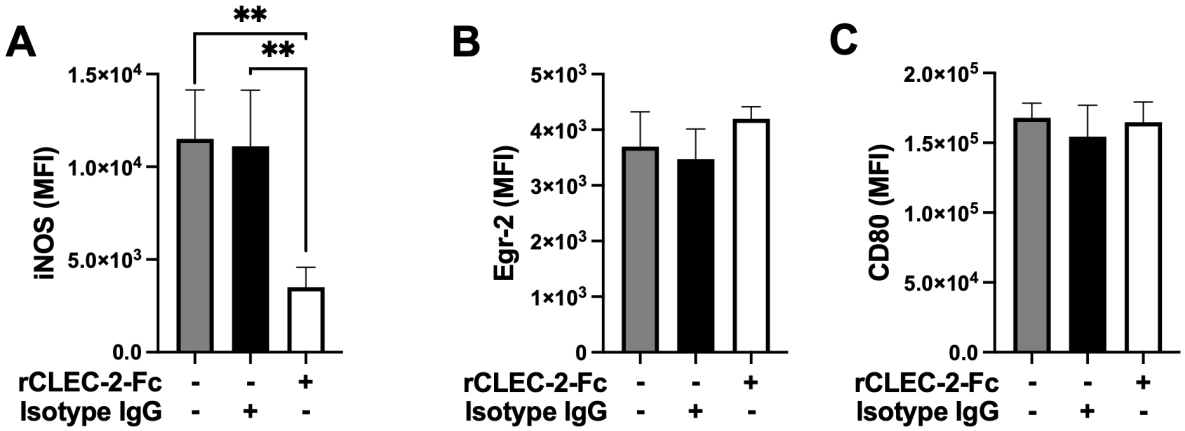

Figure 5.10 – CLEC-2 does not alter macrophage polarization. 24 h LPS-activated BMDMs (1 µg/ml) were cultured with rCLEC-2 (10 µg/ml) or IgG isotype control (10 µg/ml). Median of fluorescence intensity (MFI) for (**A)** iNOS, **(B)** Egr-2 and **(C)** CD80 was detected by flow cytometry (n=4). The statistical difference between multiple groups was tested using a one-way ANOVA with Tukey's multiple comparisons test. ** $p < 0.01$

5.3.5 rCLEC-2-Fc treatment reduces macrophage accumulation and inflammation in the peritoneum post-LPS-induced peritonitis

Inflammation is a critical process which allows the body to process trauma or pathogen infection. However, inflammation can equally be detrimental to bodily function, and can lead to organ dysfunction. Macrophage accumulation has been observed in peritonitis, ARDS, inflammation of the liver, and atherosclerosis (Rayes et al., 2017, Lax et al., 2017, Hitchcock et al., 2015, Hatakeyama et al., 2012). We have described a role for CLEC-2 in dampening the inflammatory macrophage phenotype, and inducing actin cytoskeletal remodelling *in vitro*, which may provide a promising therapeutic target. To address this, we investigated the use of rCLEC-2-Fc therapeutically during an *in vivo* model of ongoing inflammation, LPS-induced peritonitis, and assessed the accumulation of inflammatory macrophages and their activity. Mice were challenged intraperitoneally (IP) with LPS at 10 mg/kg for 18 h, before IP treatment with rCLEC-2-Fc (100 µg) or an isotype IgG (100 µg) for 4 h **(Figure 2)**.

Myeloid and lymphoid immune cell populations were detected after 22 h in the peritoneal lavage by flow cytometry. The gating strategy to identify F4/80$^+$ macrophages is shown in **Figure 5.11A**. At 22h post LPS, no significant change in the total number of cells in the peritoneum was observed in LPS-treated mice, compared to control mice **(Figure 5.11B)**. Endotoxemia did not significantly alter CD45$^+$ cell count in the PLF, compared to saline-treated mice. However, a significant reduction in CD45$^+$ was observed in the group treated with rCLEC-2-Fc **(Figure 5.11C),** more specifically CD11b$^+$ F4/80$^+$ **(Figure 5.11D, E).** The reduction in

inflammatory F4/80$^+$ cells was not due to increased cell apoptosis or death, measured by AnnexinV and Sytox staining **(Figure 5.11F)**. Podoplanin expression on F4/80$^+$ cells detected in the peritoneum was increased in the LPS groups compared to control, with no significant changes between rCLEC-2-Fc and IgG treatment **(Figure 5.11G)**. LPS increased platelet-macrophage complexes in the PLF, but this was not altered by rCLEC-2-Fc **(Figure 5.11H)**. However, a significant increase in F4/80$^+$CLEC-2$^+$ macrophages and the expression of CLEC-2 on F4/80$^+$ macrophages was observed following rCLEC-2-Fc treatment, confirming the binding of rCLEC-2-Fc to podoplanin on macrophages, without alteration in platelet-macrophage interactions **(Figure 5.11I, J)**.

These observations were shown to be specific to macrophages, as rCLEC-2-Fc did not alter neutrophil (CD45$^+$CD11b$^+$Ly6G$^+$), monocyte (CD45$^+$CD11b$^+$Ly6C$^+$), T cells (CD45$^+$CD11b$^-$CD3$^+$CD4$^+$ and CD8$^+$), B cells (CD45$^+$CD11b$^-$CD3$^-$CD19$^+$) or dendritic cells (CD45$^+$CD11b$^-$CD3$^-$CD11c$^+$) in the PLF **(Figure 5.12A-F)**. rCLEC-2 treatment did not induce bleeding in the peritoneum, measured using red blood cell marker, Ter 119 **(Figure 5.12G)**.

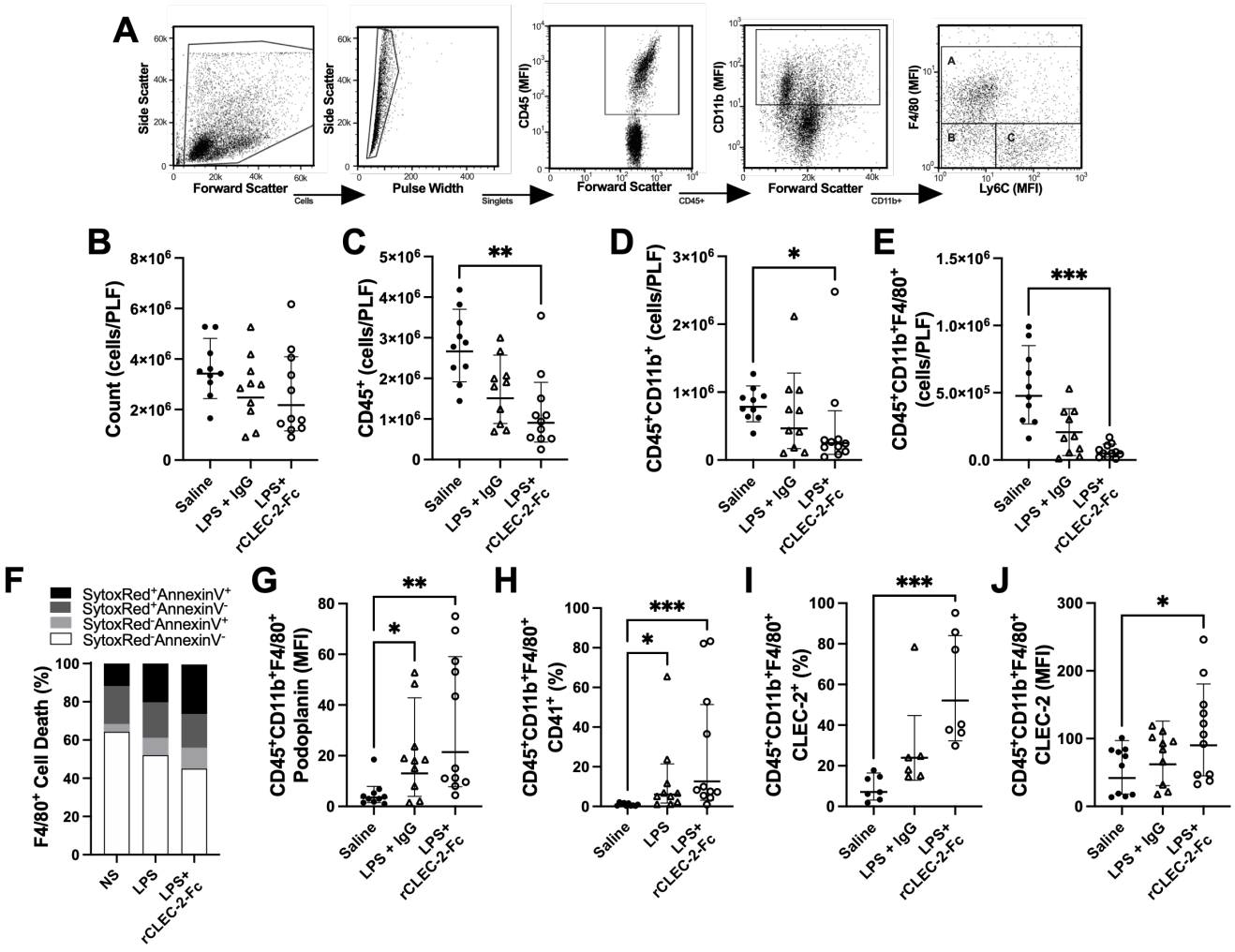

Figure 5.11 - rCLEC-2-Fc decreases macrophage number in the peritoneum following endotoxemia. Mice were intraperitoneally injected with LPS (10 mg/kg) for 18 h followed by rCLEC-2-Fc or IgG isotype control (100 µg) for 4 h (n=11). Immune cell and platelet infiltration in the peritoneal lavage (PLF) were measured using flow cytometry. **(A)** Gating strategy to identify A: macrophages ($CD11b^+F4/80^+$), B: monocytes ($CD11b^+Ly6C^+$) and C: neutrophils ($CD11b^+F4/80^-Ly6C^-$). **(B)** Total number of cells from the peritoneal lavage, **(C)** leukocytes ($CD45^+$), **(D)** myeloid cells ($CD45^+CD11b^+$) and **(E)** macrophages ($CD45^+CD11b^+F4/80^+$) were measured in the PLF. **(F)** $F4/80^+$ macrophage viability was quantified using SytoxRed and AnnexinV staining. **(G)** Median fluorescence intensity (MFI) of

podoplanin expressed on the surface of macrophages was quantified. **(H)** The percentage of platelet-macrophage complexes in the peritoneum ($F4/80^{+}CD41^{+}$), **(I)** the percentage of CLEC-2-positive macrophages and **(H)** the MFI of CLEC-2 expression on macrophages was assessed. The statistical difference between multiple groups was tested using a one-way ANOVA with Tukey's multiple comparisons test, *$p<0.05$ **$p < 0.01$ ***$p<0.001$.

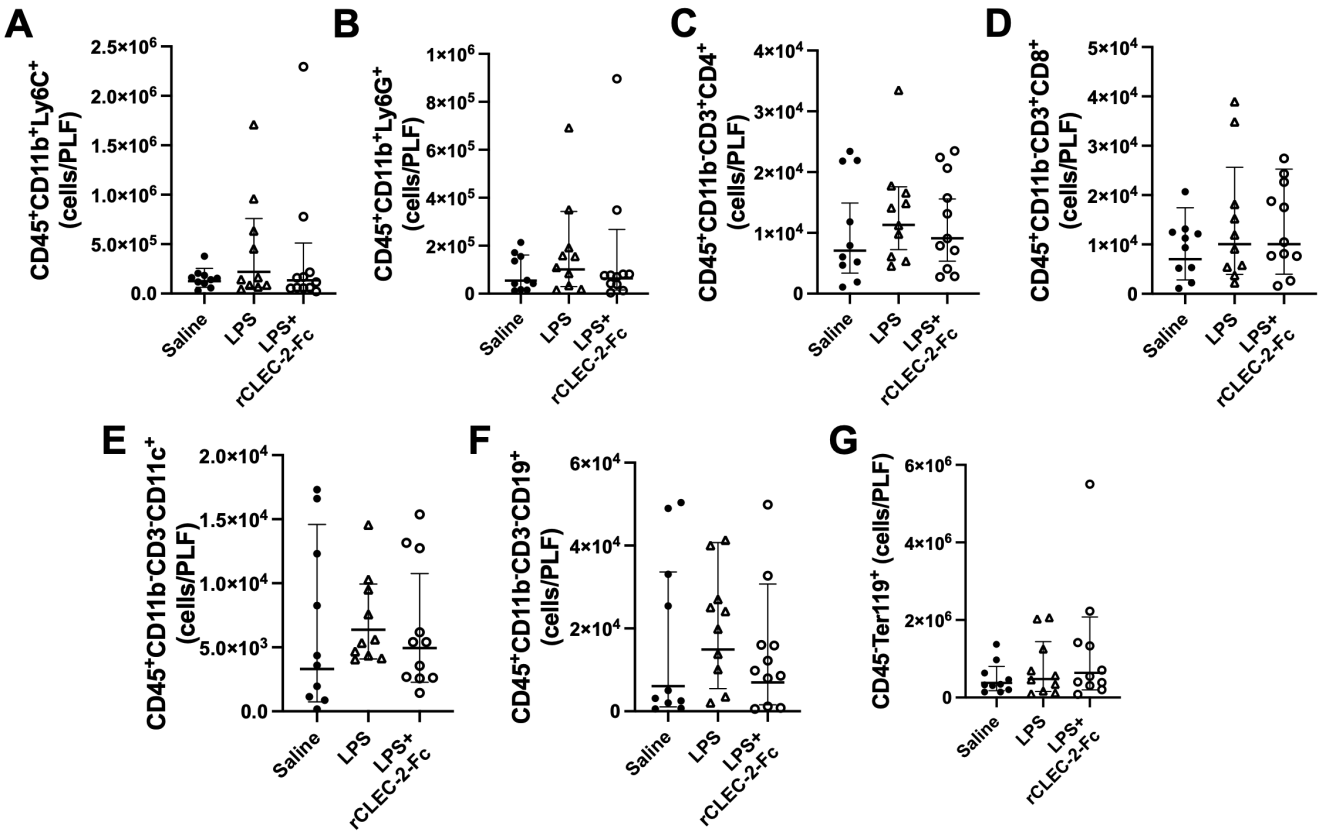

Figure 5.12 - rCLEC-2-Fc treatment does not alter immune cell accumulation aside from macrophages during peritonitis. Mice were intraperitoneally injected with LPS (10 mg/kg) for 18 h followed by rCLEC-2-Fc or IgG isotype control (100 µg) for an additional 4 h (n=11. Total count of **(A)** monocytes ($CD45^+CD11b^+Ly6C^+$) and **(B)** neutrophils ($CD45^+CD11b^+Ly6G^+$), **(C)** CD4+ and **(D)** CD8+ T cells ($CD45^+CD11b^-CD3^+$), **(E)** B cells ($CD45^+CD11b^-CD3^-CD19^+$), **(F)** dendritic cells ($CD45^+CD11b^-CD3^-CD11c^+$) and **(G)** erythrocytes ($CD45^-Ter119^+$) in the peritoneum was acquired by flow cytometry. The statistical difference between multiple groups was tested using a one-way ANOVA with Tukey's multiple comparisons test.

We assessed whether the change in macrophage accumulation in the inflamed peritoneum is accompanied by an alteration in cytokine and chemokine release. Similar to our *in vitro* observations, rCLEC-2-Fc decreased TNF-α secretion in the PLF of LPS-treated mice **(Figure 5.13A)** and increased the levels of the anti-inflammatory cytokine IL-10 **(Figure 5.13B)**. Furthermore, chemokines CCL2, CCL5 and CXCL1 were also significantly increased **(Figure 5.13C-E)**. Interestingly, CCL21, a soluble ligand for podoplanin (Tejchman et al., 2017), was not significantly altered in the peritoneum in rCLEC-2-Fc-treated mice **(Figure 5.13F)**. Alongside previous observation that increased $Ter119^{+}$ cells were not detected in the peritoneum in the group treated with rCLEC-2-Fc, we saw that the emigration of macrophages was not associated with increased vascular permeability, as measured by angiopoietin-2 secretion **(Figure 5.13G)**. There was no change in MMP-9, CXCL2, CCL4, C5a, IL-6 or IL1-β secretion following rCLEC-2-Fc treatment **(Figure 5.13H-L).**

Together, these results show that rCLEC-2-Fc preferentially reduces inflammation through multiple mechanisms. Not only does rCLEC-2-Fc reduce podoplanin-positive inflammatory macrophage accumulation and retention in the inflamed peritoneum, but we observe that this is associated with an alteration in the inflammatory environment, in particular a reduction in pro-inflammatory TNF-α levels and increase in anti-inflammatory IL-10. However, the fate of the macrophages which have emigrated from the peritoneum is unknown.

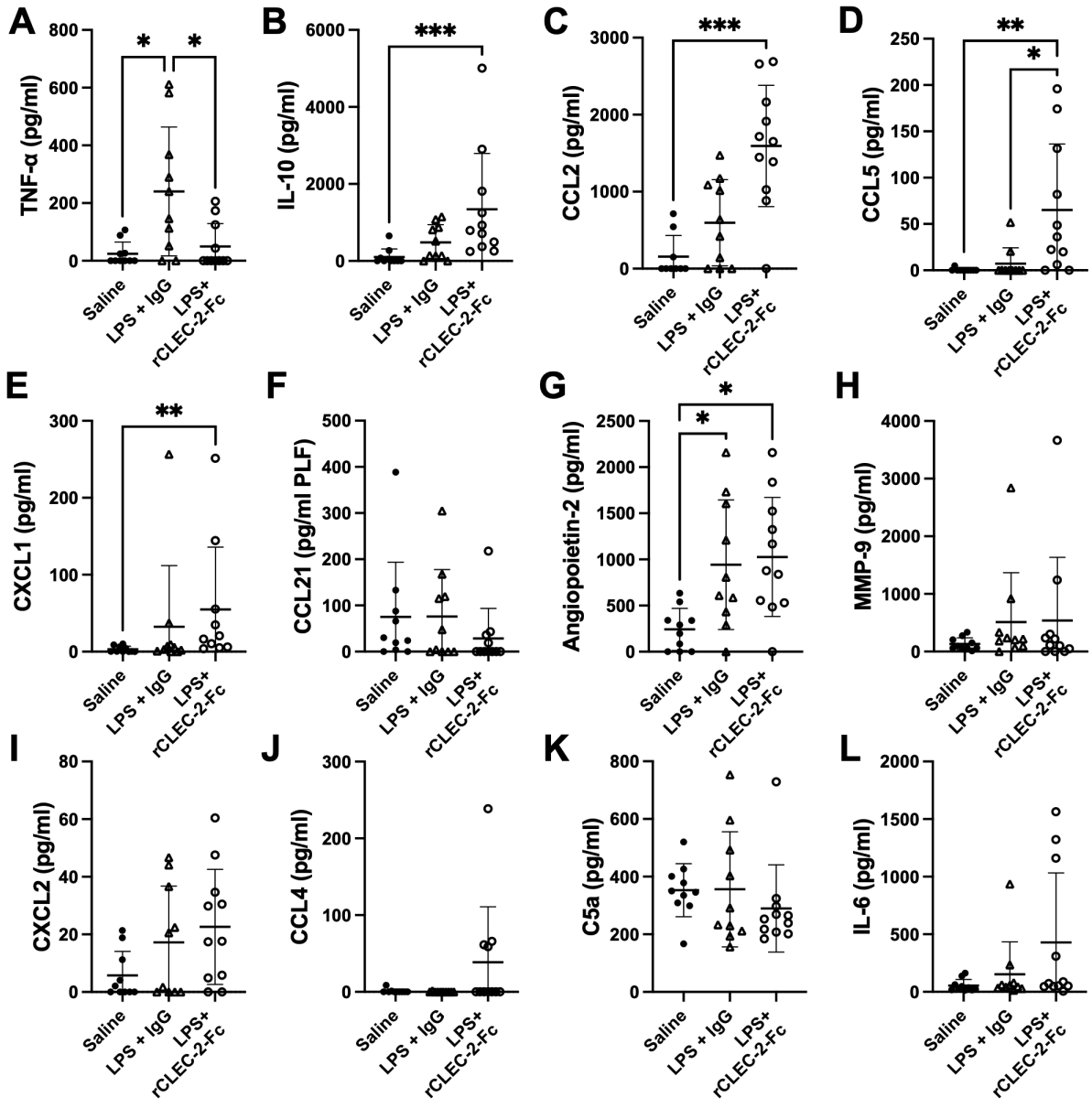

Figure 5.13 – rCLEC-2-Fc reduces inflammation in the peritoneum during endotoxemia. Mice were intraperitoneally injected with LPS (10 mg/kg) for 18 h followed by rCLEC-2-Fc or IgG isotype control (100 µg) for an additional 4 h (n=11). Chemokine and cytokine secretion in the peritoneal lavage fluid (PLF) of **(A)** TNF-α, **(B)** IL-10, **(C)** CCL2, **(D)** CCL5, **(E)** CXCL1, **(F)** CCL21 **(G)** angiopoietin-2, **(H)** MMP-9, **(I)** CXCL2, **(J)** CCL4, **(K)** C5a, and **(L)** IL-6 was measured by ELISA. The statistical difference between multiple groups was tested using a one-way ANOVA with Tukey's multiple comparisons test. *p < 0.05 **p < 0.01 ***p < 0.001

5.3.6 rCLEC-2-Fc treatment during endotoxemia increases inflammatory macrophage emigration from the spleen and lung

The decrease in macrophage count in the peritoneum could be explained by increased cell death, increased adhesion or emigration to secondary sites. Since rCLEC-2-Fc did not increase macrophage death and our *in vitro* experiments suggests accelerated migration, we investigated the infiltration of macrophage in the draining lymphoid organs. No significant increase in spleen weight or $CD45^+$ cell count was observed post-LPS-challenge **(Figure 5.14A, B)**. However, LPS injection increases the total number of myeloid $CD11b^+$ cells, in particular $F4/80^+$, in the spleen compared to control **(Figure 5.14C, D)**, which was abrogated in rCLEC-2-Fc-treated mice. Despite that LPS-challenge induced podoplanin expression on splenic $F4/80^+$, it was not significantly altered by rCLEC-2 compared to control **(Figure 5.14E)**. Although, a significant increase in $F4/80^+podoplanin^+CLEC\text{-}2^+$ is observed **(Figure 5.14F, G)**. Immunofluorescent imaging shows a decrease in platelet-positive macrophages in the spleen compared to IgG control **(Figure 5.14H)**.

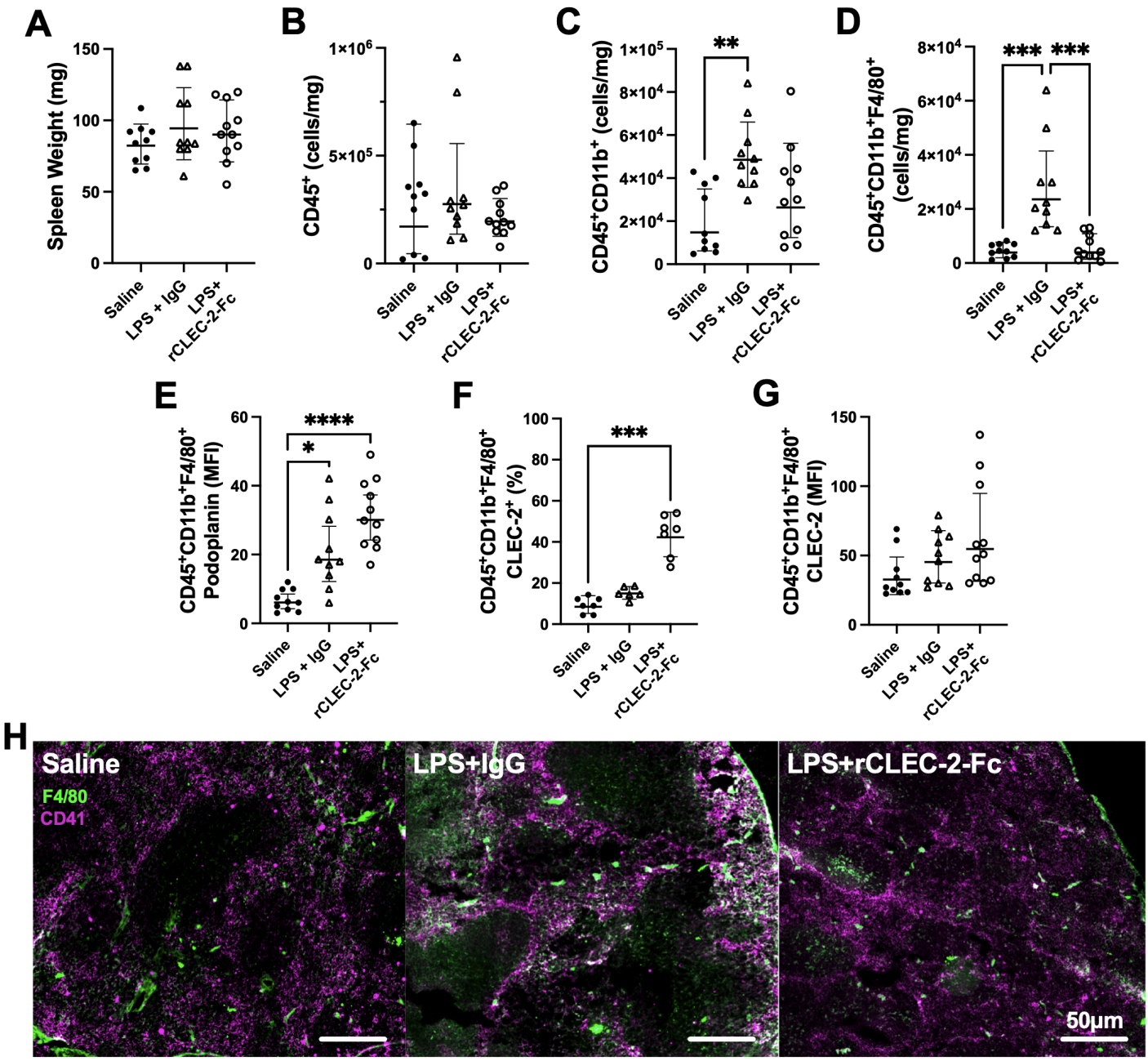

Figure 5.14 - rCLEC-2-Fc treatment induces macrophage emigration from the spleen during endotoxemia. Mice were intraperitoneally injected with LPS (10 mg/kg) for 18 h followed by rCLEC-2-Fc or IgG isotype control (100 µg) for an additional 4 h (n=11). Total splenocytes were collected, red blood cells lysed and immune cell populations were detected by flow cytometry. Cell number was normalised to **(A)** spleen weight. **(B)** Total count of immune cells ($CD45^+$), **(C)** myeloid cells ($CD45^+CD11b^+$) and **(D)** macrophages ($CD45^+CD11b^+F4/80^+$) were analysed, alongside **(E)** median

fluorescent intensity (MFI) of podoplanin expressed on the surface of macrophages, **(F)** CLEC-2-positive macrophages (%) and **(G)** F4/80$^+$CLEC-2 expression was assessed using flow cytometry. **(H)** Immunofluorescent staining of platelets (CD41; purple) and macrophages (F4/80; green) in frozen spleen sections was imaged by a Zeiss Axioscan 7. The statistical difference between multiple groups was tested using a one-way ANOVA with Tukey's multiple comparisons test. **p < 0.01 ***p < 0.001 ****p < 0.0001.

As rCLEC-2 did not induce F4/80$^+$ migration to the spleen, and were not found in the peritoneum, we investigated the presence of macrophages in the liver, kidney and lungs **(Figure 5.15A-C)** and quantified by F4/80$^+$ thresholding **(Figure 5.15A-C)**. We observed resident macrophages (Kupffer cells) in the liver of unchallenged mice, with an infiltration of F4/80$^+$ macrophages upon LPS-challenge, unchanged by rCLEC-2-Fc treatment **(Figure 5.15A, D)**. There were few kidney resident macrophages in unchallenged mice, again with an infiltration of F4/80+ cells upon LPS-challenge, unchanged by rCLEC-2-Fc treatment **(Figure 5.15B, E)**. Finally, we observed alveolar macrophages in the lungs of unchallenged mice, but interestingly, whilst we observe F4/80$^+$ lung infiltration upon LPS-challenge, there was macrophage emigration from the lungs with rCLEC-2-Fc treatment **(Figure 5.15C, F)**.

Our results demonstrate that macrophages do not emigrate to organs upon rCLEC-2-Fc treatment, but in fact show a loss of macrophages in the lung. This does not explain the loss of macrophages observed in the spleen or peritoneum.

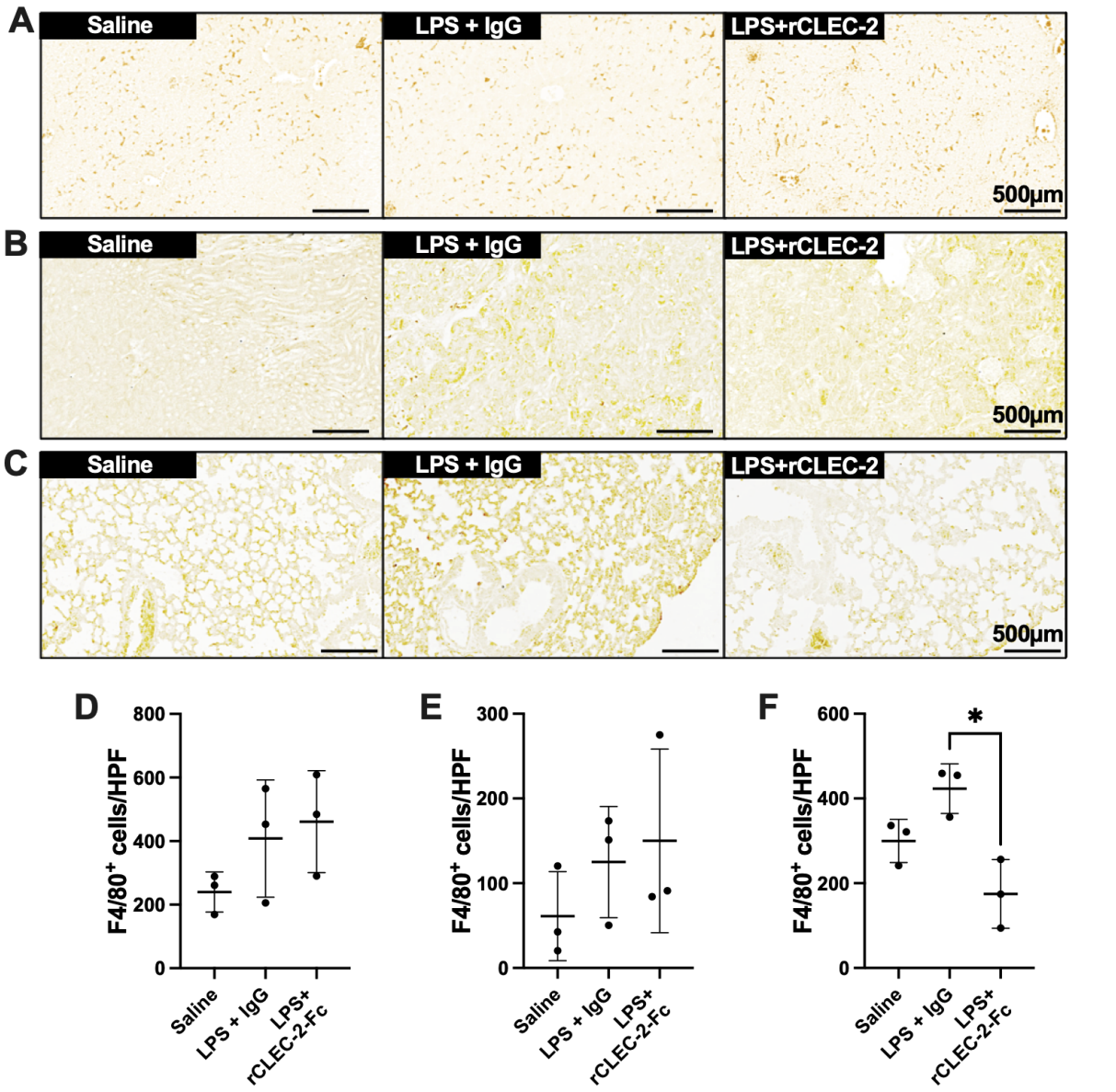

Figure 5.15 - rCLEC-2-Fc treatment induces macrophage emigration from the lungs during endotoxemia. Mice were intraperitoneally injected with LPS (10 mg/kg) for 18 h followed by rCLEC-2-Fc or IgG isotype control (100µg) for 4 h. **(A-C)** F4/80-DAB stained paraffin embedded organs: **(A)** liver, **(B)** kidney and **(C)** lungs were imaged using a Zeiss Axioscan 7. **(D-F)** F4/80$^+$ cells were quantified per high power field (HPF) using an ImageJ script: **(D)** liver, **(E)** kidney and **(F)** lungs. The statistical difference between multiple groups was tested using a one-way ANOVA with Tukey's multiple comparisons test. **p < 0.01

5.3.7 Macrophages emigrate to draining mesenteric lymph nodes upon rCLEC-2-Fc treatment during endotoxemia to prime T cells

We next investigated the infiltration of inflammatory peritoneal macrophages to the draining lymph nodes. F4/80$^+$ population was detected in the mesenteric lymph nodes (MLN) by flow cytometry and immunofluorescence. A significant increase in myeloid cells, in particular F4/80$^+$ cells, was observed in rCLEC-2-Fc treated mice compared to IgG control **(Figure 5.16A-C)**. There was also a notable increase in CLEC-2-bound F4/80$^+$ cells in rCLEC-2-Fc-treated mice **(Figure 5.16D)**. The increase in CLEC-2 MFI might be due to the enhanced podoplanin expression, increasing the binding sites for CLEC-2. The increase in CLEC-2 density on F4/80$^+$ cells positively correlated with F4/80$^+$ frequency in the MLN (r^2=0.67, p=0.0011; **Figure 5.16E)**, demonstrating that rCLEC-2-Fc binding to inflammatory peritoneal macrophages promotes their emigration from the inflamed peritoneum to the MLN.

In order to assess whether emigrated macrophages prime T cells in the draining lymph nodes, we first assessed the location of these macrophages. Unchallenged lymph nodes showed platelets were localised in the medulla, and around the medullary chords. Following LPS challenge, there was no significant staining for F4/80$^+$ cells. However, following rCLEC-2-Fc treatment, a significant influx of F4/80$^+$ cells was observed in the draining lymph nodes, with a concentration of cells in the medulla, in close contact with T cells **(Figure 5.16F)**. We did not detect macrophages bound to platelets in this zone, however macrophages localised in the lymph nodes post-rCLEC-2-Fc are seen to be CLEC-2- and podoplanin-positive compared to IgG control **(Figure 5.16G)**.

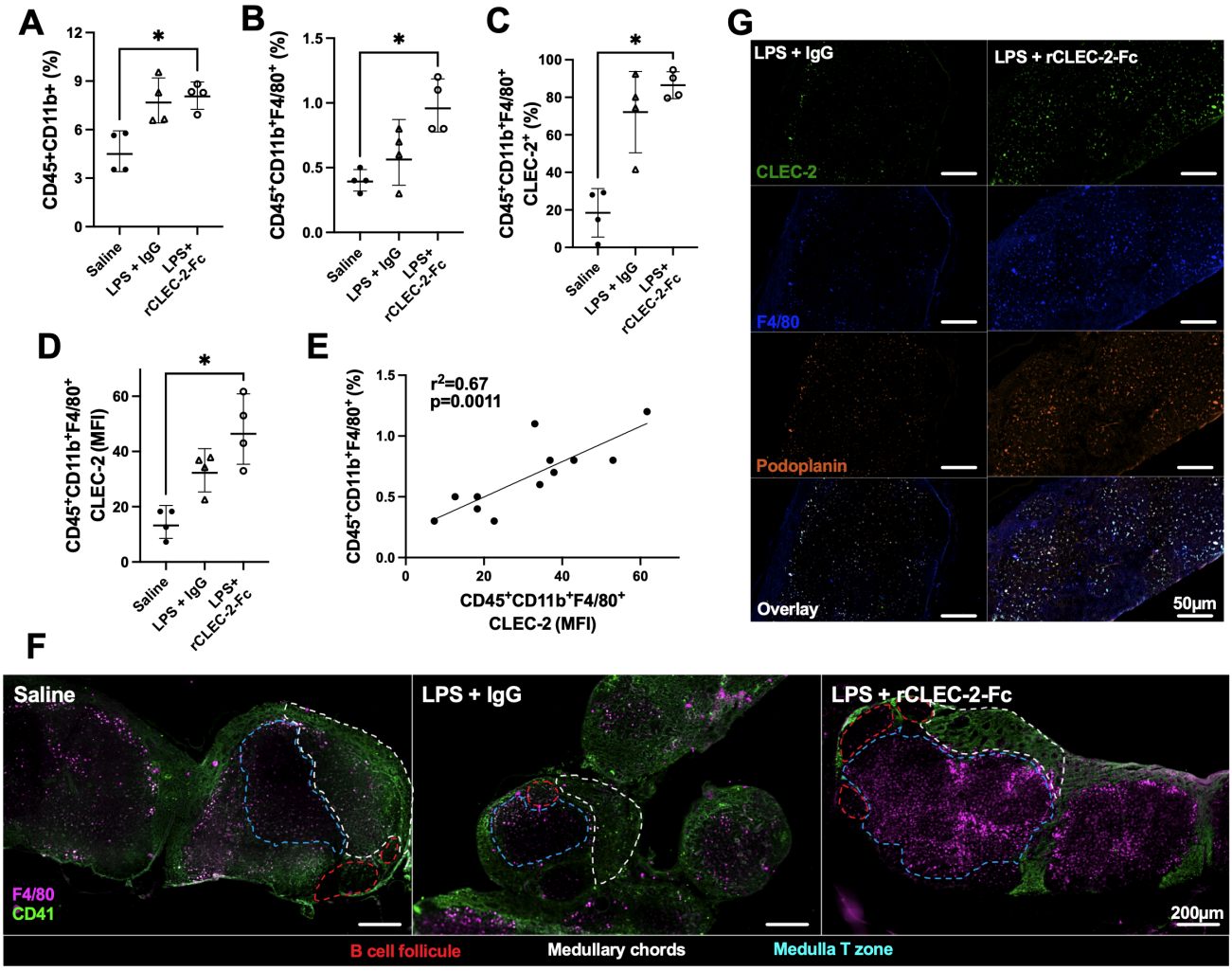

Figure 5.16 - Peritoneal macrophage emigration to mesenteric lymph nodes during endotoxemia is induced by rCLEC-2-Fc treatment. Mice were intraperitoneally injected with LPS (10 mg/kg) for 18 h followed by rCLEC-2-Fc or IgG isotype control (100µg) for an additional 4 h (n=4). **(A-E)** Mesenteric lymph node (MLN) cells were collected and immune cell population detected by flow cytometry. **(A)** Percentage of myeloid cells ($CD45^+CD11b^+$), **(B)** macrophages ($CD45^+CD11b^+F4/80^+$), **(C)** CLEC-2-positive macrophages and **(D)** the MFI of CLEC-2 expression on macrophages were detected by flow cytometry. **(E)** The correlation between the percentage of macrophages in the MLN and the MFI of CLEC-2 expression on macrophages by is shown by simple linear regression. **(F)**

Immunofluorescent staining of macrophages (F4/80; purple) and platelets (CD41; green) and **(G)** macrophages (F4/80; blue), CLEC-2 (green) and podoplanin (orange) in frozen MLN sections was imaged using a Zeiss Axioscan 7. The statistical significance was analysed using a Kruskal-Wallis multiple comparisons test. *$p < 0.05$.

Macrophage influx to the MLN is likely a result of a response to a chemoattract gradient generated. We investigated CCL21, a chemoattractant secreted from LECs and soluble ligand for podoplanin (Farnsworth et al., 2019). However, similar to the peritoneum, we did not observe an alteration of CCL21 expression in MLN upon rCLEC-2-Fc treatment **(Figure 5.17A)**. In order to assess whether increased podoplanin expression and actin remodelling upon CLEC-2-crosslinking increases macrophage chemoattraction towards CCL21, we evaluated inflammatory BMDM migration towards CCL21 *in vitro* using a Boyden chamber. Addition of rCLEC-2-Fc to LPS-treated BMDM increased the number of macrophages migrating towards CCL21 **(Figure 5.17B)**. This was not due to an increase in CCL21 receptors, CCR4 and CCR7 **(Figure 5.17C, D)**. This suggests that CLEC-2-dependent podoplanin and CD44 upregulation, associated with accelerated actin rearrangement, was responsible for increased migration towards CCL21.

We observed macrophages in the medulla post rCLEC-2-Fc treatment during peritonitis, whereby they can interact with lymphoid cells. This hinted that macrophages may be migrating to the MLN to prime T cells. We investigated this by stimulating homogenised MLN *ex vivo* with low-dose LPS (10 ng/ml) for 24 h. IL-2 secretion, a marker for T cell priming, was not detected post-low-dose LPS in MLN

cells isolated from saline- or LPS-treated mice **(Figure 5.17E)**. In contrast, a significant increase in IL-2 levels was observed in rCLEC-2-Fc treated mice, suggesting that increased macrophage efflux to the medulla T zone promotes T cell priming.

Altogether, these results suggest that rCLEC-2-Fc alters the expression of podoplanin and its interaction with ligands CD44, ERM and CCL21. This accelerates the removal of inflammatory macrophages from the inflamed peritoneum, reducing macrophage inflammation and promotes macrophage emigration to mesenteric lymph nodes to promote T cell priming. Overall this reduces inflammation in the peritoneum, and may initiate the adaptive immune system to promote the resolution of inflammation.

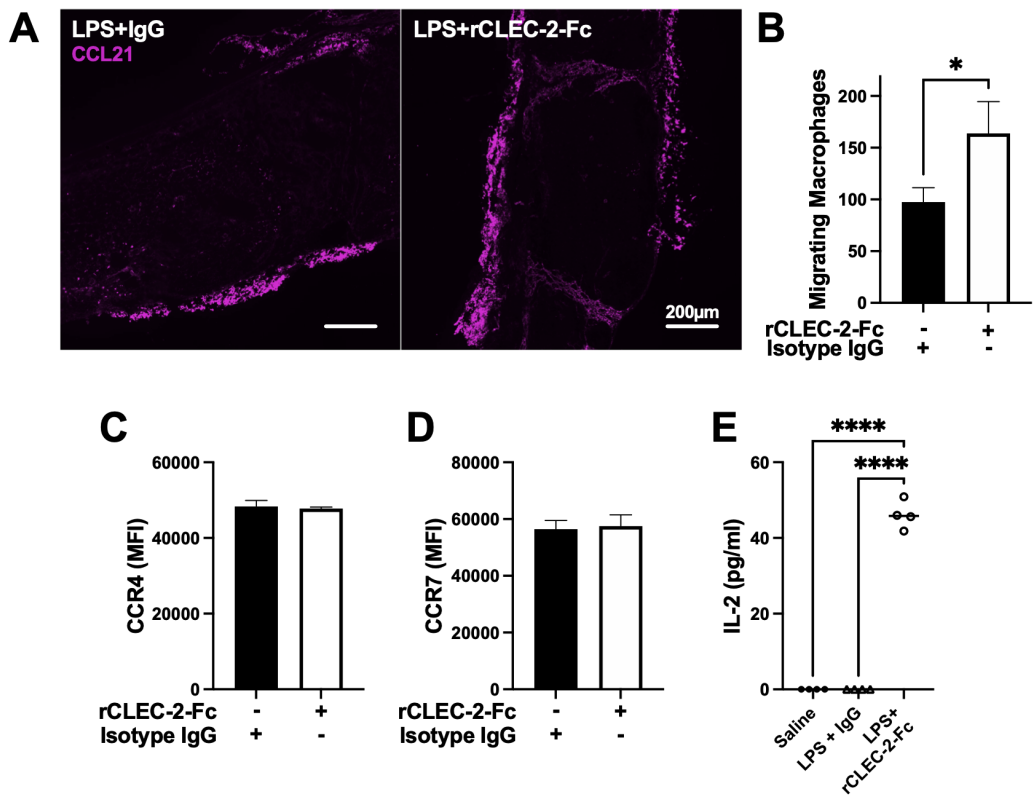

Figure 5.17 - Inflammatory macrophages migrate toward CCL21 during endotoxemia and primes T cells in mesenteric lymph nodes. Mice were intraperitoneally injected with LPS (10 mg/kg) for 18 h followed by rCLEC-2-Fc or IgG isotype control (100µg) for an additional 4 h (n=4). **(A)** Immunofluorescent staining of CCL21 (purple) in frozen sections of MLN, and images taken using a Zeiss Axioscan 7. **(B-D)** 24 h LPS-stimulated (1 µg/ml) BMDMs were treated with rCLEC-2-Fc or IgG isotype control (10 µg/ml) for 4 h. **(B)** The migration of inflammatory BMDMs with rCLEC-2-Fc or IgG Isotype control (10 µg/ml) toward CCL21 (30 ng/ml) was analysed using a Boyden chamber for 4 h (n=3). Surface expression of **(C)** CCR4 and **(D)** CCR7 median fluorescence intensity (MFI) was detected by flow cytometry (n=4). **(E)** IL-2 secretion from MLN cells *in vitro* culture with LPS (10 ng/ml) for 16 h was quantified by ELISA. The statistical significance between 2 groups was analysed using an unpaired t-test and a one-way ANOVA with Tukey's multiple comparisons test for multiple groups, *$p < 0.05$ ****$p < 0.0001$.

5.4 Discussion

In this study, we report that crosslinking podoplanin expressed on inflammatory macrophages using rCLEC-2-Fc limits the inflammatory environment by reducing inflammatory macrophage accumulation in the inflamed tissue and directly reducing their inflammatory phenotype. During ongoing peritonitis induced by LPS, rCLEC-2-Fc accelerates the removal of inflammatory macrophages from the site of inflammation to a draining lymph node and primes T cells. CLEC-2-podoplanin crosslinking inflammatory macrophages promotes their mobility through (i) the dephosphorylation of podoplanin intracellular serine residues, (ii) upregulation and rearrangement of podoplanin and CD44 expression on macrophage membrane protrusions, (iii) reorganisation of the actin cytoskeleton through ERM protein distribution on cell protrusions and (iv) inflammatory macrophage interaction with CCL21. Simultaneously, CLEC-2 reduces TNF-α secretion from inflammatory macrophages and delays their phagocytic activity without changing macrophage polarisation, in a podoplanin-dependant manner. We propose that during ongoing inflammation, CLEC-2-podoplanin crosslinking reduces tissue inflammation by reducing accumulation and retention of inflammatory macrophages and promotes their emigration to draining lymph nodes.

During inflammation, macrophages play three main functions: phagocytosis of debris and dead/apoptotic cells and pathogens, antigen presentation and immunoregulation by secreting an arsenal of cytokines and chemokines. After the first inflammatory phase subsides, macrophages also play a role in tissue repair and wound healing (Duffield et al., 2005). Alteration in the acute or repair phases can lead to chronic

inflammation and pathogenic fibrosis. Recent studies showed that platelet interaction with macrophages can alter macrophage function, dependant on the receptor, insult, organ and disease progression (Scull et al., 2010, Linke et al., 2017, Carestia et al., 2019, Barrett et al., 2019, Rolfes et al., 2020, Heffron et al., 2021). Using acute inflammatory models, we and others have shown a significant upregulation of podoplanin on inflammatory macrophages. Although many studies have shown that platelet secretion is the main regulator of macrophage function, partly through Prostaglandin E_2 (Xiang et al., 2013, Heffron et al., 2021), we show for the first time that CLEC-2 immunomodulation independent of platelet activation and secretion. Deletion of CLEC-2 from platelets did not alter the binding of platelets to inflammatory macrophages, suggesting that CLEC-2 is not involved this heterotypic interaction, but exerts an immunomodulatory effect. GPIb, CD40L, P-selectin or other receptors might be responsible for binding and differentially regulate macrophage functions (Carestia et al., 2019, Inwald et al., 2003, Ye et al., 2019).

The use of rCLEC-2-Fc overcomes the limitation of using platelets during ongoing inflammation, as the variety of platelet receptors have both pro- and anti-inflammatory roles which limit clinical translation. CLEC-2 induces a rapid (<1 h) translocation of podoplanin from intracellular stores to the surface of inflammatory macrophages. This is associated with a loss of phosphorylation of the serine residues in the intracellular podoplanin tail, which has been demonstrated to promote fibroblast migratory activity (Krishnan et al., 2013, Krishnan et al., 2015). Classically, macrophages migrate through actin polymerisation-driven elongation of the leading edge towards a gradient, followed by integrin mediated adhesion to matrix proteins and finally actomyosin contraction and trailing edge de-adhesion (Pixley, 2012).

CLEC-2 induced the reorganisation of the actin cytoskeleton and increased podoplanin interaction with ERM proteins and CD44, promoting macrophage migration. Furthermore, CD44 expression is required for podoplanin-induced migration in squamous stratified epithelia (Martín-Villar et al., 2010). This provides evidence for a signalling pathway linking podoplanin serine phosphorylation, ERM proteins and CD44 association to dictate cell migration. This cell- and protein-specific strategy to promote inflammatory macrophage migration, without inducing inflammatory bleeding or thrombosis, avoids major complications associated with platelet targeting in inflammation.

The induction of macrophage removal is unclear, although it has previously been speculated that it could be through local death and/or increased migration to draining lymph nodes (Bellingan et al., 1996, Cao et al., 2005, Gautier et al., 2013). Here, we show the absence of macrophages from the inflamed peritoneum is not secondary to macrophage local death or increased macrophage adherence through integrin $\alpha_D\beta_2$ and $\alpha_M\beta_2$ (Mac-1) upregulation, but rather due to macrophage emigration to a secondary site. Furthermore, the increase in macrophage emigration was not due to matrix metalloprotease 9 secretion, dysregulated vascular integrity, or by increase in other chemotactic molecules such as complement C5a levels, as previously described (Gong et al., 2008, Xie et al., 2020). Peritoneal macrophages are comprised of 2 functionally and phenotypically distinct subsets, the large (LPM) and small peritoneal macrophages (SPM) (Cassado Ados et al., 2015). LPM ($F4/80^{high}CD11b^{high}Ly6C^{-}$) largely outnumber SPM ($F4/80^{low}CD11b^{low}Ly6C^{+}$), and are responsible for phagocytosis of cell debris and apoptotic cells and mediate tissue repair (Cassado Ados et al., 2015). During a sterile liver injury, a sub-population of

resident peritoneal macrophages, GATA-6$^+$, is rapidly mobilised to the injured liver in CD44-dependent manner, expressing M2 macrophage markers and promoting tissue repair (Wang and Kubes, 2016). Following inflammation, LPM rapidly migrates to draining lymph nodes, whereas SPM numbers increases with monocyte influx from the circulation into the peritoneum. Combining our *in vitro* and *in vivo* data suggests a role for the strong chemoattractant and podoplanin ligand released from the draining lymph node LECs, CCL21 (Farnsworth et al., 2019). CCL21 has previously been described as a key regulator of podoplanin$^+$ dendritic cells migrating to lymph nodes (Lira, 2005, Manzo et al., 2007). Dendritic cell emigration to draining lymph nodes by a CCL21 gradient during inflammation was shown to be regulated by CCR7 upregulation on the cell surface (Luster et al., 2005). However, here we show CCL21 receptors, CCR4 and CCR7, had indifferent expression with rCLEC-2-Fc treatment, demonstrating a distinct role for podoplanin-CCL21. This directed migration and retention in lymph nodes represents advantages, through limitation of peritoneal inflammation and potential development of an adaptive immune response.

CLEC-2-mediated macrophage migration to draining lymph nodes was not restricted to reduce peritoneal inflammation and macrophage accumulation, but also increased T cell priming in the lymph nodes. Macrophages are not solely innate immune cells but can also process and present antigens to naïve T cells in secondary lymphoid organs, driving CD4$^+$ T helper cell activation and polarisation to Th1, Th2 or Th17 effector cells (Muntjewerff et al., 2020). Macrophage presence in the medulla, alongside IL-2 secretion, indicates T cell priming. Whether macrophages function as antigen presenting cells, express co-stimulatory molecules or release activating cytokines to prime T cells needs further investigation. Moreover, T cell priming,

polarisation and survival following clonal expansion requires further investigation. The beneficial targeting of macrophage emigration to lymph nodes is dependent on the disease, as the association of podoplanin-positive macrophages with tumour lymphatic vessels in mammary tumour model correlates with increased lymph node and distant organ metastasis (Bieniasz-Krzywiec et al., 2019).

We have previously shown that platelet-CLEC-2-deficiency in mice exacerbated the cytokine storm during endotoxemia and caecal ligation and puncture, associated with impaired macrophage number in the peritoneum. Complex alterations in the inflammatory response in these mice limited the use of rCLEC-2-Fc treatment during endotoxemia, due to a drastic early increase in the clinical severity. Therefore, the mechanisms driving the dysregulated inflammatory response in CLEC-2-deficient mice require further investigation.

In conclusion, we show a novel, key immunomodulatory role for CLEC-2-podoplanin interaction to limit the accumulation and retention of highly inflamed macrophages in tissues, a major complication observed in many sterile thromboinflammatory diseases such as atherosclerosis and metabolic syndrome. rCLEC-2-Fc may present a novel pathway to reduce the accumulation of inflammatory macrophages, limiting tissue inflammation and subsequent progression a to chronic inflammatory state.

Chapter 6

General Discussion

6.1 Summary of Results

The work presented in this thesis describes the dynamic characteristics of CLEC-2 in thrombosis, thromboinflammation and inflammation. We identified: **(i)** a role for CLEC-2 in thrombus growth and stability in mice, but not humans, **(ii)** a novel platelet-activating ligand for CLEC-2, hemin, which is limited by anti-malarial drug, hydroxychloroquine, **(iii)** a mechanism for CLEC-2 in promoting macrophage emigration during ongoing inflammation, through podoplanin. This data supports therapeutic interventions to either block CLEC-2-mediated thrombosis or to use recombinant CLEC-2 to reduce tissue inflammation. This data also supports a disease- and organ-dependent function of CLEC-2, which will require to be adjusted to the disease and organ involved.

6.2 A negligible role for CLEC-2 in thrombosis and haemostasis

The role of platelet CLEC-2 in arterial thrombosis until now was ambiguous. It had been suggested that CLEC-2 could be a novel anti-thrombotic target to replace P2Y12 or COX inhibitors, after promising observations in mice (May et al., 2009, Suzuki-Inoue, 2011, Bender et al., 2013, Haining et al., 2017). However, here we observe that the role of platelet-CLEC-2 to thrombus growth in arterial thrombosis in mice is not translated to humans. Whether this is the result of a ligand which does not exist in humans which is seen in mouse blood, or if it is due to dissimilar CLEC-2 copy numbers, it is not clear. This theory needs to be confirmed using a humanised platelet-CLEC-2 mouse model, which may elude to an answer. However, based on research to date, we can conclude that platelet-CLEC-2 inhibition in humans will not

detriment thrombosis and haemostasis, therefore making it a promising therapeutic target in other diseases.

6.3 Targeting CLEC-2 in thromboinflammation

CLEC-2 has well established roles in thromboinflammation, and has been described to contribute to venous thrombus formation in both sterile- and infection-driven thrombosis in a podoplanin-dependent manner (Hitchcock et al., 2015, Payne et al., 2017). However, no clinical trials targeting CLEC-2 in thromboinflammatory are ongoing, perhaps due to concern surrounding the contribution of CLEC-2 to haemostasis (Harbi et al., 2021). Our data demonstrating its negligible role in thrombus growth in humans provides justification to inhibit CLEC-2 to limit thrombus growth. Alternatively, CLEC-2 ligands could be targeted to limit thromboinflammation. Here, we show that HCQ limits hemin-induced platelet aggregation through CLEC-2 by scavenging hemin, similar to its mechanism of action as an anti-malarial. Hitchcock et al. demonstrated that a deletion of haematopoietic-podoplanin impaired thrombus generation post-*Salmonella* infection, similar to platelet-CLEC-2-deletion. However, targeting podoplanin therapeutically may be challenging, due to its expression on a wide variety of cell types, unlike CLEC-2, which is restricted to platelets and $CD11b^{hi}Gr\text{-}1^{hi}$ cells (Lowe et al., 2015). That being said, whilst inhibiting CLEC-2 during sterile thromboinflammation (such as DVT) may be without risk, impairment of the immunomodulatory function of CLEC-2 to regulate the inflammatory response during pathogen-induce thrombosis may prove counterintuitive.

6.4 Intracellular and Extracellular inhibition of CLEC-2

Classically, antibodies are used to inhibit receptor-ligand binding due to their high affinity, however they are not orally available. There are very few effective CLEC-2-blocking reagents. Cobalt hematoporphyrin blocks podoplanin and rhodocytin-induced aggregation (Tsukiji et al., 2018). Furthermore, non-cytotoxic 5-nitrobenzoate compound, 2CP, was shown to limit $FeCl_3$-induced vascular occlusion in mice, and podoplanin, but not rhodocytin-induced platelet aggregation (Chang et al., 2015). The drugs' toxicity, low potency and lack of oral availability has led to their discard from clinical trial pursuit. We show that monoclonal antibody, AYP1, blocks podoplanin and rhodocytin-induced platelet aggregation. The bioavailability, stability and efficacy of this antibody *in vivo* is the subject of ongoing research. Issues using extracellular inhibitors provide justification for CLEC-2 inhibition by other methods.

Intracellular targeting by downstream kinases linked to CLEC-2 hemITAM domain is effective. Specific kinases such as Bruton (BTK), syk and src, are essential to CLEC-2-regulated platelet activation (Outlined in **Figure 1.4**), and are approved for treatment of solid tumours, haematological malignancies and immuno thrombocytopaenia (Harbi et al., 2021). **Syk inhibitor**, Fostamatinib, is clinically approved to treat immune thrombocytopaenia, but has also been shown to inhibit CLEC-2- and GPVI-mediated platelet activation. Alternatively, **BTK inhibitors** have been developed and are in clinical trial such as Ibrutinib, which binds to the BTK H3 domain (Byrd et al., 2013, Byrd et al., 2015, Wen et al., 2021). Interestingly, low-dose BTK inhibitors have been shown to selectively inhibit CLEC-2- and not GPVI-induced platelet activation (Nicolson et al., 2021). This could be particularly

promising for treatment of thromboinflammatory, CLEC-2-mediated disease, without detriment to GPVI-mediated platelet activation.

A novel and exciting method for receptor blocking is nanobodies. They have the same specificity and affinity of antigen binding, but are 1/10th of the size, which allows for much greater tissue infiltration (Yang and Shah, 2020). In our lab, we have recently generated more than 50 different nanobodies to GPVI, some of which have been characterised to block ligand-induced platelet activation (Slater et al., 2021). There is currently no published nanobody to CLEC-2, however this could be an exciting, highly specific prospect for CLEC-2-specific inhibition in humans.

6.5 Difficulties in targeting CLEC-2 during inflammation

Inflammation is dynamic, and during major inflammatory diseases such as sepsis, can range from SIRS phase to the polar opposite CARS phase. The lack of distinction between these phases, alongside patient immune heterogeneity, makes treatment challenging. Whereas patients during the SIRS phase would benefit from anti-inflammatory therapy (Vincent et al., 2013), an immune adjuvant treatment would be more beneficial in immune suppressed patients, such as GM-CSF or IL-7 therapies (Marshall, 2014). Here, we have demonstrated a cell-specific axis which limits the inflammatory response during LPS-induced peritonitis, which limited local inflammation (**Figure 6**). Utilisation of this therapeutic target depends on the stimuli, location and timepoint of inflammation.

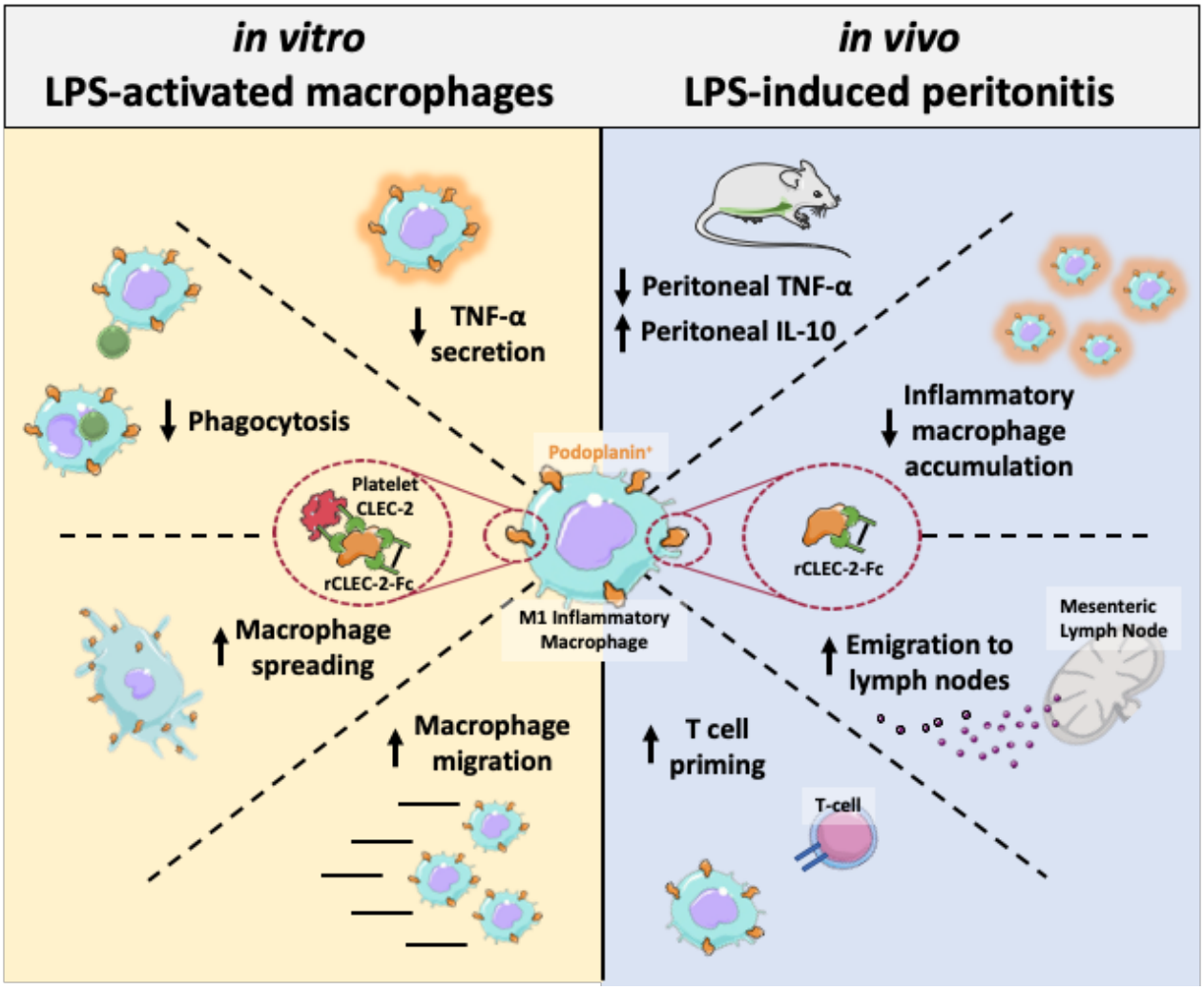

Figure 6 – The reduction of the pro-inflammatory phenotype of M1 macrophages during a mouse model of LPS-induced peritonitis by CLEC-2. Podoplanin crosslinking by rCLEC-2-Fc or platelet-CLEC-2 *in vitro* reduces macrophage TNF-α secretion and phagocytic activity, but increases their migration. Treatment using rCLEC-2 *in vivo* reduces inflammatory macrophage accumulation by increasing their emigration to lymph nodes, to reduce tissue inflammation. *Figure made using BioRender*.

The podoplanin-CLEC-2 axis has been demonstrated to benefit and detriment inflammation. The axis is protective during ARDS; deletion of podoplanin- or CLEC-2 exacerbated lung function post-intratracheal LPS instillations (Lax et al., 2017). Their deletion during sepsis exacerbates the cytokine storm and limited macrophage recruitment/secretion (Rayes et al., 2017). During EAE, it is neuroprotective, whereby deletion of podoplanin or CLEC-2 increased EAE-induced inflammatory responses (Constantinescu et al., 2011, Peters et al., 2015, Nylander et al., 2017). Interestingly, during a mouse model of ischaemic stroke, the podoplanin-CLEC-2 axis was shown to promote neurodegeneration, contradictory to that observed during EAE – both cortical inflammatory events (Meng et al., 2021). Furthermore, overexpression of podoplanin on Th17 cells during rheumatoid arthritis promoted the inflammatory response (Noack et al., 2016). CLEC-2 also limits liver recovery post-toxic injury by inhibiting neutrophil recruitment (Chauhan et al., 2020). This demonstrates that an organ, alongside the stimuli can dictate the activity of the CLEC-2-podoplanin axis determining its benefit or detriment.

During acute infectious disease, inflammatory macrophages are critical in clearing pathogens, and also removing inflammatory/dead neutrophils and debris. However, during chronic inflammatory diseases such as obesity or metabolic disorders, inflammatory macrophage accumulation and retention can harm tissue (Zheng et al., 2016). Therefore, promoting macrophage emigration by crosslinking CLEC-2 and podoplanin may benefit patients in reducing both the inflammatory phenotype of M1 macrophages, and reducing tissue inflammation. It is clear that patient stratification is crucial for a treatment success, and a specialised identification of stimuli, location

and timepoint is necessary to utilise the CLEC-2-podoplanin axis as a therapeutic target during inflammation.

6.6 Future work – Crosslinking CLEC-2

Although we have shown that CLEC-2-podoplanin crosslinking induces macrophage emigration from the site of inflammation, due to animal licensing, we have not been able to assess the subsequent adaptive immune response. We can predict that rCLEC-2-Fc-induced T cell priming may initiate the resolution of inflammation, however this is speculative. Should this be the case, delivery of recombinant proteins to crosslink podoplanin in patients during chronic inflammatory disease could be promising. This could be achieved using pH sensitive nanoparticles, which are in development to treat cancer, but could be applied to selectively target the acidic microenvironment within inflammatory tissue (Lv et al., 2016).

6.7 Conclusion

Data and discussion in this thesis identify CLEC-2 as a therapeutic target in thromboinflammation and inflammatory disease. The negligible contribution of CLEC-2 to arterial thrombosis and haemostasis allows targeting without inducing bleeding defects. This could be accomplished specifically through low-dose BTK inhibition, or perhaps in the future through nanobody generation. Targeting hemin-induced platelet activation by CLEC-2 using hydroxychloroquine could remove the need for invasive treatment during haemolytic disease. Furthermore, crosslinking CLEC-2 during chronic inflammatory disease, with consideration for inflammatory

stimuli, tissue and timescale, could limit inflammation. Future research into synthetically crosslinking CLEC-2 has a prospect for therapeutic use in patients.

References

ABRAM, C. L., ROBERGE, G. L., HU, Y. & LOWELL, C. A. 2014. Comparative analysis of the efficiency and specificity of myeloid-Cre deleting strains using ROSA-EYFP reporter mice. *J Immunol Methods,* 408**,** 89-100.

ABTAHIAN, F., GUERRIERO, A., SEBZDA, E., LU, M. M., ZHOU, R., MOCSAI, A., MYERS, E. E., HUANG, B., JACKSON, D. G., FERRARI, V. A., TYBULEWICZ, V., LOWELL, C. A., LEPORE, J. J., KORETZKY, G. A. & KAHN, M. L. 2003. Regulation of blood and lymphatic vascular separation by signaling proteins SLP-76 and Syk. *Science,* 299**,** 247-51.

ADAM, F., VERBEUREN, T. J., FAUCHÈRE, J. L., GUILLIN, M. C. & JANDROT-PERRUS, M. 2003. Thrombin-induced platelet PAR4 activation: role of glycoprotein Ib and ADP. *J Thromb Haemost,* 1**,** 798-804.

ADAMZIK, M., HAMBURGER, T., PETRAT, F., PETERS, J., DE GROOT, H. & HARTMANN, M. 2012. Free hemoglobin concentration in severe sepsis: methods of measurement and prediction of outcome. *Crit Care,* 16**,** R125.

AGENO, W., GALLUS, A. S., WITTKOWSKY, A., CROWTHER, M., HYLEK, E. M. & PALARETI, G. 2012. Oral anticoagulant therapy: Antithrombotic Therapy and Prevention of Thrombosis, 9th ed: American College of Chest Physicians Evidence-Based Clinical Practice Guidelines. *Chest,* 141**,** e44S-e88S.

ALITALO, K. & CARMELIET, P. 2002. Molecular mechanisms of lymphangiogenesis in health and disease. *Cancer Cell,* 1**,** 219-27.

ALLAN, D. & RAVAL, P. 1983. Some morphological consequences of uncoupling the lipid bilayer from the plasma membrane skeleton in intact erythrocytes. *Biomed Biochim Acta,* 42**,** S11-6.

ALLEN, R. D., ZACHARSKI, L. R., WIDIRSTKY, S. T., ROSENSTEIN, R., ZAITLIN, L. M. & BURGESS, D. R. 1979. Transformation and motility of human platelets: details of the shape change and release reaction observed by optical and electron microscopy. *J Cell Biol,* 83**,** 126-42.

ALSHEHRI, O. M., HUGHES, C. E., MONTAGUE, S., WATSON, S. K., FRAMPTON, J., BENDER, M. & WATSON, S. P. 2015a. Fibrin activates GPVI in human and mouse platelets. *Blood,* 126**,** 1601-8.

ALSHEHRI, O. M., MONTAGUE, S., WATSON, S., CARTER, P., SARKER, N., MANNE, B. K., MILLER, J. L., HERR, A. B., POLLITT, A. Y., O'CALLAGHAN, C. A., KUNAPULI, S., ARMAN, M., HUGHES, C. E. & WATSON, S. P. 2015b. Activation of glycoprotein VI (GPVI) and C-type lectin-like receptor-2 (CLEC-2) underlies platelet activation by diesel exhaust particles and other charged/hydrophobic ligands. *Biochem J,* 468**,** 459-73.

AMIN, M. A., VOLPERT, O. V., WOODS, J. M., KUMAR, P., HARLOW, L. A. & KOCH, A. E. 2003. Migration inhibitory factor mediates angiogenesis via mitogen-activated protein kinase and phosphatidylinositol kinase. *Circ Res,* 93**,** 321-9.

ANDREWS, R. K., GARDINER, E. E., SHEN, Y. & BERNDT, M. C. 2003. Structure-activity relationships of snake toxins targeting platelet receptors, glycoprotein Ib-IX-V and glycoprotein VI. *Curr Med Chem Cardiovasc Hematol Agents,* 1**,** 143-9.

ANDREWS, R. K., KARUNAKARAN, D., GARDINER, E. E. & BERNDT, M. C. 2007. Platelet receptor proteolysis: a mechanism for downregulating platelet reactivity. *Arterioscler Thromb Vasc Biol,* 27**,** 1511-20.

ANTONIOLI, L., PACHER, P., VIZI, E. S. & HASKÓ, G. 2013. CD39 and CD73 in immunity and inflammation. *Trends Mol Med,* 19**,** 355-67.

ARACHICHE, A., MUMAW, M. M., DE LA FUENTE, M. & NIEMAN, M. T. 2013. Protease-activated receptor 1 (PAR1) and PAR4 heterodimers are required for PAR1-enhanced cleavage of PAR4 by α-thrombin. *J Biol Chem,* 288**,** 32553-32562.

ARMAN, M., KRAUEL, K., TILLEY, D. O., WEBER, C., COX, D., GREINACHER, A., KERRIGAN, S. W. & WATSON, S. P. 2014. Amplification of bacteria-induced platelet activation is triggered by FcγRIIA, integrin αIIbβ3, and platelet factor 4. *Blood,* 123**,** 3166-74.

ARPIN, M., CHIRIVINO, D., NABA, A. & ZWAENEPOEL, I. 2011. Emerging role for ERM proteins in cell adhesion and migration. *Cell Adh Migr,* 5**,** 199-206.

ASSINGER, A., SCHROTTMAIER, W. C., SALZMANN, M. & RAYES, J. 2019. Platelets in Sepsis: An Update on Experimental Models and Clinical Data. *Front Immunol,* 10**,** 1687.

AYALA, A., MUNOZ, M. F. & ARGUELLES, S. 2014. Lipid peroxidation: production, metabolism, and signaling mechanisms of malondialdehyde and 4-hydroxy-2-nonenal. *Oxid Med Cell Longev,* 2014**,** 360438.

BADRNYA, S., SCHROTTMAIER, W. C., KRAL, J. B., YAIW, K. C., VOLF, I., SCHABBAUER, G., SÖDERBERG-NAUCLÉR, C. & ASSINGER, A. 2014. Platelets mediate oxidized low-density lipoprotein-induced monocyte extravasation and foam cell formation. *Arterioscler Thromb Vasc Biol,* 34**,** 571-80.

BAHL, N., DU, R., WINARSIH, I., HO, B., TUCKER-KELLOGG, L., TIDOR, B. & DING, J. L. 2011. Delineation of lipopolysaccharide (LPS)-binding sites on hemoglobin: from in silico predictions to biophysical characterization. *J Biol Chem,* 286**,** 37793-803.

BAHL, N., WINARSIH, I., TUCKER-KELLOGG, L. & DING, J. L. 2014. Extracellular haemoglobin upregulates and binds to tissue factor on macrophages: implications for coagulation and oxidative stress. *Thromb Haemost,* 111**,** 67-78.

BAO, Z., HUANG, Y., CHEN, J., WANG, Z., QIAN, J., XU, J. & ZHAO, Y. 2019. Validation of Reference Genes for Gene Expression Normalization in RAW264.7 Cells under Different Conditions. *Biomed Res Int,* 2019**,** 6131879.

BARRETT, T. J., SCHLEGEL, M., ZHOU, F., GORENCHTEIN, M., BOLSTORFF, J., MOORE, K. J., FISHER, E. A. & BERGER, J. S. 2019. Platelet regulation of myeloid suppressor of cytokine signaling 3 accelerates atherosclerosis. *Sci Transl Med,* 11.

BARRY, K. C., FONTANA, M. F., PORTMAN, J. L., DUGAN, A. S. & VANCE, R. E. 2013. IL-1alpha signaling initiates the inflammatory response to virulent Legionella pneumophila in vivo. *J Immunol,* 190**,** 6329-39.

BEARER, E. L., PRAKASH, J. M. & LI, Z. 2002. Actin dynamics in platelets. *Int Rev Cytol,* 217**,** 137-82.

BECK-SCHIMMER, B., SCHWENDENER, R., PASCH, T., REYES, L., BOOY, C. & SCHIMMER, R. C. 2005. Alveolar macrophages regulate neutrophil recruitment in endotoxin-induced lung injury. *Respir Res,* 6**,** 61.

BELCHER, J. D., CHEN, C., NGUYEN, J., MILBAUER, L., ABDULLA, F., ALAYASH, A. I., SMITH, A., NATH, K. A., HEBBEL, R. P. & VERCELLOTTI, G. M. 2014. Heme triggers TLR4 signaling leading to endothelial cell activation and vaso-occlusion in murine sickle cell disease. *Blood,* 123**,** 377-90.

BELLINGAN, G. J., CALDWELL, H., HOWIE, S. E., DRANSFIELD, I. & HASLETT, C. 1996. In vivo fate of the inflammatory macrophage during the resolution of inflammation: inflammatory macrophages do not die locally, but emigrate to the draining lymph nodes. *J Immunol,* 157**,** 2577-85.

BENDER, M., HAGEDORN, I. & NIESWANDT, B. 2011. Genetic and antibody-induced glycoprotein VI deficiency equally protects mice from mechanically and FeCl(3) - induced thrombosis. *J Thromb Haemost,* 9**,** 1423-6.

BENDER, M., HOFMANN, S., STEGNER, D., CHALARIS, A., BÖSL, M., BRAUN, A., SCHELLER, J., ROSE-JOHN, S. & NIESWANDT, B. 2010. Differentially regulated GPVI ectodomain shedding by multiple platelet-expressed proteinases. *Blood,* 116**,** 3347-55.

BENDER, M., MAY, F., LORENZ, V., THIELMANN, I., HAGEDORN, I., FINNEY, B. A., VÖGTLE, T., REMER, K., BRAUN, A., BÖSL, M., WATSON, S. P. & NIESWANDT, B. 2013. Combined in vivo depletion of glycoprotein VI and C-type lectin-like receptor 2 severely compromises hemostasis and abrogates arterial thrombosis in mice. *Arterioscler Thromb Vasc Biol,* 33**,** 926-34.

BENNETT, J. S. 2005. Structure and function of the platelet integrin alphaIIbbeta3. *J Clin Invest,* 115**,** 3363-9.

BENNETT, J. S. 2015. Regulation of integrins in platelets. *Biopolymers,* 104**,** 323-33.

BERCHICHE, Y. A., GRAVEL, S., PELLETIER, M. E., ST-ONGE, G. & HEVEKER, N. 2011. Different effects of the different natural CC chemokine receptor 2b ligands on beta-arrestin recruitment, Galphai signaling, and receptor internalization. *Mol Pharmacol,* 79**,** 488-98.

BERGMEIER, W., BOUVARD, D., EBLE, J. A., MOKHTARI-NEJAD, R., SCHULTE, V., ZIRNGIBL, H., BRAKEBUSCH, C., FÄSSLER, R. & NIESWANDT, B. 2001. Rhodocytin (aggretin) activates platelets lacking alpha(2)beta(1) integrin, glycoprotein VI, and the ligand-binding domain of glycoprotein Ibalpha. *J Biol Chem,* 276**,** 25121-6.

BERLANGA, O., TULASNE, D., BORI, T., SNELL, D. C., MIURA, Y., JUNG, S., MOROI, M., FRAMPTON, J. & WATSON, S. P. 2002. The Fc receptor gamma-chain is necessary and sufficient to initiate signalling through glycoprotein VI in transfected cells by the snake C-type lectin, convulxin. *Eur J Biochem,* 269**,** 2951-60.

BERTOZZI, C. C., SCHMAIER, A. A., MERICKO, P., HESS, P. R., ZOU, Z., CHEN, M., CHEN, C. Y., XU, B., LU, M. M., ZHOU, D., SEBZDA, E., SANTORE, M. T., MERIANOS, D. J., STADTFELD, M., FLAKE, A. W., GRAF, T., SKODA, R., MALTZMAN, J. S., KORETZKY, G. A. & KAHN, M. L. 2010. Platelets regulate lymphatic vascular development through CLEC-2-SLP-76 signaling. *Blood,* 116**,** 661-70.

BEST, D., SENIS, Y. A., JARVIS, G. E., EAGLETON, H. J., ROBERTS, D. J., SAITO, T., JUNG, S. M., MOROI, M., HARRISON, P., GREEN, F. R. & WATSON, S. P. 2003. GPVI levels in platelets: relationship to platelet function at high shear. *Blood,* 102**,** 2811-8.

BIENIASZ-KRZYWIEC, P., MARTÍN-PÉREZ, R., EHLING, M., GARCÍA-CABALLERO, M., PINIOTI, S., PRETTO, S., KROES, R., ALDENI, C., DI MATTEO, M., PRENEN, H., TRIBULATTI, M. V., CAMPETELLA, O., SMEETS, A., NOEL, A., FLORIS, G., VAN GINDERACHTER, J. A. & MAZZONE, M. 2019. Podoplanin-Expressing Macrophages Promote Lymphangiogenesis and Lymphoinvasion in Breast Cancer. *Cell Metab,* 30**,** 917-936.e10.

BLUTEAU, O., LANGLOIS, T., RIVERA-MUNOZ, P., FAVALE, F., RAMEAU, P., MEURICE, G., DESSEN, P., SOLARY, E., RASLOVA, H., MERCHER, T., DEBILI, N. & VAINCHENKER, W. 2013. Developmental changes in human megakaryopoiesis. *J Thromb Haemost,* 11**,** 1730-41.

BOBRYSHEV, Y. V., IVANOVA, E. A., CHISTIAKOV, D. A., NIKIFOROV, N. G. & OREKHOV, A. N. 2016. Macrophages and Their Role in Atherosclerosis: Pathophysiology and Transcriptome Analysis. *Biomed Res Int,* 2016**,** 9582430.

BOULAFTALI, Y., HESS, P. R., KAHN, M. L. & BERGMEIER, W. 2014. Platelet immunoreceptor tyrosine-based activation motif (ITAM) signaling and vascular integrity. *Circ Res,* 114**,** 1174-84.

BOURNE, J. H., BERISTAIN-COVARRUBIAS, N., ZUIDSCHERWOUDE, M., CAMPOS, J., DI, Y., GARLICK, E., COLICCHIA, M., TERRY, L. V., THOMAS, S. G., BRILL, A., BAYRY, J., WATSON, S. P. & RAYES, J. 2021. CLEC-2 Prevents Accumulation and Retention of Inflammatory Macrophages During Murine Peritonitis. *Front Immunol,* 12**,** 693974.

BOURNE, J. H., COLICCHIA, M., DI, Y., MARTIN, E., SLATER, A., ROUMENINA, L. T., DIMITROV, J. D., WATSON, S. P. & RAYES, J. 2020. Heme induces human and mouse platelet activation through C-type-lectin-like receptor-2. *Haematologica*.

BOYDEN, S. 1962. The chemotactic effect of mixtures of antibody and antigen on polymorphonuclear leucocytes. *J Exp Med,* 115**,** 453-66.

BRANDT, J. T., ISENHART, C. E., OSBORNE, J. M., AHMED, A. & ANDERSON, C. L. 1995. On the role of platelet Fc gamma RIIa phenotype in heparin-induced thrombocytopenia. *Thromb Haemost,* 74**,** 1564-72.

BRIDDELL, R. A., BRANDT, J. E., STRANEVA, J. E., SROUR, E. F. & HOFFMAN, R. 1989. Characterization of the human burst-forming unit-megakaryocyte. *Blood,* 74**,** 145-51.

BYRD, J. C., FURMAN, R. R., COUTRE, S. E., BURGER, J. A., BLUM, K. A., COLEMAN, M., WIERDA, W. G., JONES, J. A., ZHAO, W., HEEREMA, N. A., JOHNSON, A. J., SHAW, Y., BILOTTI, E., ZHOU, C., JAMES, D. F. & O'BRIEN, S. 2015. Three-year follow-up of treatment-naive and previously treated patients with CLL and SLL receiving single-agent ibrutinib. *Blood,* 125**,** 2497-506.

BYRD, J. C., FURMAN, R. R., COUTRE, S. E., FLINN, I. W., BURGER, J. A., BLUM, K. A., GRANT, B., SHARMAN, J. P., COLEMAN, M., WIERDA, W. G., JONES, J. A., ZHAO, W., HEEREMA, N. A., JOHNSON, A. J., SUKBUNTHERNG, J., CHANG, B. Y., CLOW, F., HEDRICK, E., BUGGY, J. J., JAMES, D. F. & O'BRIEN, S. 2013. Targeting BTK with ibrutinib in relapsed chronic lymphocytic leukemia. *N Engl J Med,* 369**,** 32-42.

CALAMINUS, S. D., GUITART, A. V., GUITART, A., SINCLAIR, A., SCHACHTNER, H., WATSON, S. P., HOLYOAKE, T. L., KRANC, K. R. & MACHESKY, L. M. 2012. Lineage tracing of Pf4-Cre marks hematopoietic stem cells and their progeny. *PLoS One,* 7**,** e51361.

CAMEJO, G., HALBERG, C., MANSCHIK-LUNDIN, A., HURT-CAMEJO, E., ROSENGREN, B., OLSSON, H., HANSSON, G. I., FORSBERG, G. B. & YLHEN, B. 1998. Hemin binding and oxidation of lipoproteins in serum: mechanisms and effect on the interaction of LDL with human macrophages. *J Lipid Res,* 39**,** 755-66.

CAMPOS, J., PONOMARYOV, T., DE PRENDERGAST, A., WHITWORTH, K., SMITH, C. W., KHAN, A. O., KAVANAGH, D. & BRILL, A. 2021. Neutrophil extracellular traps and inflammasomes cooperatively promote venous thrombosis in mice. *Blood Adv,* 5**,** 2319-2324.

CAO, C., LAWRENCE, D. A., STRICKLAND, D. K. & ZHANG, L. 2005. A specific role of integrin Mac-1 in accelerated macrophage efflux to the lymphatics. *Blood,* 106**,** 3234-41.

CAPEL, P. J., VAN DE WINKEL, J. G., VAN DEN HERIK-OUDIJK, I. E. & VERBEEK, J. S. 1994. Heterogeneity of human IgG Fc receptors. *Immunomethods,* 4**,** 25-34.

CARESTIA, A., MENA, H. A., OLEXEN, C. M., ORTIZ WILCZYÑSKI, J. M., NEGROTTO, S., ERRASTI, A. E., GÓMEZ, R. M., JENNE, C. N., CARRERA SILVA, E. A. & SCHATTNER, M. 2019. Platelets Promote Macrophage Polarization toward Pro-inflammatory Phenotype and Increase Survival of Septic Mice. *Cell Rep,* 28**,** 896-908.e5.

CASSADO ADOS, A., D'IMPERIO LIMA, M. R. & BORTOLUCI, K. R. 2015. Revisiting mouse peritoneal macrophages: heterogeneity, development, and function. *Front Immunol,* 6**,** 225.

CATTANEO, M. 2015. P2Y12 receptors: structure and function. *J Thromb Haemost,* 13 Suppl 1**,** S10-6.

ČERMÁK, V., GANDALOVIČOVÁ, A., MERTA, L., FUČÍKOVÁ, J., ŠPÍŠEK, R., RÖSEL, D. & BRÁBEK, J. 2018. RNA-seq of macrophages of amoeboid or mesenchymal migratory phenotype due to specific structure of environment. *Scientific Data,* 5**,** 180198.

CHAIPAN, C., SOILLEUX, E. J., SIMPSON, P., HOFMANN, H., GRAMBERG, T., MARZI, A., GEIER, M., STEWART, E. A., EISEMANN, J., STEINKASSERER, A., SUZUKI-INOUE, K., FULLER, G. L., PEARCE, A. C., WATSON, S. P., HOXIE, J. A., BARIBAUD, F. & PÖHLMANN, S. 2006. DC-SIGN and CLEC-2 mediate human immunodeficiency virus type 1 capture by platelets. *J Virol,* 80**,** 8951-60.

CHANG, Y. W., HSIEH, P. W., CHANG, Y. T., LU, M. H., HUANG, T. F., CHONG, K. Y., LIAO, H. R., CHENG, J. C. & TSENG, C. P. 2015. Identification of a novel platelet antagonist that binds to CLEC-2 and suppresses podoplanin-induced platelet aggregation and cancer metastasis. *Oncotarget,* 6**,** 42733-48.

CHAPLIN, H., JR. & ZARKOWSKY, H. S. 1981. Combined sickle cell disease and autoimmune hemolytic anemia. *Arch Intern Med,* 141**,** 1091-3.

CHAUHAN, A., SHERIFF, L., HUSSAIN, M. T., WEBB, G. J., PATTEN, D. A., SHEPHERD, E. L., SHAW, R., WESTON, C. J., HALDAR, D., BOURKE, S., BHANDARI, R., WATSON, S., ADAMS, D. H., WATSON, S. P. & LALOR, P. F. 2020. The platelet receptor CLEC-2 blocks neutrophil mediated hepatic recovery in acetaminophen induced acute liver failure. *Nat Commun,* 11**,** 1939.

CHÁVEZ-GALÁN, L., OLLEROS, M. L., VESIN, D. & GARCIA, I. 2015. Much More than M1 and M2 Macrophages, There are also CD169+ and TCR+ Macrophages. *Frontiers in Immunology,* 6.

CHEN, G., ZHANG, D., FUCHS, T. A., MANWANI, D., WAGNER, D. D. & FRENETTE, P. S. 2014. Heme-induced neutrophil extracellular traps contribute to the pathogenesis of sickle cell disease. *Blood,* 123**,** 3818-27.

CHEN, Z., MONDAL, N. K., DING, J., GAO, J., GRIFFITH, B. P. & WU, Z. J. 2015. Shear-induced platelet receptor shedding by non-physiological high shear stress with short exposure time: glycoprotein Ibα and glycoprotein VI. *Thromb Res,* 135**,** 692-8.

CHIABRANDO, D., VINCHI, F., FIORITO, V., MERCURIO, S. & TOLOSANO, E. 2014. Heme in pathophysiology: a matter of scavenging, metabolism and trafficking across cell membranes. *Front Pharmacol,* 5**,** 61.

CHICHARRO-ALCÁNTARA, D., RUBIO-ZARAGOZA, M., DAMIÁ-GIMÉNEZ, E., CARRILLO-POVEDA, J. M., CUERVO-SERRATO, B., PELÁEZ-GORREA, P. & SOPENA-JUNCOSA, J. J. 2018. Platelet Rich Plasma: New Insights for Cutaneous Wound Healing Management. *J Funct Biomater,* 9.

CHIMEN, M., EVRYVIADOU, A., BOX, C. L., HARRISON, M. J., HAZELDINE, J., DIB, L. H., KURAVI, S. J., PAYNE, H., PRICE, J. M. J., KAVANAGH, D., IQBAL, A. J., LAX, S., KALIA, N., BRILL, A., THOMAS, S. G., BELLI, A., CROMBIE, N., ADAMS, R. A., EVANS, S. A., DECKMYN, H., LORD, J. M., HARRISON, P., WATSON, S. P., NASH, G. B. & RAINGER, G. E. 2020. Appropriation of GPIbalpha from platelet-derived extracellular vesicles supports monocyte recruitment in systemic inflammation. *Haematologica,* 105**,** 1248-1261.

CHRISTOU, C. M., PEARCE, A. C., WATSON, A. A., MISTRY, A. R., POLLITT, A. Y., FENTON-MAY, A. E., JOHNSON, L. A., JACKSON, D. G., WATSON, S. P. & O'CALLAGHAN, C. A. 2008. Renal cells activate the platelet receptor CLEC-2 through podoplanin. *Biochem J,* 411**,** 133-40.

CHUNG, S. W., LIU, X., MACIAS, A. A., BARON, R. M. & PERRELLA, M. A. 2008. Heme oxygenase-1-derived carbon monoxide enhances the host defense response to microbial sepsis in mice. *J Clin Invest,* 118**,** 239-47.

CLOUTIER, N., ALLAEYS, I., MARCOUX, G., MACHLUS, K. R., MAILHOT, B., ZUFFEREY, A., LEVESQUE, T., BECKER, Y., TESSANDIER, N., MELKI, I., ZHI, H., POIRIER, G., RONDINA, M. T., ITALIANO, J. E., FLAMAND, L., MCKENZIE, S. E., COTE, F., NIESWANDT, B., KHAN, W. I., FLICK, M. J., NEWMAN, P. J., LACROIX, S., FORTIN, P. R. & BOILARD, E. 2018. Platelets release pathogenic serotonin and return to circulation after immune complex-mediated sequestration. *Proc Natl Acad Sci U S A,* 115**,** E1550-E1559.

COLONNA, M., SAMARIDIS, J. & ANGMAN, L. 2000. Molecular characterization of two novel C-type lectin-like receptors, one of which is selectively expressed in human dendritic cells. *Eur J Immunol,* 30**,** 697-704.

COMBRINCK, J. M., MABOTHA, T. E., NCOKAZI, K. K., AMBELE, M. A., TAYLOR, D., SMITH, P. J., HOPPE, H. C. & EGAN, T. J. 2013. Insights into the role of heme in the mechanism of action of antimalarials. *ACS Chem Biol,* 8**,** 133-7.

CONSTANTINESCU, C. S., FAROOQI, N., O'BRIEN, K. & GRAN, B. 2011. Experimental autoimmune encephalomyelitis (EAE) as a model for multiple sclerosis (MS). *Br J Pharmacol,* 164**,** 1079-106.

CUENI, L. N. & DETMAR, M. 2009. Galectin-8 interacts with podoplanin and modulates lymphatic endothelial cell functions. *Exp Cell Res,* 315**,** 1715-23.

CUI, K., ARDELL, C. L., PODOLNIKOVA, N. P. & YAKUBENKO, V. P. 2018. Distinct Migratory Properties of M1, M2, and Resident Macrophages Are Regulated by alphaDbeta2 and alphaMbeta2 Integrin-Mediated Adhesion. *Front Immunol,* 9**,** 2650.

DE WINDE, C. M., MAKRIS, S., MILLWARD, L. J., CANTORAL-REBORDINOS, J. A., BENJAMIN, A. C., MARTÍNEZ, V. G. & ACTON, S. E. 2021. Fibroblastic reticular cell response to dendritic cells requires coordinated activity of podoplanin, CD44 and CD9. *J Cell Sci,* 134.

DEMPSEY, P. W., VAIDYA, S. A. & CHENG, G. 2003. The art of war: Innate and adaptive immune responses. *Cell Mol Life Sci,* 60**,** 2604-21.

DEPPERMANN, C. & KUBES, P. 2016. Platelets and infection. *Semin Immunol,* 28**,** 536-545.

DESHMANE, S. L., KREMLEV, S., AMINI, S. & SAWAYA, B. E. 2009. Monocyte chemoattractant protein-1 (MCP-1): an overview. *J Interferon Cytokine Res,* 29**,** 313-26.

DHALIWAL, G., CORNETT, P. A. & TIERNEY, L. M., JR. 2004. Hemolytic anemia. *Am Fam Physician,* 69**,** 2599-606.

DIETRICH, H. H., ELLSWORTH, M. L., SPRAGUE, R. S. & DACEY, R. G., JR. 2000. Red blood cell regulation of microvascular tone through adenosine triphosphate. *Am J Physiol Heart Circ Physiol,* 278**,** H1294-8.

DIXON, S. J., LEMBERG, K. M., LAMPRECHT, M. R., SKOUTA, R., ZAITSEV, E. M., GLEASON, C. E., PATEL, D. N., BAUER, A. J., CANTLEY, A. M., YANG, W. S., MORRISON, B., 3RD & STOCKWELL, B. R. 2012. Ferroptosis: an iron-dependent form of nonapoptotic cell death. *Cell,* 149**,** 1060-72.

DRECHSLER, M., MEGENS, R. T., VAN ZANDVOORT, M., WEBER, C. & SOEHNLEIN, O. 2010. Hyperlipidemia-triggered neutrophilia promotes early atherosclerosis. *Circulation,* 122**,** 1837-45.

DUFFIELD, J. S., FORBES, S. J., CONSTANDINOU, C. M., CLAY, S., PARTOLINA, M., VUTHOORI, S., WU, S., LANG, R. & IREDALE, J. P. 2005. Selective depletion of macrophages reveals distinct, opposing roles during liver injury and repair. *J Clin Invest,* 115**,** 56-65.

DUNSTER, J. L., UNSWORTH, A. J., BYE, A. P., HAINING, E. J., SOWA, M. A., DI, Y., SAGE, T., PALLINI, C., PIKE, J. A., HARDY, A. T., NIESWANDT, B., GARCÍA, Á., WATSON, S. P., POULTER, N. S., GIBBINS, J. M. & POLLITT, A. Y. 2020. Interspecies differences in protein expression do not impact the spatiotemporal regulation of glycoprotein VI mediated activation. *J Thromb Haemost,* 18**,** 485-496.

DURRANT, T. N., VAN DEN BOSCH, M. T. & HERS, I. 2017. Integrin α. *Blood,* 130**,** 1607-1619.

EISEMANN, T., COSTA, B., PETERZIEL, H. & ANGEL, P. 2019. Podoplanin Positive Myeloid Cells Promote Glioma Development by Immune Suppression. *Front Oncol,* 9**,** 187.

EISINGER, F., PATZELT, J. & LANGER, H. F. 2018. The Platelet Response to Tissue Injury. *Front Med (Lausanne),* 5**,** 317.

ETULAIN, J., MARTINOD, K., WONG, S. L., CIFUNI, S. M., SCHATTNER, M. & WAGNER, D. D. 2015. P-selectin promotes neutrophil extracellular trap formation in mice. *Blood,* 126**,** 242-6.

FARNDALE, R. W., SIXMA, J. J., BARNES, M. J. & DE GROOT, P. G. 2004. The role of collagen in thrombosis and hemostasis. *J Thromb Haemost,* 2**,** 561-73.

FARNSWORTH, R. H., KARNEZIS, T., MACIBURKO, S. J., MUELLER, S. N. & STACKER, S. A. 2019. The Interplay Between Lymphatic Vessels and Chemokines. *Front Immunol,* 10**,** 518.

FARR, A. G., BERRY, M. L., KIM, A., NELSON, A. J., WELCH, M. P. & ARUFFO, A. 1992. Characterization and cloning of a novel glycoprotein expressed by stromal cells in T-dependent areas of peripheral lymphoid tissues. *J Exp Med,* 176**,** 1477-82.

FARZAMNIA, H., RABIEI, K., SADEGHI, M. & ROGHANI, F. 2011. The predictive factors of recurrent deep vein thrombosis. *ARYA Atheroscler,* 7**,** 123-8.

FINNEY, B. A., SCHWEIGHOFFER, E., NAVARRO-NÚÑEZ, L., BÉNÉZECH, C., BARONE, F., HUGHES, C. E., LANGAN, S. A., LOWE, K. L., POLLITT, A. Y., MOURAO-SA, D., SHEARDOWN, S., NASH, G. B., SMITHERS, N., REIS E SOUSA, C., TYBULEWICZ, V. L. & WATSON, S. P. 2012. CLEC-2 and Syk in the megakaryocytic/platelet lineage are essential for development. *Blood,* 119**,** 1747-56.

FITCH, C. D. 1998. Involvement of heme in the antimalarial action of chloroquine. *Trans Am Clin Climatol Assoc,* 109**,** 97-105; discussion 105-6.

FLAUMENHAFT, R. 2003. Molecular basis of platelet granule secretion. *Arterioscler Thromb Vasc Biol,* 23**,** 1152-60.

FLEETWOOD, A. J., COOK, A. D. & HAMILTON, J. A. 2005. Functions of granulocyte-macrophage colony-stimulating factor. *Crit Rev Immunol,* 25**,** 405-28.

FOX, R. I. 1993. Mechanism of action of hydroxychloroquine as an antirheumatic drug. *Semin Arthritis Rheum,* 23**,** 82-91.

FREDRIKSSON, R., LAGERSTRÖM, M. C., LUNDIN, L. G. & SCHIÖTH, H. B. 2003. The G-protein-coupled receptors in the human genome form five main families. Phylogenetic analysis, paralogon groups, and fingerprints. *Mol Pharmacol,* 63**,** 1256-72.

FRENETTE, P. S., DENIS, C. V., WEISS, L., JURK, K., SUBBARAO, S., KEHREL, B., HARTWIG, J. H., VESTWEBER, D. & WAGNER, D. D. 2000. P-Selectin glycoprotein ligand 1 (PSGL-1) is

expressed on platelets and can mediate platelet-endothelial interactions in vivo. *J Exp Med,* 191**,** 1413-22.
FRIMODT-MØLLER, N. 1993. The mouse peritonitis model: present and future use. *J Antimicrob Chemother,* 31 Suppl D**,** 55-60.
FRITZ, E., LUDWIG, H., SCHEITHAUER, W. & SINZINGER, H. 1986. Shortened platelet half-life in multiple myeloma. *Blood,* 68**,** 514-20.
FUJITA, H., HASHIMOTO, Y., RUSSELL, S., ZIEGER, B. & WARE, J. 1998. In vivo expression of murine platelet glycoprotein Ibalpha. *Blood,* 92**,** 488-95.
FURMAN, M. I., GRIGORYEV, D., BRAY, P. F., DISE, K. R. & GOLDSCHMIDT-CLERMONT, P. J. 1994. Platelet tyrosine kinases and fibrinogen receptor activation. *Circ Res,* 75**,** 172-80.
GALE, N. W., PREVO, R., ESPINOSA, J., FERGUSON, D. J., DOMINGUEZ, M. G., YANCOPOULOS, G. D., THURSTON, G. & JACKSON, D. G. 2007. Normal lymphatic development and function in mice deficient for the lymphatic hyaluronan receptor LYVE-1. *Mol Cell Biol,* 27**,** 595-604.
GALT, S. W., LINDEMANN, S., MEDD, D., ALLEN, L. L., KRAISS, L. W., HARRIS, E. S., PRESCOTT, S. M., MCINTYRE, T. M., WEYRICH, A. S. & ZIMMERMAN, G. A. 2001. Differential regulation of matrix metalloproteinase-9 by monocytes adherent to collagen and platelets. *Circ Res,* 89**,** 509-16.
GARCIA LOPEZ, M. A., AGUADO MARTINEZ, A., LAMAZE, C., MARTINEZ, A. C. & FISCHER, T. 2009. Inhibition of dynamin prevents CCL2-mediated endocytosis of CCR2 and activation of ERK1/2. *Cell Signal,* 21**,** 1748-57.
GARDINER, E. E., ARTHUR, J. F., KAHN, M. L., BERNDT, M. C. & ANDREWS, R. K. 2004. Regulation of platelet membrane levels of glycoprotein VI by a platelet-derived metalloproteinase. *Blood,* 104**,** 3611-7.
GARDINER, E. E., KARUNAKARAN, D., SHEN, Y., ARTHUR, J. F., ANDREWS, R. K. & BERNDT, M. C. 2007. Controlled shedding of platelet glycoprotein (GP)VI and GPIb-IX-V by ADAM family metalloproteinases. *J Thromb Haemost,* 5**,** 1530-7.
GAUTIER, E. L., IVANOV, S., LESNIK, P. & RANDOLPH, G. J. 2013. Local apoptosis mediates clearance of macrophages from resolving inflammation in mice. *Blood,* 122**,** 2714-22.
GEER, M. J., VAN GEFFEN, J. P., GOPALASINGAM, P., VÖGTLE, T., SMITH, C. W., HEISING, S., KUIJPERS, M. J. E., TULLEMANS, B. M. E., JARVIS, G. E., EBLE, J. A., JEEVES, M., OVERDUIN, M., HEEMSKERK, J. W. M., MAZHARIAN, A. & SENIS, Y. A. 2018. Uncoupling ITIM receptor G6b-B from tyrosine phosphatases Shp1 and Shp2 disrupts murine platelet homeostasis. *Blood,* 132**,** 1413-1425.
GHOSH, D. K. & SALERNO, J. C. 2003. Nitric oxide synthases: domain structure and alignment in enzyme function and control. *Front Biosci,* 8**,** d193-209.
GHOSHAL, K. & BHATTACHARYYA, M. 2014. Overview of platelet physiology: its hemostatic and nonhemostatic role in disease pathogenesis. *ScientificWorldJournal,* 2014**,** 781857.
GINSBURG, H. & GEARY, T. G. 1987. Current concepts and new ideas on the mechanism of action of quinoline-containing antimalarials. *Biochem Pharmacol,* 36**,** 1567-76.
GITZ, E., POLLITT, A. Y., GITZ-FRANCOIS, J. J., ALSHEHRI, O., MORI, J., MONTAGUE, S., NASH, G. B., DOUGLAS, M. R., GARDINER, E. E., ANDREWS, R. K., BUCKLEY, C. D., HARRISON, P. & WATSON, S. P. 2014. CLEC-2 expression is maintained on activated platelets and on platelet microparticles. *Blood,* 124**,** 2262-70.

GLICK, D., BARTH, S. & MACLEOD, K. F. 2010. Autophagy: cellular and molecular mechanisms. *J Pathol,* 221**,** 3-12.
GOLEBIEWSKA, E. M. & POOLE, A. W. 2015. Platelet secretion: From haemostasis to wound healing and beyond. *Blood Rev,* 29**,** 153-62.
GONG, Y., HART, E., SHCHURIN, A. & HOOVER-PLOW, J. 2008. Inflammatory macrophage migration requires MMP-9 activation by plasminogen in mice. *J Clin Invest,* 118**,** 3012-24.
GOUVEIA, Z., CARLOS, A. R., YUAN, X., AIRES-DA-SILVA, F., STOCKER, R., MAGHZAL, G. J., LEAL, S. S., GOMES, C. M., TODOROVIC, S., IRANZO, O., RAMOS, S., SANTOS, A. C., HAMZA, I., GONCALVES, J. & SOARES, M. P. 2017. Characterization of plasma labile heme in hemolytic conditions. *FEBS J,* 284**,** 3278-3301.
GRABHER, C., CLIFFE, A., MIURA, K., HAYFLICK, J., PEPPERKOK, R., RORTH, P. & WITTBRODT, J. 2007. Birth and life of tissue macrophages and their migration in embryogenesis and inflammation in medaka. *J Leukoc Biol,* 81**,** 263-71.
GRACA-SOUZA, A. V., ARRUDA, M. A., DE FREITAS, M. S., BARJA-FIDALGO, C. & OLIVEIRA, P. L. 2002. Neutrophil activation by heme: implications for inflammatory processes. *Blood,* 99**,** 4160-5.
GREENLEE-WACKER, M. C. 2016. Clearance of apoptotic neutrophils and resolution of inflammation. *Immunol Rev,* 273**,** 357-70.
GROS, A., SYVANNARATH, V., LAMRANI, L., OLLIVIER, V., LOYAU, S., GOERGE, T., NIESWANDT, B., JANDROT-PERRUS, M. & HO-TIN-NOÉ, B. 2015. Single platelets seal neutrophil-induced vascular breaches via GPVI during immune-complex-mediated inflammation in mice. *Blood,* 126**,** 1017-26.
GUIET, R., VÉROLLET, C., LAMSOUL, I., COUGOULE, C., POINCLOUX, R., LABROUSSE, A., CALDERWOOD, D. A., GLOGAUER, M., LUTZ, P. G. & MARIDONNEAU-PARINI, I. 2012. Macrophage mesenchymal migration requires podosome stabilization by filamin A. *J Biol Chem,* 287**,** 13051-62.
GÜNDÜZ, D., HIRCHE, F., HÄRTEL, F. V., RODEWALD, C. W., SCHÄFER, M., PFITZER, G., PIPER, H. M. & NOLL, T. 2003. ATP antagonism of thrombin-induced endothelial barrier permeability. *Cardiovascular Research,* 59**,** 470-478.
GUPTA, S., KONRADT, C., CORKEN, A., WARE, J., NIESWANDT, B., DI PAOLA, J., YU, M., WANG, D., NIEMAN, M. T., WHITEHEART, S. W. & BRASS, L. F. 2020. Hemostasis vs. homeostasis: Platelets are essential for preserving vascular barrier function in the absence of injury or inflammation. *Proc Natl Acad Sci U S A,* 117**,** 24316-24325.
GUYTON, J. R., BLACK, B. L. & SEIDEL, C. L. 1990. Focal toxicity of oxysterols in vascular smooth muscle cell culture. A model of the atherosclerotic core region. *Am J Pathol,* 137**,** 425-34.
HAHL, P., DAVIS, T., WASHBURN, C., ROGERS, J. T. & SMITH, A. 2013. Mechanisms of neuroprotection by hemopexin: modeling the control of heme and iron homeostasis in brain neurons in inflammatory states. *J Neurochem,* 125**,** 89-101.
HAINING, E. J., CHERPOKOVA, D., WOLF, K., BECKER, I. C., BECK, S., EBLE, J. A., STEGNER, D., WATSON, S. P. & NIESWANDT, B. 2017. CLEC-2 contributes to hemostasis independently of classical hemITAM signaling in mice. *Blood,* 130**,** 2224-2228.
HAINING, E. J., LOWE, K. L., WICHAIYO, S., KATARU, R. P., NAGY, Z., KAVANAGH, D. P., LAX, S., DI, Y., NIESWANDT, B., HO-TIN-NOÉ, B., MEHRARA, B. J., SENIS, Y. A., RAYES, J. & WATSON, S. P. 2020. Lymphatic blood filling in CLEC-2-deficient mouse models. *Platelets***,** 1-16.

HAMANAKA, R. B. & CHANDEL, N. S. 2010. Mitochondrial reactive oxygen species regulate cellular signaling and dictate biological outcomes. *Trends Biochem Sci,* 35**,** 505-13.
HAMILTON, J. A. 2008. Colony-stimulating factors in inflammation and autoimmunity. *Nat Rev Immunol,* 8**,** 533-44.
HARBI, M. H., SMITH, C. W., NICOLSON, P. L. R., WATSON, S. P. & THOMAS, M. R. 2021. Novel antiplatelet strategies targeting GPVI, CLEC-2 and tyrosine kinases. *Platelets,* 32**,** 29-41.
HARGROVE, M. S., WHITAKER, T., OLSON, J. S., VALI, R. J. & MATHEWS, A. J. 1997. Quaternary structure regulates hemin dissociation from human hemoglobin. *J Biol Chem,* 272**,** 17385-9.
HARRISON, P. & CRAMER, E. M. 1993. Platelet alpha-granules. *Blood Rev,* 7**,** 52-62.
HASHIMOTO, D., CHOW, A., NOIZAT, C., TEO, P., BEASLEY, M. B., LEBOEUF, M., BECKER, C. D., SEE, P., PRICE, J., LUCAS, D., GRETER, M., MORTHA, A., BOYER, S. W., FORSBERG, E. C., TANAKA, M., VAN ROOIJEN, N., GARCIA-SASTRE, A., STANLEY, E. R., GINHOUX, F., FRENETTE, P. S. & MERAD, M. 2013. Tissue-resident macrophages self-maintain locally throughout adult life with minimal contribution from circulating monocytes. *Immunity,* 38**,** 792-804.
HATAKEYAMA, K., KANEKO, M. K., KATO, Y., ISHIKAWA, T., NISHIHIRA, K., TSUJIMOTO, Y., SHIBATA, Y., OZAKI, Y. & ASADA, Y. 2012. Podoplanin expression in advanced atherosclerotic lesions of human aortas. *Thromb Res,* 129**,** e70-6.
HATZIOANNOU, A., NAYAR, S., GAITANIS, A., BARONE, F., ANAGNOSTOPOULOS, C. & VERGINIS, P. 2016. Intratumoral accumulation of podoplanin-expressing lymph node stromal cells promote tumor growth through elimination of CD4. *Oncoimmunology,* 5**,** e1216289.
HECHLER, B. & GACHET, C. 2011. P2 receptors and platelet function. *Purinergic Signal,* 7**,** 293-303.
HEFFRON, S. P., WEINSTOCK, A., SCOLARO, B., CHEN, S., SANSBURY, B. E., MARECKI, G., ROLLING, C. C., EL BANNOUDI, H., BARRETT, T., CANARY, J. W., SPITE, M., BERGER, J. S. & FISHER, E. A. 2021. Platelet-conditioned media induces an anti-inflammatory macrophage phenotype through EP4. *J Thromb Haemost,* 19**,** 562-573.
HEIJNEN, H. & VAN DER SLUIJS, P. 2015. Platelet secretory behaviour: as diverse as the granules … or not? *J Thromb Haemost,* 13**,** 2141-51.
HEMKER, H. C. 2016. A century of heparin: past, present and future. *J Thromb Haemost,* 14**,** 2329-2338.
HILLGRUBER, C., PÖPPELMANN, B., WEISHAUPT, C., STEINGRÄBER, A. K., WESSEL, F., BERDEL, W. E., GESSNER, J. E., HO-TIN-NOÉ, B., VESTWEBER, D. & GOERGE, T. 2015. Blocking neutrophil diapedesis prevents hemorrhage during thrombocytopenia. *J Exp Med,* 212**,** 1255-66.
HITCHCOCK, J. R., COOK, C. N., BOBAT, S., ROSS, E. A., FLORES-LANGARICA, A., LOWE, K. L., KHAN, M., DOMINGUEZ-MEDINA, C. C., LAX, S., CARVALHO-GASPAR, M., HUBSCHER, S., RAINGER, G. E., COBBOLD, M., BUCKLEY, C. D., MITCHELL, T. J., MITCHELL, A., JONES, N. D., VAN ROOIJEN, N., KIRCHHOFER, D., HENDERSON, I. R., ADAMS, D. H., WATSON, S. P. & CUNNINGHAM, A. F. 2015. Inflammation drives thrombosis after Salmonella infection via CLEC-2 on platelets. *J Clin Invest,* 125**,** 4429-46.
HO-TIN-NOÉ, B., BOULAFTALI, Y. & CAMERER, E. 2018. Platelets and vascular integrity: how platelets prevent bleeding in inflammation. *Blood,* 131**,** 277-288.

HOPPE, C. C., STYLES, L., HEATH, L. E., ZHOU, C., JAKUBOWSKI, J. A., WINTERS, K. J., BROWN, P. B., REES, D. C. & HEENEY, M. M. 2016. Design of the DOVE (Determining Effects of Platelet Inhibition on Vaso-Occlusive Events) trial: A global Phase 3 double-blind, randomized, placebo-controlled, multicenter study of the efficacy and safety of prasugrel in pediatric patients with sickle cell anemia utilizing a dose titration strategy. *Pediatr Blood Cancer,* 63**,** 299-305.

HOVIG, T., MCKENZIE, F. N. & ARFORS, K. E. 1974. Measruement of the platelet response to laserinduced microvascular injury. Ultrastructural studies. *Thromb Diath Haemorrh,* 32**,** 695-703.

HOYLAERTS, M., LIJNEN, H. R. & COLLEN, D. 1981. Studies on the mechanism of the antifibrinolytic action of tranexamic acid. *Biochim Biophys Acta,* 673**,** 75-85.

HUANG, T. F., LIU, C. Z. & YANG, S. H. 1995. Aggretin, a novel platelet-aggregation inducer from snake (Calloselasma rhodostoma) venom, activates phospholipase C by acting as a glycoprotein Ia/IIa agonist. *Biochem J,* 309 (Pt 3)**,** 1021-7.

HUANG, Y. X., WU, Z. J., MEHRISHI, J., HUANG, B. T., CHEN, X. Y., ZHENG, X. J., LIU, W. J. & LUO, M. 2011. Human red blood cell aging: correlative changes in surface charge and cell properties. *J Cell Mol Med,* 15**,** 2634-42.

HUGHES, C. E., NAVARRO-NÚÑEZ, L., FINNEY, B. A., MOURÃO-SÁ, D., POLLITT, A. Y. & WATSON, S. P. 2010a. CLEC-2 is not required for platelet aggregation at arteriolar shear. *J Thromb Haemost,* 8**,** 2328-2332.

HUGHES, C. E., POLLITT, A. Y., MORI, J., EBLE, J. A., TOMLINSON, M. G., HARTWIG, J. H., O'CALLAGHAN, C. A., FÜTTERER, K. & WATSON, S. P. 2010b. CLEC-2 activates Syk through dimerization. *Blood,* 115**,** 2947-55.

HUGHES, C. E., SINHA, U., PANDEY, A., EBLE, J. A., O'CALLAGHAN, C. A. & WATSON, S. P. 2013. Critical Role for an acidic amino acid region in platelet signaling by the HemITAM (hemi-immunoreceptor tyrosine-based activation motif) containing receptor CLEC-2 (C-type lectin receptor-2). *J Biol Chem,* 288**,** 5127-35.

HUO, Y. & XIA, L. 2009. P-selectin glycoprotein ligand-1 plays a crucial role in the selective recruitment of leukocytes into the atherosclerotic arterial wall. *Trends Cardiovasc Med,* 19**,** 140-5.

HYUN, Y.-M., CHOE, Y. H., PARK, S. A. & KIM, M. 2019. LFA-1 (CD11a/CD18) and Mac-1 (CD11b/CD18) distinctly regulate neutrophil extravasation through hotspots I and II. *Experimental & Molecular Medicine,* 51**,** 1-13.

IMMENSCHUH, S., VIJAYAN, V., JANCIAUSKIENE, S. & GUELER, F. 2017. Heme as a Target for Therapeutic Interventions. *Front Pharmacol,* 8**,** 146.

INOUE, O., HOKAMURA, K., SHIRAI, T., OSADA, M., TSUKIJI, N., HATAKEYAMA, K., UMEMURA, K., ASADA, Y., SUZUKI-INOUE, K. & OZAKI, Y. 2015. Vascular Smooth Muscle Cells Stimulate Platelets and Facilitate Thrombus Formation through Platelet CLEC-2: Implications in Atherothrombosis. *PLoS One,* 10**,** e0139357.

INOUE, O., SUZUKI-INOUE, K., MCCARTY, O. J., MOROI, M., RUGGERI, Z. M., KUNICKI, T. J., OZAKI, Y. & WATSON, S. P. 2006. Laminin stimulates spreading of platelets through integrin alpha6beta1-dependent activation of GPVI. *Blood,* 107**,** 1405-12.

INWALD, D. P., MCDOWALL, A., PETERS, M. J., CALLARD, R. E. & KLEIN, N. J. 2003. CD40 is constitutively expressed on platelets and provides a novel mechanism for platelet activation. *Circ Res,* 92**,** 1041-8.

ITALIANI, P. & BORASCHI, D. 2014. From Monocytes to M1/M2 Macrophages: Phenotypical vs. Functional Differentiation. *Front Immunol,* 5**,** 514.

JACKSON, S. P., DARBOUSSET, R. & SCHOENWAELDER, S. M. 2019. Thromboinflammation: challenges of therapeutically targeting coagulation and other host defense mechanisms. *Blood,* 133**,** 906-918.

JAMBUSARIA, A., HONG, Z., ZHANG, L., SRIVASTAVA, S., JANA, A., TOTH, P. T., DAI, Y., MALIK, A. B. & REHMAN, J. 2020. Endothelial heterogeneity across distinct vascular beds during homeostasis and inflammation. *Elife,* 9.

JANZ, D. R., BASTARACHE, J. A., PETERSON, J. F., SILLS, G., WICKERSHAM, N., MAY, A. K., ROBERTS, L. J., 2ND & WARE, L. B. 2013. Association between cell-free hemoglobin, acetaminophen, and mortality in patients with sepsis: an observational study. *Crit Care Med,* 41**,** 784-90.

KARDEBY, C., FÄLKER, K., HAINING, E. J., CRIEL, M., LINDKVIST, M., BARROSO, R., PÅHLSSON, P., LJUNGBERG, L. U., TENGDELIUS, M., RAINGER, G. E., WATSON, S., EBLE, J. A., HOYLAERTS, M. F., EMSLEY, J., KONRADSSON, P., WATSON, S. P., SUN, Y. & GRENEGÅRD, M. 2019. Synthetic glycopolymers and natural fucoidans cause human platelet aggregation via PEAR1 and GPIbα. *Blood Adv,* 3**,** 275-287.

KATO, G. J., PIEL, F. B., REID, C. D., GASTON, M. H., OHENE-FREMPONG, K., KRISHNAMURTI, L., SMITH, W. R., PANEPINTO, J. A., WEATHERALL, D. J., COSTA, F. F. & VICHINSKY, E. P. 2018. Sickle cell disease. *Nat Rev Dis Primers,* 4**,** 18010.

KATO, K., KANAJI, T., RUSSELL, S., KUNICKI, T. J., FURIHATA, K., KANAJI, S., MARCHESE, P., REININGER, A., RUGGERI, Z. M. & WARE, J. 2003a. The contribution of glycoprotein VI to stable platelet adhesion and thrombus formation illustrated by targeted gene deletion. *Blood,* 102**,** 1701-7.

KATO, Y., FUJITA, N., KUNITA, A., SATO, S., KANEKO, M., OSAWA, M. & TSURUO, T. 2003b. Molecular identification of Aggrus/T1alpha as a platelet aggregation-inducing factor expressed in colorectal tumors. *J Biol Chem,* 278**,** 51599-605.

KAUSHANSKY, K. 2005. The molecular mechanisms that control thrombopoiesis. *J Clin Invest,* 115**,** 3339-47.

KAUSHANSKY, K. & DRACHMAN, J. G. 2002. The molecular and cellular biology of thrombopoietin: the primary regulator of platelet production. *Oncogene,* 21**,** 3359-67.

KERRIGAN, A. M., DENNEHY, K. M., MOURÃO-SÁ, D., FARO-TRINDADE, I., WILLMENT, J. A., TAYLOR, P. R., EBLE, J. A., REIS E SOUSA, C. & BROWN, G. D. 2009. CLEC-2 is a phagocytic activation receptor expressed on murine peripheral blood neutrophils. *J Immunol,* 182**,** 4150-7.

KERRIGAN, A. M., NAVARRO-NUÑEZ, L., PYZ, E., FINNEY, B. A., WILLMENT, J. A., WATSON, S. P. & BROWN, G. D. 2012. Podoplanin-expressing inflammatory macrophages activate murine platelets via CLEC-2. *J Thromb Haemost,* 10**,** 484-6.

KHAN, A. R., JS; BOURNE, JH; COLICCHIA, M; NEWBY, ML; ALLEN, JD; CRISPIN, M; YOUD, E; MURRAY, PG; TAYLOR, G; STAMATAKI, Z; RICHTER, AG; CUNNINGHAM, AF; PUGH, M; RAYES, J 2021. Stimulation of vascular organoids with SARS-CoV-2 antigens increases endothelial permeability and regulates vasculopathy. *medRxiV*.

KIM, N. D. & LUSTER, A. D. 2015. The role of tissue resident cells in neutrophil recruitment. *Trends Immunol,* 36**,** 547-55.

KIM, S. J. & JENNE, C. N. 2016. Role of platelets in neutrophil extracellular trap (NET) production and tissue injury. *Semin Immunol,* 28**,** 546-554.

KINGMA, J. G., PLANTE, S. & BOGATY, P. 2000. Platelet GPIIb/IIIa receptor blockade reduces infarct size in a canine model of ischemia-reperfusion. *J Am Coll Cardiol,* 36**,** 2317-24.

KOCH, T., GEIGER, S. & RAGALLER, M. J. 2001. Monitoring of organ dysfunction in sepsis/systemic inflammatory response syndrome: novel strategies. *J Am Soc Nephrol,* 12 Suppl 17**,** S53-9.

KONO, M., SAIGO, K., TAKAGI, Y., TAKAHASHI, T., KAWAUCHI, S., WADA, A., HASHIMOTO, M., MINAMI, Y., IMOTO, S., TAKENOKUCHI, M., MORIKAWA, T. & FUNAKOSHI, K. 2014. Heme-related molecules induce rapid production of neutrophil extracellular traps. *Transfusion,* 54**,** 2811-9.

KOSZALKA, P., OZÜYAMAN, B., HUO, Y., ZERNECKE, A., FLÖGEL, U., BRAUN, N., BUCHHEISER, A., DECKING, U. K., SMITH, M. L., SÉVIGNY, J., GEAR, A., WEBER, A. A., MOLOJAVYI, A., DING, Z., WEBER, C., LEY, K., ZIMMERMANN, H., GÖDECKE, A. & SCHRADER, J. 2004. Targeted disruption of cd73/ecto-5'-nucleotidase alters thromboregulation and augments vascular inflammatory response. *Circ Res,* 95**,** 814-21.

KOUPENOVA, M., CORKREY, H. A., VITSEVA, O., MANNI, G., PANG, C. J., CLANCY, L., YAO, C., RADE, J., LEVY, D., WANG, J. P., FINBERG, R. W., KURT-JONES, E. A. & FREEDMAN, J. E. 2019. The role of platelets in mediating a response to human influenza infection. *Nat Commun,* 10**,** 1780.

KRISHNAN, H., OCHOA-ALVAREZ, J. A., SHEN, Y., NEVEL, E., LAKSHMINARAYANAN, M., WILLIAMS, M. C., RAMIREZ, M. I., MILLER, W. T. & GOLDBERG, G. S. 2013. Serines in the intracellular tail of podoplanin (PDPN) regulate cell motility. *J Biol Chem,* 288**,** 12215-21.

KRISHNAN, H., RETZBACH, E. P., RAMIREZ, M. I., LIU, T., LI, H., MILLER, W. T. & GOLDBERG, G. S. 2015. PKA and CDK5 can phosphorylate specific serines on the intracellular domain of podoplanin (PDPN) to inhibit cell motility. *Exp Cell Res,* 335**,** 115-22.

KRISTIANSEN, M., GRAVERSEN, J. H., JACOBSEN, C., SONNE, O., HOFFMAN, H. J., LAW, S. K. & MOESTRUP, S. K. 2001. Identification of the haemoglobin scavenger receptor. *Nature,* 409**,** 198-201.

KROLL, M. H., HARRIS, T. S., MOAKE, J. L., HANDIN, R. I. & SCHAFER, A. I. 1991. von Willebrand factor binding to platelet GpIb initiates signals for platelet activation. *J Clin Invest,* 88**,** 1568-73.

KUCKLEBURG, C. J., YATES, C. M., KALIA, N., ZHAO, Y., NASH, G. B., WATSON, S. P. & RAINGER, G. E. 2011. Endothelial cell-borne platelet bridges selectively recruit monocytes in human and mouse models of vascular inflammation. *Cardiovasc Res,* 91**,** 134-41.

KUMAR, S. & BANDYOPADHYAY, U. 2005. Free heme toxicity and its detoxification systems in human. *Toxicol Lett,* 157**,** 175-88.

KUYPERS, F. A. 2014. Hemoglobin s polymerization and red cell membrane changes. *Hematol Oncol Clin North Am,* 28**,** 155-79.

LÄMMERMANN, T., BADER, B. L., MONKLEY, S. J., WORBS, T., WEDLICH-SÖLDNER, R., HIRSCH, K., KELLER, M., FÖRSTER, R., CRITCHLEY, D. R., FÄSSLER, R. & SIXT, M. 2008. Rapid leukocyte migration by integrin-independent flowing and squeezing. *Nature,* 453**,** 51-55.

LARSEN, R., GOZZELINO, R., JENEY, V., TOKAJI, L., BOZZA, F. A., JAPIASSU, A. M., BONAPARTE, D., CAVALCANTE, M. M., CHORA, A., FERREIRA, A., MARGUTI, I., CARDOSO, S., SEPULVEDA, N., SMITH, A. & SOARES, M. P. 2010. A central role for free heme in the pathogenesis of severe sepsis. *Sci Transl Med,* 2**,** 51ra71.

LAX, S., RAYES, J., WICHAIYO, S., HAINING, E. J., LOWE, K., GRYGIELSKA, B., LALOO, R., FLODBY, P., BOROK, Z., CRANDALL, E. D., THICKETT, D. R. & WATSON, S. P. 2017.

Platelet CLEC-2 protects against lung injury via effects of its ligand podoplanin on inflammatory alveolar macrophages in the mouse. *Am J Physiol Lung Cell Mol Physiol,* 313**,** L1016-L1029.
LEBOIS, M. & JOSEFSSON, E. C. 2016. Regulation of platelet lifespan by apoptosis. *Platelets,* 27**,** 497-504.
LEE, D., FONG, K. P., KING, M. R., BRASS, L. F. & HAMMER, D. A. 2012. Differential dynamics of platelet contact and spreading. *Biophys J,* 102**,** 472-82.
LEFRANÇAIS, E., ORTIZ-MUÑOZ, G., CAUDRILLIER, A., MALLAVIA, B., LIU, F., SAYAH, D. M., THORNTON, E. E., HEADLEY, M. B., DAVID, T., COUGHLIN, S. R., KRUMMEL, M. F., LEAVITT, A. D., PASSEGUÉ, E. & LOONEY, M. R. 2017. The lung is a site of platelet biogenesis and a reservoir for haematopoietic progenitors. *Nature,* 544**,** 105-109.
LI, D., ZHANG, X., ZHANG, H. & LI, X. 2020a. Synergic effect of GPIBA and von Willebrand factor in pathogenesis of deep vein thrombosis. *Vascular,* 28**,** 309-313.
LI, J., CAO, F., YIN, H. L., HUANG, Z. J., LIN, Z. T., MAO, N., SUN, B. & WANG, G. 2020b. Ferroptosis: past, present and future. *Cell Death Dis,* 11**,** 88.
LI, W., NIEMAN, M. & SEN GUPTA, A. 2016. Ferric Chloride-induced Murine Thrombosis Models. *J Vis Exp*.
LIN, T., MAITA, D., THUNDIVALAPPIL, S. R., RILEY, F. E., HAMBSCH, J., VAN MARTER, L. J., CHRISTOU, H. A., BERRA, L., FAGAN, S., CHRISTIANI, D. C. & WARREN, H. S. 2015. Hemopexin in severe inflammation and infection: mouse models and human diseases. *Crit Care,* 19**,** 166.
LINKE, B., SCHREIBER, Y., PICARD-WILLEMS, B., SLATTERY, P., NÜSING, R. M., HARDER, S., GEISSLINGER, G. & SCHOLICH, K. 2017. Activated Platelets Induce an Anti-Inflammatory Response of Monocytes/Macrophages through Cross-Regulation of PGE. *Mediators Inflamm,* 2017**,** 1463216.
LIRA, S. A. 2005. A passport into the lymph node. *Nat Immunol,* 6**,** 866-8.
LIVAK, K. J. & SCHMITTGEN, T. D. 2001. Analysis of relative gene expression data using real-time quantitative PCR and the 2(-Delta Delta C(T)) Method. *Methods,* 25**,** 402-8.
LOCKYER, S., OKUYAMA, K., BEGUM, S., LE, S., SUN, B., WATANABE, T., MATSUMOTO, Y., YOSHITAKE, M., KAMBAYASHI, J. & TANDON, N. N. 2006. GPVI-deficient mice lack collagen responses and are protected against experimentally induced pulmonary thromboembolism. *Thromb Res,* 118**,** 371-80.
LOMBARD, S. E., POLLITT, A. Y., HUGHES, C. E., DI, Y., MCKINNON, T., O'CALLAGHAN, C. A. & WATSON, S. P. 2018. Mouse podoplanin supports adhesion and aggregation of platelets under arterial shear: A novel mechanism of haemostasis. *Platelets,* 29**,** 716-722.
LONG, M. W., WILLIAMS, N. & EBBE, S. 1982. Immature megakaryocytes in the mouse: physical characteristics, cell cycle status, and in vitro responsiveness to thrombopoietic stimulatory factor. *Blood,* 59**,** 569-75.
LOWE, K. L., NAVARRO-NÚÑEZ, L., BÉNÉZECH, C., NAYAR, S., KINGSTON, B. L., NIESWANDT, B., BARONE, F., WATSON, S. P., BUCKLEY, C. D. & DESANTI, G. E. 2015. The expression of mouse CLEC-2 on leucocyte subsets varies according to their anatomical location and inflammatory state. *Eur J Immunol,* 45**,** 2484-93.
LUSTER, A. D., ALON, R. & VON ANDRIAN, U. H. 2005. Immune cell migration in inflammation: present and future therapeutic targets. *Nat Immunol,* 6**,** 1182-90.

LV, Y., HAO, L., HU, W., RAN, Y., BAI, Y. & ZHANG, L. 2016. Novel multifunctional pH-sensitive nanoparticles loaded into microbubbles as drug delivery vehicles for enhanced tumor targeting. *Sci Rep,* 6**,** 29321.

MACHOGU, E. M. & MACHADO, R. F. 2018. How I treat hypoxia in adults with hemoglobinopathies and hemolytic disorders. *Blood,* 132**,** 1770-1780.

MADABHUSHI, S. R., ZHANG, C., KELKAR, A., DAYANANDA, K. M. & NEELAMEGHAM, S. 2014. Platelet GpIba binding to von Willebrand Factor under fluid shear:contributions of the D'D3-domain, A1-domain flanking peptide and O-linked glycans. *J Am Heart Assoc,* 3**,** e001420.

MAEDA, T., WAKASAWA, T., SHIMA, Y., TSUBOI, I., AIZAWA, S. & TAMAI, I. 2006. Role of polyamines derived from arginine in differentiation and proliferation of human blood cells. *Biol Pharm Bull,* 29**,** 234-9.

MAINES, M. D., TRAKSHEL, G. M. & KUTTY, R. K. 1986. Characterization of two constitutive forms of rat liver microsomal heme oxygenase. Only one molecular species of the enzyme is inducible. *J Biol Chem,* 261**,** 411-9.

MANGIN, P. H., ONSELAER, M. B., RECEVEUR, N., LE LAY, N., HARDY, A. T., WILSON, C., SANCHEZ, X., LOYAU, S., DUPUIS, A., BABAR, A. K., MILLER, J. L., PHILIPPOU, H., HUGHES, C. E., HERR, A. B., ARIËNS, R. A., MEZZANO, D., JANDROT-PERRUS, M., GACHET, C. & WATSON, S. P. 2018. Immobilized fibrinogen activates human platelets through glycoprotein VI. *Haematologica,* 103**,** 898-907.

MANZO, A., BUGATTI, S., CAPORALI, R., PREVO, R., JACKSON, D. G., UGUCCIONI, M., BUCKLEY, C. D., MONTECUCCO, C. & PITZALIS, C. 2007. CCL21 expression pattern of human secondary lymphoid organ stroma is conserved in inflammatory lesions with lymphoid neogenesis. *Am J Pathol,* 171**,** 1549-62.

MARSHALL, J. C. 2014. Why have clinical trials in sepsis failed? *Trends Mol Med,* 20**,** 195-203.

MARTIN, E. M., ZUIDSCHERWOUDE, M., MORÁN, L. A., DI, Y., GARCÍA, A. & WATSON, S. P. 2021. The structure of CLEC-2: mechanisms of dimerization and higher-order clustering. *Platelets***,** 1-11.

MARTIN, R. E., MARCHETTI, R. V., COWAN, A. I., HOWITT, S. M., BROER, S. & KIRK, K. 2009. Chloroquine transport via the malaria parasite's chloroquine resistance transporter. *Science,* 325**,** 1680-2.

MARTÍN-VILLAR, E., FERNÁNDEZ-MUÑOZ, B., PARSONS, M., YURRITA, M. M., MEGÍAS, D., PÉREZ-GÓMEZ, E., JONES, G. E. & QUINTANILLA, M. 2010. Podoplanin associates with CD44 to promote directional cell migration. *Mol Biol Cell,* 21**,** 4387-99.

MARTÍN-VILLAR, E., MEGÍAS, D., CASTEL, S., YURRITA, M. M., VILARÓ, S. & QUINTANILLA, M. 2006. Podoplanin binds ERM proteins to activate RhoA and promote epithelial-mesenchymal transition. *J Cell Sci,* 119**,** 4541-53.

MARTÍN-VILLAR, E., SCHOLL, F. G., GAMALLO, C., YURRITA, M. M., MUÑOZ-GUERRA, M., CRUCES, J. & QUINTANILLA, M. 2005. Characterization of human PA2.26 antigen (T1alpha-2, podoplanin), a small membrane mucin induced in oral squamous cell carcinomas. *Int J Cancer,* 113**,** 899-910.

MARTYANOV, A. A., BALABIN, F. A., DUNSTER, J. L., PANTELEEV, M. A., GIBBINS, J. M. & SVESHNIKOVA, A. N. 2020. Control of Platelet CLEC-2-Mediated Activation by Receptor Clustering and Tyrosine Kinase Signaling. *Biophys J,* 118**,** 2641-2655.

MASSBERG, S., BRAND, K., GRUNER, S., PAGE, S., MULLER, E., MULLER, I., BERGMEIER, W., RICHTER, T., LORENZ, M., KONRAD, I., NIESWANDT, B. & GAWAZ, M. 2002. A critical

role of platelet adhesion in the initiation of atherosclerotic lesion formation. *J Exp Med,* 196**,** 887-96.
MATSUI, K., BREITENDER-GELEFF, S., SOLEIMAN, A., KOWALSKI, H. & KERJASCHKI, D. 1999. Podoplanin, a novel 43-kDa membrane protein, controls the shape of podocytes. *Nephrol Dial Transplant,* 14 Suppl 1**,** 9-11.
MAY, A. E., KÄLSCH, T., MASSBERG, S., HEROUY, Y., SCHMIDT, R. & GAWAZ, M. 2002. Engagement of glycoprotein IIb/IIIa (alpha(IIb)beta3) on platelets upregulates CD40L and triggers CD40L-dependent matrix degradation by endothelial cells. *Circulation,* 106**,** 2111-7.
MAY, F., HAGEDORN, I., PLEINES, I., BENDER, M., VÖGTLE, T., EBLE, J., ELVERS, M. & NIESWANDT, B. 2009. CLEC-2 is an essential platelet-activating receptor in hemostasis and thrombosis. *Blood,* 114**,** 3464-72.
MAZHARIAN, A., MORI, J., WANG, Y. J., HEISING, S., NEEL, B. G., WATSON, S. P. & SENIS, Y. A. 2013. Megakaryocyte-specific deletion of the protein-tyrosine phosphatases Shp1 and Shp2 causes abnormal megakaryocyte development, platelet production, and function. *Blood,* 121**,** 4205-20.
MAZHARIAN, A., WANG, Y. J., MORI, J., BEM, D., FINNEY, B., HEISING, S., GISSEN, P., WHITE, J. G., BERNDT, M. C., GARDINER, E. E., NIESWANDT, B., DOUGLAS, M. R., CAMPBELL, R. D., WATSON, S. P. & SENIS, Y. A. 2012. Mice lacking the ITIM-containing receptor G6b-B exhibit macrothrombocytopenia and aberrant platelet function. *Sci Signal,* 5**,** ra78.
MCCRACKEN, J. M. & ALLEN, L. A. 2014. Regulation of human neutrophil apoptosis and lifespan in health and disease. *J Cell Death,* 7**,** 15-23.
MCDONALD, B. & KUBES, P. 2015. Interactions between CD44 and Hyaluronan in Leukocyte Trafficking. *Front Immunol,* 6**,** 68.
MCGANN, P. T. & WARE, R. E. 2015. Hydroxyurea therapy for sickle cell anemia. *Expert Opin Drug Saf,* 14**,** 1749-58.
MCKENZIE, S. E., TAYLOR, S. M., MALLADI, P., YUHAN, H., CASSEL, D. L., CHIEN, P., SCHWARTZ, E., SCHREIBER, A. D., SURREY, S. & REILLY, M. P. 1999. The role of the human Fc receptor Fc gamma RIIA in the immune clearance of platelets: a transgenic mouse model. *J Immunol,* 162**,** 4311-8.
MENG, D., MA, X., LI, H., WU, X., CAO, Y., MIAO, Z. & ZHANG, X. 2021. A Role of the Podoplanin-CLEC-2 Axis in Promoting Inflammatory Response After Ischemic Stroke in Mice. *Neurotox Res,* 39**,** 477-488.
MITCHELL, J. A., ALI, F., BAILEY, L., MORENO, L. & HARRINGTON, L. S. 2008. Role of nitric oxide and prostacyclin as vasoactive hormones released by the endothelium. *Exp Physiol,* 93**,** 141-7.
MIURA, Y., TAKAHASHI, T., JUNG, S. M. & MOROI, M. 2002. Analysis of the interaction of platelet collagen receptor glycoprotein VI (GPVI) with collagen. A dimeric form of GPVI, but not the monomeric form, shows affinity to fibrous collagen. *J Biol Chem,* 277**,** 46197-204.
MONTAGUE, S. J., DELIERNEUX, C., LECUT, C., LAYIOS, N., DINSDALE, R. J., LEE, C. S., POULTER, N. S., ANDREWS, R. K., HAMPSON, P., WEARN, C. M., MAES, N., BISHOP, J., BAMFORD, A., GARDINER, C., LEE, W. M., IQBAL, T., MOIEMEN, N., WATSON, S. P., OURY, C., HARRISON, P. & GARDINER, E. E. 2018. Soluble GPVI is elevated in injured patients: shedding is mediated by fibrin activation of GPVI. *Blood Adv,* 2**,** 240-251.

MOROI, M., INDURUWA, I., FARNDALE, R. W. & JUNG, S. M. 2021. Dimers of the platelet collagen receptor glycoprotein VI bind specifically to fibrin fibers during clot formation, but not to intact fibrinogen. *J Thromb Haemost,* 19**,** 2056-2067.

MORRELL, C. N., AGGREY, A. A., CHAPMAN, L. M. & MODJESKI, K. L. 2014. Emerging roles for platelets as immune and inflammatory cells. *Blood,* 123**,** 2759-67.

MOURÃO-SÁ, D., ROBINSON, M. J., ZELENAY, S., SANCHO, D., CHAKRAVARTY, P., LARSEN, R., PLANTINGA, M., VAN ROOIJEN, N., SOARES, M. P., LAMBRECHT, B. & REIS E SOUSA, C. 2011. CLEC-2 signaling via Syk in myeloid cells can regulate inflammatory responses. *Eur J Immunol,* 41**,** 3040-53.

MUNRO, J. M., LO, S. K., CORLESS, C., ROBERTSON, M. J., LEE, N. C., BARNHILL, R. L., WEINBERG, D. S. & BEVILACQUA, M. P. 1992. Expression of sialyl-Lewis X, an E-selectin ligand, in inflammation, immune processes, and lymphoid tissues. *Am J Pathol,* 141**,** 1397-408.

MUNTJEWERFF, E. M., MEESTERS, L. D. & VAN DEN BOGAART, G. 2020. Antigen Cross-Presentation by Macrophages. *Front Immunol,* 11**,** 1276.

NAGAE, M., MORITA-MATSUMOTO, K., KATO, M., KANEKO, M. K., KATO, Y. & YAMAGUCHI, Y. 2014. A platform of C-type lectin-like receptor CLEC-2 for binding O-glycosylated podoplanin and nonglycosylated rhodocytin. *Structure,* 22**,** 1711-1721.

NAGEL, M., BRAUCKMANN, S., MOEGLE-HOFACKER, F., EFFENBERGER-NEIDNICHT, K., HARTMANN, M., DE GROOT, H. & MAYER, C. 2015. Impact of bacterial endotoxin on the structure of DMPC membranes. *Biochim Biophys Acta,* 1848**,** 2271-6.

NAGY, M., PERRELLA, G., DALBY, A., BECERRA, M. F., GARCIA QUINTANILLA, L., PIKE, J. A., MORGAN, N. V., GARDINER, E. E., HEEMSKERK, J. W. M., AZÓCAR, L., MIQUEL, J. F., MEZZANO, D. & WATSON, S. P. 2020. Flow studies on human GPVI-deficient blood under coagulating and noncoagulating conditions. *Blood Adv,* 4**,** 2953-2961.

NAGY, Z., VÖGTLE, T., GEER, M. J., MORI, J., HEISING, S., DI NUNZIO, G., GAREUS, R., TARAKHOVSKY, A., WEISS, A., NEEL, B. G., DESANTI, G. E., MAZHARIAN, A. & SENIS, Y. A. 2019. The Gp1ba-Cre transgenic mouse: a new model to delineate platelet and leukocyte functions. *Blood,* 133**,** 331-343.

NAKAZAWA, Y., SATO, S., NAITO, M., KATO, Y., MISHIMA, K., ARAI, H., TSURUO, T. & FUJITA, N. 2008. Tetraspanin family member CD9 inhibits Aggrus/podoplanin-induced platelet aggregation and suppresses pulmonary metastasis. *Blood,* 112**,** 1730-9.

NAVARRO-NÚÑEZ, L., POLLITT, A. Y., LOWE, K., LATIF, A., NASH, G. B. & WATSON, S. P. 2015. Platelet adhesion to podoplanin under flow is mediated by the receptor CLEC-2 and stabilised by Src/Syk-dependent platelet signalling. *Thromb Haemost,* 113**,** 1109-20.

NAVEENKUMAR, S. K., HEMSHEKHAR, M., KEMPARAJU, K. & GIRISH, K. S. 2019. Hemin-induced platelet activation and ferroptosis is mediated through ROS-driven proteasomal activity and inflammasome activation: Protection by Melatonin. *Biochim Biophys Acta Mol Basis Dis,* 1865**,** 2303-2316.

NAVEENKUMAR, S. K., SHARATHBABU, B. N., HEMSHEKHAR, M., KEMPARAJU, K., GIRISH, K. S. & MUGESH, G. 2018. The Role of Reactive Oxygen Species and Ferroptosis in Heme-Mediated Activation of Human Platelets. *ACS Chem Biol,* 13**,** 1996-2002.

NEEL, N. F., SCHUTYSER, E., SAI, J., FAN, G. H. & RICHMOND, A. 2005. Chemokine receptor internalization and intracellular trafficking. *Cytokine Growth Factor Rev,* 16**,** 637-58.

NICOLSON, P. L. R., NOCK, S. H., HINDS, J., GARCIA-QUINTANILLA, L., SMITH, C. W., CAMPOS, J., BRILL, A., PIKE, J. A., KHAN, A. O., POULTER, N. S., KAVANAGH, D. M., WATSON, S., WATSON, C. N., CLIFFORD, H., HUISSOON, A. P., POLLITT, A. Y., EBLE, J. A., PRATT, G.,

WATSON, S. P. & HUGHES, C. E. 2021. Low-dose Btk inhibitors selectively block platelet activation by CLEC-2. *Haematologica,* 106**,** 208-219.
NIESWANDT, B., BERGMEIER, W., SCHULTE, V., RACKEBRANDT, K., GESSNER, J. E. & ZIRNGIBL, H. 2000. Expression and function of the mouse collagen receptor glycoprotein VI is strictly dependent on its association with the FcRgamma chain. *J Biol Chem,* 275**,** 23998-4002.
NIESWANDT, B., BRAKEBUSCH, C., BERGMEIER, W., SCHULTE, V., BOUVARD, D., MOKHTARI-NEJAD, R., LINDHOUT, T., HEEMSKERK, J. W., ZIRNGIBL, H. & FÄSSLER, R. 2001a. Glycoprotein VI but not alpha2beta1 integrin is essential for platelet interaction with collagen. *EMBO J,* 20**,** 2120-30.
NIESWANDT, B., KLEINSCHNITZ, C. & STOLL, G. 2011. Ischaemic stroke: a thrombo-inflammatory disease? *J Physiol,* 589**,** 4115-23.
NIESWANDT, B., SCHULTE, V., BERGMEIER, W., MOKHTARI-NEJAD, R., RACKEBRANDT, K., CAZENAVE, J. P., OHLMANN, P., GACHET, C. & ZIRNGIBL, H. 2001b. Long-term antithrombotic protection by in vivo depletion of platelet glycoprotein VI in mice. *J Exp Med,* 193**,** 459-69.
NIESWANDT, B. & WATSON, S. P. 2003. Platelet-collagen interaction: is GPVI the central receptor? *Blood,* 102**,** 449-61.
NOACK, M., NDONGO-THIAM, N. & MIOSSEC, P. 2016. Interaction among activated lymphocytes and mesenchymal cells through podoplanin is critical for a high IL-17 secretion. *Arthritis Res Ther,* 18**,** 148.
NOSE, K., SAITO, H. & KUROKI, T. 1990. Isolation of a gene sequence induced later by tumor-promoting 12-O-tetradecanoylphorbol-13-acetate in mouse osteoblastic cells (MC3T3-E1) and expressed constitutively in ras-transformed cells. *Cell Growth Differ,* 1**,** 511-8.
NUNNARI, J. & SUOMALAINEN, A. 2012. Mitochondria: in sickness and in health. *Cell,* 148**,** 1145-59.
NUTESCU, E. A., BURNETT, A., FANIKOS, J., SPINLER, S. & WITTKOWSKY, A. 2016. Pharmacology of anticoagulants used in the treatment of venous thromboembolism. *J Thromb Thrombolysis,* 41**,** 15-31.
NYLANDER, A. N., PONATH, G. D., AXISA, P. P., MUBARAK, M., TOMAYKO, M., KUCHROO, V. K., PITT, D. & HAFLER, D. A. 2017. Podoplanin is a negative regulator of Th17 inflammation. *JCI Insight,* 2.
O'BRIEN, C. D., CAO, G., MAKRIGIANNAKIS, A. & DELISSER, H. M. 2004. Role of immunoreceptor tyrosine-based inhibitory motifs of PECAM-1 in PECAM-1-dependent cell migration. *Am J Physiol Cell Physiol,* 287**,** C1103-13.
OFFERMANNS, S. 2006. Activation of platelet function through G protein-coupled receptors. *Circ Res,* 99**,** 1293-304.
OFORI-ACQUAH, S. F., HAZRA, R., ORIKOGBO, O. O., CROSBY, D., FLAGE, B., ACKAH, E. B., LENHART, D., TAN, R. J., VITTURI, D. A., PAINTSIL, V., OWUSU-DABO, E., GHOSH, S. & SICKLEGENAFRICA, N. 2020. Hemopexin deficiency promotes acute kidney injury in sickle cell disease. *Blood,* 135**,** 1044-1048.
OGAWA, M. 1993. Differentiation and proliferation of hematopoietic stem cells. *Blood,* 81**,** 2844-53.
OISHI, S., TSUKIJI, N., OTAKE, S., OISHI, N., SASAKI, T., SHIRAI, T., YOSHIKAWA, Y., TAKANO, K., SHINMORI, H., INUKAI, T., KONDO, T. & SUZUKI-INOUE, K. 2021. Heme activates

platelets and exacerbates rhabdomyolysis-induced acute kidney injury via CLEC-2 and GPVI/FcRγ. *Blood Adv,* 5**,** 2017-2026.
OKUBO, K., KUROSAWA, M., KAMIYA, M., URANO, Y., SUZUKI, A., YAMAMOTO, K., HASE, K., HOMMA, K., SASAKI, J., MIYAUCHI, H., HOSHINO, T., HAYASHI, M., MAYADAS, T. N. & HIRAHASHI, J. 2018. Macrophage extracellular trap formation promoted by platelet activation is a key mediator of rhabdomyolysis-induced acute kidney injury. *Nat Med,* 24**,** 232-238.
ORF, K. & CUNNINGTON, A. J. 2015. Infection-related hemolysis and susceptibility to Gram-negative bacterial co-infection. *Front Microbiol,* 6**,** 666.
PALLINI, C., PIKE, J. A., O'SHEA, C., ANDREWS, R. K., GARDINER, E. E., WATSON, S. P. & POULTER, N. S. 2021. Immobilized collagen prevents shedding and induces sustained GPVI clustering and signaling in platelets. *Platelets,* 32**,** 59-73.
PATEL, S. R., HARTWIG, J. H. & ITALIANO, J. E. 2005. The biogenesis of platelets from megakaryocyte proplatelets. *J Clin Invest,* 115**,** 3348-54.
PATRIGNANI, P., SCIULLI, M. G., MANARINI, S., SANTINI, G., CERLETTI, C. & EVANGELISTA, V. 1999. COX-2 is not involved in thromboxane biosynthesis by activated human platelets. *J Physiol Pharmacol,* 50**,** 661-7.
PAUL, B. Z., JIN, J. & KUNAPULI, S. P. 1999. Molecular mechanism of thromboxane A(2)-induced platelet aggregation. Essential role for p2t(ac) and alpha(2a) receptors. *J Biol Chem,* 274**,** 29108-14.
PAYNE, H., PONOMARYOV, T., WATSON, S. P. & BRILL, A. 2017. Mice with a deficiency in CLEC-2 are protected against deep vein thrombosis. *Blood,* 129**,** 2013-2020.
PENG, L., MUNDADA, L., STOMEL, J. M., LIU, J. J., SUN, J., YET, S. F. & FAY, W. P. 2004. Induction of heme oxygenase-1 expression inhibits platelet-dependent thrombosis. *Antioxid Redox Signal,* 6**,** 729-35.
PERTUY, F., AGUILAR, A., STRASSEL, C., ECKLY, A., FREUND, J. N., DULUC, I., GACHET, C., LANZA, F. & LÉON, C. 2015. Broader expression of the mouse platelet factor 4-cre transgene beyond the megakaryocyte lineage. *J Thromb Haemost,* 13**,** 115-25.
PETERS, A., BURKETT, P. R., SOBEL, R. A., BUCKLEY, C. D., WATSON, S. P., BETTELLI, E. & KUCHROO, V. K. 2015. Podoplanin negatively regulates CD4+ effector T cell responses. *J Clin Invest,* 125**,** 129-40.
PETRI, B., PHILLIPSON, M. & KUBES, P. 2008. The physiology of leukocyte recruitment: an in vivo perspective. *J Immunol,* 180**,** 6439-46.
PETROVIC, S., ARSIC, A., RISTIC-MEDIC, D., CVETKOVIC, Z. & VUCIC, V. 2020. Lipid Peroxidation and Antioxidant Supplementation in Neurodegenerative Diseases: A Review of Human Studies. *Antioxidants (Basel),* 9.
PIERCE, K. L., PREMONT, R. T. & LEFKOWITZ, R. J. 2002. Seven-transmembrane receptors. *Nat Rev Mol Cell Biol,* 3**,** 639-50.
PIXLEY, F. J. 2012. Macrophage Migration and Its Regulation by CSF-1. *Int J Cell Biol,* 2012**,** 501962.
PIXLEY, F. J. & STANLEY, E. R. 2004. CSF-1 regulation of the wandering macrophage: complexity in action. *Trends Cell Biol,* 14**,** 628-38.
PLUSKOTA, E., WOODY, N. M., SZPAK, D., BALLANTYNE, C. M., SOLOVIEV, D. A., SIMON, D. I. & PLOW, E. F. 2008. Expression, activation, and function of integrin alphaMbeta2 (Mac-1) on neutrophil-derived microparticles. *Blood,* 112**,** 2327-35.

POILLERAT, V., GENTINETTA, T., LEON, J., WASSMER, A., EDLER, M., TORSET, C., LUO, D., TUFFIN, G. & ROUMENINA, L. T. 2020. Hemopexin as an Inhibitor of Hemolysis-Induced Complement Activation. *Front Immunol,* 11**,** 1684.

POLANOWSKA-GRABOWSKA, R., WALLACE, K., FIELD, J. J., CHEN, L., MARSHALL, M. A., FIGLER, R., GEAR, A. R. & LINDEN, J. 2010. P-selectin-mediated platelet-neutrophil aggregate formation activates neutrophils in mouse and human sickle cell disease. *Arterioscler Thromb Vasc Biol,* 30**,** 2392-9.

POLLITT, A. Y., GRYGIELSKA, B., LEBLOND, B., DÉSIRÉ, L., EBLE, J. A. & WATSON, S. P. 2010. Phosphorylation of CLEC-2 is dependent on lipid rafts, actin polymerization, secondary mediators, and Rac. *Blood,* 115**,** 2938-46.

POLLITT, A. Y., POULTER, N. S., GITZ, E., NAVARRO-NUÑEZ, L., WANG, Y. J., HUGHES, C. E., THOMAS, S. G., NIESWANDT, B., DOUGLAS, M. R., OWEN, D. M., JACKSON, D. G., DUSTIN, M. L. & WATSON, S. P. 2014. Syk and Src family kinases regulate C-type lectin receptor 2 (CLEC-2)-mediated clustering of podoplanin and platelet adhesion to lymphatic endothelial cells. *J Biol Chem,* 289**,** 35695-710.

POON, I. K., LUCAS, C. D., ROSSI, A. G. & RAVICHANDRAN, K. S. 2014. Apoptotic cell clearance: basic biology and therapeutic potential. *Nat Rev Immunol,* 14**,** 166-80.

POSCHL, J. M., LERAY, C., RUEF, P., CAZENAVE, J. P. & LINDERKAMP, O. 2003. Endotoxin binding to erythrocyte membrane and erythrocyte deformability in human sepsis and in vitro. *Crit Care Med,* 31**,** 924-8.

POULTER, N. S., POLLITT, A. Y., DAVIES, A., MALINOVA, D., NASH, G. B., HANNON, M. J., PIKRAMENOU, Z., RAPPOPORT, J. Z., HARTWIG, J. H., OWEN, D. M., THRASHER, A. J., WATSON, S. P. & THOMAS, S. G. 2015. Platelet actin nodules are podosome-like structures dependent on Wiskott-Aldrich syndrome protein and ARP2/3 complex. *Nat Commun,* 6**,** 7254.

POULTER, N. S., POLLITT, A. Y., OWEN, D. M., GARDINER, E. E., ANDREWS, R. K., SHIMIZU, H., ISHIKAWA, D., BIHAN, D., FARNDALE, R. W., MOROI, M., WATSON, S. P. & JUNG, S. M. 2017. Clustering of glycoprotein VI (GPVI) dimers upon adhesion to collagen as a mechanism to regulate GPVI signaling in platelets. *J Thromb Haemost,* 15**,** 549-564.

PRAME KUMAR, K., NICHOLLS, A. J. & WONG, C. H. Y. 2018. Partners in crime: neutrophils and monocytes/macrophages in inflammation and disease. *Cell Tissue Res,* 371**,** 551-565.

QIAN, Q., NATH, K. A., WU, Y., DAOUD, T. M. & SETHI, S. 2010. Hemolysis and acute kidney failure. *Am J Kidney Dis,* 56**,** 780-4.

QUINN, C. T., SMITH, E. P., ARBABI, S., KHERA, P. K., LINDSELL, C. J., NISS, O., JOINER, C. H., FRANCO, R. S. & COHEN, R. M. 2016. Biochemical surrogate markers of hemolysis do not correlate with directly measured erythrocyte survival in sickle cell anemia. *Am J Hematol,* 91**,** 1195-1201.

QUINTANILLA, M., MONTERO-MONTERO, L., RENART, J. & MARTÍN-VILLAR, E. 2019. Podoplanin in Inflammation and Cancer. *Int J Mol Sci,* 20.

RAINGER, G., CHIMEN, M., HARRISON, M. J., YATES, C. M., HARRISON, P., WATSON, S. P., LORDKIPANIDZE, M. & NASH, G. B. 2015. The role of platelets in the recruitment of leukocytes during vascular disease. *Platelets,* 26**,** 507-20.

RAPIDO, F., BRITTENHAM, G. M., BANDYOPADHYAY, S., LA CARPIA, F., L'ACQUA, C., MCMAHON, D. J., REBBAA, A., WOJCZYK, B. S., NETTERWALD, J., WANG, H., SCHWARTZ, J., EISENBERGER, A., SOFFING, M., YEH, R., DIVGI, C., GINZBURG, Y. Z., SHAZ, B. H., SHETH, S., FRANCIS, R. O., SPITALNIK, S. L. & HOD, E. A. 2017. Prolonged

red cell storage before transfusion increases extravascular hemolysis. *J Clin Invest,* 127**,** 375-382.
RAVANAT, C., STRASSEL, C., HECHLER, B., SCHUHLER, S., CHICANNE, G., PAYRASTRE, B., GACHET, C. & LANZA, F. 2010. A central role of GPIb-IX in the procoagulant function of platelets that is independent of the 45-kDa GPIbalpha N-terminal extracellular domain. *Blood,* 116**,** 1157-64.
RAYES, J., BOURNE, J. H., BRILL, A. & WATSON, S. P. 2020. The dual role of platelet-innate immune cell interactions in thrombo-inflammation. *Res Pract Thromb Haemost,* 4**,** 23-35.
RAYES, J., JADOUI, S., LAX, S., GROS, A., WICHAIYO, S., OLLIVIER, V., DENIS, C. V., WARE, J., NIESWANDT, B., JANDROT-PERRUS, M., WATSON, S. P. & HO-TIN-NOÉ, B. 2018. The contribution of platelet glycoprotein receptors to inflammatory bleeding prevention is stimulus and organ dependent. *Haematologica,* 103**,** e256-e258.
RAYES, J., LAX, S., WICHAIYO, S., WATSON, S. K., DI, Y., LOMBARD, S., GRYGIELSKA, B., SMITH, S. W., SKORDILIS, K. & WATSON, S. P. 2017. The podoplanin-CLEC-2 axis inhibits inflammation in sepsis. *Nat Commun,* 8**,** 2239.
RAYES, J., WATSON, S. P. & NIESWANDT, B. 2019. Functional significance of the platelet immune receptors GPVI and CLEC-2. *J Clin Invest,* 129**,** 12-23.
REILLY, M. P., TAYLOR, S. M., HARTMAN, N. K., AREPALLY, G. M., SACHAIS, B. S., CINES, D. B., PONCZ, M. & MCKENZIE, S. E. 2001. Heparin-induced thrombocytopenia/thrombosis in a transgenic mouse model requires human platelet factor 4 and platelet activation through FcgammaRIIA. *Blood,* 98**,** 2442-7.
RETH, M. 1989. Antigen receptor tail clue. *Nature,* 338**,** 383-4.
RIBATTI, D. & CRIVELLATO, E. 2007. Giulio Bizzozero and the discovery of platelets. *Leuk Res,* 31**,** 1339-41.
RIEDL, J., FLYNN, K. C., RADUCANU, A., GÄRTNER, F., BECK, G., BÖSL, M., BRADKE, F., MASSBERG, S., ASZODI, A., SIXT, M. & WEDLICH-SÖLDNER, R. 2010. Lifeact mice for studying F-actin dynamics. *Nat Methods,* 7**,** 168-9.
RISHI, A. K., JOYCE-BRADY, M., FISHER, J., DOBBS, L. G., FLOROS, J., VANDERSPEK, J., BRODY, J. S. & WILLIAMS, M. C. 1995. Cloning, characterization, and development expression of a rat lung alveolar type I cell gene in embryonic endodermal and neural derivatives. *Dev Biol,* 167**,** 294-306.
ROGERS, S. C., ROSS, J. G., D'AVIGNON, A., GIBBONS, L. B., GAZIT, V., HASSAN, M. N., MCLAUGHLIN, D., GRIFFIN, S., NEUMAYR, T., DEBAUN, M., DEBAUN, M. R. & DOCTOR, A. 2013. Sickle hemoglobin disturbs normal coupling among erythrocyte O2 content, glycolysis, and antioxidant capacity. *Blood,* 121**,** 1651-62.
ROLFES, V., RIBEIRO, L. S., HAWWARI, I., BÖTTCHER, L., ROSERO, N., MAASEWERD, S., SANTOS, M. L. S., PRÓCHNICKI, T., SILVA, C. M. S., WANDERLEY, C. W. S., ROTHE, M., SCHMIDT, S. V., STUNDEN, H. J., BERTHELOOT, D., RIVAS, M. N., FONTES, C. J., CARVALHO, L. H., CUNHA, F. Q., LATZ, E., ARDITI, M. & FRANKLIN, B. S. 2020. Platelets Fuel the Inflammasome Activation of Innate Immune Cells. *Cell Rep,* 31**,** 107615.
ROUMENINA, L. T., RAYES, J., LACROIX-DESMAZES, S. & DIMITROV, J. D. 2016. Heme: Modulator of Plasma Systems in Hemolytic Diseases. *Trends Mol Med,* 22**,** 200-213.
SADRZADEH, S. M. & BOZORGMEHR, J. 2004. Haptoglobin phenotypes in health and disorders. *Am J Clin Pathol,* 121 Suppl**,** S97-104.

SAVAGE, B., ALMUS-JACOBS, F. & RUGGERI, Z. M. 1998. Specific synergy of multiple substrate-receptor interactions in platelet thrombus formation under flow. *Cell,* 94**,** 657-66.

SCHAER, D. J., SCHAER, C. A., BUEHLER, P. W., BOYKINS, R. A., SCHOEDON, G., ALAYASH, A. I. & SCHAFFNER, A. 2006. CD163 is the macrophage scavenger receptor for native and chemically modified hemoglobins in the absence of haptoglobin. *Blood,* 107**,** 373-80.

SCHEUERER, B., ERNST, M., DURRBAUM-LANDMANN, I., FLEISCHER, J., GRAGE-GRIEBENOW, E., BRANDT, E., FLAD, H. D. & PETERSEN, F. 2000. The CXC-chemokine platelet factor 4 promotes monocyte survival and induces monocyte differentiation into macrophages. *Blood,* 95**,** 1158-66.

SCHMITT, A., GUICHARD, J., MASSÉ, J. M., DEBILI, N. & CRAMER, E. M. 2001. Of mice and men: comparison of the ultrastructure of megakaryocytes and platelets. *Exp Hematol,* 29**,** 1295-302.

SCHOLL, F. G., GAMALLO, C., VILARÓ, S. & QUINTANILLA, M. 1999. Identification of PA2.26 antigen as a novel cell-surface mucin-type glycoprotein that induces plasma membrane extensions and increased motility in keratinocytes. *J Cell Sci,* 112 (Pt 24)**,** 4601-13.

SCHREZENMEIER, E. & DORNER, T. 2020. Mechanisms of action of hydroxychloroquine and chloroquine: implications for rheumatology. *Nat Rev Rheumatol,* 16**,** 155-166.

SCHUBERT, J. & ROTH, A. 2015. Update on paroxysmal nocturnal haemoglobinuria: on the long way to understand the principles of the disease. *Eur J Haematol,* 94**,** 464-73.

SCHWARZ, M., NORDT, T., BODE, C. & PETER, K. 2002. The GP IIb/IIIa inhibitor abciximab (c7E3) inhibits the binding of various ligands to the leukocyte integrin Mac-1 (CD11b/CD18, alphaMbeta2). *Thromb Res,* 107**,** 121-8.

SCULL, C. M., HAYS, W. D. & FISCHER, T. H. 2010. Macrophage pro-inflammatory cytokine secretion is enhanced following interaction with autologous platelets. *J Inflamm (Lond),* 7**,** 53.

SEIZER, P. & MAY, A. E. 2013. Platelets and matrix metalloproteinases. *Thromb Haemost,* 110**,** 903-9.

SEMPLE, J. W. & FREEDMAN, J. 2010. Platelets and innate immunity. *Cell Mol Life Sci,* 67**,** 499-511.

SERHAN, C. N. & SAVILL, J. 2005. Resolution of inflammation: the beginning programs the end. *Nat Immunol,* 6**,** 1191-7.

SHAMRI, R., GRABOVSKY, V., GAUGUET, J. M., FEIGELSON, S., MANEVICH, E., KOLANUS, W., ROBINSON, M. K., STAUNTON, D. E., VON ANDRIAN, U. H. & ALON, R. 2005. Lymphocyte arrest requires instantaneous induction of an extended LFA-1 conformation mediated by endothelium-bound chemokines. *Nat Immunol,* 6**,** 497-506.

SIEGEMUND, S., SHEPHERD, J., XIAO, C. & SAUER, K. 2015. hCD2-iCre and Vav-iCre mediated gene recombination patterns in murine hematopoietic cells. *PLoS One,* 10**,** e0124661.

SIM, X., PONCZ, M., GADUE, P. & FRENCH, D. L. 2016. Understanding platelet generation from megakaryocytes: implications for in vitro-derived platelets. *Blood,* 127**,** 1227-33.

SIXMA, J. J., VAN ZANTEN, G. H., HUIZINGA, E. G., VAN DER PLAS, R. M., VERKLEY, M., WU, Y. P., GROS, P. & DE GROOT, P. G. 1997. Platelet adhesion to collagen: an update. *Thromb Haemost,* 78**,** 434-8.

SIXMA, J. J., VAN ZANTEN, G. H., SAELMAN, E. U., VERKLEIJ, M., LANKHOF, H., NIEUWENHUIS, H. K. & DE GROOT, P. G. 1995. Platelet adhesion to collagen. *Thromb Haemost,* 74**,** 454-9.

SLATER, A., DI, Y., CLARK, J. C., JOOSS, N. J., MARTIN, E. M., ALENAZY, F., THOMAS, M. R., ARIËNS, R. A. S., HERR, A. B., POULTER, N. S., EMSLEY, J. & WATSON, S. P. 2021. Structural characterization of a novel GPVI-nanobody complex reveals a biologically active domain-swapped GPVI dimer. *Blood,* 137**,** 3443-3453.

SMITH, C. W., RASLAN, Z., PARFITT, L., KHAN, A. O., PATEL, P., SENIS, Y. A. & MAZHARIAN, A. 2018. TREM-like transcript 1: a more sensitive marker of platelet activation than P-selectin in humans and mice. *Blood Adv,* 2**,** 2072-2078.

SOEHNLEIN, O., ZERNECKE, A., ERIKSSON, E. E., ROTHFUCHS, A. G., PHAM, C. T., HERWALD, H., BIDZHEKOV, K., ROTTENBERG, M. E., WEBER, C. & LINDBOM, L. 2008. Neutrophil secretion products pave the way for inflammatory monocytes. *Blood,* 112**,** 1461-71.

SOHRABI, S. & LIU, Y. 2017. A Cellular Model of Shear-Induced Hemolysis. *Artif Organs,* 41**,** E80-E91.

SPETH, C., RAMBACH, G. & LASS-FLÖRL, C. 2014. Platelet immunology in fungal infections. *Thromb Haemost,* 112**,** 632-9.

STALKER, T. J. 2020. Mouse laser injury models: variations on a theme. *Platelets,* 31**,** 423-431.

STARK, K., PHILIPPI, V., STOCKHAUSEN, S., BUSSE, J., ANTONELLI, A., MILLER, M., SCHUBERT, I., HOSEINPOUR, P., CHANDRARATNE, S., VON BRÜHL, M. L., GAERTNER, F., LORENZ, M., AGRESTI, A., COLETTI, R., ANTOINE, D. J., HEERMANN, R., JUNG, K., REESE, S., LAITINEN, I., SCHWAIGER, M., WALCH, A., SPERANDIO, M., NAWROTH, P. P., REINHARDT, C., JÄCKEL, S., BIANCHI, M. E. & MASSBERG, S. 2016. Disulfide HMGB1 derived from platelets coordinates venous thrombosis in mice. *Blood,* 128**,** 2435-2449.

STENBERG, P. E., SHUMAN, M. A., LEVINE, S. P. & BAINTON, D. F. 1984. Redistribution of alpha-granules and their contents in thrombin-stimulated platelets. *J Cell Biol,* 98**,** 748-60.

STITHAM, J., AREHART, E., GLEIM, S. R., LI, N., DOUVILLE, K. & HWA, J. 2007. New insights into human prostacyclin receptor structure and function through natural and synthetic mutations of transmembrane charged residues. *Br J Pharmacol,* 152**,** 513-22.

STONE, J., HANGGE, P., ALBADAWI, H., WALLACE, A., SHAMOUN, F., KNUTTIEN, M. G., NAIDU, S. & OKLU, R. 2017. Deep vein thrombosis: pathogenesis, diagnosis, and medical management. *Cardiovasc Diagn Ther,* 7**,** S276-S284.

STOWELL, S. R., WINKLER, A. M., MAIER, C. L., ARTHUR, C. M., SMITH, N. H., GIRARD-PIERCE, K. R., CUMMINGS, R. D., ZIMRING, J. C. & HENDRICKSON, J. E. 2012. Initiation and regulation of complement during hemolytic transfusion reactions. *Clin Dev Immunol,* 2012**,** 307093.

SUGIYAMA, T., OKUMA, M., USHIKUBI, F., SENSAKI, S., KANAJI, K. & UCHINO, H. 1987. A novel platelet aggregating factor found in a patient with defective collagen-induced platelet aggregation and autoimmune thrombocytopenia. *Blood,* 69**,** 1712-20.

SUZUKI-INOUE, K. 2011. Essential in vivo roles of the platelet activation receptor CLEC-2 in tumour metastasis, lymphangiogenesis and thrombus formation. *J Biochem,* 150**,** 127-32.

SUZUKI-INOUE, K., FULLER, G. L., GARCÍA, A., EBLE, J. A., PÖHLMANN, S., INOUE, O., GARTNER, T. K., HUGHAN, S. C., PEARCE, A. C., LAING, G. D., THEAKSTON, R. D., SCHWEIGHOFFER, E., ZITZMANN, N., MORITA, T., TYBULEWICZ, V. L., OZAKI, Y. & WATSON, S. P. 2006. A novel Syk-dependent mechanism of platelet activation by the C-type lectin receptor CLEC-2. *Blood,* 107**,** 542-9.

SUZUKI-INOUE, K., INOUE, O., DING, G., NISHIMURA, S., HOKAMURA, K., ETO, K., KASHIWAGI, H., TOMIYAMA, Y., YATOMI, Y., UMEMURA, K., SHIN, Y., HIRASHIMA, M. & OZAKI, Y. 2010. Essential in vivo roles of the C-type lectin receptor CLEC-2: embryonic/neonatal lethality of CLEC-2-deficient mice by blood/lymphatic misconnections and impaired thrombus formation of CLEC-2-deficient platelets. *J Biol Chem,* 285**,** 24494-507.

SUZUKI-INOUE, K., KATO, Y., INOUE, O., KANEKO, M. K., MISHIMA, K., YATOMI, Y., YAMAZAKI, Y., NARIMATSU, H. & OZAKI, Y. 2007. Involvement of the snake toxin receptor CLEC-2, in podoplanin-mediated platelet activation, by cancer cells. *J Biol Chem,* 282**,** 25993-6001.

SUZUKI-INOUE, K., OZAKI, Y., KAINOH, M., SHIN, Y., WU, Y., YATOMI, Y., OHMORI, T., TANAKA, T., SATOH, K. & MORITA, T. 2001. Rhodocytin induces platelet aggregation by interacting with glycoprotein Ia/IIa (GPIa/IIa, Integrin alpha 2beta 1). Involvement of GPIa/IIa-associated src and protein tyrosine phosphorylation. *J Biol Chem,* 276**,** 1643-52.

TAKAKUBO, Y., OKI, H., NAGANUMA, Y., SASKI, K., SASAKI, A., TAMAKI, Y., SURAN, Y., KONTA, T. & TAKAGI, M. 2017. Distribution of Podoplanin in Synovial Tissues in Rheumatoid Arthritis Patients Using Biologic or Conventional Disease-Modifying Anti-Rheumatic Drugs. *Curr Rheumatol Rev,* 13**,** 72-78.

TANG, T., LI, L., TANG, J., LI, Y., LIN, W. Y., MARTIN, F., GRANT, D., SOLLOWAY, M., PARKER, L., YE, W., FORREST, W., GHILARDI, N., ORAVECZ, T., PLATT, K. A., RICE, D. S., HANSEN, G. M., ABUIN, A., EBERHART, D. E., GODOWSKI, P., HOLT, K. H., PETERSON, A., ZAMBROWICZ, B. P. & DE SAUVAGE, F. J. 2010. A mouse knockout library for secreted and transmembrane proteins. *Nat Biotechnol,* 28**,** 749-55.

TEJCHMAN, A., LAMERANT-FAYEL, N., JACQUINET, J. C., BIELAWSKA-POHL, A., MLECZKO-SANECKA, K., GRILLON, C., CHOUAIB, S., UGORSKI, M. & KIEDA, C. 2017. Tumor hypoxia modulates podoplanin/CCL21 interactions in CCR7+ NK cell recruitment and CCR7+ tumor cell mobilization. *Oncotarget,* 8**,** 31876-31887.

TENHUNEN, R., MARVER, H. S. & SCHMID, R. 1969. Microsomal heme oxygenase. Characterization of the enzyme. *J Biol Chem,* 244**,** 6388-94.

THEURL, I., HILGENDORF, I., NAIRZ, M., TYMOSZUK, P., HASCHKA, D., ASSHOFF, M., HE, S., GERHARDT, L. M., HOLDERRIED, T. A., SEIFERT, M., SOPPER, S., FENN, A. M., ANZAI, A., RATTIK, S., MCALPINE, C., THEURL, M., WIEGHOFER, P., IWAMOTO, Y., WEBER, G. F., HARDER, N. K., CHOUSTERMAN, B. G., ARVEDSON, T. L., MCKEE, M., WANG, F., LUTZ, O. M., REZOAGLI, E., BABITT, J. L., BERRA, L., PRINZ, M., NAHRENDORF, M., WEISS, G., WEISSLEDER, R., LIN, H. Y. & SWIRSKI, F. K. 2016. On-demand erythrocyte disposal and iron recycling requires transient macrophages in the liver. *Nat Med,* 22**,** 945-51.

THON, J. N. & ITALIANO, J. E. 2010. Platelet formation. *Semin Hematol,* 47**,** 220-6.

TIEDT, R., SCHOMBER, T., HAO-SHEN, H. & SKODA, R. C. 2007. Pf4-Cre transgenic mice allow the generation of lineage-restricted gene knockouts for studying megakaryocyte and platelet function in vivo. *Blood,* 109**,** 1503-6.

TOMAIUOLO, M., BRASS, L. F. & STALKER, T. J. 2017. Regulation of Platelet Activation and Coagulation and Its Role in Vascular Injury and Arterial Thrombosis. *Interv Cardiol Clin,* 6**,** 1-12.

TSENG, M. T., DOZIER, A., HARIBABU, B. & GRAHAM, U. M. 2006. Transendothelial migration of ferric ion in FeCl3 injured murine common carotid artery. *Thromb Res,* 118**,** 275-80.

TSUKIJI, N., OSADA, M., SASAKI, T., SHIRAI, T., SATOH, K., INOUE, O., UMETANI, N., MOCHIZUKI, C., SAITO, T., KOJIMA, S., SHINMORI, H., OZAKI, Y. & SUZUKI-INOUE, K. 2018. Cobalt hematoporphyrin inhibits CLEC-2-podoplanin interaction, tumor metastasis, and arterial/venous thrombosis in mice. *Blood Adv,* 2**,** 2214-2225.

TSUNEKI, M., MARUYAMA, S., YAMAZAKI, M., XU, B., ESSA, A., ABÉ, T., BABKAIR, H., CHENG, J., YAMAMOTO, T. & SAKU, T. 2013. Extracellular heat shock protein A9 is a novel interaction partner of podoplanin in oral squamous cell carcinoma cells. *Biochem Biophys Res Commun,* 434**,** 124-30.

TULL, S. P., ANDERSON, S. I., HUGHAN, S. C., WATSON, S. P., NASH, G. B. & RAINGER, G. E. 2006. Cellular pathology of atherosclerosis: smooth muscle cells promote adhesion of platelets to cocultured endothelial cells. *Circ Res,* 98**,** 98-104.

UHRIN, P., ZAUJEC, J., BREUSS, J. M., OLCAYDU, D., CHRENEK, P., STOCKINGER, H., FUERTBAUER, E., MOSER, M., HAIKO, P., FÄSSLER, R., ALITALO, K., BINDER, B. R. & KERJASCHKI, D. 2010. Novel function for blood platelets and podoplanin in developmental separation of blood and lymphatic circulation. *Blood,* 115**,** 3997-4005.

UNDERHILL, D. M. & GOODRIDGE, H. S. 2007. The many faces of ITAMs. *Trends Immunol,* 28**,** 66-73.

UNSWORTH, A. J., KRIEK, N., BYE, A. P., NARAN, K., SAGE, T., FLORA, G. D. & GIBBINS, J. M. 2017. PPARγ agonists negatively regulate αIIbβ3 integrin outside-in signaling and platelet function through up-regulation of protein kinase A activity. *J Thromb Haemost,* 15**,** 356-369.

VAN GEFFEN, J. P., BROUNS, S. L. N., BATISTA, J., MCKINNEY, H., KEMPSTER, C., NAGY, M., SIVAPALARATNAM, S., BAATEN, C. C. F. M., BOURRY, N., FRONTINI, M., JURK, K., KRAUSE, M., PILLITTERI, D., SWIERINGA, F., VERDOOLD, R., CAVILL, R., KUIJPERS, M. J. E., OUWEHAND, W. H., DOWNES, K. & HEEMSKERK, J. W. M. 2019. High-throughput elucidation of thrombus formation reveals sources of platelet function variability. *Haematologica,* 104**,** 1256-1267.

VARGA-SZABO, D., BRAUN, A. & NIESWANDT, B. 2009. Calcium signaling in platelets. *J Thromb Haemost,* 7**,** 1057-66.

VERKLEIJ, M. W., MORTON, L. F., KNIGHT, C. G., DE GROOT, P. G., BARNES, M. J. & SIXMA, J. J. 1998. Simple collagen-like peptides support platelet adhesion under static but not under flow conditions: interaction via alpha2 beta1 and von Willebrand factor with specific sequences in native collagen is a requirement to resist shear forces. *Blood,* 91**,** 3808-16.

VINCENT, J. L., OPAL, S. M., MARSHALL, J. C. & TRACEY, K. J. 2013. Sepsis definitions: time for change. *Lancet,* 381**,** 774-5.

VON HUNDELSHAUSEN, P., KOENEN, R. R., SACK, M., MAUSE, S. F., ADRIAENS, W., PROUDFOOT, A. E., HACKENG, T. M. & WEBER, C. 2005. Heterophilic interactions of platelet factor 4 and RANTES promote monocyte arrest on endothelium. *Blood,* 105**,** 924-30.

WAGNER, M. C., ECKMAN, J. R. & WICK, T. M. 2004. Sickle cell adhesion depends on hemodynamics and endothelial activation. *J Lab Clin Med,* 144**,** 260-7; discussion 227-8.

WANG, J. & KUBES, P. 2016. A Reservoir of Mature Cavity Macrophages that Can Rapidly Invade Visceral Organs to Affect Tissue Repair. *Cell,* 165**,** 668-78.

WANG, L., OLIVECRONA, G., GOTBERG, M., OLSSON, M. L., WINZELL, M. S. & ERLINGE, D. 2005a. ADP acting on P2Y13 receptors is a negative feedback pathway for ATP release from human red blood cells. *Circ Res,* 96**,** 189-96.

WANG, Y., SAKUMA, M., CHEN, Z., USTINOV, V., SHI, C., CROCE, K., ZAGO, A. C., LOPEZ, J., ANDRE, P., PLOW, E. & SIMON, D. I. 2005b. Leukocyte engagement of platelet glycoprotein Ibalpha via the integrin Mac-1 is critical for the biological response to vascular injury. *Circulation,* 112**,** 2993-3000.

WATSON, A. A., BROWN, J., HARLOS, K., EBLE, J. A., WALTER, T. S. & O'CALLAGHAN, C. A. 2007. The crystal structure and mutational binding analysis of the extracellular domain of the platelet-activating receptor CLEC-2. *J Biol Chem,* 282**,** 3165-72.

WATSON, A. A., CHRISTOU, C. M., JAMES, J. R., FENTON-MAY, A. E., MONCAYO, G. E., MISTRY, A. R., DAVIS, S. J., GILBERT, R. J., CHAKERA, A. & O'CALLAGHAN, C. A. 2009. The platelet receptor CLEC-2 is active as a dimer. *Biochemistry,* 48**,** 10988-96.

WATSON, C. N., KERRIGAN, S. W., COX, D., HENDERSON, I. R., WATSON, S. P. & ARMAN, M. 2016. Human platelet activation by Escherichia coli: roles for FcγRIIA and integrin αIIbβ3. *Platelets,* 27**,** 535-40.

WATSON, S. P., AUGER, J. M., MCCARTY, O. J. & PEARCE, A. C. 2005. GPVI and integrin alphaIIb beta3 signaling in platelets. *J Thromb Haemost,* 3**,** 1752-62.

WEISCHENFELDT, J. & PORSE, B. 2008. Bone Marrow-Derived Macrophages (BMM): Isolation and Applications. *CSH Protoc,* 2008**,** pdb.prot5080.

WEISS, L. J., MANUKJAN, G., PFLUG, A., WINTER, N., WEIGEL, M., NAGLER, N., KREDEL, M., LÂM, T. T., NIESWANDT, B., WEISMANN, D. & SCHULZE, H. 2021. Acquired platelet GPVI receptor dysfunction in critically ill patients with sepsis. *Blood,* 137**,** 3105-3115.

WEN, T., WANG, J., SHI, Y., QIAN, H. & LIU, P. 2021. Inhibitors targeting Bruton's tyrosine kinase in cancers: drug development advances. *Leukemia,* 35**,** 312-332.

WETTERWALD, A., HOFFSTETTER, W., CECCHINI, M. G., LANSKE, B., WAGNER, C., FLEISCH, H. & ATKINSON, M. 1996. Characterization and cloning of the E11 antigen, a marker expressed by rat osteoblasts and osteocytes. *Bone,* 18**,** 125-32.

WICHAIYO, S., LAX, S., MONTAGUE, S. J., LI, Z., GRYGIELSKA, B., PIKE, J. A., HAINING, E. J., BRILL, A., WATSON, S. P. & RAYES, J. 2019. Platelet glycoprotein VI and C-type lectin-like receptor 2 deficiency accelerates wound healing by impairing vascular integrity in mice. *Haematologica,* 104**,** 1648-1660.

WIESNER, C., LE-CABEC, V., EL AZZOUZI, K., MARIDONNEAU-PARINI, I. & LINDER, S. 2014. Podosomes in space: macrophage migration and matrix degradation in 2D and 3D settings. *Cell Adh Migr,* 8**,** 179-91.

WOLF, A. A., YÁÑEZ, A., BARMAN, P. K. & GOODRIDGE, H. S. 2019. The Ontogeny of Monocyte Subsets. *Frontiers in Immunology,* 10.

WOODMAN, R. C., JOHNSTON, B., HICKEY, M. J., TEOH, D., REINHARDT, P., POON, B. Y. & KUBES, P. 1998. The functional paradox of CD43 in leukocyte recruitment: a study using CD43-deficient mice. *J Exp Med,* 188**,** 2181-6.

WORTH, R. G., CHIEN, C. D., CHIEN, P., REILLY, M. P., MCKENZIE, S. E. & SCHREIBER, A. D. 2006. Platelet FcgammaRIIA binds and internalizes IgG-containing complexes. *Exp Hematol,* 34**,** 1490-5.

WU, C. C., KO, F. N., HUANG, T. F. & TENG, C. M. 1996. Mechanisms-regulated platelet spreading after initial platelet contact with collagen. *Biochem Biophys Res Commun,* 220**,** 388-93.

XIANG, B., ZHANG, G., GUO, L., LI, X. A., MORRIS, A. J., DAUGHERTY, A., WHITEHEART, S. W., SMYTH, S. S. & LI, Z. 2013. Platelets protect from septic shock by inhibiting macrophage-dependent inflammation via the cyclooxygenase 1 signalling pathway. *Nat Commun,* 4**,** 2657.

XIE, Z., SHAO, B., HOOVER, C., MCDANIEL, M., SONG, J., JIANG, M., MA, Z., YANG, F., HAN, J., BAI, X., RUAN, C. & XIA, L. 2020. Monocyte upregulation of podoplanin during early sepsis induces complement inhibitor release to protect liver function. *JCI Insight,* 5.

XUAN, W., QU, Q., ZHENG, B., XIONG, S. & FAN, G. H. 2015. The chemotaxis of M1 and M2 macrophages is regulated by different chemokines. *J Leukoc Biol,* 97**,** 61-9.

YANG, E. Y. & SHAH, K. 2020. Nanobodies: Next Generation of Cancer Diagnostics and Therapeutics. *Front Oncol,* 10**,** 1182.

YANG, W. S. & STOCKWELL, B. R. 2008. Synthetic lethal screening identifies compounds activating iron-dependent, nonapoptotic cell death in oncogenic-RAS-harboring cancer cells. *Chem Biol,* 15**,** 234-45.

YAU, J. W., TEOH, H. & VERMA, S. 2015. Endothelial cell control of thrombosis. *BMC Cardiovasc Disord,* 15**,** 130.

YE, Y., WAN, W., WANG, J., HU, W., WANG, H., LI, L., SANG, P., GU, Y., LI, D., WANG, Z. & MENG, Z. 2020. The CEACAM1-derived peptide QLSN impairs collagen-induced human platelet activation through glycoprotein VI. *Biosci Biotechnol Biochem,* 84**,** 85-94.

YE, Z., ZHONG, L., ZHU, S., WANG, Y., ZHENG, J., WANG, S., ZHANG, J. & HUANG, R. 2019. The P-selectin and PSGL-1 axis accelerates atherosclerosis via activation of dendritic cells by the TLR4 signaling pathway. *Cell Death Dis,* 10**,** 507.

YLITALO, R., OKSALA, O., YLÄ-HERTTUALA, S. & YLITALO, P. 1994. Effects of clodronate (dichloromethylene bisphosphonate) on the development of experimental atherosclerosis in rabbits. *J Lab Clin Med,* 123**,** 769-76.

ZAIDEL-BAR, R., MILO, R., KAM, Z. & GEIGER, B. 2007. A paxillin tyrosine phosphorylation switch regulates the assembly and form of cell-matrix adhesions. *J Cell Sci,* 120**,** 137-48.

ZEILER, M., MOSER, M. & MANN, M. 2014. Copy number analysis of the murine platelet proteome spanning the complete abundance range. *Mol Cell Proteomics,* 13**,** 3435-45.

ZERNECKE, A., BIDZHEKOV, K., OZÜYAMAN, B., FRAEMOHS, L., LIEHN, E. A., LÜSCHER-FIRZLAFF, J. M., LÜSCHER, B., SCHRADER, J. & WEBER, C. 2006. CD73/ecto-5'-nucleotidase protects against vascular inflammation and neointima formation. *Circulation,* 113**,** 2120-7.

ZHANG, D., EBRAHIM, M., ADLER, K., BLANCHET, X., JAMASBI, J., MEGENS, R. T. A., UHLAND, K., UNGERER, M., MÜNCH, G., DECKMYN, H., WEBER, C., ELIA, N., LORENZ, R. & SIESS, W. 2020. Glycoprotein VI is not a Functional Platelet Receptor for Fibrin Formed in Plasma or Blood. *Thromb Haemost,* 120**,** 977-993.

ZHANG, D., XU, C., MANWANI, D. & FRENETTE, P. S. 2016. Neutrophils, platelets, and inflammatory pathways at the nexus of sickle cell disease pathophysiology. *Blood,* 127**,** 801-9.

ZHARIKOV, S. & SHIVA, S. 2013. Platelet mitochondrial function: from regulation of thrombosis to biomarker of disease. *Biochem Soc Trans,* 41**,** 118-23.

ZHENG, C., YANG, Q., CAO, J., XIE, N., LIU, K., SHOU, P., QIAN, F., WANG, Y. & SHI, Y. 2016. Local proliferation initiates macrophage accumulation in adipose tissue during obesity. *Cell Death Dis,* 7**,** e2167.

ZHOU, Z., CONNELL, M. C. & MACEWAN, D. J. 2007. TNFR1-induced NF-kappaB, but not ERK, p38MAPK or JNK activation, mediates TNF-induced ICAM-1 and VCAM-1 expression on endothelial cells. *Cell Signal,* 19**,** 1238-48.

ZIBERNA, L., MARTELANC, M., FRANKO, M. & PASSAMONTI, S. 2016. Bilirubin is an Endogenous Antioxidant in Human Vascular Endothelial Cells. *Sci Rep,* 6**,** 29240.

Appendix 1 – Heme induces human and mouse platelet activation through C-type lectin-like receptor 2. Haematologica.

Heme induces human and mouse platelet activation through C-type-lectin-like receptor-2

Intravascular hemolysis is a serious complication developed in many severe infections such as malaria, sepsis,[1] typical hemolytic uremic syndrome[2] and congenital diseases such as sickle cell disease.[3] Hemolysis is accompanied by thrombocytopenia, platelet activation, platelet-leukocyte aggregates, inflammation, vascular obstruction and organ damage. During hemolysis, red blood cell destruction leads to the release of molecules such as ADP, hemoglobin and heme which exert potent prothrombotic and proinflammatory actions.

Under physiological conditions, free heme is scavenged by the plasma protein hemopexin, and is subsequently catabolized by heme oxygenase-1 into carbon monoxide, biliverdin and ferrous iron (Fe^{2+}). However, acute or/and chronic hemolysis exhausts the scavenging system leading to an increase in free heme in the blood. Upon release, reduced heme is rapidly and spontaneously oxidized in the blood into ferric (Fe^{3+}) form, hemin, with increased levels observed in hemolytic diseases. It was recently shown that hemin induces human platelet activation and platelet death through ferroptosis, an intracellular iron-mediated cell death.[4] However, the mechanisms and receptors involved in platelet activation by hemin are not known.

In this study, we investigated hemin-mediated human and mouse platelet activation *in vitro*. An increase in labile (i.e., weakly bound and free) heme/hemin is detected in patients with hemolytic diseases with plasma concentrations ranging between 2 μM and 50 μM.[5,6] Similar concentrations of heme are detected in mice with chronic or acute hemolysis such as sickle cell mice or Escherichia coli-induced hemolysis.[1,7] In this study, we show that hemin (2-12 μM) induces rapid aggregation of human washed platelets, while aggregation is slower and reduced in magnitude at higher (≥ 25 μM) concentrations (Figure 1A, B). Platelet aggregation was associated with increased P-selectin expression and GPIIbIIIa activation as measured by flow cytometry (Figure 1C, D). High (≥25 μM) but not lower concentrations of hemin significantly increased phosphatidylserine (PS) exposure on platelets as assessed using Annexin V staining (Figure 1E). Moreover, high concentrations of hemin induced toxicity as measured by increased levels of lactate dehydrogenase (LDH) in the supernatant of activated platelets (Figure 1F). Recent data have shown that a high concentration of hemin (25 μM) triggers lipid peroxidation and human platelet death through ferroptosis but not apoptosis or necroptosis.[4] Whether the increase in PS exposure modulates the contribution of platelets to the coagulopathies observed in hemolytic diseases requires further investigation.

Hemin is known to bind to Toll-like receptor (TLR) TLR4 on endothelial cells resulting in endothelial cell activation including secretion of Weibel-Palade bodies.[3] However, blocking TLR4 signaling in platelets using TAK-242 did not alter activation by hemin, suggesting a TLR-4-independent pathway of activation (Figure 1H). At low concentrations, human platelet aggregation by hemin was blocked by inhibitors of Syk (PRT-060318), Src family kinases (PP2) and Btk (Ibrutinib), and partially by GPIIbIIIa inhibitor eptifibatide (Integrilin) (Figure 1G, H). These results suggest that hemin induces human platelet activation *via* an immunoreceptor-tyrosine-based activation-motif (ITAM) receptor-based pathway.[8] Indeed, low concentrations of hemin provoked phosphorylation of Syk and PLCγ2 (Figure 1I). In order to identify the receptor triggering platelet activation by hemin, we used recombinant dimeric forms of C-type-lectin-like receptor-2 (CLEC-2) and collagen receptor glycoprotein VI (GPVI) (hFc-CLEC-2 and hFc-GPVI, respectively) as a blocking strategy. Pre-incubation of hemin with hFc-CLEC-2 but not hFc-GPVI abolished platelet aggregation by hemin identifying CLEC-2 as the receptor mediating human platelet activation by hemin (Figure 1G, H). These results also suggest a direct interaction between hemin and CLEC-2. However, while we believe that the inhibition is likely the result of competition between recombinant and platelet CLEC-2, we cannot rule out that recombinant CLEC-2-hemin complex may interfere with CLEC-2 clustering thereby inhibiting platelet activation. Platelet aggregation was not altered by AYP1, 9, an antibody that blocks the interaction between CLEC-2 and podoplanin, providing indirect evidence that hemin binds to a distinct site on CLEC-2 to podoplanin (Figure 1H). Protoporphyrin IX, the precursor of heme, and cobalt hematoporphyrin were shown to bind to CLEC-2 and inhibit podoplanin-CLEC-2 interaction without inducing platelet activation.[10] The type of interactions by which different porphyrins selectively bind to CLEC-2 and induce platelet activation requires further investigation. Platelet aggregation mediated by low concentrations of hemin (6.25 μM) was not altered by cyclooxygenase (COX) (indomethacin) or P2Y12 (cangrelor) inhibitors, showing that, in contrast to podoplanin, secondary mediators are not required for hemin-mediated platelet activation (Figure 1G, H). This may reflect the ability of hemin to induce higher oligomers of CLEC-2 increasing signal transduction. Platelet aggregation does not depend on oxidative stress as hemin-mediated platelet aggregation was not altered by the antioxidant N-acetyl cysteine (NAC) (Figure 1H; Online Supplementary Figure S1). At higher concentrations (>25 μM), platelet aggregation was not inhibited by integrilin or inhibitors of Src, Syk and Btk, suggesting that higher concentrations of hemin induce agglutination (*Online Supplementary Figure S2*). Increasing the concentrations of inhibitors did not alter platelet agglutination/aggregation (*not shown*). The distinct mechanisms of platelet activation by low and high concentrations of hemin might be related to formation of hemin aggregates at high concentrations, which might exert different activities as compared to monomeric or dimeric hemin present at low concentrations.

Hemin induces mouse platelet aggregation, albeit at a slightly higher concentration (Figure 2A). Similar to human platelets, aggregation by low concentrations of hemin was inhibited by inhibitors of Src, Syk and Btk tyrosine kinases, recombinant mouse Fc-mCLEC-2 and GPIIbIIIa blockade (Figure 2B, C). In contrast, inhibitors of TLR4, COX and $P2Y_{12}$ had no effect on platelet aggregation by hemin (Figure 2C). Platelet aggregation by hemin was significantly reduced in CLEC-2-deficient platelets confirming a key role for CLEC-2 (Figure 2D, E). However, deletion of CLEC-2 did not inhibit platelet shape change suggesting that one or more other receptors support platelet activation by hemin in mice.

The fact that recombinant CLEC-2 inhibits hemin-mediated platelet aggregation suggests a direct interaction between hemin and CLEC-2. Using surface plasmon resonance-based technique, we demonstrated that hemin binds to both murine and human recombinant CLEC-2 with K_D values of ~200 nM in both cases (Figure 3A, C). Hemin binding to mouse CLEC-2 was characterized by kinetic rate association (k_a) and dissociation (k_d) constants of k_a=2.77±0.08×104 mol^{-1} s^{-1} and 5.76±0.09×10^{-3} s^{-1}.

Similar values of kinetic rate constants were determined for hemin binding to human CLEC-2, ka=2.65±0.09×10^4 mol^{-1} s^{-1} and kd=5.06±0.05×10^{-3} s^{-1}. The interaction of hemin with human and mouse CLEC-2 was further confirmed by UV-vis absorbance spectroscopy (Figure 3B, D). The differential absorbance spectra profiles revealed significant shifts of the spectra of hemin towards higher wavelength by human and mouse CLEC-2 demonstrating a direct binding. The differences in the spectral changes of hemin in the presence of human and mouse CLEC-2 can be explained by distinct residues coordinating heme's iron. The blue shift in the Soret region observed with mCLEC-2 suggests the involvement of sulfur containing amino acid (cysteine)[11] whereas the red shift observed with human CLEC-2 suggests histidine coordination.

Altogether, these results show that hemin is an endogenous agonist for CLEC-2 leading to platelet activa-

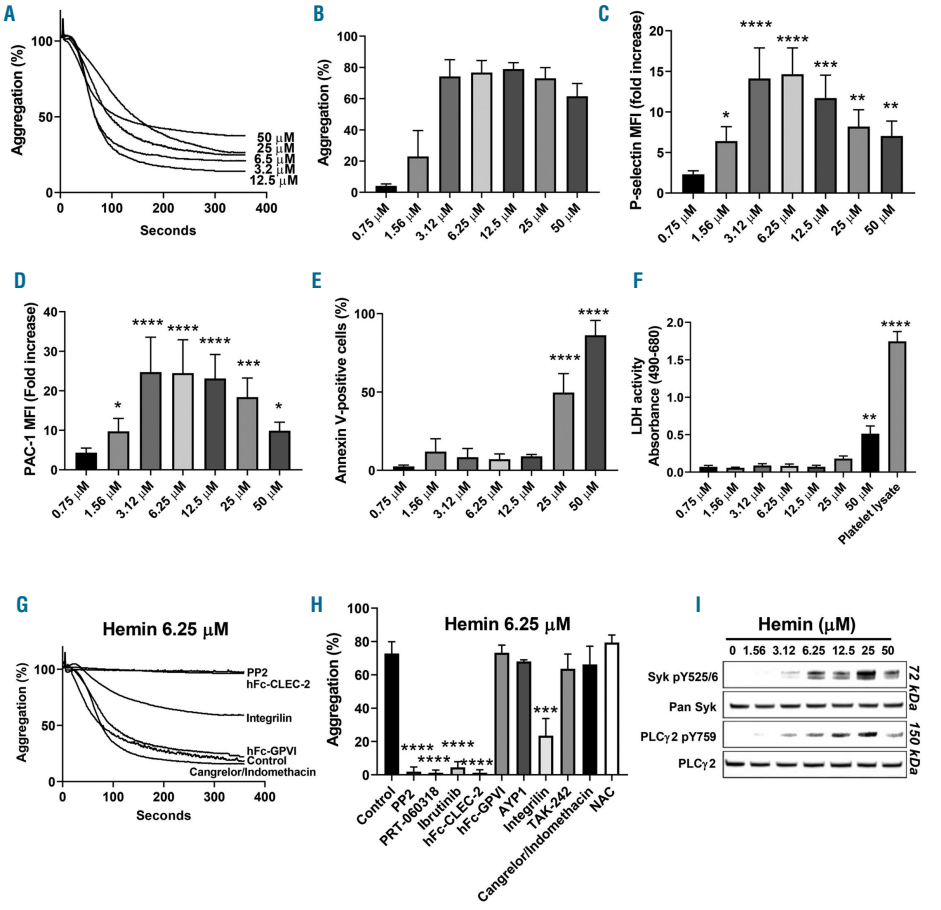

Figure 1. Hemin mediates human platelet activation through C-type-lectin-like receptor-2. (A, B) Human washed platelets (2x108/mL) were incubated with increasing concentrations of hemin in the presence of Ca^{2+} (2 mM). Platelet aggregation was assessed for 6 minutes (min) using light transmission aggregometry (n=5). (C, D) For flow cytometry analysis, 1x10^6 platelets were incubated with different concentrations of hemin for 20 min at 37°C. Platelet activation was determined by flow cytometry using (C) anti-P-selectin and (D) GPIIbIIIa PAC-1 antibodies (n=4). Data is shown as fold increase of median of fluorescence (MFI) of treated platelets over control (absence of hemin). (E) Phosphatidylserine exposure was assessed using Annexin V staining. (F) Lactate dehydrogenase (LDH) levels were measured in the supernatant following platelet aggregation (6 min). Platelet lysate was used to detect the total level of LDH in platelets. (G, H) Platelet aggregation by hemin was assessed using Btk inhibitor Ibrutinib (500 nM), Src family kinase inhibitor PP2 (20 µM), Syk inhibitor PRT-060318 (20 µM), TLR4 inhibitor TAK-242 (10 µM), $P2Y_{12}$ inhibitor Cangrelor (10 µM) or cyclooxygenase inhibitor indomethacin (10 µM). Platelets were pre-incubated with different inhibitors for 5 min at 37 °C prior to the addition of hemin. Dimeric C-type-lectin-like receptor-2 (CLEC-2) (hFc-CLEC-2, 20 µg/mL) or dimeric collagen receptor glycoprotein VI (GPVI) (hFc-GPVI, 20 µg/mL) were pre-incubated with hemin for 20 min at 37 °C prior to addition to platelets (n=5). (H) Histogram data are shown as mean ± standard deviation. (I) Protein levels of the phosphorylation of Syk and PLCγ2, and total Syk and PLCγ2 in platelet lysates were determined by western blotting after 6 min aggregation. Western blots are representative of five independent experiments. The statistical significance was analyzed using a one-way ANOVA with Tukey's multiple comparisons test using Prism 8 (GraphPad Software Inc, USA). Significance is shown compared to control (absence of hemin), *P<0.05, **P<0.01, ***P<0.001, ****P<0.0001.

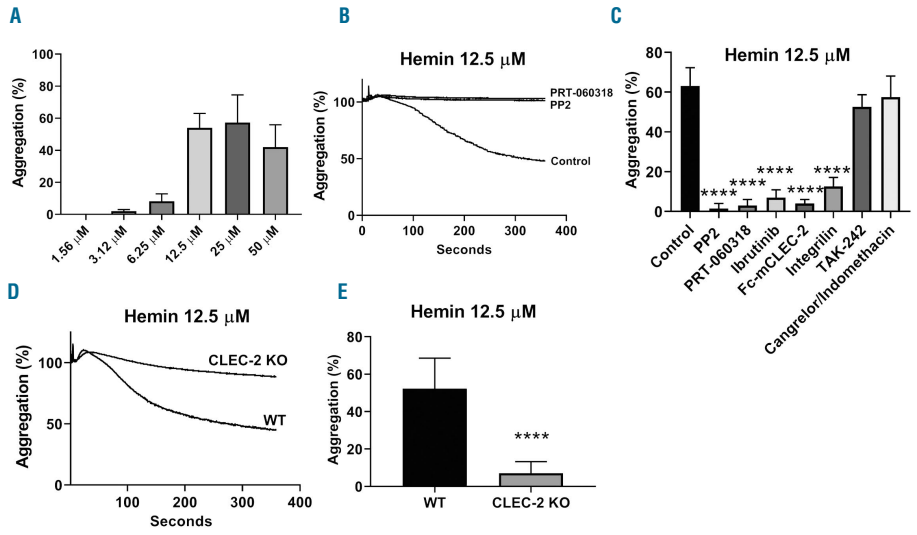

Figure 2. Hemin induces mouse platelet aggregation. (A) Mouse washed platelets ($2x10^8$/mL) were incubated with increasing concentrations of hemin in the presence of Ca^{2+} (2 mM). Platelet aggregation was assessed using light transmission aggregometry. (B, C) Hemin-mediated platelet aggregation (12.5 μM hemin) was assessed in the presence of Ibrutinib (2 μM), PP2 (20 μM), PRT-060318 (20 μM), TAK-242 (10 μM), Cangrelor (10 μM), recombinant mouse C-type-lectin-like receptor-2 (CLEC-2) (Fc-mCLEC-2, 10 μg/mL) (n=4). (D, E) Washed platelets from wild-type (WT) or Clec-2 deficient (Clec-1bfl/fl PF4cre, Clec-2 KO) were incubated with hemin (12.5 μM) in the presence of Ca^{2+} (2 mM) (n=5). (E) Histogram data are shown as mean ± standard deviation. The statistical significance was analyzed using a one-way ANOVA with Tukey's multiple comparisons test using Prism 8. Significance is shown compared to control ****P<0.0001.

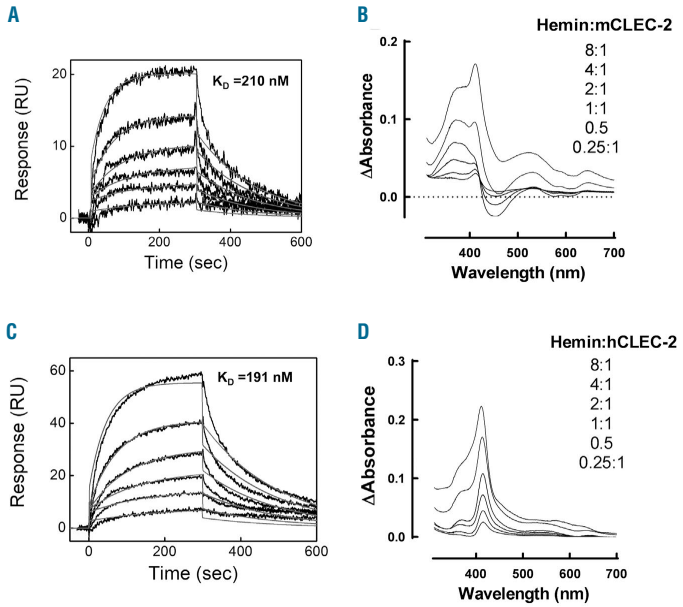

Figure 3. Hemin binds to mouse and human recombinant C-type-lectin-like receptor-2. (A, C) For surface plasma resonance, real-time interaction profiles were obtained after injection of increasing concentrations of hemin (19.5–625 nM) over recombinant mouse (A) and human (C) C-type-lectin-like receptor-2 (CLEC-2) immobilized on CM5 sensor chip. The association and dissociation phases were followed for 5 minutes, each. The black lines show the experimental data, the grey lines depict the fit obtained using Langmuir global analyses model. (B, D) For UV-vis absorbance spectroscopy, differential spectra were generated after titration of (B) mouse or (D) human dimeric CLEC-2 (2 μM) with increasing concentrations of hemin (0.5–16 μM). The differential spectra were obtained after subtraction of the spectra of hemin at a given concentration from the spectra of the same concentration of hemin in the presence of the protein. The measurements were done at 25°C in optical cell with 10 mm light path.

tion through activation of integrin GPIIbIIIa at low concentrations and agglutination at high concentrations. Recombinant CLEC-2 inhibits platelet activation by both mechanisms suggesting that this may represent a novel form of therapeutic intervention to inhibit platelet activation in hemolytic disease.

Ethical approval for collecting blood from healthy volunteers was granted by Birmingham University Internal Ethical Review (ERN_11-0175). Mice experiments were performed in accordance with UK laws (Animal [Scientific Procedures] Act 1986) with approval of the local ethical committee and UK Home Office approval (PPL P0e98D513).

Human and mouse washed platelets were prepared as previously described.[12,13] Platelet aggregation was assessed using light transmission aggregometry for 6 minutes (ChronoLog, Havertown, PA, USA). Fresh synthetic hemin solution was freshly prepared (Frontiers Scientific, USA) for each experiment. PP2 (Tocris/Biotechne Ltd), PRT-060318 (Caltag medsystems), indomethacin (Sigma-Aldrich), cangrelor (The Medicines Company), Ibrutinib (Stratech Scientific), N-Acetyl-L-cysteine (Sigma-Aldrich) and TAK-242 (Sigma-Aldrich) were preincubated for 5 minutes (min) at 37°C with platelets prior to addition of hemin. Human (h) and mouse (m) CLEC-2 and GPVI were produced as Fc fusion proteins (hFc-CLEC-2, hFc-GPVI, Fc-mCLEC-2) in human embryonic kidney HEK293 cells and purified using chromatography affinity. Recombinant human and mouse CLEC-2 were preincubated with hemin for 15 min at 37°C before addition to platelets. Following aggregation, platelets were centrifuged at 1,000g for 10 min and LDH was measured in the supernatant using CyQUANT™ LDH Cytotoxicity Assay (ThermoFisher Scientific). Clec-2 deficient mice (Clec-1bfl/fl PF4cre) and littermate controls were previously described.[14]

Platelet activation (106 platelets) by different concentrations of hemin (20 min at 37°C) was assessed by flow cytometry with antibodies against CD62P (PE/Cy5 anti-human CD62P antibody, biolegend) and activated GPIIbIIIa (Alexa Fluor® 647 anti-human CD41/CD61 antibody PAC1, Biolegend) using BD Accuri C6 Plus flow cytometer (BD Bioscience). For western blotting, Phospho-Syk (Tyr525/526) (C87C1) Rabbit mAb (#2710), Phospho-PLCγ2 (Tyr759) antibody (#3874), Syk antibody (#2712) and PLCγ2 antibody (#3872) were used (Cell signalling). Protein phosphorylation was assessed after 6 min of aggregation as previously described.[12]

The binding of human and mouse dimeric CLEC-2 to hemin was performed at 25°C and assessed using surface plasma resonance and UV-spectroscopy methods.[15]

Joshua H. Bourne,[1] Martina Colicchia,[1*] Ying Di,[1] Eleyna Martin,[1] Alexander Slater,[1] Lubka T. Roumenina,[2] Jordan D. Dimitrov,[2] Steve P. Watson,[1,3] and Julie Rayes[1,3]*

[1]Institute of Cardiovascular Sciences, College of Medical and Dental Sciences, University of Birmingham, Birmingham, UK; [2]Centre de Recherche des Cordeliers, INSERM, Sorbonne Université, USPC, Université Paris Descartes, Université Paris Diderot, Paris, France and [3]Center of Membrane Proteins and Receptors (COMPARE), Universities of Birmingham and Nottingham, The Midlands, UK

**JHB and MC contributed equally as co-first authors*

Correspondence:

JULIE RAYES - j.rayes@bham.ac.uk

doi:10.3324/haematol.2020.246488

Disclosures: no conflicts of interests to disclose.

Contributions: JHB, MC performed experiments and analyzed data; YD, AS, EM generated reagents; LTR contributed to data interpretation; JDD contributed to research design, performed experiments and interpreted data; SPW contributed to research and data interpretation and provided reagents; JR designed and performed research, collected data, analyzed and interpreted data and wrote the manuscript. All authors reviewed and approved the manuscript.

Acknowledgments: the authors would like to thank Dr B. Grygielska for genotyping of mice.

Funding: this work was supported by a BHF Accelerator Award (AA/18/2/34218), BHF programme grant (RG/13/18/30563), Wellcome Trust 4 year studentship (204951), Wellcome Trust Joint Investigator Award (204951/Z/16/Z) and the Centre of Membrane Proteins and Receptors. JDD hold an H2020 ERC starting grant (CoBABATI 678905). SPW holds a BHF Chair (CH/03/003).

References

1. Martins R, Maier J, Gorki AD, et al. Heme drives hemolysis-induced susceptibility to infection via disruption of phagocyte functions. Nat Immunol. 2016;17(12):1361-1372.
2. Frimat M, Tabarin F, Dimitrov JD, et al. Complement activation by heme as a secondary hit for atypical hemolytic uremic syndrome. Blood. 2013; 122(2):282-292.
3. Belcher JD, Chen C, Nguyen J, et al. Heme triggers TLR4 signaling leading to endothelial cell activation and vaso-occlusion in murine sickle cell disease. Blood. 2014;123(3):377-390.
4. NaveenKumar SK, SharathBabu BN, Hemshekhar M, Kemparaju K, Girish KS, Mugesh G. The Role of Reactive Oxygen Species and Ferroptosis in Heme-Mediated Activation of Human Platelets. ACS Chem Biol. 2018;13(8):1996-2002.
5. Muller-Eberhard U, Javid J, Liem HH, Hanstein A, Hanna M. Plasma concentrations of hemopexin, haptoglobin and heme in patients with various hemolytic diseases. Blood. 1968;32(5):811-815.
6. Gouveia Z, Carlos AR, Yuan X, et al. Characterization of plasma labile heme in hemolytic conditions. FEBS J. 2017;284(19):3278-3301.
7. Belcher JD, Chen C, Nguyen J, et al. Haptoglobin and hemopexin inhibit vaso-occlusion and inflammation in murine sickle cell disease: Role of heme oxygenase-1 induction. PLoS One. 2018; 13(4):e0196455.
8. Rayes J, Watson SP, Nieswandt B. Functional significance of the platelet immune receptors GPVI and CLEC-2. J Clin Invest. 2019;129(1):12-23.
9. Gitz E, Pollitt AY, Gitz-Francois JJ, et al. CLEC-2 expression is maintained on activated platelets and on platelet microparticles. Blood. 2014; 124(14):2262-2270.
10. Tsukiji N, Osada M, Sasaki T, et al. Cobalt hematoporphyrin inhibits CLEC-2-podoplanin interaction, tumor metastasis, and arterial/venous thrombosis in mice. Blood Adv. 2018;2(17):2214-2225.
11. Kuhl T, Wissbrock A, Goradia N, et al. Analysis of Fe(III) heme binding to cysteine-containing heme-regulatory motifs in proteins. ACS Chem Biol. 2013;8(8):1785-1793.
12. Nicolson PLR, Hughes CE, Watson S, et al. Inhibition of Btk by Btk-specific concentrations of ibrutinib and acalabrutinib delays but does not block platelet aggregation mediated by glycoprotein VI. Haematologica. 2018;103(12):2097-2108.
13. Hughes CE, Pollitt AY, Mori J, et al. CLEC-2 activates Syk through dimerization. Blood. 2010;115(14):2947-2955.
14. Finney BA, Schweighoffer E, Navarro-Nunez L, et al. CLEC-2 and Syk in the megakaryocytic/platelet lineage are essential for development. Blood. 2012;119(7):1747-1756.
15. Wiatr M, Merle NS, Boudhabhay I, et al. Anti-inflammatory activity of intravenous immunoglobulin through scavenging of heme. Mol Immunol. 2019;111:205-208.

Appendix 2 – CLEC-2 prevents accumulation and retention of Inflammatory macrophages during murine peritonitis

frontiers in Immunology

ORIGINAL RESEARCH
published: 07 June 2021
doi: 10.3389/fimmu.2021.693974

CLEC-2 Prevents Accumulation and Retention of Inflammatory Macrophages During Murine Peritonitis

*Joshua H. Bourne[1], Nonantzin Beristain-Covarrubias[1], Malou Zuidscherwoude[1,2], Joana Campos[1], Ying Di[1], Evelyn Garlick[1,2], Martina Colicchia[1], Lauren V. Terry[3], Steven G. Thomas[1,2], Alexander Brill[1,4], Jagadeesh Bayry[5,6], Steve P. Watson[1,2] and Julie Rayes[1,2]**

[1] Institute of Cardiovascular Sciences, College of Medical and Dental Sciences, University of Birmingham, Birmingham, United Kingdom, [2] Centre of Membrane Proteins and Receptors (COMPARE), Universities of Birmingham and Nottingham, The Midlands, United Kingdom, [3] Institute of Immunology and Immunotherapy, University of Birmingham, Birmingham, United Kingdom, [4] Department of Pathophysiology, Sechenov First Moscow State Medical University (Sechenov University), Moscow, Russia, [5] Institut National de la Santé et de la Recherche Médicale, Centre de Recherche des Cordeliers, Equipe - Immunopathologie et Immunointervention Thérapeutique, Sorbonne Université, Université de Paris, Paris, France, [6] Biological Sciences and Engineering, Indian Institute of Technology Palakkad, Kerala, India

OPEN ACCESS

Edited by:
Amiram Ariel,
University of Haifa, Israel

Reviewed by:
Andreas Von Knethen,
Goethe University Frankfurt, Germany
Prasenjit Guchhait,
Regional Centre for Biotechnology (RCB), India

***Correspondence:**
Julie Rayes
j.rayes@bham.ac.uk

Specialty section:
This article was submitted to Inflammation, a section of the journal Frontiers in Immunology

Received: *12 April 2021*
Accepted: *20 May 2021*
Published: *07 June 2021*

Citation:
Bourne JH, Beristain-Covarrubias N, Zuidscherwoude M, Campos J, Di Y, Garlick E, Colicchia M, Terry LV, Thomas SG, Brill A, Bayry J, Watson SP and Rayes J (2021) CLEC-2 Prevents Accumulation and Retention of Inflammatory Macrophages During Murine Peritonitis. Front. Immunol. 12:693974. doi: 10.3389/fimmu.2021.693974

Platelets play a key role in the development, progression and resolution of the inflammatory response during sterile inflammation and infection, although the mechanism is not well understood. Here we show that platelet CLEC-2 reduces tissue inflammation by regulating inflammatory macrophage activation and trafficking from the inflamed tissues. The immune regulatory function of CLEC-2 depends on the expression of its ligand, podoplanin, upregulated on inflammatory macrophages and is independent of platelet activation and secretion. Mechanistically, platelet CLEC-2 and also recombinant CLEC-2-Fc accelerates actin rearrangement and macrophage migration by increasing the expression of podoplanin and CD44, and their interaction with the ERM proteins. During ongoing inflammation, induced by lipopolysaccharide, treatment with rCLEC-2-Fc induces the rapid emigration of peritoneal inflammatory macrophages to mesenteric lymph nodes, thus reducing the accumulation of inflammatory macrophages in the inflamed peritoneum. This is associated with a significant decrease in pro-inflammatory cytokine, TNF-α and an increase in levels of immunosuppressive, IL-10 in the peritoneum. Increased podoplanin expression and actin remodelling favour macrophage migration towards CCL21, a soluble ligand for podoplanin and chemoattractant secreted by lymph node lymphatic endothelial cells. Macrophage efflux to draining lymph nodes induces T cell priming. In conclusion, we show that platelet CLEC-2 reduces the inflammatory phenotype of macrophages and their accumulation, leading to diminished tissue inflammation. These immunomodulatory functions of CLEC-2 are a novel strategy to reduce tissue inflammation and could be therapeutically exploited through rCLEC-2-Fc, to limit the progression to chronic inflammation.

Keywords: CLEC-2, podoplanin, macrophage, inflammation, platelet

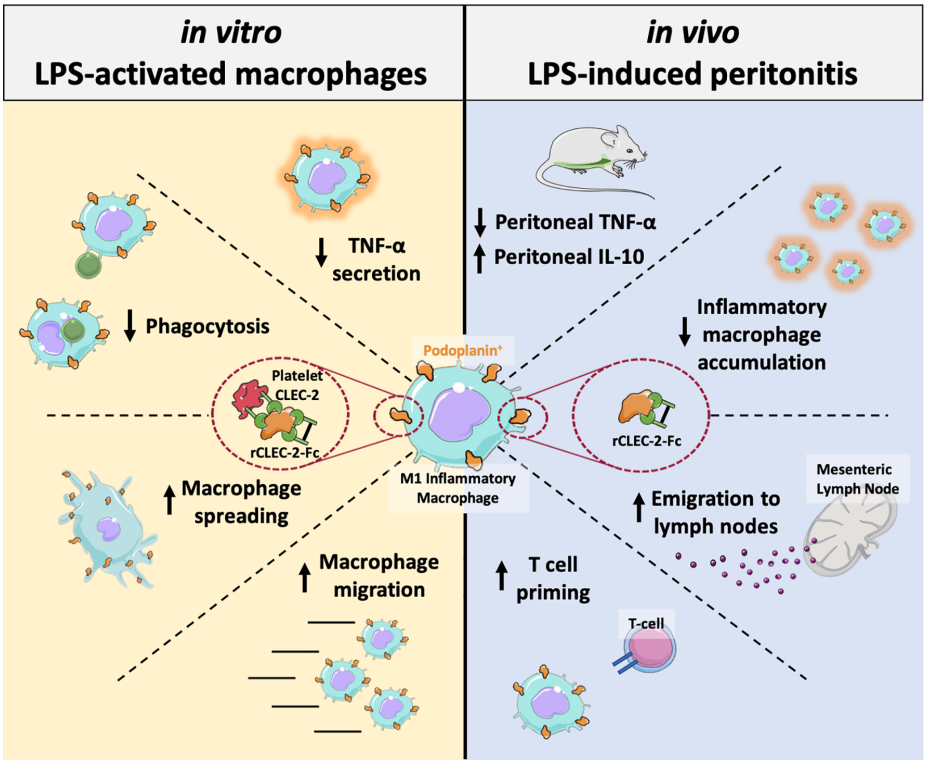

GRAPHICAL ABSTRACT |

INTRODUCTION

Alongside their role in thrombosis and haemostasis, platelets are emerging as vital regulators of the inflammatory response under sterile and infectious conditions (1, 2). Platelet immunoregulatory functions are tightly regulated by the nature of the insult and the environment. Interestingly, distinct platelet receptors are engaged in different vascular beds and differentially regulate vascular integrity, thrombosis and inflammation (3, 4). Platelet-innate immune cell interactions play a pivotal role in balancing the immune response, however little is known on the functional relevance of these interaction during ongoing inflammation, and how it regulates the resolution of the inflammation. Platelet-leukocyte aggregates are observed in the blood during sterile inflammation and following bacterial, viral and fungal infections (5–8). Platelets are also found in inflamed tissues, such as the lung and peritoneum, primarily in complexes with monocytes, neutrophils and macrophages (3, 9–14). Among the receptors reported to regulate the inflammatory response, the adhesion receptors glycoprotein I (GPIb) and C-type lectin-like receptor 2 (CLEC-2) were shown to differentially regulate macrophage polarization and activation in the inflamed peritoneum, with distinct receptors engaged during the time course of the inflammatory response (10, 12, 13). An increase in macrophage recruitment and activation, drives tissue inflammation observed in atherosclerosis and metabolic disorders, as well as non-resolved infection-driven inflammation (15).

CLEC-2 is a hemi-immunoreceptor tyrosine-based activation motif (hemi-ITAM) receptor constitutively expressed on platelets and a sub-set of dendritic cells. CLEC-2 induces platelet activation through its interaction with its endogenous ligands podoplanin or heme (16, 17). Podoplanin is a small, transmembrane O-glycosylated mucin-type protein constituently expressed on type I lung epithelial cells, fibroblastic reticular cells, lymphatic endothelial cells and podocytes, and is upregulated on inflammatory macrophages, TH17 cells, fibroblasts and cancer cells (18, 19). Beside the role of CLEC-2-podoplanin in thrombosis (20, 21), deletion of platelet-

CLEC-2 or haematopoietic-podoplanin increases the cytokine storm and bacterial growth and spreading during caecal ligation and puncture-mediated peritonitis (10, 22). Whether crosslinking podoplanin can regulate macrophage phenotype, fate or resultant tissue inflammation is not known. This is highly relevant in diseases describing platelet-bound podoplanin-positive macrophages such as atherosclerosis (23), rheumatoid arthritis (24), and breast cancer (25).

In this study, we investigate the mechanisms by which CLEC-2 regulates macrophage activation, accumulation and fate during ongoing inflammation. Our study shows a key role for CLEC-2 in macrophage trafficking from the inflamed tissues. This provides a rational to use recombinant CLEC-2-Fc as a therapeutic protein to limit macrophage accumulation in inflamed tissues and progression to chronic inflammation.

METHODS

Mice

Wild type (WT) C57BL/6 mice (12-14 weeks; males and females) were purchased from Harlan Laboratories (Oxford, UK). Platelet-specific CLEC-2-deficient (26) (CLEC1b$^{fl/fl}$GPIbCre), haematopoietic-specific podoplanin deficient (10) (PDPN$^{fl/fl}$ Vav-iCre) and LifeAct-GFP (27) mice were used. All experiments were performed in accordance with UK law (Animal Scientific Procedures Act 1986) with approval of the local ethics committee and UK Home Office approval under PPL P2E63AE7B, PP9677279 and P0E98D513 granted to the University of Birmingham.

Cell Culture

RAW264.7 cells (Sigma Aldrich) were cultured as previously described (28). Bone marrow cells were isolated from WT mice or PDPN$^{fl/fl}$Vav-iCre^{+} (tibias and femurs) and differentiated into bone marrow-derived macrophages (BMDM) with L-929 conditioned medium for 7 days (29). RAW264.7 cells and BMDM were maintained in Dulbecco's Modified Eagle Media (DMEM, Thermofisher) supplemented with 10% heat-inactivated foetal bovine serum (FBS), 1% *penicillin*-streptomycin and 2mM L-*glutamine* in a humidified incubator at 5% CO_2 and 37°C.

Platelet Preparation

Mouse platelets were prepared as previously described (28).

Lipopolysaccharide (LPS)-Induced Endotoxemia in Mice

LPS (*Escherichia Coli* 055:B5, Sigma) was injected intraperitoneally (IP) to age- and sex-matched C57BL/6 mice in 200µl saline (10mg/kg). 18h post-LPS-challenge, mice received an intraperitoneal injection of rCLEC-2-Fc or IgG isotype control (100µg/mouse) for an additional 4h. EDTA-treated blood was used to assess blood haematological parameters. Lymph nodes were homogenised, ammonium-Chloride-Potassium (ACK) treated (5mM) and Fc-receptors blocked before antibody staining. Peritoneal cells were collected in 2ml of PBS-EDTA (10mM). Peritoneal lavage fluid (PLF), lymph node cell populations were measured using a CyAn ADP High-Performance Flow Cytometer.

Immunofluorescent Tissue Staining

Organs were snapped frozen and 6 microns sections used for immunofluorescent staining as previously described (10). Sections were flat-mounted with VECTASHIELD antifade mounting medium (Vector Labs). Antibody mixes are shown in **Supplementary Table 1**. Images were acquired using a Zeiss AxioScan.Z1 microscope and analysed using ZEN software.

STATISTICS

All data is presented as mean±SEM. The statistical significance between 2 groups was analyzed using a student's paired t-test and the statistical difference between multiple groups *in vitro* using one-way ANOVA with Tukey's multiple comparisons test. The statistical significance for *in vivo* experiments were determined by a Kruskal-Wallis test using Prism 8 (GraphPad Software Inc, USA). Statistical significance was represented by stars: $*p < 0.05$ $**p < 0.01$ $***p < 0.001$ $****<0.0001$.

DATA SHARING STATEMENT

For original data, please contact the corresponding author. Additional methodology available in supplemental methods.

RESULTS

Platelet CLEC-2 Delays Inflammatory Macrophage Phagocytic Capacity, Reduces TNF-α Secretion and Accelerates Wound Closure *In Vitro*

Upregulation of podoplanin is observed on inflammatory mouse macrophage cell line, RAW264.7, primary macrophages such as bone marrow-derived macrophages (BMDM), peritoneal macrophage following peritonitis, tumour-associated macrophages and monocyte-derived macrophages in the inflamed lung, liver, skin and other organs (3, 10, 12, 20, 28, 30–32). The expression of podoplanin is associated with macrophage migration. In this study, we assessed the effect of crosslinking podoplanin by platelet CLEC-2 on macrophage function and migration.

Using BMDM, we show that addition of wild type (WT), but not CLEC-2-deficient platelets (CLEC2$^{-/-}$), to LPS-challenged BMDM delayed the uptake of pH-sensitive fluorescent *E. Coli*-bound bioparticles compared to control, as assessed by Incucyte systems for live-cell microscopy (**Figures 1A–C**). Podoplanin deficiency in BMDM generated from hematopoietic-specific podoplanin-deficient mice was confirmed in the presence on LPS (**Supplementary Figure 1A**). Podoplanin deficiency from

BMDM did not affect their phagocytic activity (**Supplemental Figures 1B–C**) suggesting a distinct role for podoplanin-crosslinking by CLEC-2. Crosslinking podoplanin by CLEC-2 expressed on WT platelets inhibited TNF-α secretion from BMDM, whereas the levels of TNF-α were not altered by the addition of CLEC2$^{-/-}$ platelets compared to control (**Figure 1D**). No significant change in IL-10 was observed following platelet addition (**Figure 1E**). In a wound scratch assay, addition of WT platelets to a scratched monolayer of inflammatory BMDM (**Figures 1F–H**) accelerated wound closure by two-fold (36% ± 7.4 wound closure for control versus 86% ±12.6 closure in the presence of WT platelets) (**Figures 1F–H**). Wound closure was also accelerated in the presence of CLEC2$^{-/-}$ platelets, although the maximal coverage did not exceed 66% ±18.2. Podoplanin deficiency did not significantly alter wound closure, compared to WT BMDM (**Supplementary Figures 1D–F**), nor did the addition of WT or CLEC-2$^{-/-}$ platelets (**Supplementary Figures 1D, G–H**).

Together these data suggest that platelet CLEC-2 binding to inflammatory BMDM decreased their inflammatory phenotype and regulated their migration.

Platelet CLEC-2 Upregulates the Expression of Inflammatory Macrophage-Podoplanin to Drive Actin Remodelling

We assessed the effect of CLEC-2 on the expression and distribution of podoplanin, and podoplanin transmembrane and intracellular ligands CD44 and ezrin-radixin-moesin (ERM) proteins, respectively. Addition of WT, but not CLEC2$^{-/-}$ platelets for 1h to LPS-stimulated BMDM potentiates

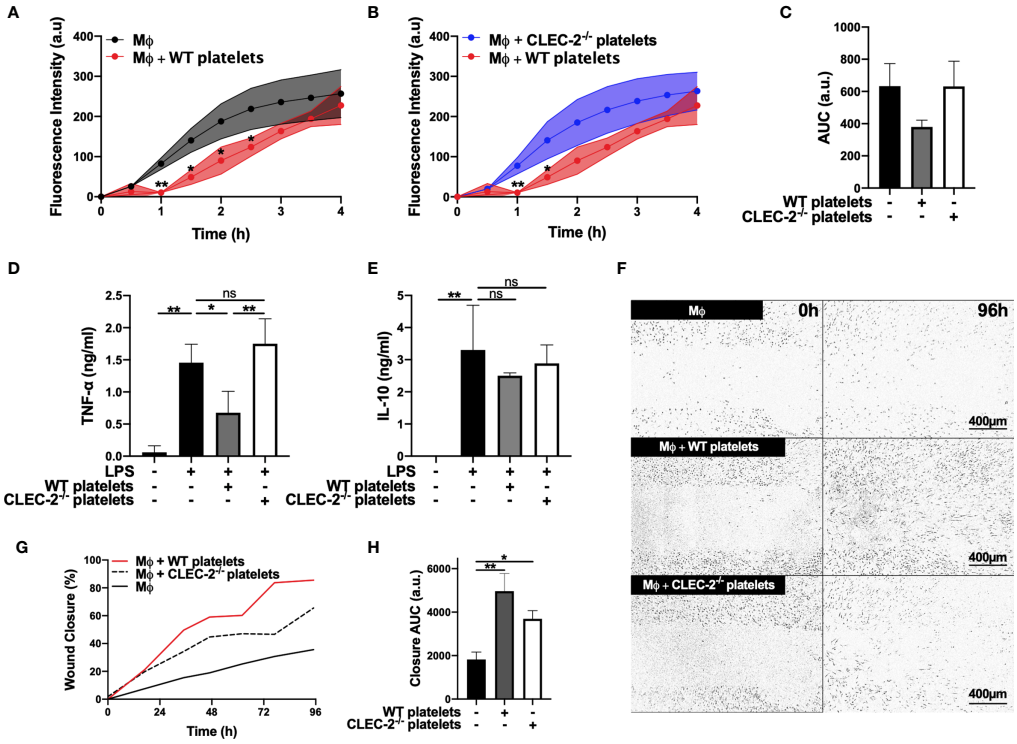

FIGURE 1 | Platelet CLEC-2 delays inflammatory BMDM phagocytic capacity and reduces TNF-α secretion **(A–C)** pH sensitive Alexa Fluor-488 conjugated *Escherichia Coli* bioparticles (3x10^6 beads/condition) were added to LPS-treated BMDM (Mϕ) in the absence or presence of **(A)** WT platelets or **(B)** CLEC-2-deficient platelets (100 platelets: 1 Mϕ) for 4h. **(A, B)** Phagocytosis was visualised and quantified by time lapse-imaging using an Incucyte Live-cell analysis system. **(C)** Phagocytosis profiles were quantified at 4h by detecting fluorescence/mm^3 using area under the curve (AUC; a.u. = arbitrary units; n=3). **(D)** TNF-α and **(E)** IL-10 secretion from control Mϕ or in the presence of WT or CLEC-2-deficient platelets was quantified in the supernatant by ELISA (n=4). **(F–H)** Scratch wound migration of Mϕ was monitored every 2h for 96h using an Incucyte ZOOM system. Following wound scratch, **(F)** WT or CLEC-2-deficient platelets (100 platelets:1 Mϕ) were added to Mϕ. **(G)** Wound closure was quantified as percentage of closure using ImageJ. **(H)** Total wound closure was quantified by AUC at 96h (n=3). The statistical significance between 2 groups was analyzed using a student's paired t-test and the statistical difference between multiple groups using one-way ANOVA with Tukey's multiple comparisons test. *$p < 0.05$ **$p < 0.01$. NS, non-stimulated.

podoplanin and CD44 expression, as assessed by flow cytometry (**Figures 2A–C**). The expression of classical activation markers, such as CD80 and CD86, were not altered (not shown). The distribution of podoplanin and CD44 was also altered by CLEC-2, associated with increased BMDM spreading, measured by increased cell area and loss of circularity (**Figures 2D–F**). Platelet-mediated cell spreading and pseudopods formation was confirmed using scanning electron microscopy (**Figure 2G**). Podoplanin and CD44 colocalized on the pseudopod of BMDM in the presence of WT but not CLEC2$^{-/-}$ platelets. Similar effects on podoplanin expression, distribution and spreading was observed in RAW264.7 cells (**Supplementary Figures 2A–C**). The podoplanin intracellular tail contains 2 serines, 167 and 171, that are constitutively phosphorylated

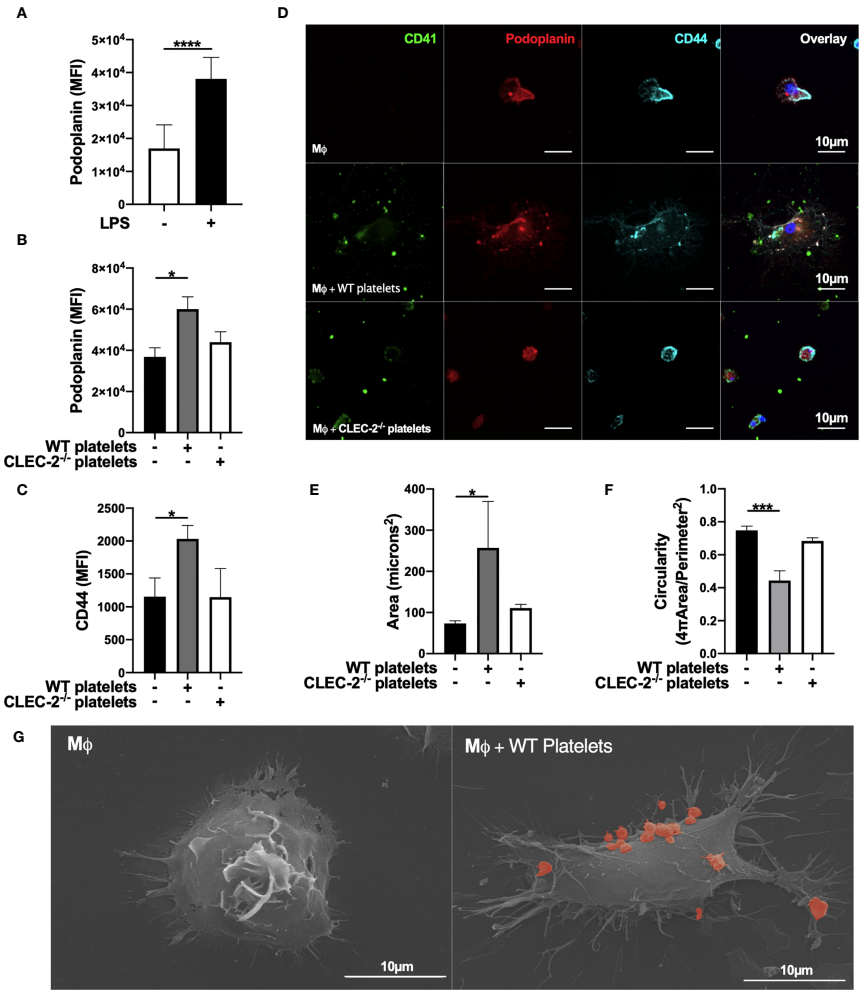

FIGURE 2 | Platelet CLEC-2 upregulates podoplanin and CD44 expression on LPS-stimulated BMDM. **(A)** BMDM were incubated in the presence or absence of LPS (1μg/ml) for 24h. **(B, C)** LPS-stimulated BMDM (Mϕ) were co-cultured in the absence or presence of WT or CLEC-2-deficient platelets (100 platelets: 1 Mϕ). **(A–C)** Median of fluorescence intensity (MFI) of podoplanin (n=4) and CD44 (n=3) was detected by flow cytometry. **(D)** Mϕ were cultured on glass, and WT or CLEC-2-deficient platelets were added for 1h. Platelets (CD41, green), podoplanin (red) and CD44 (cyan) were detected using confocal microscopy. Images are representative of 4 independent experiments. **(E)** Cell area and **(F)** circularity were analysed using ImageJ. **(G)** Mϕ were cultured on glass in the presence or absence of WT platelets (red) for 1h, before fixing and imaging by electron microscopy. The statistical significance between 2 groups was analyzed using a student's paired t-test and the statistical difference between multiple groups using one-way ANOVA with Tukey's multiple comparisons test. *$p < 0.05$, ***$p < 0.001$, ****$p < 0.0001$.

and are critical for the association with the ERM proteins and cell migration (33, 34). Immunoprecipitation of podoplanin demonstrated a reduction in the presence of podoplanin phospho-serine residues in the presence of WT but not CLEC2$^{-/-}$ platelets, which promotes podoplanin association with the ERM proteins (**Supplementary Figure 2D**).

In order to confirm the role of platelet on actin remodelling, we imaged LifeAct-GFP-derived inflammatory BMDM in the presence of platelets using diSPIM LightSheet microscopy for 1h. As expected, inflammatory macrophages are sessile, and addition of WT platelets to LPS-activated BMDM increased pseudopod formation, actin remodelling and mobility, compared to control (**Supplementary Video 1, 2**). In contrast, actin remodelling, spreading and pseudopod formation decreased after the phagocytosis of platelets, showing distinct mechanism of cell-cell interaction and platelet phagocytosis on actin remodelling.

These results show that platelet CLEC-2 binding to podoplanin on inflammatory BMDM, or RAW264.7 cells, increases the expression and distribution of podoplanin and its transmembrane ligand CD44, promoting actin remodelling and cell mobility.

CLEC-2-Mediated Platelet Activation and Secretion Are Dispensable for the Immunomodulatory Functions of CLEC-2

In order to assess whether CLEC-2-dependent platelet activation and secretion, or crosslinking podoplanin is responsible for the immunomodulatory functions of CLEC-2, we performed similar experiments using recombinant dimeric CLEC-2 (rCLEC-2-Fc) and IgG control (17). Addition of rCLEC-2-Fc to LPS-stimulated RAW264.7 cells or LPS-treated BMDM for 1h increased podoplanin expression similar to WT platelets (**Figures 3A, B**). Crosslinking podoplanin with rCLEC-2-Fc decreased TNF-α secretion (**Figure 3C**). In line with this, rCLEC-2-Fc reduced the levels of iNOS, a marker of M1 inflammatory macrophages, without altering Early Growth Response Gene-2 (Egr-2), a marker of M2 anti-inflammatory macrophages (**Supplementary Figures 3A, B**), suggesting a decrease in BMDM inflammatory phenotype without altering their polarization.

rCLEC-2-Fc induced LPS-stimulated BMDM elongation along collagen fibres compared isotype IgG control (**Figure 3D**) and accelerated wound closure (**Figures 3E–G**), confirming the role of podoplanin crosslinking on macrophage migration. The addition of rCLEC-2-Fc to podoplanin-deficient BMDM did not induce wound closure (**Supplementary Figures 4A–C**). Podoplanin was shown to bind to ERM proteins to regulate cell migration. We therefore investigated the interaction and distribution of the ERM proteins and podoplanin in inflammatory macrophages using 3D-SIM microscopy. Surprisingly, podoplanin did not colocalize with the ERM proteins in LPS-treated BMDM. However, addition of rCLEC-2-Fc increased the expression of the ERM proteins and their colocalization with podoplanin (**Figure 3H**), with an enrichment on the filopodia and migrating edges of the cell.

Altogether, our results show that crosslinking podoplanin by CLEC-2, rather than platelet activation and secretion, is responsible for the immunomodulatory effect of CLEC-2 regulating macrophage inflammatory phenotype and their migration.

rCLEC-2-Fc Decreases Inflammatory Macrophage Accumulation in the Peritoneum During Ongoing Inflammation Induced by LPS

The accumulation of podoplanin-positive macrophages is observed in many infectious and inflammatory diseases such as peritonitis, lung inflammation, liver infection and atherosclerosis (10, 12, 20, 23, 30). We assessed the relevance of crosslinking podoplanin using rCLEC-2-Fc during ongoing peritonitis induced by LPS on the accumulation of inflammatory macrophages in the inflamed peritoneum. WT mice were intraperitoneally injected with LPS or saline for 18h to allow inflammatory macrophage accumulation in the inflamed peritoneum, and rCLEC-2-Fc or IgG isotype control were injected for an additional 4h.

Myeloid and lymphoid immune cell populations were detected in the peritoneal lavage using flow cytometry. Gating strategy to identify F4/80+ macrophages is shown in **Figure 4A**. At 22h post LPS, no significant change in the total number of cells in the peritoneum was observed in LPS-treated mice compared to control mice (**Figure 4B**). LPS injection did not significantly alter CD45$^+$ cell count in the PLF compared to saline-treated mice. However, a significant reduction in CD45$^+$ was observed in the peritonitis group treated with rCLEC-2-Fc (**Figure 4C**), more specifically CD11b$^+$ F4/80$^+$ (**Figures 4D, E**). The reduction in inflammatory F4/80$^+$ cells was not due to increased cell apoptosis or death, measured by AnnexinV and Sytox staining (**Supplementary Figure 5A**). Podoplanin expression on F4/80$^+$ cells detected in the peritoneum was increased in the LPS groups compared to control, with no significant changes between rCLEC-2-Fc and IgG treatment (**Figure 4F**). LPS increased platelet-macrophage complexes in the PLF, but this was not altered by rCLEC-2-Fc (**Supplementary Figure 5B**). However, a significant increase in F4/80$^+$CLEC-2$^+$ macrophages was observed following rCLEC-2-Fc treatment, confirming the binding of rCLEC-2-Fc to podoplanin on macrophages, without alteration in platelet-macrophage interactions (**Figures 4G, H**). rCLEC-2-Fc did not alter neutrophil, monocyte, T cells (CD4$^+$ and CD8$^+$), CD19$^+$ or CD45$^+$CD11b$^-$CD11c$^+$ in the PLF (**Supplementary Figures 5C–H**), suggesting a preferential effect of rCLEC-2-Fc on inflammatory F4/80$^+$ cells. rCLEC-2 treatment did not induce bleeding in the peritoneum as measured using red blood cell marker Ter 119 (**Supplementary Figure 5I**).

These results show that rCLEC-2-Fc preferentially alters peritoneal podoplanin-positive inflammatory macrophage accumulation and retention in the inflamed peritoneum.

rCLEC-2-Fc Treatment Reduces TNF-α and Increases IL-10, CCL2, CCL5 and CXCL1 Levels in the Inflamed Peritoneum

We assessed whether the change in macrophage accumulation in the inflamed peritoneum is accompanied by an alteration in

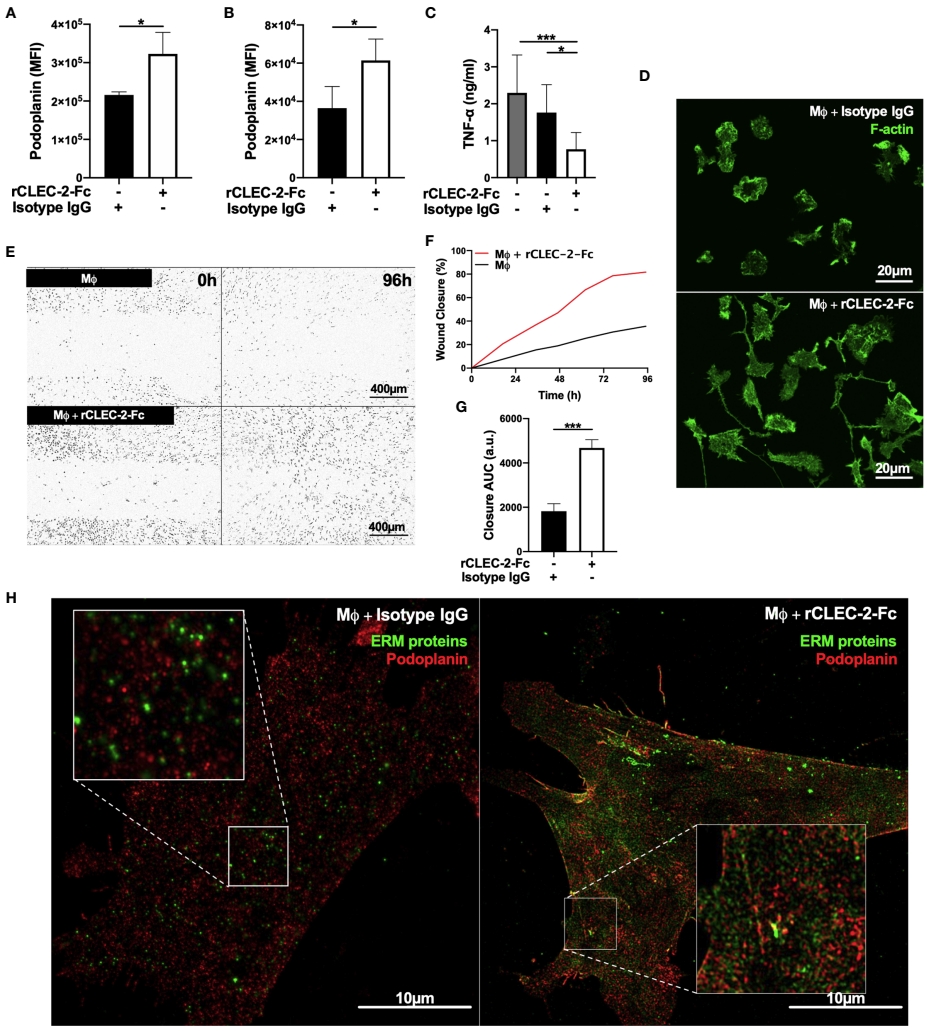

FIGURE 3 | rCLEC-2-Fc upregulates podoplanin expression, and promotes macrophage spreading and migration *in vitro*. **(A, B)** Surface podoplanin expression was detected by flow cytometry using a conjugated anti-podoplanin antibody. 24h LPS-stimulated (1μg/ml) **(A)** RAW264.7 cells (n=3) or **(B)** BMDM (Mϕ; n=4), were washed and incubated with recombinant CLEC-2-Fc (rCLEC-2-Fc; 10μg/ml) or IgG isotype control (10μg/ml) for 1h. **(C)** Mϕ were washed, and cultured with rCLEC-2-Fc (10μg/ml) or IgG isotype control (10μg/ml) for 2h before TNF-α secretion was quantified in the media supernatant by ELISA (n=4). **(D)** LifeAct-GFP-derived Mϕ were spread on collagen in the presence of rCLEC-2-Fc or IgG isotype control (10μg/ml) for 2h and measured with immunofluorescence by confocal microscopy. **(E–G)** Scratch wound migration of Mϕ was monitored every 2h for a total of 96h using an Incucyte ZOOM system. Following wound scratch, **(E)** rCLEC-2-Fc (10μg/ml) was added to Mϕ. **(F)** Wound closure was quantified as percentage of closure compared to initial scratch size using ImageJ. **(G)** Total wound closure was quantified using area under the curve (AUC) at 96h (a.u.= arbitrary units; n=3). **(H)** Mϕ were cultured on collagen in the presence of rCLEC-2-Fc or IgG isotype control (10μg/ml) for 2h. Podoplanin (red) and ERM protein (green) localisation was visualised using immunofluorescence by 3D-structured illumination microscopy (3D-SIM). The statistical significance between 2 groups was analyzed using a student's paired t-test and the statistical difference between multiple groups using one-way ANOVA with Tukey's multiple comparisons test. $^{*}p < 0.05$ $^{***}p < 0.001$.

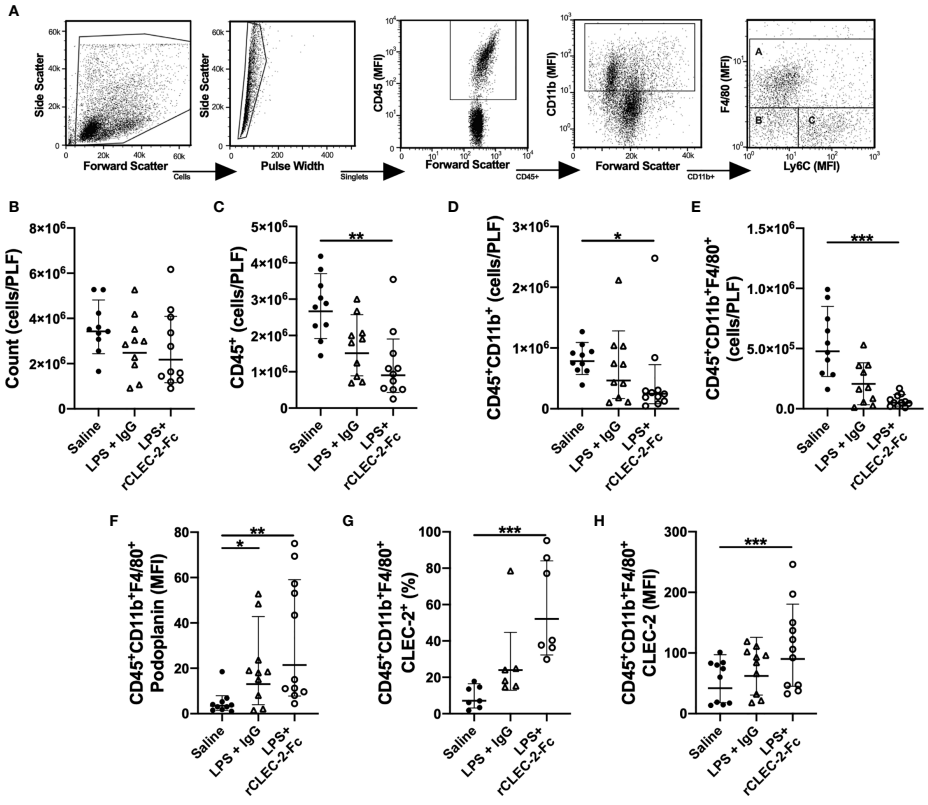

FIGURE 4 | rCLEC-2-Fc decreases macrophage number in the peritoneum following endotoxemia. WT mice were intraperitoneally injected with LPS (10mg/kg) for 18h followed by rCLEC-2-Fc or IgG isotype control (100μg/mouse) for and additional 4h (n=11). Immune cell and platelet infiltration in the peritoneal lavage (PLF) were measured using flow cytometry. **(A)** Gating strategy to identify A: macrophages ($CD11b^+F4/80^+$), B: monocytes ($CD11b^+Ly6C^+$) and C: neutrophils ($CD11b^+F4/80^-Ly6C^-$). **(B)** Total number of cells from the peritoneal lavage, **(C)** leukocytes ($CD45^+$), **(D)** myeloid cells ($CD45^+CD11b^+$) and **(E)** macrophages ($CD45^+CD11b^+F4/80^+$) were measured in the PLF. **(F)** MFI of podoplanin expressed on the surface of macrophages. **(G)** Percentage of CLEC-2-positive macrophages and **(H)** the MFI of CLEC-2 expression on macrophages. The statistical significance was analyzed using a Kruskal-Wallis multiple comparisons test. $^*p < 0.05$, $^{**}p < 0.01$, $^{***}p < 0.001$.

cytokine and chemokine release. Similar to our *in vitro* observations, rCLEC-2-Fc decreased TNF-α secretion in the PLF of LPS-treated mice (**Supplemental Figure 6A**) and increased the levels of the anti-inflammatory cytokine IL-10 (**Supplementary Figure 6B**) and the chemokines CCL2, CCL5 and CXCL1 (**Supplemental Figures 6C–E**). The level of CCL21, the soluble ligand for podoplanin, was not significantly altered in the peritoneum in rCLEC-2-Fc-treated mice (**Supplemental Figure 6F**). The emigration of macrophages was not associated with increased vascular permeability, as measured by angiopoietin-2 secretion (**Supplementary Figure 6G**). There was no change in MMP-9, CXCL2, CCL4, C5a, IL-6 or IL1-β secretion following rCLEC-2-Fc treatment (**Supplementary Figures 6H–L**).

Together, our results show that reduction in macrophage accumulation is associated with an alteration in the inflammatory environment, in particular a reduction in TNF-α levels and increase in IL-10.

rCLEC-2-Fc Promotes Peritoneal Macrophage Emigration to Mesenteric Lymph Nodes

We next investigated the infiltration of inflammatory peritoneal macrophages to the draining lymph nodes. $F4/80^+$ population was detected in the mesenteric lymph nodes (MLN) by flow cytometry and immunofluorescence. A significant increase in myeloid cells, in particular $F4/80^+CLEC2^+$, was observed in rCLEC-2-Fc treated mice compared to IgG control (**Figures 5A–D**). The increase in CLEC-2 MFI might be due to the enhanced podoplanin expression, increasing the binding sites for CLEC-2 (**Figure 5D**). The increase in CLEC-2 density on $F4/80^+$

cells positively correlated with F4/80$^+$ frequency in the MLN (r^2 = 0.67, p=0.0011; **Figure 5E**).

These results show that rCLEC-2-Fc binding to inflammatory peritoneal macrophages promotes their emigration from the inflamed peritoneum to the MLN.

rCLEC-2-Fc-Driven Macrophage Migration to Mesenteric Lymph Nodes Prime T Cells

In order to assess whether emigrated macrophages prime T cells in the draining lymph nodes, we first assessed the location of these macrophages. MLNs were collected 22h post-LPS challenge and macrophages (F4/80$^+$) and platelets (CD41$^+$) localisation in the lymph nodes was assessed using immunofluorescence (**Figure 5F**). In unchallenged lymph nodes, platelets were localised in the medulla and around the medullary chords. Following LPS challenge, there was no significant staining for F4/80$^+$ cells. However, following rCLEC-2-Fc treatment, a significant influx of F4/80$^+$ cells was observed in the draining lymph nodes with a concentration of cells in the medulla, in close contact with T cells. We did not detect macrophages bound to platelets in this zone, however macrophages localised in the lymph nodes post-rCLEC-2-Fc are seen to be CLEC-2- and podoplanin-positive compared to IgG control (**Figure 5G**).

We next investigated whether increased macrophage influx in the MLN is due to an increase in CCL21, a chemoattractant secreted from lymphatic endothelial cells (LECs) and soluble ligand for podoplanin (35). However, we did not observe alteration in CCL21 expression in MLN was observed upon rCLEC-2-Fc treatment (**Figure 6A**). In order to assess whether

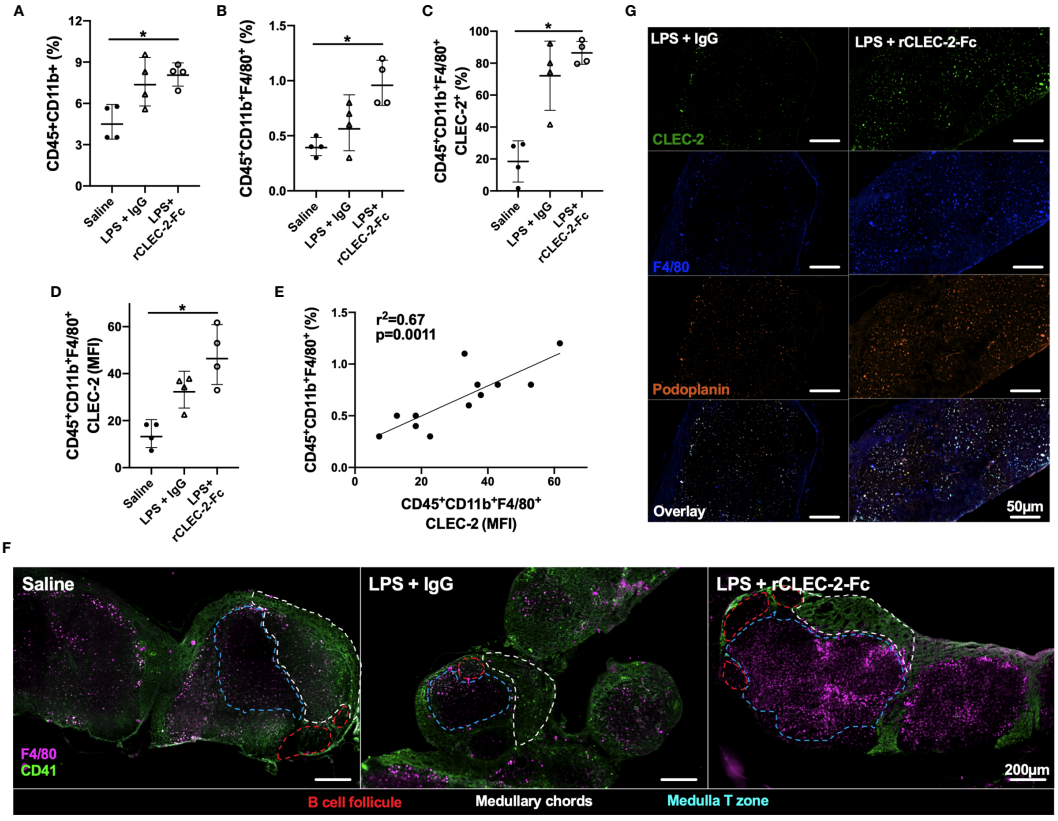

FIGURE 5 | rCLEC-2-Fc increases peritoneal macrophage migration to mesenteric lymph nodes during endotoxemia. WT mice were intraperitoneally injected with LPS (10mg/kg) for 18h followed by rCLEC-2-Fc or IgG isotype control (100µg/mouse) for an additional 4h (n=4). **(A–E)** Mesenteric lymph node (MLN) cells were collected and immune cell population detected by flow cytometry. **(A)** Percentage of myeloid cells (CD45$^+$CD11b$^+$) and **(B)** macrophages (CD45$^+$CD11b$^+$F4/80$^+$). **(C)** CLEC-2-positive macrophages and **(D)** the MFI of CLEC-2 expression on macrophages in MLN. **(E)** Correlation between the percentage of MLN macrophages and the MFI of CLEC-2 expression on macrophages by Simple Linear Regression. **(F)** Immunofluorescent staining of macrophages (F4/80; purple) and platelets (CD41; green) in frozen MLN sections. **(G)** Immunofluorescent staining of macrophages (F4/80; blue), CLEC-2 (green) and podoplanin (orange) in frozen MLN sections. The statistical significance was analyzed using a Kruskal-Wallis multiple comparisons test. *$p < 0.05$.

increased podoplanin expression and actin remodelling increases macrophage chemoattraction towards CCL21, we evaluated LPS-treated macrophage migration towards CCL21 *in vitro* using a Boyden chamber. Addition of rCLEC-2-Fc to LPS-treated BMDM increased the number of macrophages migrating towards CCL21 (**Figure 6B**). This was not due to an increase in CCL21 receptors CCR4 and CCR7 (**Figures 6C, D**). This suggested that CLEC-2-dependent podoplanin and CD44 upregulation, associated with accelerated actin rearrangement, was responsible for increased migration towards CCL21.

In order to assess whether macrophage infiltration into lymph node medulla primes T cells, we stimulated homogenised lymph nodes from different groups *ex vivo* with low-dose LPS (10ng/ml) for 24h. IL-2 secretion, as a readout of T cell priming, was measured in the supernatants by ELISA (**Figure 6E**). Low-dose LPS did not induce IL-2 secretion in MLN cells isolated from saline- or LPS-treated mice. In contrast, a significant increase in IL-2 levels was observed in rCLEC-2-Fc treated mice, suggesting that increased macrophage efflux to the medulla T zone promotes T cell priming.

Altogether, these results suggest that rCLEC-2-Fc alters the expression of podoplanin and its interaction with ligands CD44, ERM and CCL21. This accelerates the removal of inflammatory macrophages from the inflamed peritoneum and their emigration to mesenteric lymph nodes to promote T cell priming, reducing peritoneal inflammation.

DISCUSSION

In this study, we report that crosslinking podoplanin using recombinant CLEC-2-Fc limits the inflammatory environment by reducing inflammatory macrophage accumulation in the inflamed tissue and reduces their inflammatory phenotype. During ongoing peritonitis induced by LPS, rCLEC-2-Fc accelerates the removal of inflammatory macrophages from the site of inflammation to the draining lymph nodes and induces T cell priming. The interaction of CLEC-2 with podoplanin upregulated on inflammatory macrophages promotes their mobility through (i) the dephosphorylation of podoplanin intracellular serine residues, (ii) upregulation and rearrangement of podoplanin and CD44 expression on macrophage membrane protrusions, (iii) reorganisation of actin cytoskeleton and ERM protein distribution

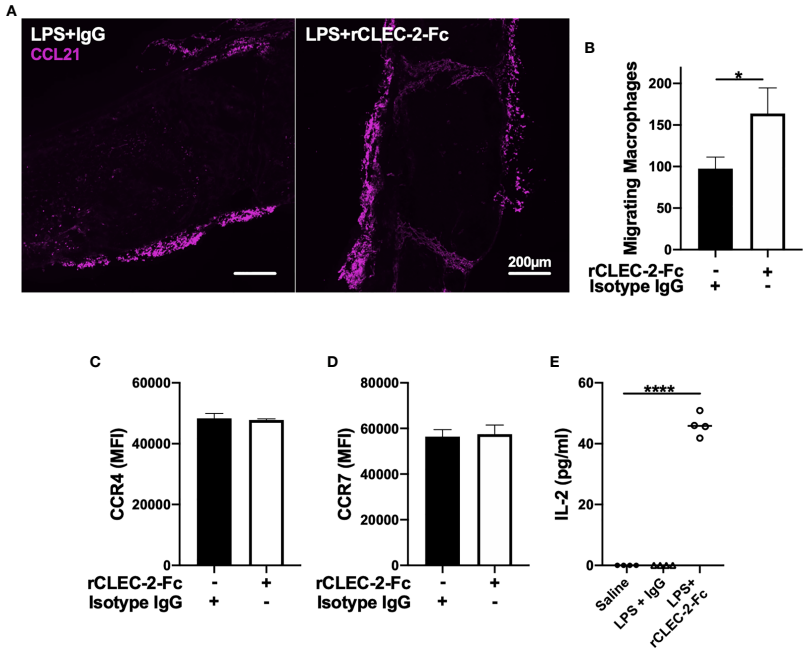

FIGURE 6 | rCLEC-2-Fc increases inflammatory macrophage migration towards CCL21 and primes T cells in mesenteric lymph nodes. WT mice were intraperitoneally injected with LPS (10mg/kg) for 18h followed by rCLEC-2-Fc or IgG isotype control (100µg/mouse) for an additional 4h (n=4). **(A)** Immunofluorescent staining of CCL21 (purple) in frozen MLN taken from LPS-challenged mice. **(B, C)** 24h LPS-stimulated (1µg/ml) BMDM were treated with rCLEC-2-Fc (10µg/ml) or IgG isotype control (10µg/ml) for 4h. Surface expression of **(B)** CCR4 and **(C)** CCR7 median fluorescence intensity (MFI) was detected by flow cytometry (n=4). **(D)** Migration of inflammatory BMDM co-cultured with rCLEC-2-Fc or IgG Isotype control (10µg/ml) toward CCL21 (30ng/ml) was analysed using a Boyden chamber assay for 4h (n=3). **(E)** IL-2 secretion from MLN cells isolated from different mice cultured *in vitro* with LPS (10ng/ml) for 16h was quantified by ELISA.The statistical significance was analyzed using a Kruskal-Wallis multiple comparisons test. $*p < 0.05$, $****p < 0.0001$.

on cell protrusions and (iv) inflammatory macrophage interaction with CCL21 secreted by lymphatic endothelial cells (LECs). In parallel, CLEC-2 crosslinks podoplanin and reduces TNF-α secretion from inflammatory macrophages and delays their phagocytic activity without changing macrophage polarisation, suggesting a reduction in their inflammatory phenotype. We propose that during acute, ongoing inflammation, CLEC-2-podoplanin crosslinking reduces tissue inflammation by reducing accumulation and retention of inflammatory macrophages and promotes their emigration to draining lymph nodes.

During inflammation, macrophages play three main functions: phagocytosis of debris and dead/apoptotic cells and pathogens, antigen presentation and immunoregulation by secreting an arsenal of cytokines and chemokines. After the first inflammatory phase subsides, macrophages also play a role in tissue repair and wound healing (36). Alteration in the acute or repair phases can lead to chronic inflammation and pathogenic fibrosis. Recent studies showed that platelet interaction with macrophages can alter macrophage function, dependant on the receptor, insult, organ and disease progression (13, 14, 37–40). Using acute inflammatory models, we and others have shown a significant upregulation of podoplanin on inflammatory macrophages (10, 12, 28, 30, 31). Here we show that podoplanin expressed on inflammatory macrophages can be targeted to regulate local inflammation and macrophage trafficking from the site of inflammation. Although many studies have shown that platelet secretion is the main regulator of macrophage function, partly through Prostaglandin E_2 (11, 40), we show for the first time that the immunomodulatory effect of CLEC-2 is not dependent on platelet activation and secretion, but rather through crosslinking podoplanin. Deletion of CLEC-2 from platelets did not alter the binding of platelets to inflammatory macrophages, suggesting that CLEC-2 is not involved this heterotypic interaction, but exerts an immunomodulatory effect. GPIb (13), CD40L (41), P-selectin (42) or other receptors might be responsible for binding and differentially regulate macrophage functions.

Our study describes a novel mechanism by which crosslinking podoplanin with CLEC-2 reduces tissue inflammation. The use of rCLEC-2-Fc overcomes the limitation of using platelets during ongoing inflammation, in particular due the differential roles of platelet receptors and secretory repertoire in inflammation which can limit clinical translation. Platelet CLEC-2, as well as rCLEC-2-Fc, induces a rapid translocation of podoplanin from intracellular stores to the surface of inflammatory macrophages. This is associated with a loss of phosphorylation of the serine residues in the intracellular podoplanin tail, which has been demonstrated to promote fibroblast migratory activity (33, 34). Classically, macrophages migrate through actin polymerisation-driven elongation of the leading edge towards a gradient, followed by integrin mediated adhesion to matrix proteins and finally actomyosin contraction and trailing edge de-adhesion (43). CLEC-2 induced the reorganisation of the actin cytoskeleton and increased podoplanin interaction with ERM proteins and CD44, promoting macrophage migration. Indeed, CD44 expression is required for podoplanin-induced migration in squamous stratified epithelia (44), suggesting that CLEC-2 may increase podoplanin and CD44 expression and their association, leading to macrophage migration. This cell-specific strategy to limit the accumulation of highly inflamed macrophages in tissues does not induce inflammatory bleeding or thrombosis, which are the major complications associated with platelet-targeting.

Peritoneal macrophages are comprised of 2 functionally and phenotypically distinct subsets, the large and small peritoneal macrophages (LPM and SPM). LPM ($F4/80^{high}CD11b^{high}Ly6C^{-}$) largely outnumber SPM ($F4/80^{low}CD11b^{low}Ly6C^{+}$), and are responsible for phagocytosis of cell debris and apoptotic cells and mediate tissue repair (45). In a model of liver sterile injury, in a recent study showed that a sub-population of resident peritoneal macrophages, GATA-6^{+}, is rapidly mobilised to the injured liver in CD44-dependent manner, expressing M2 macrophage markers and promoting tissue repair (46). Following intraperitoneal inflammation, LPM rapidly migrate to draining lymph nodes, whereas SPM numbers increases with monocyte influx from the circulation into the peritoneum. These monocytes clear apoptotic neutrophils and subsequently differentiate into macrophages or dendritic cells. Monocyte-derived inflammatory macrophages upregulate podoplanin in response to inflammatory stimuli such as Zymosan and LPS. During the resolution of inflammation, monocytes infiltration and macrophage removal regulates peritoneal inflammation. Macrophage removal could be through local death and/or increased migration to draining lymph nodes (47–49). Here we show that the expression of podoplanin on peritoneal inflammatory macrophages can be targeted to accelerate their removal from the peritoneum. Crosslinking podoplanin using recombinant CLEC-2 induces a series of intracellular changes and receptor redistribution on the cell membrane, increasing their migration. The absence of macrophages from the inflamed peritoneum is not secondary to (i) macrophage local death (49), (ii) increased macrophage adherence through integrin $\alpha_D\beta_2$ and $\alpha_M\beta_2$ (Mac-1) upregulation (50) but rather due to macrophage emigration to a secondary site (48), in particular draining lymph nodes. The increase in macrophage emigration was not due to matrix metalloprotease 9 secretion (51), or dysregulated vascular integrity, neither by increase in other chemotactic molecules such as complement C5a levels (22). Combining our *in vitro* and *in vivo* data suggests that a chemoattractant released from the draining lymph nodes is responsible for the directed migration. The directed migration to the draining lymph nodes suggests a potential role for CCL21, constituently secreted by LECs (35) and soluble ligand for podoplanin. CCL21 has previously been described as a key regulator of podoplanin^{+} dendritic cells migrating to lymph nodes (52, 53). This directed migration and retention in lymph nodes represents advantages, including limitation of local peritoneal and potential development of an adaptive immune response.

rCLEC-2-mediated macrophage migration to draining lymph nodes was not restricted to reduce peritoneal inflammation and macrophage accumulation, but also increased T cell priming in the lymph nodes. Macrophages are not solely innate immune cells but can also process and present antigens to naïve T cells in secondary lymphoid organs, driving $CD4^{+}$ T helper cell activation and polarisation to Th1, Th2 or Th17 effector cells. The co-

localisation of macrophages with T cells in the medulla increases antigen presentation and T cell priming, observed by increased IL-2 secretion from MLN cells isolated from rCLEC-2-Fc-treated mice. These results suggest that rCLEC-2 not only limits the accumulation of inflammatory macrophages in the peritoneum, but can also direct macrophages to the draining lymph nodes and prime T cell activation. Whether macrophages function as antigen presenting cells, express co-stimulatory molecules or release activating cytokines to prime T cells needs further investigation. Moreover, T cell priming, polarisation and survival following clonal expansion requires further investigation. The beneficial targeting of macrophage emigration to lymph nodes is dependent on the disease, as the association of podoplanin^{+} macrophages with tumour lymphatic vessels in mammary tumour model correlates with increased lymph node and distant organ metastasis (32).

We have previously shown that platelet-CLEC-2-deficiency in mice exacerbated the cytokine storm during endotoxemia and caecal ligation and puncture (10); this is associated with impaired macrophage number in the peritoneum. Complex alterations in the inflammatory response in these mice limited the use of rCLEC-2-Fc treatment during endotoxemia, due to a drastic early increase in the clinical severity. Therefore, the mechanisms driving the dysregulated inflammatory response in CLEC-2-deficient mice require further investigation.

In conclusion, we show a novel, key immunomodulatory role for CLEC-2-podoplanin interaction to limit the accumulation and retention of highly inflamed macrophages in tissues, a major complication observed in many sterile thromboinflammatory diseases such as atherosclerosis and metabolic syndrome. rCLEC-2-Fc may present a novel pathway to reduce the accumulation of inflammatory macrophages, limiting tissue inflammation and subsequent progression a to chronic inflammatory state.

DATA AVAILABILITY STATEMENT

The original contributions presented in the study are included in the article/**Supplementary Material**. Further inquiries can be directed to the corresponding author.

ETHICS STATEMENT

The animal study was reviewed and approved by UK Home office.

AUTHOR CONTRIBUTIONS

JB designed and performed research, collected, analysed and interpreted data, and wrote the manuscript. NB-C performed experiments and contributed to data analysis. MZ, JC, EG, and MC performed experiments. YD and ST provided reagents. LT contributed to data analysis. AB and JB contributed to data interpretation. SW contributed to data interpretation and provided reagents. JR designed and performed research, interpreted data and wrote the manuscript. All authors contributed to the article and approved the submitted version.

FUNDING

This work was supported by a College-funded PhD studentship (University of Birmingham), a BHF Accelerator Award (AA/18/2/34218) and the Centre of Membrane Proteins and Receptors. JR is supported by a BHF Intermediate Basic Science Fellowship Application (FS/IBSRF/20/25039) and Wellcome Trust 4-year studentship for MC (204951). AB is supported by BHF Senior basic Science Research Fellowship (FS/19/30/34173). SPW holds a BHF Chair (CH/03/003).

ACKNOWLEDGMENTS

The authors would like to thank Dr. Beata Grygielska for genotyping of mice, Dr. Elisabeth Haining for colony maintenance, Dr. Christopher Smith for laboratory assistance throughout, and Mr. Paul Stanley within the Centre of Electron Microscopy (UoB) for image acquisition. A CC, BY, or equivalent license is applied to AAM arising from this submission, in accordance with the grant's open access conditions. Electron microscopy pseudocolour was generated by Bourne Design. Visual abstract was created using Servier Medical Art templates, licensed under Creative Commons Attribution 3.0 Unported License; https://smart.servier.com.

SUPPLEMENTARY MATERIAL

The Supplementary Material for this article can be found online at: https://www.frontiersin.org/articles/10.3389/fimmu.2021.693974/full#supplementary-material

REFERENCES

1. Rayes J, Bourne JH, Brill A, Watson SP. The Dual Role of Platelet-Innate Immune Cell Interactions in Thrombo-Inflammation. *Res Pract Thromb Haemost* (2020) 4:23–35. doi: 10.1002/rth2.12266
2. Morrell CN, Aggrey AA, Chapman LM, Modjeski KL. Emerging Roles for Platelets as Immune and Inflammatory Cells. *Blood* (2014) 123:2759–67. doi: 10.1182/blood-2013-11-462432
3. Rayes J, Jadoui S, Lax S, Gros A, Wichaiyo S, Ollivier V, et al. The Contribution of Platelet Glycoprotein Receptors to Inflammatory Bleeding Prevention is Stimulus and Organ Dependent. *Haematologica* (2018) 103: e256–8. doi: 10.3324/haematol.2017.182162
4. Ho-Tin-Noé B, Boulaftali Y, Camerer E. Platelets and Vascular Integrity: How Platelets Prevent Bleeding in Inflammation. *Blood* (2018) 131:277–88. doi: 10.1182/blood-2017-06-742676
5. Assinger A, Schrottmaier WC, Salzmann M, Rayes J. Platelets in Sepsis: An Update on Experimental Models and Clinical Data. *Front Immunol* (2019) 10:1687. doi: 10.3389/fimmu.2019.01687
6. Koupenova M, Corkrey HA, Vitseva O, Manni G, Pang CJ, Clancy L, et al. The Role of Platelets in Mediating a Response to Human

Influenza Infection. *Nat Commun* (2019) 10:1780. doi: 10.1038/s41467-019-09607-x
7. Deppermann C, Kubes P. Platelets and Infection. *Semin Immunol* (2016) 28:536–45. doi: 10.1016/j.smim.2016.10.005
8. Speth C, Rambach G, Lass-Flörl C. Platelet Immunology in Fungal Infections. *Thromb Haemost* (2014) 112:632–9. doi: 10.1160/TH14-01-0074
9. Claushuis TAM, de Vos AF, Nieswandt B, Boon L, Roelofs JJTH, de Boer OJ, et al. Platelet Glycoprotein VI Aids in Local Immunity During Pneumonia-Derived Sepsis Caused by Gram-Negative Bacteria. *Blood* (2018) 131:864–76. doi: 10.1182/blood-2017-06-788067
10. Rayes J, Lax S, Wichaiyo S, Watson SK, Di Y, Lombard S, et al. The podoplanin-CLEC-2 Axis Inhibits Inflammation in Sepsis. *Nat Commun* (2017) 8:2239. doi: 10.1038/s41467-017-02402-6
11. Xiang B, Zhang G, Guo L, Li XA, Morris AJ, Daugherty A, et al. Platelets Protect From Septic Shock by Inhibiting Macrophage-Dependent Inflammation Via the Cyclooxygenase 1 Signalling Pathway. *Nat Commun* (2013) 4:2657. doi: 10.1038/ncomms3657
12. Lax S, Rayes J, Wichaiyo S, Haining EJ, Lowe K, Grygielska B, et al. Platelet CLEC-2 Protects Against Lung Injury Via Effects of its Ligand Podoplanin on Inflammatory Alveolar Macrophages in the Mouse. *Am J Physiol Lung Cell Mol Physiol* (2017) 313:L1016–29. doi: 10.1152/ajplung.00023.2017
13. Carestia A, Mena HA, Olexen CM, Ortiz Wilczyński JM, Negrotto S, Errasti AE, et al. Platelets Promote Macrophage Polarization Toward Pro-inflammatory Phenotype and Increase Survival of Septic Mice. *Cell Rep* (2019) 28:896–908.e5. doi: 10.1016/j.celrep.2019.06.062
14. Rolfes V, Ribeiro LS, Hawwari I, Böttcher L, Rosero N, Maasewerd S, et al. Platelets Fuel the Inflammasome Activation of Innate Immune Cells. *Cell Rep* (2020) 31:107615. doi: 10.1016/j.celrep.2020.107615
15. Huang X, Venet F, Wang YL, Lepape A, Yuan Z, Chen Y, et al. PD-1 Expression by Macrophages Plays a Pathologic Role in Altering Microbial Clearance and the Innate Inflammatory Response to Sepsis. *Proc Natl Acad Sci U S A* (2009) 106:6303–8. doi: 10.1073/pnas.0809422106
16. Suzuki-Inoue K, Kato Y, Inoue O, Kaneko MK, Mishima K, Yatomi Y, et al. Involvement of the Snake Toxin Receptor CLEC-2, in Podoplanin-Mediated Platelet Activation, by Cancer Cells. *J Biol Chem* (2007) 282:25993–6001. doi: 10.1074/jbc.M702327200
17. Bourne JH, Colicchia M, Di Y, Martin E, Slater A, Roumenina LT, et al. Heme Induces Human and Mouse Platelet Activation Through C-type-lectin-like Receptor-2. *Haematologica* (2020) 106:2. doi: 10.3324/haematol.2020.246488
18. Quintanilla M, Montero-Montero L, Renart J, Martín-Villar E. Podoplanin in Inflammation and Cancer. *Int J Mol Sci* (2019) 20(3):707–45. doi: 10.3390/ijms20030707
19. Retzbach EP, Sheehan SA, Nevel EM, Batra A, Phi T, Nguyen ATP, et al. Podoplanin Emerges as a Functionally Relevant Oral Cancer Biomarker and Therapeutic Target. *Oral Oncol* (2018) 78:126–36. doi: 10.1016/j.oraloncology.2018.01.011
20. Hitchcock JR, Cook CN, Bobat S, Ross EA, Flores-Langarica A, Lowe KL, et al. Inflammation Drives Thrombosis After Salmonella Infection Via CLEC-2 on Platelets. *J Clin Invest* (2015) 125:4429–46. doi: 10.1172/JCI79070
21. Payne H, Ponomaryov T, Watson SP, Brill A. Mice With a Deficiency in CLEC-2 are Protected Against Deep Vein Thrombosis. *Blood* (2017) 129:2013–20. doi: 10.1182/blood-2016-09-742999
22. Xie Z, Shao B, Hoover C, McDaniel M, Song J, Jiang M, et al. Monocyte Upregulation of Podoplanin During Early Sepsis Induces Complement Inhibitor Release to Protect Liver Function. *JCI Insight* (2020) 5. doi: 10.1172/jci.insight.134749
23. Inoue O, Hokamura K, Shirai T, Osada M, Tsukiji N, Hatakeyama K, et al. Vascular Smooth Muscle Cells Stimulate Platelets and Facilitate Thrombus Formation Through Platelet Clec-2: Implications in Atherothrombosis. *PloS One* (2015) 10:e0139357. doi: 10.1371/journal.pone.0139357
24. Takakubo Y, Oki H, Naganuma Y, Saski K, Sasaki A, Tamaki Y, et al. Distribution of Podoplanin in Synovial Tissues in Rheumatoid Arthritis Patients Using Biologic or Conventional Disease-Modifying Anti-Rheumatic Drugs. *Curr Rheumatol Rev* (2017) 13:72–8. doi: 10.2174/1573397112666160331143607
25. Hatzioannou A, Nayar S, Gaitanis A, Barone F, Anagnostopoulos C, Verginis P. Intratumoral Accumulation of Podoplanin-Expressing Lymph Node Stromal Cells Promote Tumor Growth Through Elimination of CD4. *Oncoimmunology* (2016) 5:e1216289. doi: 10.1080/2162402X.2016.1216289
26. Haining EJ, Lowe KL, Wichaiyo S, Kataru RP, Nagy Z, Kavanagh DP, et al. Lymphatic Blood Filling in CLEC-2-deficient Mouse Models. *Platelets* (2020) 32(3)352–67. doi: 10.1080/09537104.2020.1734784
27. Riedl J, Flynn KC, Raducanu A, Gärtner F, Beck G, Bösl M, et al. Lifeact Mice for Studying F-actin Dynamics. *Nat Methods* (2010) 7:168–9. doi: 10.1038/nmeth0310-168
28. Kerrigan AM, Navarro-Nuñez L, Pyz E, Finney BA, Willment JA, Watson SP, et al. Podoplanin-Expressing Inflammatory Macrophages Activate Murine Platelets Via CLEC-2. *J Thromb Haemost* (2012) 10:484–6. doi: 10.1111/j.1538-7836.2011.04614.x
29. Weischenfeldt J, Porse B. Bone Marrow-Derived Macrophages (Bmm): Isolation and Applications. *CSH Protoc* (2008) 2008:pdb.prot5080. doi: 10.1101/pdb.prot5080
30. Hou TZ, Bystrom J, Sherlock JP, Qureshi O, Parnell SM, Anderson G, et al. A Distinct Subset of Podoplanin (gp38) Expressing F4/80+ Macrophages Mediate Phagocytosis and are Induced Following Zymosan Peritonitis. *FEBS Lett* (2010) 584:3955–61. doi: 10.1016/j.febslet.2010.07.053
31. Wichaiyo S, Lax S, Montague SJ, Li Z, Grygielska B, Pike JA, et al. Platelet Glycoprotein VI and C-type Lectin-Like Receptor 2 Deficiency Accelerates Wound Healing by Impairing Vascular Integrity in Mice. *Haematologica* (2019) 104:1648–60. doi: 10.3324/haematol.2018.208363
32. Bieniasz-Krzywiec P, Martín-Pérez R, Ehling M, García-Caballero M, Pinioti S, Pretto S, et al. Podoplanin-Expressing Macrophages Promote Lymphangiogenesis and Lymphoinvasion in Breast Cancer. *Cell Metab* (2019) 30:917–36.e10. doi: 10.1016/j.cmet.2019.07.015
33. Krishnan H, Ochoa-Alvarez JA, Shen Y, Nevel E, Lakshminarayanan M, Williams MC, et al. Serines in the Intracellular Tail of Podoplanin (PDPN) Regulate Cell Motility. *J Biol Chem* (2013) 288:12215–21. doi: 10.1074/jbc.C112.446823
34. Krishnan H, Retzbach EP, Ramirez MI, Liu T, Li H, Miller WT, et al. PKA and CDK5 can Phosphorylate Specific Serines on the Intracellular Domain of Podoplanin (PDPN) to Inhibit Cell Motility. *Exp Cell Res* (2015) 335:115–22. doi: 10.1016/j.yexcr.2015.04.019
35. Farnsworth RH, Karnezis T, Maciburko SJ, Mueller SN, Stacker SA. The Interplay Between Lymphatic Vessels and Chemokines. *Front Immunol* (2019) 10:518. doi: 10.3389/fimmu.2019.00518
36. Duffield JS, Forbes SJ, Constandinou CM, Clay S, Partolina M, Vuthoori S, et al. Selective Depletion of Macrophages Reveals Distinct, Opposing Roles During Liver Injury and Repair. *J Clin Invest* (2005) 115:56–65. doi: 10.1172/JCI200522675
37. Scull CM, Hays WD, Fischer TH. Macrophage Pro-Inflammatory Cytokine Secretion is Enhanced Following Interaction With Autologous Platelets. *J Inflammation (Lond)* (2010) 7:53. doi: 10.1186/1476-9255-7-53
38. Barrett TJ, Schlegel M, Zhou F, Gorenchtein M, Bolstorff J, Moore KJ, et al. Platelet Regulation of Myeloid Suppressor of Cytokine Signaling 3 Accelerates Atherosclerosis. *Sci Transl Med* (2019) 11. doi: 10.1126/scitranslmed.aax0481
39. Linke B, Schreiber Y, Picard-Willems B, Slattery P, Nüsing RM, Harder S, et al. Activated Platelets Induce an Anti-Inflammatory Response of Monocytes/Macrophages Through Cross-Regulation of PGE. *Mediators Inflammation* (2017) 2017:1463216. doi: 10.1155/2017/1463216
40. Heffron SP, Weinstock A, Scolaro B, Chen S, Sansbury BE, Marecki G, et al. Platelet-Conditioned Media Induces an Anti-Inflammatory Macrophage Phenotype Through EP4. *J Thromb Haemost* (2021) 19:562–73. doi: 10.1111/jth.15172
41. Inwald DP, McDowall A, Peters MJ, Callard RE, Klein NJ. CD40 is Constitutively Expressed on Platelets and Provides a Novel Mechanism for Platelet Activation. *Circ Res* (2003) 92:1041–8. doi: 10.1161/01.RES.0000070111.98158.6C
42. Ye Z, Zhong L, Zhu S, Wang Y, Zheng J, Wang S, et al. The P-selectin and PSGL-1 Axis Accelerates Atherosclerosis Via Activation of Dendritic Cells by the TLR4 Signaling Pathway. *Cell Death Dis* (2019) 10:507. doi: 10.1038/s41419-019-1736-5
43. Pixley FJ. Macrophage Migration and Its Regulation by CSF-1. *Int J Cell Biol* (2012) 2012:501962. doi: 10.1155/2012/501962

44. Martín-Villar E, Fernández-Muñoz B, Parsons M, Yurrita MM, Megías D, Pérez-Gómez E, et al. Podoplanin Associates With CD44 to Promote Directional Cell Migration. *Mol Biol Cell* (2010) 21:4387–99. doi: 10.1091/mbc.e10-06-0489
45. Cassado ADA, D'Império Lima MR, Bortoluci KR. Revisiting Mouse Peritoneal Macrophages: Heterogeneity, Development, and Function. *Front Immunol* (2015) 6:225. doi: 10.3389/fimmu.2015.00225
46. Wang J, Kubes P. A Reservoir of Mature Cavity Macrophages That Can Rapidly Invade Visceral Organs to Affect Tissue Repair. *Cell* (2016) 165:668–78. doi: 10.1016/j.cell.2016.03.009
47. Cao C, Lawrence DA, Strickland DK, Zhang L. A Specific Role of Integrin Mac-1 in Accelerated Macrophage Efflux to the Lymphatics. *Blood* (2005) 106:3234–41. doi: 10.1182/blood-2005-03-1288
48. Bellingan GJ, Caldwell H, Howie SE, Dransfield I, Haslett C. In Vivo Fate of the Inflammatory Macrophage During the Resolution of Inflammation: Inflammatory Macrophages do Not Die Locally, But Emigrate to the Draining Lymph Nodes. *J Immunol* (1996) 157:2577–85.
49. Gautier EL, Ivanov S, Lesnik P, Randolph GJ. Local Apoptosis Mediates Clearance of Macrophages From Resolving Inflammation in Mice. *Blood* (2013) 122:2714–22. doi: 10.1182/blood-2013-01-478206
50. Yakubenko VP, Belevych N, Mishchuk D, Schurin A, Lam SC, Ugarova TP. The Role of Integrin Alpha D Beta2 (CD11d/CD18) in Monocyte/Macrophage Migration. *Exp Cell Res* (2008) 314:2569–78. doi: 10.1016/j.yexcr.2008.05.016
51. Gong Y, Hart E, Shchurin A, Hoover-Plow J. Inflammatory Macrophage Migration Requires MMP-9 Activation by Plasminogen in Mice. *J Clin Invest* (2008) 118:3012–24. doi: 10.1172/JCI32750
52. Lira SA. A Passport Into the Lymph Node. *Nat Immunol* (2005) 6:866–8. doi: 10.1038/ni0905-866
53. Manzo A, Bugatti S, Caporali R, Prevo R, Jackson DG, Uguccioni M, et al. CCL21 Expression Pattern of Human Secondary Lymphoid Organ Stroma is Conserved in Inflammatory Lesions With Lymphoid Neogenesis. *Am J Pathol* (2007) 171:1549–62. doi: 10.2353/ajpath.2007.061275

Conflict of Interest: The authors declare that the research was conducted in the absence of any commercial or financial relationships that could be construed as a potential conflict of interest.